PHOTOCHROMIC TEXTILES

Martina Viková MSc.

In accordance with the requirements for the degree of

Doctor of Philosophy

to Heriot-Watt University

The work embodied in this text was carried out at the Scottish Borders
Campus, School of Textiles and Design and off campus at the Technical University in
Liberec, Czech Republic

<u>March 2011</u>

ABSTRACT

This thesis describes a new investigation into the relationship between the developed colour intensity of photochromic textiles and the time of UV exposure and also the time of relaxation. As a result of this relationship the potential of flexible textile-based sensor constructions which might be used for the identification of radiation intensity is demonstrated. In addition the differences between photochromic pigment behaviour in solution and incorporated into prints on textiles are demonstrated. Differences in the effect of the spectral power distributions of light sources on the photochromic response are also examined. Bi-exponential functions, which are used in optical yield (O_y) calculations, have been described to provide a good description of the kinetics of colour change intensity of photochromic pigments, giving a good fit. The optical yield of the photochromic reaction O_y is linearly related to the intensity of illumination E.

The optical yield obtained from the photochromic reaction curves are described by a kinetic model, which defines the rate of colour change initiated by external stimulus of UV light. Verification of the kinetic model is demonstrated for textile sensors with photochromic pigments applied by textile printing and by fibre mass dyeing.

The thesis also describes a unique instrument developed by author, which measures colour differences ΔE^* and spectral remission curves derived from photochromic colour change simultaneously with UV irradiation.

In this theses the photochromic behaviour of selected pigments in three different applications (type of media – textile prints, non-woven textiles and solution is investigated.

Acknowledgement

Many thanks are due to Professor R.M. Christie of the School of Textiles and Design, the Scottish Border Campus for his guidance, expert supervision, and encouragement throughout. Thanks are also due to Professor Jiří Militký as co-supervisor from Technical University of Liberec.

My special thanks are devoted to all the people who helped me during the time of the writing of the thesis. Great thanks are directed to my mother Mary and my husband Michael for their stand - by support.

With all my love

Martina

TABLE OF CONTENTS

Chapter 1
INTRODUCTION

Solar radiation is an important natural feature because it is a critical factor in determining the Earth's climate and has a significant influence on the environment. The ultraviolet part of the solar spectrum (UV) plays an important role in many processes in the biosphere. UV radiation has several beneficial effects but it may also be very harmful if the UV level exceeds "safe" limits. If the level of UV radiation is sufficiently high, the self-protection ability of some biological species is exhausted and the subject may be severely damaged. This is of concern to the human organism, in particular with regard to the effect on the skin and the eyes. To avoid damage from high UV exposure, both acute and chronic, people should limit their exposure to solar radiation by using protective measures [1, 2].

The diurnal and annual variability of solar UV radiation reaching the ground is governed by astronomical and geographical parameters as well as by the atmospheric conditions. Since human activities affect the atmosphere, such as polluting the air and influencing the ozone layer, they also affect the UV radiation reaching the ground. Consequently, the level of solar UV radiation is a highly variable environmental parameter that differs widely in time and location.

The need to reach the public with simple-to-understand information about UV and its possible detrimental effects has led scientists to define a parameter that can be used as an indicator of the UV exposure (in this thesis the parameter is colour change) [1, 2, 3].

The commercial, scientific and industrial applications of ultraviolet radiation and the consequent need for UV measurements have increased enormously over the last 20 years. Ultraviolet radiation has found application in semiconductor photolithography, material curing, non-destructive testing, acceleration of chemical processes, water purification, sterilisation, phototherapy and solarium appliances. Concerns over the environmental and health effects of solar UV radiation penetrating into the biosphere through the depleted ozone layer have also greatly emphasised the urgency for accurate and reliable UV radiometry.

The measurement problems in terms of the UV wavelengths are much more severe than in the visible wavelength range, since both sources and detectors tend to be unstable in the UV region of the electromagnetic spectrum [4-8].

There is considerable interest in photochromic materials arising from the many potential applications, which are associated with their ability to undergo reversible, light-induced colour change. Two chemical species showing a reversible transformation differ from one another not only in their absorption spectra but also in their physical and chemical properties. Photochromic materials are used most widely in ophthalmic sun-screening applications, and also find applications in security printing, optical recording and switching, solar energy storage, nonlinear optics and biological systems [9-19]. The existing ranges of commercial products generally undergo positive photochromism, a light-induced transition from colourless to coloured due to a ring-opening reaction.

Major attention has been given to research, development and perfection of protective clothes, especially their barrier features. For these protective barriers, it is important to understand how clothes or textiles protect the wearer against the above-mentioned dangerous conditions associated with UV irradiation and if the protection is only partial or the protection is time limited by ambient conditions. Most protective fabrics are not developed for long periods of wear. In the development of these barrier structures, it is important also to keep in mind the comfort of individuals. This concept of protective fabrics can be considered as involving intelligent structures. A disadvantage of such intelligent structures is a fixed response to the external stimulus and the situation would be improved by a means for monitoring of external dangerous conditions. Such structures are referred to as passive intelligent textiles structures. Textile structures that produce adequate responses and are able to modulate the degree of protection in accordance to the external stimulus (e.g., change of intensity of UV irradiation, temperature, etc.) are known as active textile structures.

Textile structures, which react and respond, and which are able modulate the degree of protection in accordance with the magnitude of the external stimulus are called SMART textiles. An example of passive intelligent textiles is optical fibres, which lead not only to a signal, but they are also sensitive to the deformation, concentration of substances, pressure, electric power etc. A specific example of an active intelligent textiles would a textile, which reacts by changing colour because of its dependence on external stimulus (light, temperature). Moreover, textile based

sensors and active protective textiles have the advantages that the textile structure is easy customizable by sewing, thermal bonding or glueing. In addition, there are advantages of easy maintenance (washing, chemical cleaning) and low specific weight with good strength and elasticity. Other good features include workability with no need for a change of technology of production and their extremely large specific surface. Other major advantages are the possible integration of soft type sensors (textile-based sensors) into protective clothing system and their reasonable price. The research described in this thesis is focused on textile-based sensors with photochromic behaviour, involving a study of dynamic, colour and spectral behaviour and sensitivity to modulation of the photochromic sensors.

The thesis is focused on research into the colour change kinetics of photochromic pigments, which are applied onto a textile substrate by printing or mass dyeing. In addition, the investigation of the pigments in organic solvent solution is described as a comparative study. Fundamental attention is given to the relationship between the colour change intensity and the intensity of illumination and also its spectral distribution. The fatigue resistance, which is related to the light fastness of the photochromic textile sensors, is also studied.

The main aim of the research described in this thesis is to investigate the potential for utilisation of photochromic pigments from the point of view of their capability of application in textile soft sensors. For the achievement of this main aim, the following objectives were pursued:

- A study of the exposure and reversal of the colour change of selected photochromic pigments
- Definition of a colour change model
- Investigation of the kinetic behaviour of photochromic textiles
- A study of photochromic response modulation with UV absorbers
- A study of the spectral sensitivity of photochromic textiles
- Evaluation of fastness properties

As a consequence of this work a new definition of optical yield of a photochromic reaction is presented, which is described by the hysteresis of a colour change curve. This optical yield obtained from the photochromic reaction curve is described by a kinetic model, which defines the rate of colour change initiated by an external stimulus – namely UV light. The kinetic model verification is demonstrated

on textile sensors with photochromic pigments applied by both textile printing and fibre mass dyeing. [20]

It is envisaged that the fulfilment of these objectives will lead to the development of simple textile sensors sensitive to UV irradiation. The colour change would be visually perceivable and approximately linear to the irradiation intensity.

Based on the extensive experimental work a unique device concept for photochromic measurement in reflectance mode is described, which has been patented in the Czech Republic in the author's name.

Chapter 2
LITERATURE REVIEW

The main aim of thesis is oriented to the application of photochromic pigments onto textile substrates. This chapter contains a review of literature, which provides a theoretical basis for the research described in later chapters of this thesis. Section 2.1 describes basic types of photochromic compounds, their main structural features and the chemical reactions leading to the photochromic effect – the change from the colourless to coloured forms. Photochromic change is described by a modified Jablonski diagram, which presents a general mechanism for photochromism in terms of electronic, radiative and nonradiative transitions. Section 2.1 thus provides an understanding of the principles of the typical chemical processes, which have an influence on the photochromic colour change.

A discussion about fundamental optical concepts and principles is given next in section 2.2 illustrating how light interacts with matter in many different ways. Most systems involve heat generation, where the light is converted into thermal energy, inducing a magnetic or structural phase transition and changes in the physical properties of the medium. The wide-ranging optical properties observed in solid-state materials can be classified into a small number of general phenomena, one of which is represented by Maxwell's equations as described in section 2.2.1, allowing a deep understanding of fundamental electromagnetic interaction between light, as part of the electromagnetic spectrum, and solid matter.

Maxwell's phenomena, together with studies of geometric optics discussed in section 2.2.3 and of radiometry in section 2.2.4 have provided an important basis, which have allowed the author to be successful in the construction of the unique device for the measurement of photochromic kinetic behaviour of selected pigments based on the pyran and naphthooxazine structures as described throughout this thesis.

Finally, colour phenomena are discussed in section 2.4 to complete the background principles for the description of colour change during a photochromic reaction, using CIELAB colour space, the Kubelka-Munk function and colour change intensity.

2.1 Photochromism of organic compounds

There are many conformational changes that can take place in the excitation process, which lead to changes in electronic absorption spectra, resulting in a visible colour change. If the changes are thermally reversible, after removal of the irradiation which activates the changes, the system returns to the state before irradiation and the induced absorption or colour spontaneously disappears. This was previously referred to as phototropism [21], and now more correctly as photochromism [22 - 32]. If the colour changes are caused by heat, then this is thermochromism. It is possible to distinguish between photochromism, a reversible coloration process, and irreversible photo-induced chemical reaction.

Simply, the photochromic processes may be described as follows [33]:

$$\text{colourless} \qquad A \underset{h\nu_2 \text{ or } \Delta T}{\overset{h\nu_1}{\rightleftharpoons}} B \qquad \text{coloured}$$
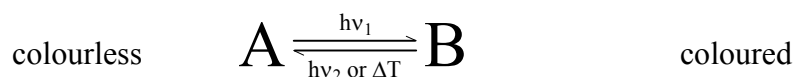
The formation of a new absorption band resulting from the transition $S_0^B \rightarrow S_1^B$ from various vibrational levels in the excitation of a colourless molecule S_1^A is schematically described in Fig. 2.1.1.

After the molecule is in the excited state S_1^B the coloured molecule is deactivated to the ground state S_0^B. Then there follows an exergonic process in which the regeneration of the colourless form occurs via a radiationless transition with the creation of the original form in its ground state S_0^A. The system B is not thermodynamically stable and therefore spontaneously returns to the state A. Frequently the backward reaction B→A, the so-called thermal conversion from S_0^B to S_0^A, proceeds via the transition state X, whose energy is higher than the singlet state of coloured form S_0^B. The process is thermally activated. The reaction B→A may also be induced with long wavelength light (infrared irradiation) or by light near to the new absorption band.

With regard to the energy difference E (S_0^B) − E (S_0^A) the photochromic change can be used to provide energy accumulation.
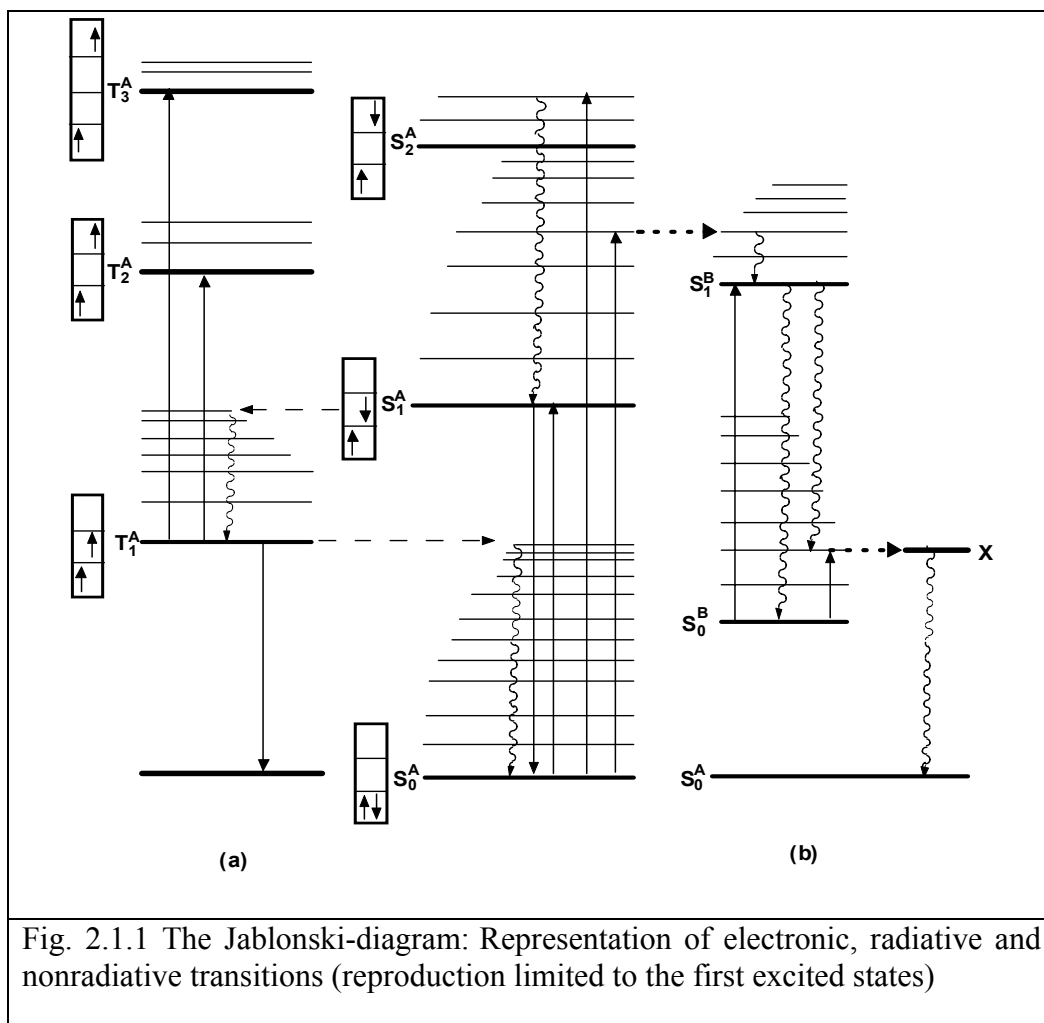
Fig. 2.1.1 The Jablonski-diagram: Representation of electronic, radiative and nonradiative transitions (reproduction limited to the first excited states)

As with the yield of the light energy conversion to the thermal energy, so the accumulative capacity (difference of heats of coloured B and colourless A forms) depends on the chemical structure of the meta-stable photoproduct, which has non-conventional bond lengths and angles and on the dissipation of resonance energy, which involves increased stability caused by delocalization of π electrons.

The limitation of the effect results from the second theory of thermodynamics. Because it may be described as a thermal machine which is working between temperatures T and T' (photochemical reaction $A(S_0^A) \rightarrow A(S_1^A) \rightarrow B(S_0^B)$ at temperature T and exothermal reaction $B(S_0^B) \rightarrow X \rightarrow A(S_0^A)$ at temperature T'), the final yield of accumulative capacity increases at temperature T', as does the energy of the ground state of the "coloured" molecule S_0^B.

The highest specific accumulative capacity of a well-known systems is around 2 kJ/kg (norbornadiene $\rightarrow$ quadricyclane, as shown in Fig. 2.1.2.).

Fig. 2.1.2 Reaction: Norbornadiene → Quadricyclane
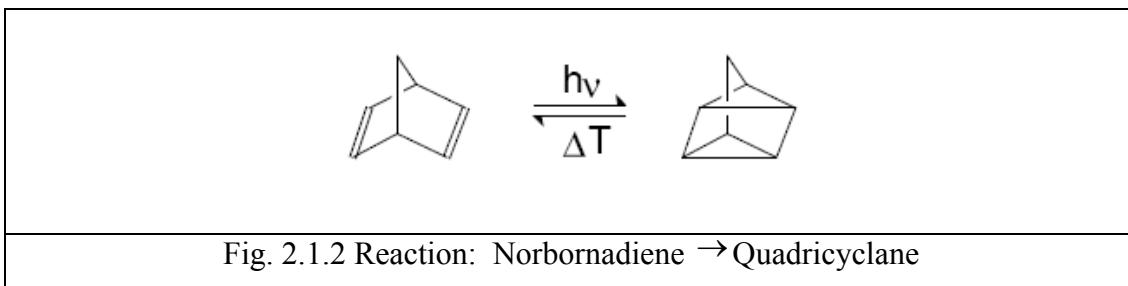
The photochromic process may be classified into several main groups as follows, according to the mechanism of conformation changes [10,34]:

a) Triplet –triplet photochromism

In this system, its own absorption band in the long wavelength region of the spectrum characterizes the coloured form B. Photochromic materials include species whose triplet state has a sufficiently long lifetime (approximately 1s) and show strong triplet-triplet excitation. Typical examples are pentacene (Fig. 2.1.3a) or dibenzanthracene (Fig. 2.1.3b)

| Fig. 2.1.3a Pentacene | Fig. 2.1.3b Dibenzanthracene |
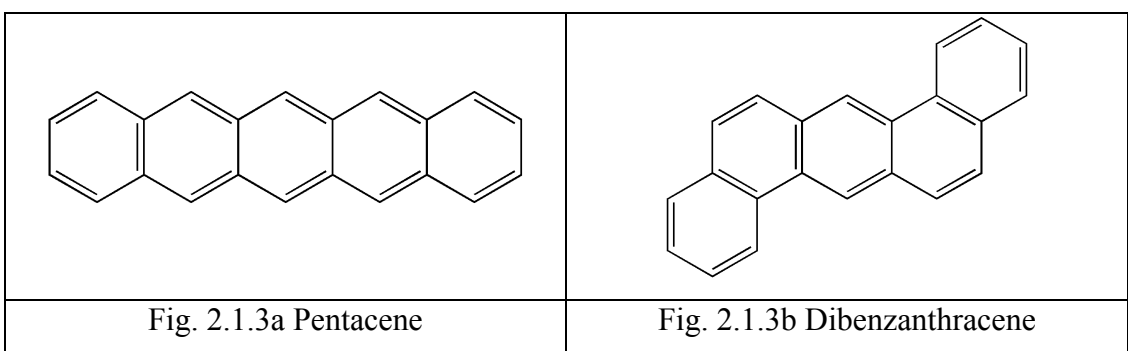
These materials provide very quick response photochromic media with a bleaching time shorter than 1 second. The bleaching time refers to term for reversion of photochromic colour change, in the case of positive photochromism, proceeding from coloured to colourless forms. The triplet state of aromatic hydrocarbons (anthracene, dibenzanthracene, etc.) is quenched by nitrobenzenes through outer sphere electron transfer reactions. This triplet state has been referred to as a contrary type [35]. This is defined in photochromic effect of the triplet type, where three independent steps are required. A chromophore quickly absorbs activating radiation to raise ground state molecules to an excited singlet state, as a second step the excited singlet state proceeds by a process known as intersystem crossing, to convert to a

triplet state; thirdly triplet state molecules absorb incident radiation to convert from the first triplet state level to a higher level.

The quantum yield of triplet-triplet photochromism depends on the concentration of oxygen in the system, because oxygen causes creation of triplet excitons. Then quantum yield depends on the relative contributions from processes, which have an influence on the population of the triplet state such as for example phosphorescence, radiationless transitions or intersystem conversion etc.

b) Heterolytic cleavage

In this type of system, a covalent bond is broken in the excited molecule and new conformations are created with zwitterionic (dipolar) structures [36,37]. The ionic species either continue to react or they are stable and they can exist separately [37, 38]. Typical structures within this photochromic group are pyrans (Fig. 2.1.4):

Fig. 2.1.4 Photochromic reaction of pyrans
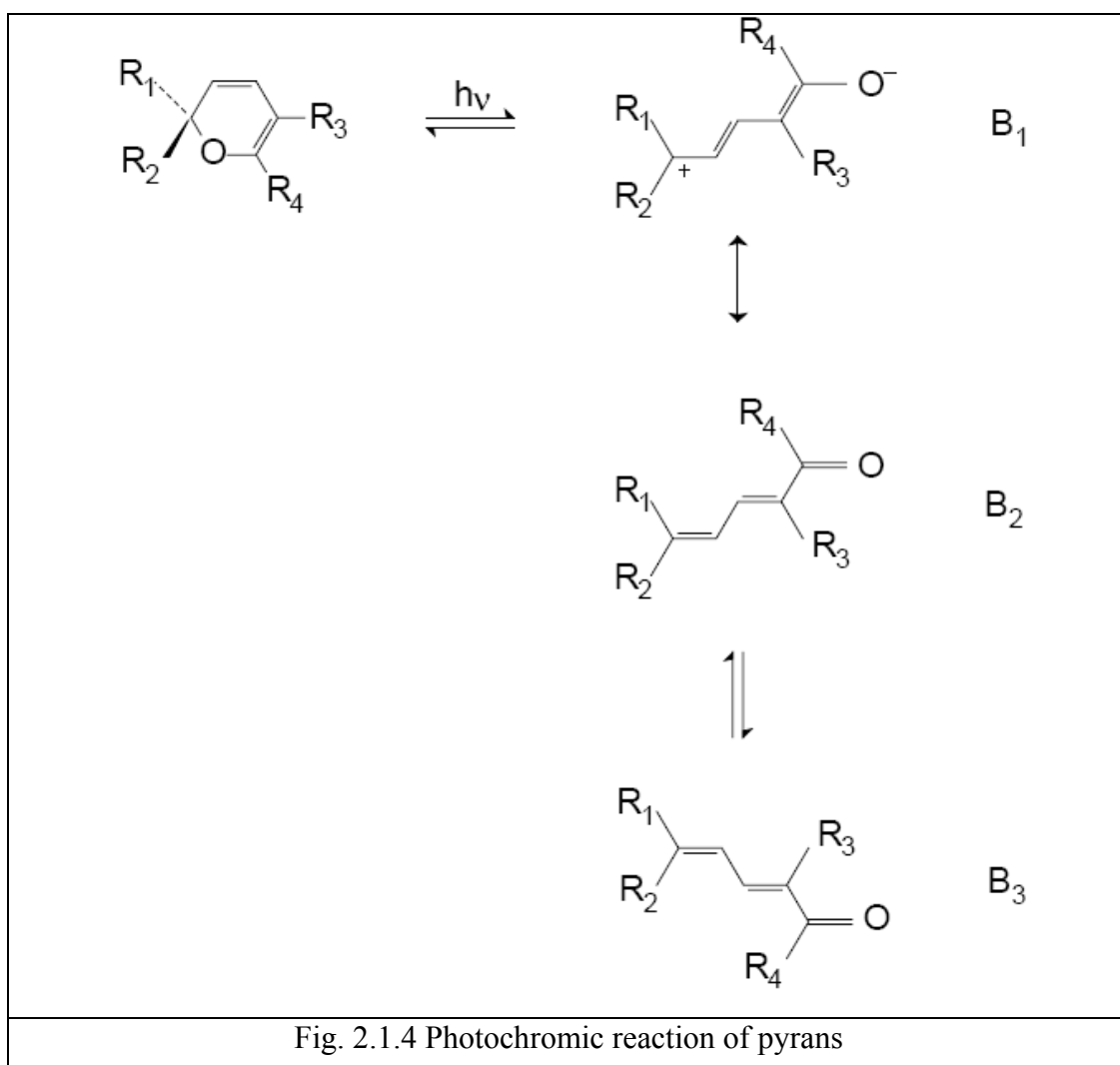
Under the influence of UV irradiation, the bond is broken between carbon and oxygen and the pyran ring is opened. Ionic structure (B_1) is formed, which is similar to merocyanine colorants and which provides intense coloration. There is also a resonance contribution from neutral form (B_2). In the photochromic process involving pyrans, cis-trans conversion (isomer B_3) and triplet–triplet absorption also play an important role. The balance between the contributing forms $(B_1, B_2$ and $B_3)$ determines the resulting colour after irradiation.

The rate of thermal bleaching depends on substituents R_3 and R_4. Electron donor substituents accelerate the reverse ring closure to the pyran ring. Similarly, steric influence, for example with a bulky substituent R_2 decreases the probability of the formation of coloured planar conformers. The reason is the fact that the sp^3 carbon creates a point of contact for the two planes of the molecules (see Fig.2.1.5), which have to rotate about 90° to create the new coloured isomers.

Fig. 2.1.5 Creation of contact point for planes with rotation about 90°
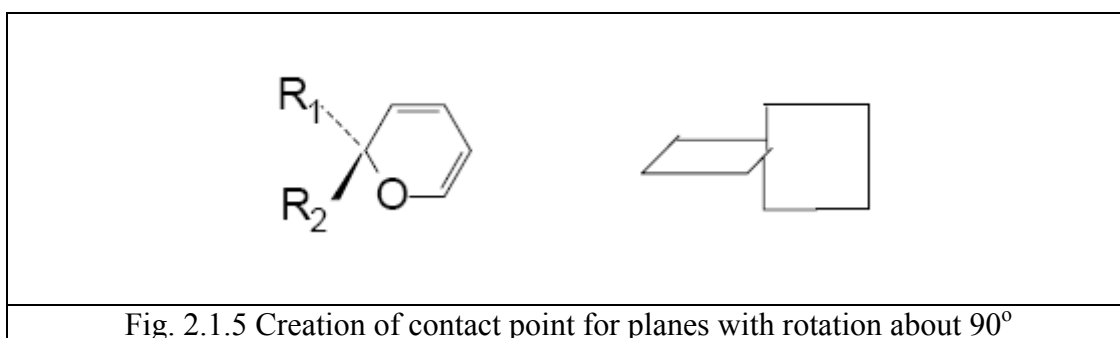
c) Homolytic cleavage

In this system, with the absorption of radiation, a bond is broken and dissociation of the molecule takes place to give two or more parts, which contain azygous electrons. In comparison with the mechanism of heterolytic cleavage, where the products have some ionic character, during homolytic cleavage, paramagnetic radical products are formed. The character of the cleavage strongly depends on the bonding configuration to accommodate the dissociation of electrons. An example is the dissociation of hexaphenylbisimidazole (Fig. 2.1.6) to the two 2,4,5 - triphenylimidazole radicals [9,34].

Fig. 2.1.6 Photochromism of Hexaphenylbisimidazole
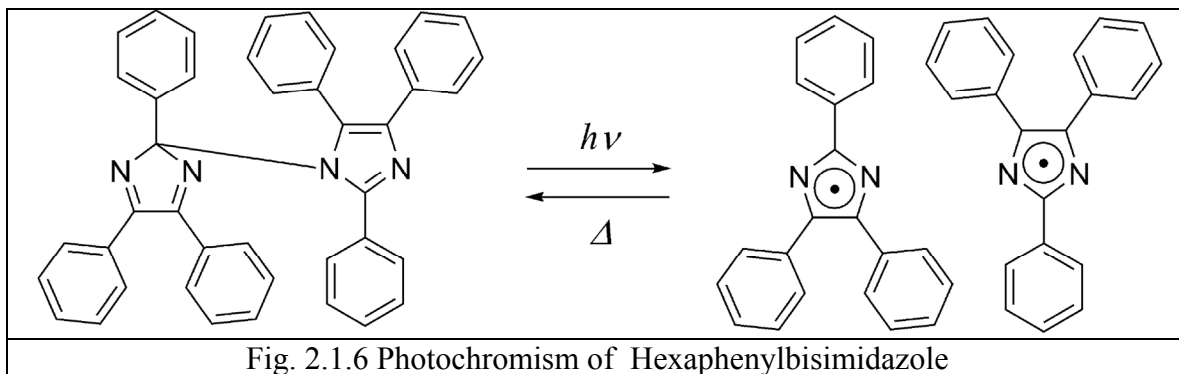
Another example is the cleavage of a C-Cl bond in 2,3,4,4- tetrachloro-1-oxo-1, 4-dihydronaphthalene (Fig. 2.1.7) with the formation of an additional chlorine radical fragment and an optical absorption around 530 nm [9].

Fig. 2.1.7 Photochromism of l–oxo–2,3,4,4–tetrachloro–l, 4–dihydronaphthalene
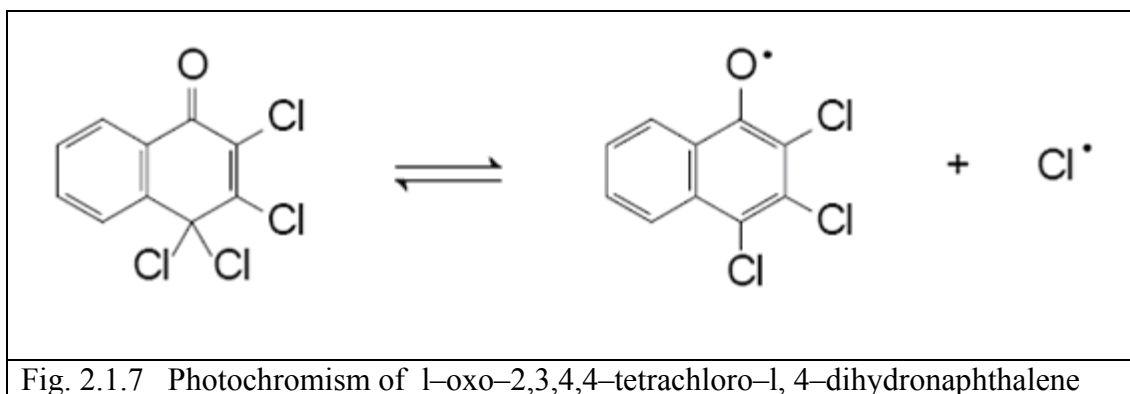
d) Trans-cis isomeration

Thermal trans-cis isomeration is common in many chemical reactions. Thermal energy can cause a change from the *trans* state to the *cis* state, in most cases around a central unsaturated bond. This type of isomeration is also involved as part of the process of vision, in which the photon absorbed by the molecule of rhodopsin changes the membrane permeability of cones so that sodium ions can pass through. The chromophoric part of the molecule of rhodopsin is created by the (nonatetraenyliden)alkylamine radical in the 11-cis, 12-cis configuration [40-49]. After absorption of a photon, part of the molecule rotates around the 11-12 bond and the trans- isomer is formed (pre–lumirhodopsin as shown in Fig. 2.1.8).

Fig. 2.1.8 Photochromic reaction of rhodopsin
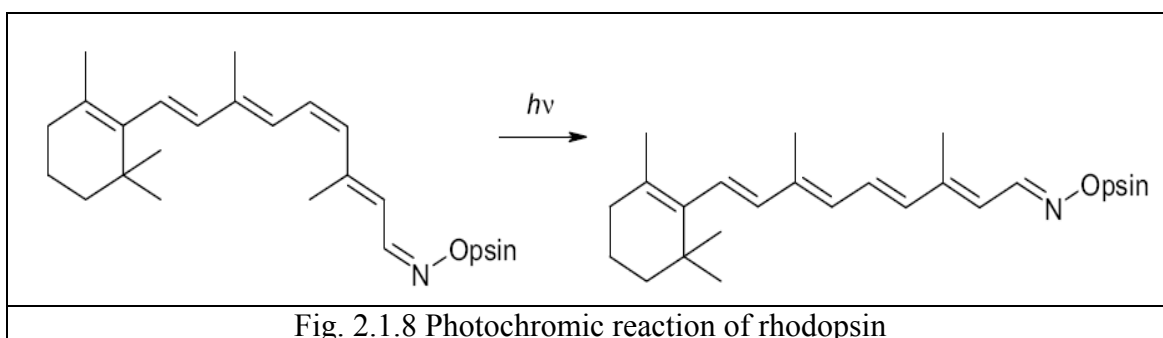
Other examples are the photochromism of stilbene (Fig. 2.1.9) and the photochromism of polymeric poly(4–methacrylaminoazobenzene) (Fig. 2.1.10) [50,51,52,53].

Fig. 2.1.9 Photochromic reaction of Stilbene

Fig. 2.1.10 Photochromic reaction of poly(4–methacrylaminoazobenzene)
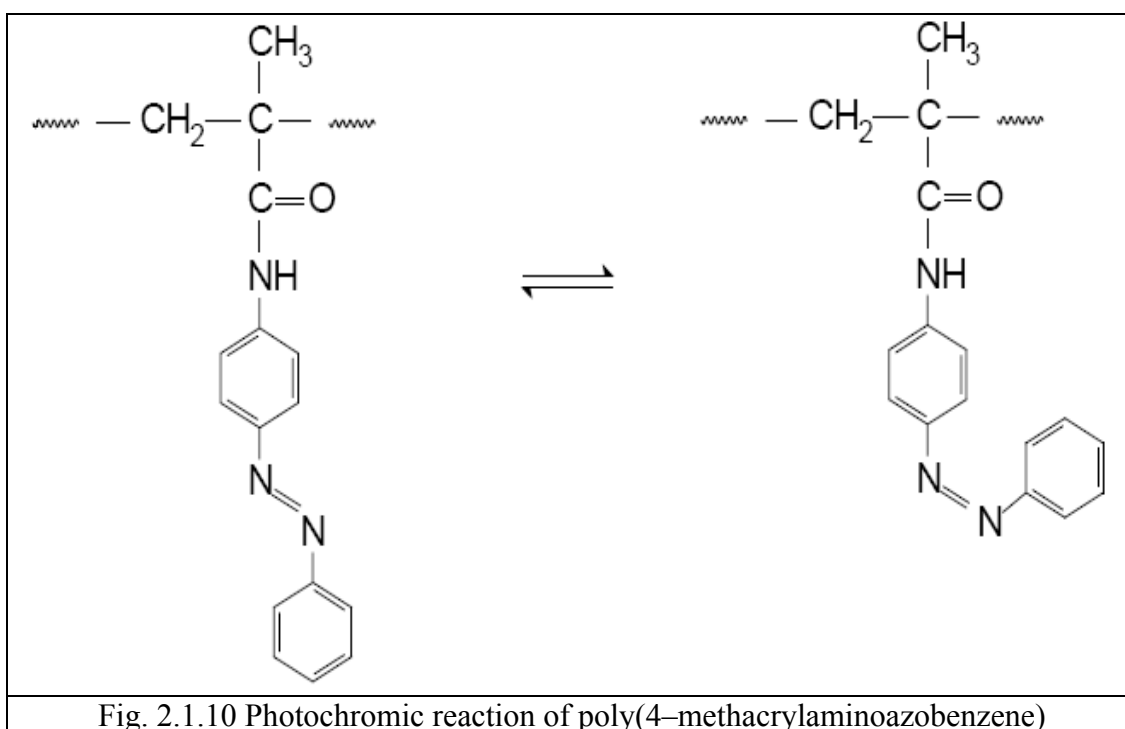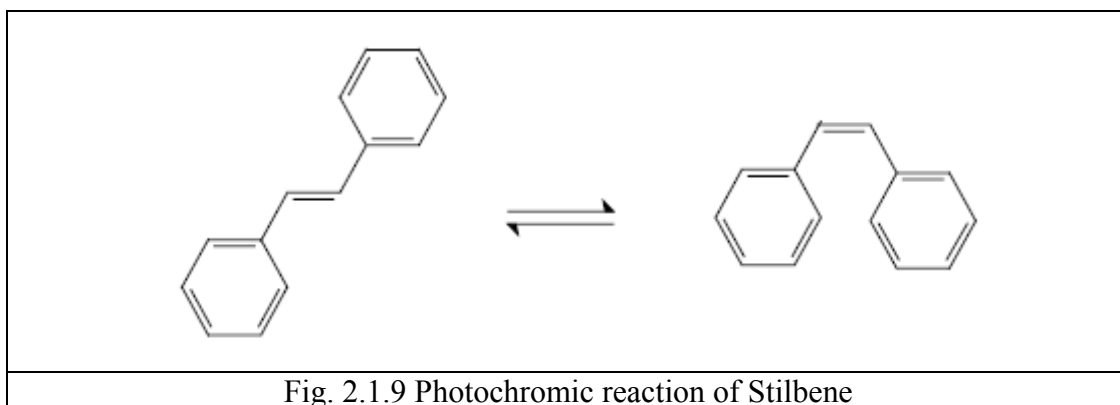
e) Photochromism based on tautomerism

Tautomerism refers in general to the reversible interconversion of isomers, which differ in the position of a hydrogen atom. In the case of photochromic tautomerism this interconversion occurs after irradiation with light. A major type of photochromic tautomerism is hydrogen transfer. A typical example of photo-tautomerism involves metal-free phthalocyanine. In the excited form at low temperature, two hydrogen atoms are shifted between four central carbon atoms [54] (see Fig.2.1.11). Another example is hydrogen tautomerism observable in (E)-2-((phenylimino)methyl)phenol (Fig.2.1.12). The enol-form (**2.1**) is pale yellow and after irradiation the keto-form (**2.2**) appears, which is reddish or brown [9].

Fig. 2.1.11 The tautomerism of phthalocyanine

Fig. 2.1.12 Photochromic reaction of (E)-2-((phenylimino)methyl)phenol
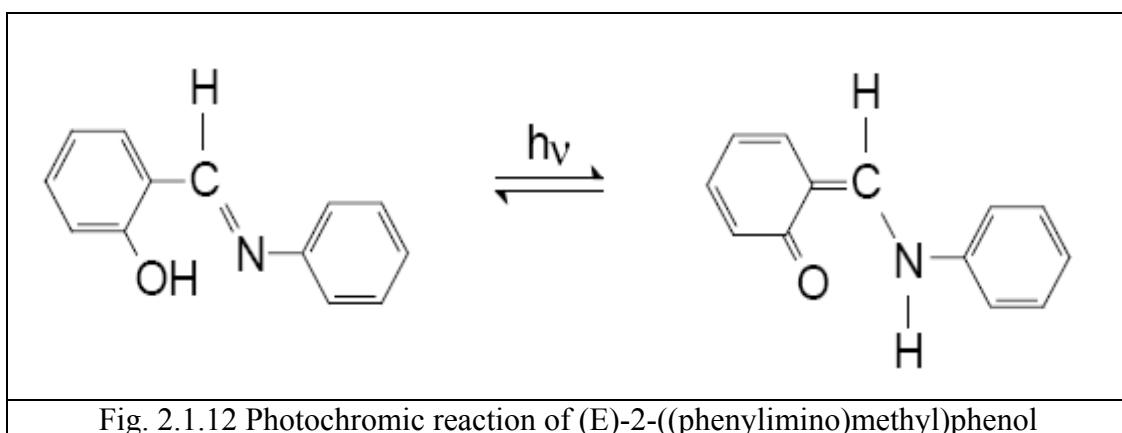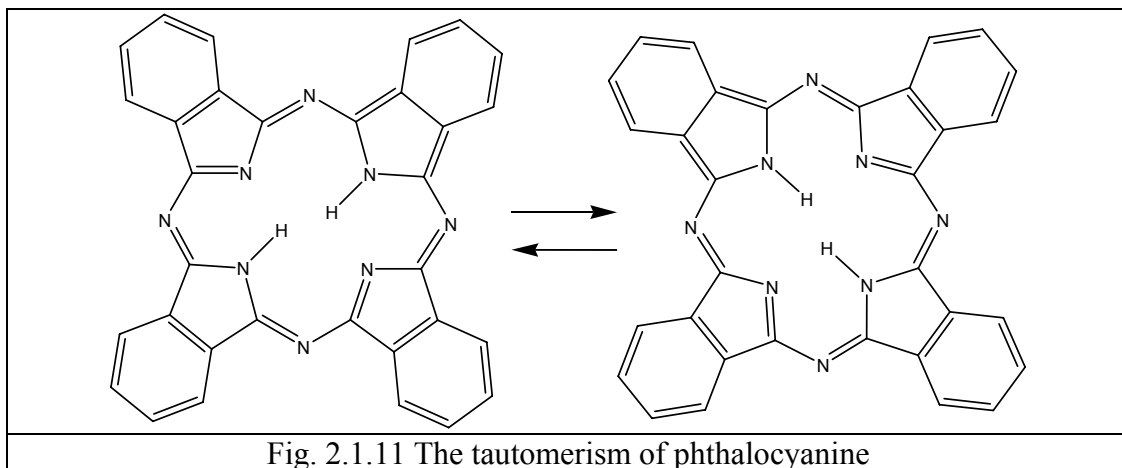
f) Photodimerisation

There are many organic compounds which during excitation by UV irradiation create excimers, in which one molecule is in the ground state and the second is in the excited state. This specific arrangement was measured by spectroscopic methods [56] and a maximum conversion rate of 75% has been determined. The creation of a complex of one photo excited molecule and one ground state molecule results during photoreaction. Different tautomeric sites lead to an additional disorder parameter adding further complexity in the photodimerisation reaction. Bond energies are so high as to create also in the solid-state a stable dimmer. An example is the pair of σ covalent bonds between two neighbouring parallel molecules in anthracene [55, 56] (see Fig.2.1.12). Anthracene absorbs light in the 240 – 290 nm and 310 – 390 nm regions and a fluorescence emission can be observed between 390 nm and 450 nm. Upon irradiation in the near ultraviolet (around 360 nm) a dimerization reaction can also occur. Note that rather intense illumination conditions and high anthracene concentrations are required for this second-order reaction to proceed at a measurable rate.

Upon irradiation, side photo-products such as photo-oxides can eventually be formed and interfere with the dimerization reaction.

Fig.2.1.12 Photodimerisation of anthracene
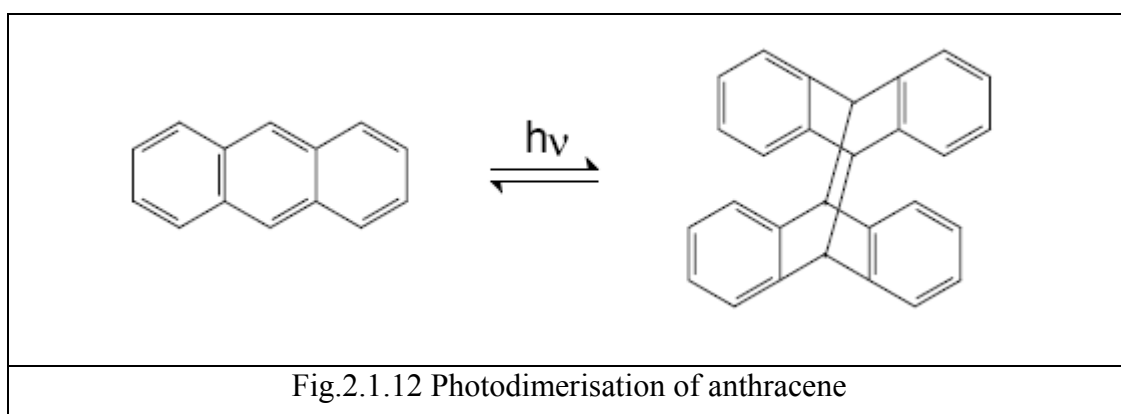
2.2 Basic Optical Concepts and Principles

Today it is well known that electromagnetic phenomena are the basis for macroscopic physics and for most microscopic processes. In particular, electromagnetic phenomena are the essence of optics and not only in the visual part of spectrum. An overview of the fundament concepts and principles of optics is presented here in view of its relevance to the photochromic phenomena and the construction of a special device, described later in this thesis, for its measurement.

2.2.1 Maxwell's Equations

Fundamental electromagnetic interactions between charged particles in a medium are described by Maxwell's equations [57, 58], which involve the electric field strength $\mathbf{E}(\mathbf{r}, t)$, the magnetic field, magnetic induction $\mathbf{B}(\mathbf{r}, t)$, the charge density $\rho(\mathbf{r}, t)$ and the electric current density $\mathbf{j}(\mathbf{r}, t)$. All vector fields are functions of position and time. Throughout this chapter, bold symbols will be used to denote vector quantities. Maxwell's equations in linear, dispersion less, time-invariant materials, with constant dielectric permittivity ε and magnetic permeability μ, are:

$$rot\mathbf{E} + \frac{\partial \mathbf{B}}{\partial t} = 0$$

$$div\mathbf{B} = 0$$

$$div\mathbf{E} = \frac{\rho}{\varepsilon} \qquad \text{(Eq. 2.2.1)}$$

$$rot\mathbf{B} - \varepsilon\mu \frac{\partial \mathbf{E}}{\partial t} = \mu\mathbf{j}$$

The fields in Maxwell's equations are generated by charges and currents. Conversely, the charges and currents are affected by the fields through the Lorentz force equation:

$$\mathbf{F} = Q(\mathbf{E} + v \times \mathbf{B}) \qquad \text{(Eq. 2.2.2)}$$

Electromagnetic wave existence is a direct effect of Maxwell's equations. It is possible to show that from Maxwell's equations in empty space, i.e., space where

ρ=0, **j**=0, wave equations for fields **E** and **B** may be deduced**.** For this solution, it is necessary to employ equations by the operator *rot*. If we use this operator for equation *rot* **E** than we will obtain the solution as given in equation 2.2.3:

$$rot\ rot\mathbf{E} = grad\ div\mathbf{E} - \Delta\mathbf{E} \qquad \text{(Eq. 2.2.3)}$$

If the rest of Maxwell's equations are considered, vector **B** can be excluded:

$$rot\ rot\mathbf{E} = -\Delta\mathbf{E} = -rot\frac{\partial\mathbf{B}}{\partial t} = -\frac{\partial}{\partial t}rot\mathbf{B} = -\varepsilon\mu\frac{\partial^2\mathbf{E}}{\partial t^2} \qquad \text{(Eq. 2.2.4)}$$

so that

$$\Delta\mathbf{E} = \varepsilon\mu\frac{\partial^2\mathbf{E}}{\partial t^2} \qquad \text{(Eq. 2.2.5)}$$

An analogous procedure allows exclusion of the electric field **E**:

$$\Delta\mathbf{B} = \varepsilon\mu\frac{\partial^2\mathbf{B}}{\partial t^2} \qquad \text{(Eq. 2.2.6)}$$

From this derivation it is also apparent that the electromagnetic waves in a homogenous environment ε, μ propagate with phase velocity:

$$v = \frac{1}{\sqrt{\varepsilon\mu}} \qquad \text{(Eq. 2.2.7)}$$

Electromagnetic waves are also able to propagate in a vacuum, where the speed of propagation is $v = c = 1/\sqrt{\varepsilon_0\mu_0}$, c is the speed of light in a vacuum and the equation for refraction index can be written as follows:

$$n = \frac{c}{v} = \sqrt{\varepsilon_r\mu_r} \approx \sqrt{\varepsilon_r} \qquad \text{(Eq. 2.2.8)}$$

For a clear understanding of the main properties of the electromagnetic waves the special space solution of Maxwell's equations can be defined, when a plane wave

propagates in the *z*-axis direction. Fields **E**, **B** will be constant in the *z*-axis perpendicular planes,

$$\mathbf{E} = \mathbf{E}(z,\,t), \quad \mathbf{B} = \mathbf{B}(z,\,t).$$

From Maxwell's equations, it is possible to see:

$$(rot\mathbf{E})_z = 0 = -\frac{\partial B_z}{\partial t}$$

$$div\mathbf{B} = \frac{\partial B_z}{\partial z} = 0$$

$$div\mathbf{E} = \frac{\partial E_z}{\partial z} = 0 \qquad\qquad \text{(Eq. 2.2.9)}$$

$$(rot\mathbf{B})_z = 0 = \frac{\partial E_z}{\partial t}$$

that longitudinal components E_z, B_z are independent of *z, t*. That means these components are constant in space and in time – thus they are not related to wave propagation. Therefore:

$$E_z(z,\,t) = 0, \qquad B_z(z,\,t) = 0.$$

The rest of Maxwell's equations for the transversal component are given as follows:

$$(rot\mathbf{E})_x = -\frac{\partial E_y}{\partial z} = -\frac{\partial B_x}{\partial t}, \quad (rot\mathbf{B})_x = -\frac{\partial B_y}{\partial z} = \varepsilon\mu\frac{\partial E_x}{\partial t},$$

$$\text{(Eq. 2.2.10)}$$

$$(rot\mathbf{E})_y = \frac{\partial E_x}{\partial z} = -\frac{\partial B_y}{\partial t}, \qquad (rot\mathbf{B})_y = -\frac{\partial B_x}{\partial z} = \varepsilon\mu\frac{\partial E_y}{\partial t}.$$

A simple solution is obtained providing that $E_y(z,\,t) = 0$. Because $\partial B_x / \partial z = \partial B_x / \partial t = 0$, therefore $B_x = 0$. For wave vectors **E** and **B** in direction z and time t : $\qquad \mathbf{E} = (E_x(z,\,t),0,0), \quad \mathbf{B} = (0,B_y(z,\,t),0)$

and after application of Maxwell's equations the following solution is obtained:

$$-\frac{\partial E_x}{\partial z} = \frac{\partial B_y}{\partial t}\,, \qquad -\frac{\partial B_y}{\partial z} = \varepsilon\mu\frac{\partial E_x}{\partial t}\,. \qquad \text{(Eq. 2.2.11)}$$

From equations 2.2.11 wave equations result:

$$-\frac{\partial^2 E_x}{\partial z^2} = \varepsilon\mu\frac{\partial^2 E_x}{\partial t^2}\,, \qquad -\frac{\partial^2 B_y}{\partial z^2} = \varepsilon\mu\frac{\partial^2 B_y}{\partial t^2}\,. \qquad \text{(Eq. 2.2.12)}$$

For waves E_x, B_y, which propagate in the positive direction of the z-axis, the d'Alembert solution for equations 2.2.12 can be written:

$$E_x(z,t) = F_E(z - vt)\,, \qquad B_y(z,t) = F_B(z - vt)\,. \quad \text{(Eq. 2.2.13)}$$

where F_E, F_B are forces of the electric and magnetic parts of electromagnetic radiation. The relationship between waves E_x, B_y is described by equations 2.2.11, from which follows:

$$F_E'(\xi) = vF_B'(\xi) \;\Rightarrow\; F_E(\xi) = F_B(\xi) + const.,$$

where $\xi = z - vt$ and the constant of integration is equal to zero. In a planar wave, which propagates in direction $+z$ it is valid to write:

$$E_x(z,t) = vB_y(z,t)\,, \quad v = \frac{1}{\sqrt{\varepsilon\mu}}\,.$$

For a harmonic (monochromatic) wave, the expression:

$$E_x(z,t) = E_0\cos(\omega t - kz + \varphi)\,, \; B_y(z,t) = B_0\cos(\omega t - kz + \varphi')\,,$$

is valid

$$E_0 = vB_0 \rangle 0\,, \qquad \varphi = \varphi'\,, \qquad \omega = vk\,,$$

as shown in Figure 2.2.1:
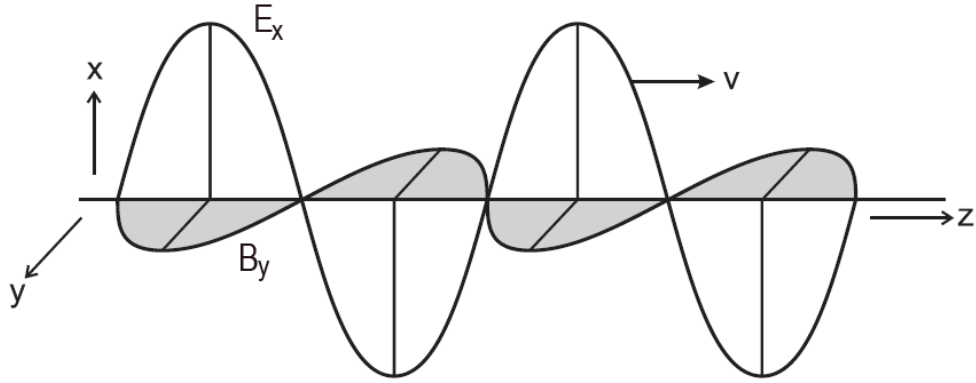
Figure 2.2.1 Planar harmonic electromagnetic wave

Based on that, related properties of electromagnetic waves can be concluded. Because waves are independent of the system of coordinates used, for a planar wave, which propagates in an arbitrary direction **s** ($|\mathbf{s}|=1$), then:

$$\mathbf{E}(\mathbf{r},t) = \mathbf{F_E}(\mathbf{s}.\mathbf{r} - vt), \qquad \mathbf{B}(\mathbf{r},t) = \mathbf{F_B}(\mathbf{s}.\mathbf{r} - vt) \quad \text{(Eq. 2.2.14)}$$

E, **B**, **s** create in this order a clockwise system of each other`s orthogonal vectors (wave is transversal);

$$E = vB, \text{ where } v = 1/\sqrt{\varepsilon\mu}. \qquad \text{(Eq. 2.2.15)}$$

Field **B(r,t)** is fully defined by field **E(r,t)**. A monochromatic planar wave is described by equations:

$$\mathbf{E}(\mathbf{r},t) = \mathbf{E}_0 \cos(\omega t - \mathbf{k}.\mathbf{r} + \varphi) \qquad \text{(Eq. 2.2.16)}$$

$$\mathbf{B}(\mathbf{r},t) = \mathbf{B}_0 \cos(\omega t - \mathbf{k}.\mathbf{r} + \varphi) \qquad \text{(Eq. 2.2.17)}$$

where $\mathbf{k} = k\mathbf{s}$ is the wave vector, $\omega = v\,|\mathbf{k}|$, $|\mathbf{s}|=1$. Vector amplitudes fulfil the properties of equations 2.2.14 and 2.2.15.

2.2.2 Energetic quantity inside a planar electromagnetic wave

An electromagnetic field as a physical object involves energy, momentum and moment of momentum. If the continual character of the field is defined, the energetic

capacity of this field is described by energy density $w(\mathbf{r},t)$, and it's volume integral $\int_V w dV$ indicates immediate energy included with arbitrary volume V.

Based on Maxwell's ideas [59], the density of an electromagnetic field in nonconductive media ε, μ is given by the quadratic equation:

$$w = \frac{1}{2}(\mathbf{E}.\mathbf{D} + \mathbf{H}.\mathbf{B}) = \frac{1}{2}(\varepsilon E^2 + \mu H^2) \qquad \text{(Eq. 2.2.18)}$$

Where $\mathbf{D}$ is electrostatic induction and $\mathbf{H}$ is the intensity of the magnetic field.

The energetic flow density $\mathbf{S}(\mathbf{r},t)$ describes the transfer of energy in space. This transfer of the energy is defined as energy quantity transferred through an area, which is perpendicular to the direction of propagation per unit time (W/m^2). In a time changeable electromagnetic field in media ε, μ, the energetic flow density is described by the Poynting vector:

$$\mathbf{S} = \mathbf{E} \times \mathbf{H}. \qquad \text{(Eq. 2.2.19)}$$

If the momentum density of the electromagnetic field in a vacuum is applied the following equation results:

$$\mathbf{g} = \mathbf{D} \times \mathbf{B} = \varepsilon_0 \mu_0 \mathbf{E} \times \mathbf{H} = \frac{\mathbf{S}}{c^2}. \qquad \text{(Eq. 2.2.20)}$$

Taking in to consideration that all equations for energetic quantities are quadratic in fields and this equation is transferred to the case of a planar electromagnetic wave equation 2.2.15 it is possible to reformulate:

$$E = vB \qquad \Leftrightarrow \qquad \sqrt{\varepsilon}E = \sqrt{\mu}H. \qquad \text{(Eq. 2.2.21)}$$

Therefore the electric and magnetic part of the energy density w are equal in a planar wave and:

$$w = \varepsilon E^2. \qquad \text{(Eq. 2.2.22)}$$

With use of equations 2.2.14 and 2.2.15:

$$\mathbf{H} = \sqrt{\frac{\varepsilon}{\mu}} \mathbf{s} \times \mathbf{E}, \qquad \text{(Eq. 2.2.23)}$$

The Poynting vector in a planar electromagnetic wave is proportional to the energy density as is visible in Figure 2.2.2:
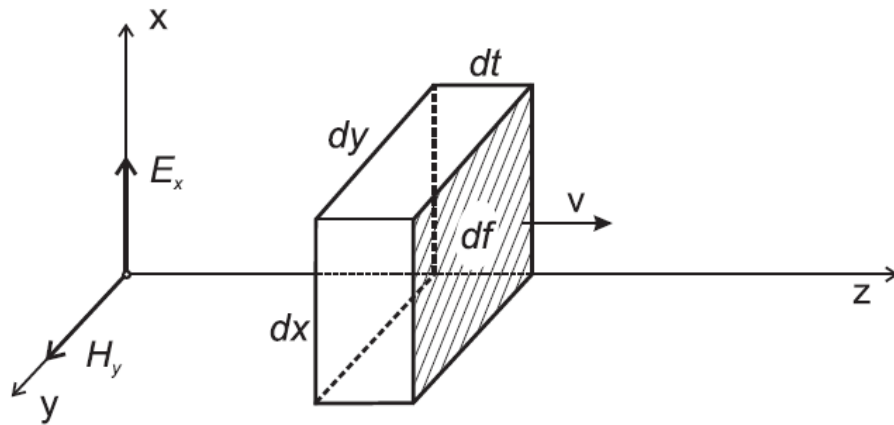
Figure 2.2.2 Description of relationship between Poynting vector **S** and energy density *w*. If speed of wave energy transfer is *v*, then through area *df = dxdy* during time *dt* will be transfered energy: *wdV = wvdtdxdy*. Density of energy flow S_Z is equal to energy, which is transferred through unitary area, that means:

(wdV)/(dSdt) = wv

$$\mathbf{S} = \sqrt{\frac{\varepsilon}{\mu}} \mathbf{E} \times (\mathbf{s} \times \mathbf{E}) = \sqrt{\frac{\varepsilon}{\mu}} \mathbf{E}^2 \mathbf{s} \qquad \text{(Eq. 2.2.24)}$$

$$\mathbf{S} = wv\mathbf{s} \qquad \text{(Eq. 2.2.25)}$$

Finally, momentum density in a vacuum is given by:

$$\mathbf{g} = \frac{\mathbf{S}}{c^2} = \frac{w}{c} \mathbf{s} \ . \qquad \text{(Eq. 2.2.26)}$$

2.2.3 Geometric Optics

Geometrical optics describes light propagation in terms of rays. We can define reflection in the case when a light ray strikes upon an object boundary or an interface between two media. In the special case of a very smooth boundary or interface the reflected light will propagate as shown in Fig. 2.2.3-a, i.e. concentrating along the direction that is planar symmetric with the incident direction about the normal surface. The reflected angle θ_r is equal to the incident angle θ_i

$$\theta_r = \theta_i \qquad \text{(Eq. 2.2.27)}$$

In the case of a transparent object, the refraction phenomena when light can enter the new media is shown in Figure 2.2.3-b. The refractive angle θ_t is given by Snell's law:

$$n_t \sin\theta_t = n_i \sin\theta_i \qquad \text{(Eq. 2.2.28)}$$

where n_t and n_i are the refractive indices of the media on the incident and transmitted sides, respectively. When light travels from a medium with a higher refractive index to one with a lower refractive index, Snell's law seems to require in some cases that the sine of the angle of refraction be greater than one. This effect is called total internal reflection.

$$\frac{n_i \sin\theta_i}{n_t} \geq 1 \qquad \text{(Eq. 2.2.29)}$$

The corresponding incident angle is referred to as the critical angle.

(a)   **(b)**
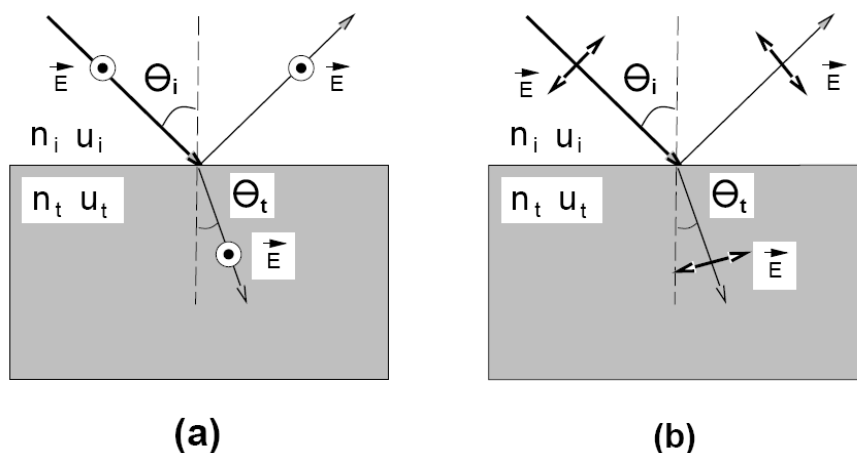
Figure 2.2.3 Reflection and refraction at the interface of two media.
a) An incident light wave with polarization perpendicular to the plane of reflection.
b) An incident light wave with polarization parallel to the plane of reflection.

The total energy in the reflected and refracted rays is equal to the energy of the incident light, but the proportion of the intensities in these two rays will depend upon the refractive index difference, the angle of incidence, the light polarization and direction in which the light is passing the border. For determination of the intensity distribution between the reflected and refracted rays the Fresnel formulae can be used [57]. The intensity reflection coefficients $R\|$ and $R\perp$ and transmission coefficients $T\|$ and $T\perp$ (for the parallel and perpendicular polarization consequently) are described by the following equations:

$$\mathbf{R_{II}} = \left(\frac{n_t \cos\theta_i - n_i \cos\theta_t}{n_t \cos\theta_i + n_i \cos\theta_t} \right)^2 = \frac{\tan^2(\theta_i - \theta_t)}{\tan^2(\theta_i + \theta_t)}$$

(Eq. 2.2.30)

$$\mathbf{R_\perp} = \left(\frac{n_i \cos\theta_i - n_t \cos\theta_t}{n_i \cos\theta_i + n_t \cos\theta_t} \right)^2 = \frac{\sin^2(\theta_i - \theta_t)}{\sin^2(\theta_i + \theta_t)}$$

$$\mathbf{T_{II}} = \frac{n_t \cos\theta_t}{n_i \cos\theta_i} \left(\frac{2n_i \cos\theta_i}{n_t \cos\theta_i + n_i \cos\theta_t} \right)^2$$

(Eq. 2.2.31)

$$\mathbf{T_\perp} = \frac{n_t \cos\theta_t}{n_i \cos\theta_i} \left(\frac{2n_i \cos\theta_i}{n_i \cos\theta_i + n_t \cos\theta_t} \right)^2$$

where the ratio of the refractive indices is due to the involvement of two different media. It can be verified that

$$\mathbf{R_{II}} + \mathbf{T_{II}} = 1$$

(Eq. 2.2.32)

$$\mathbf{R_\perp} + \mathbf{T_\perp} = 1$$

and generally $R\|$, $R\perp$, $T\|$ and $T\perp$ are called Fresnel coefficients.

2.2.4 Radiometry

Radiometry is the science of measuring light in any portion of the electromagnetic spectrum. In practice, the term is usually limited to the measurement of infrared, visible, and ultraviolet light using optical instruments [61-68]. The measured results are usually in units of energy (joules-J) or power (watts- W). An important sub-topic of radiometry is spectrophotometry, which specifically deals with the effects of reflection and transmission at object boundaries as well as absorption and scattering inside materials.

Photometry is a special case of radiometry, because photometry is the science of the measurement of light, in terms of its perceived brightness to the human eye. It is distinct from radiometry, which is the science of measurement of radiant energy (including light) in terms of absolute power; rather, in photometry, the radiant power at each wavelength is weighted by a luminosity function that models human brightness sensitivity.

Since the basic measurement concepts are applicable to both, radiometric quantities will be discussed first followed by corresponding relationships and measurement units that have developed and are peculiar to photometry.

Radiant energy is the energy of electromagnetic waves and can be defined as the energy emitted, transferred, or received in the form of electromagnetic radiation. When a physical object absorbs light, its energy is converted into some other form. A microwave oven, for example, heats a glass of water when the water molecules absorb microwave radiation. The radiant energy of the microwaves is converted into thermal energy (heat). Similarly, visible light causes an electric current to flow in a photographic light meter when its radiant energy is transferred to the electrons as kinetic energy. Radiant energy is denoted by Q and is recorded in units of joules (J).

In radiometry, radiant flux or radiant power is the rate of flow of electromagnetic energy. It may be defined as the energy emitted, transferred, or received in the form of electromagnetic radiation per unit time. It is denoted by Φ and is in units of watts (W).

It is defined as:

$$\Phi = \frac{dQ}{dt}$$

(Eq. 2.2.33)

where Q is radiant energy and t is time.

Radiant flux density is the radiant flux per unit area at a point on a surface, where the surface can be real or imaginary (i.e., a mathematical plane). There are two possible conditions. The flux can be arriving at the surface (Figure 2.2.4a), in which case the radiant flux density is referred to as irradiance.
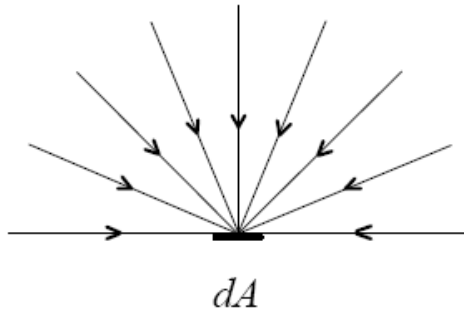
Fig. 2.2.4a Irradiance   Fig. 2.2.4b Radiant exitance
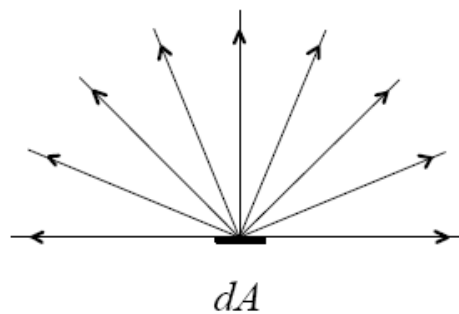
Irradiance is a radiometry term for the power per unit area of electromagnetic radiation at a surface. It is the ratio of the radiant power incident on an infinitesimally small element of a surface to the projected area of that element, dA_d, whose normal is at an angle θ_d to the direction of the radiation. Irradiance is denoted by E.

$$E = \frac{d\Phi}{\cos\theta_d dA_d}$$

(Eq. 2.2.34)

The flux can also be leaving the surface due to emission and/or reflection (Figure 2.2.4b). The radiant flux density is then referred to as radiant excitance. Radiant excitance (M) represents the power per unit area leaving a surface into a hemisphere above that surface, where dA_s is an infinitesimally small element of a source of the projected area of that element of area whose normal is at an angle θ_s to the direction of the radiation. The units usually used for both above mentioned terms are watts per square meter (Wm^{-2}).

$$M = \frac{d\Phi}{\cos\theta_s dA_s}$$

(Eq. 2.2.35)

The solid angle is defined (equation 2.2.36) as the ratio of a portion of the area on the surface of a sphere to the square of the radius r of the sphere. The solid angle is denoted by Ω and units are steradians (sr).

$$d\Omega = \frac{dA}{r^2}$$

(Eq. 2.2.36)

The definition of the radiance, illustrated in Figure 2.2.5, is the ratio of the radiant power at an angle θ to the normal of the surface element, to the infinitesimally small elements of both projected area and solid angle.

$$L = \frac{d\Phi}{\cos\theta dA d\Omega}$$

(Eq. 2.2.37)

Unit of radiance is watt per steradian meter^2 (W sr^{-1} m^{-2}).
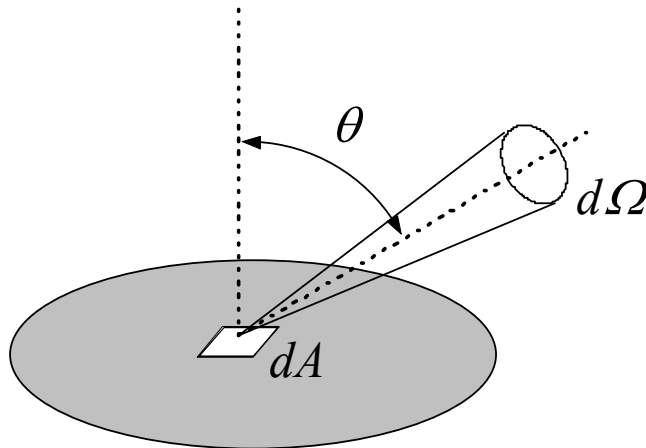
Fig. 2.2.5 The differential flux from small orthogonal surface element dA with a surface normal into the solid angle $d\Omega$ along the direction described by angle θ .

Luminance Lv describes the measurable photometric brightness of a certain location on a reflecting or emitting surface when viewed from a certain direction. It describes the luminous flux emitted or reflected from a certain location on an emitting or reflecting surface in a particular direction. The distinction between radiant and photometric quantities is that each of the radiometric quantities radiant power, radiant excitance, irradiance, radiant intensity and radiance corresponds to a photometric quantity, which is derived from the radiometric quantity by means of the spectral

luminous efficacy V_λ. Equivalently, illuminance is the total luminous flux incident on a surface, per unit area, similar to irradiance.

Radiometric term	Unit	Photometric term	Unit
Radiance	Wsr^{-1}m^{-2}	Luminance	cd.m^{-2}
Irradiance	W.m^{-2}	Iluminance	lx

Here it could be mentioned that the electromagnetic scattering is at an arbitrary boundary. In case of reflection, the behaviour is described by a bi-directional reflection distribution function (BRDF). According to the scheme in Figure 2.2.6, the polar and azimuth angles are θ and φ for the reflective direction, and are θ_0 and φ_0 for the incident direction.
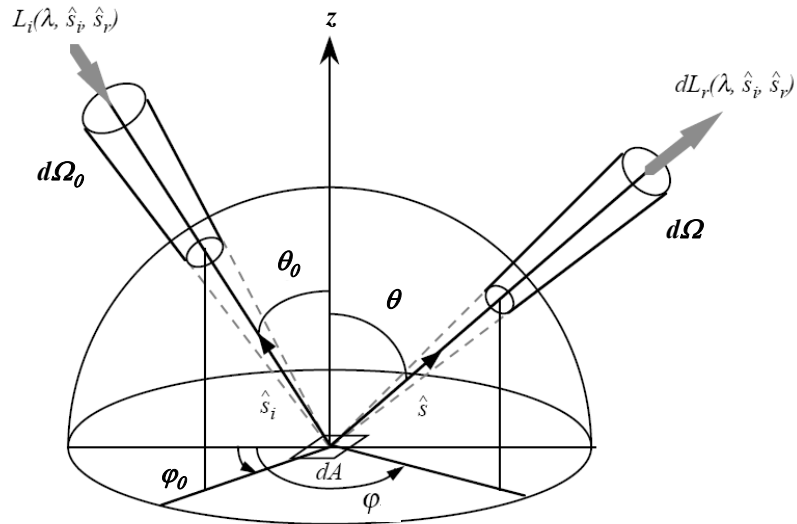
Figure 2.2.6: Scheme of BRDF definition

The value range for θ and θ_0 is [0,π/2] and for φ and φ_0 is [0,2π]. The BRDF is a four-dimensional function that defines how light is reflected at an opaque surface. It is defined as the ratio of the infinitesimally small radiance $dL(\theta,\varphi)$ for direction (θ,φ) to the infinitesimal incident flux L_o $(\theta_o,\varphi_o)d\Omega_o$ at a solid angle $d\Omega_o = \sin\theta_o\,d\theta_o\,d\varphi_0$:

$$\rho(\theta,\varphi,\theta_0,\varphi_0) = \frac{dL(\theta,\varphi)}{L_0(\theta_0,\varphi_0)d\Omega_0} = \frac{dL(\theta,\varphi)}{L_0(\theta_0,\varphi_0)\sin\theta_0 d\theta_0 d\varphi_0} \qquad \text{(Eq. 2.2.38)}$$

A BRDF has several important features. It is a fundamental radiometric concept, and accordingly is used in computer graphics for photorealistic rendering of synthetic scenes [67]. The BRDF in general depends not only on the incident and reflected directions, but also on wavelength λ and the surface location **r** where the reflection occurs. Therefore, a BRDF can generally be expressed as $\rho(\theta, \varphi, \theta_o, \varphi_o,$ **r** , λ). For most surfaces, usually two or three variables dominate the behaviour. BRDF allow also the reciprocity principle – if the incident and reflected directions are switched, a BRDF remains the same, i.e:

$$\rho(\theta_0, \varphi_0, \theta, \varphi) = \rho(\theta, \varphi, \theta_0, \varphi_0) \qquad \text{(Eq. 2.2.39)}$$

The counterpart of a BRDF for transmission is called a bi-directional transmittance distribution function (BTDF). The definition of a BTDF is similar to Eq. (2.3.38) except that the outgoing direction points to the transmission side.

2.3 Spectral Functions

Most sources of optical radiation are spectrally dependent, and the quantities radiance, intensity, etc. give no information about the distribution of these quantities over wavelength. Generally, the spectral function is a physical property that varies with wavelength and frequently is called a spectrum. The graph of a spectral function is then called a spectral curve.

2.3.1 Spectral Power Distribution

The term colour temperature is commonly used to describe the colour stimulus specification of a light source with a single number. More specifically, the colour temperature is expressed in degrees Kelvin. The colour temperature cannot substitute for the exact spectral description of a colour stimulus specification, but is in practice a rough, but tried and tested, value to describe the properties of light sources. The term colour temperature has its origin in the theory of black body radiation. The fact that with many artificial sources of radiation, the visible radiation is obtained as a result of

the heating up of a material, for example the metal filament in an electric light bulb. For these thermal radiators, the radiated energy and its spectral distribution depend on the temperature and absorption properties of the material. An ideal black body is often taken as a comparison variable for colour temperatures because there are some light sources with radiation distribution behaviour very close to that of a black body. The temperature of the black body at which the colour is most similar to the light source is called the colour temperature.

A spectral power distribution (SPD) is defined as the power of a light ray of unit wavelength in a unit area perpendicular to the propagating direction. Thus, a SPD is the light intensity according equation Eq. 2.3.4, which corresponds to the amplitude of the Poynting vector. Therefore, in the next part of this thesis, SPDs and light intensities will be used as equivalent terms.

The CIE has standardized a few SPDs and recommends that these should be used whenever possible when colorimetric characterization of materials is carried out. A further distinction is that for calculations only the relative SPD is needed. Such theoretical sources are called illuminants. There are two standard illuminants: CIE standard illuminant A and D65, and several secondary illuminants [68].

Practical realizations of a CIE illuminant are called CIE sources. Often an illuminant cannot be reproduced accurately. In such cases a simulator is referred to [68, 69]. In 1931 the CIE decided to introduce three standard illuminants, termed illuminants A, B, and C [79]. They were chosen in such a form that illuminant A should resemble the SPD of an average incandescent light, and it was thought that direct sunlight might be an appropriate second choice (illuminant B) with average daylight (illuminant C) as a further selection. During the years, it turned out that illuminant B was very seldom used and was soon dropped. Illuminant C is still in use in some industries, but in 1964 the CIE recommended a new set of daylight illuminants, where the SPD was also defined in the ultraviolet (UV) part of the spectrum [88].

One phase of daylight was selected as the most representative and is now known as CIE standard illuminant D65. A single letter has defined one further illuminant: Illuminant E has an SPD independent of wavelength, and it represents the equienergy spectrum.
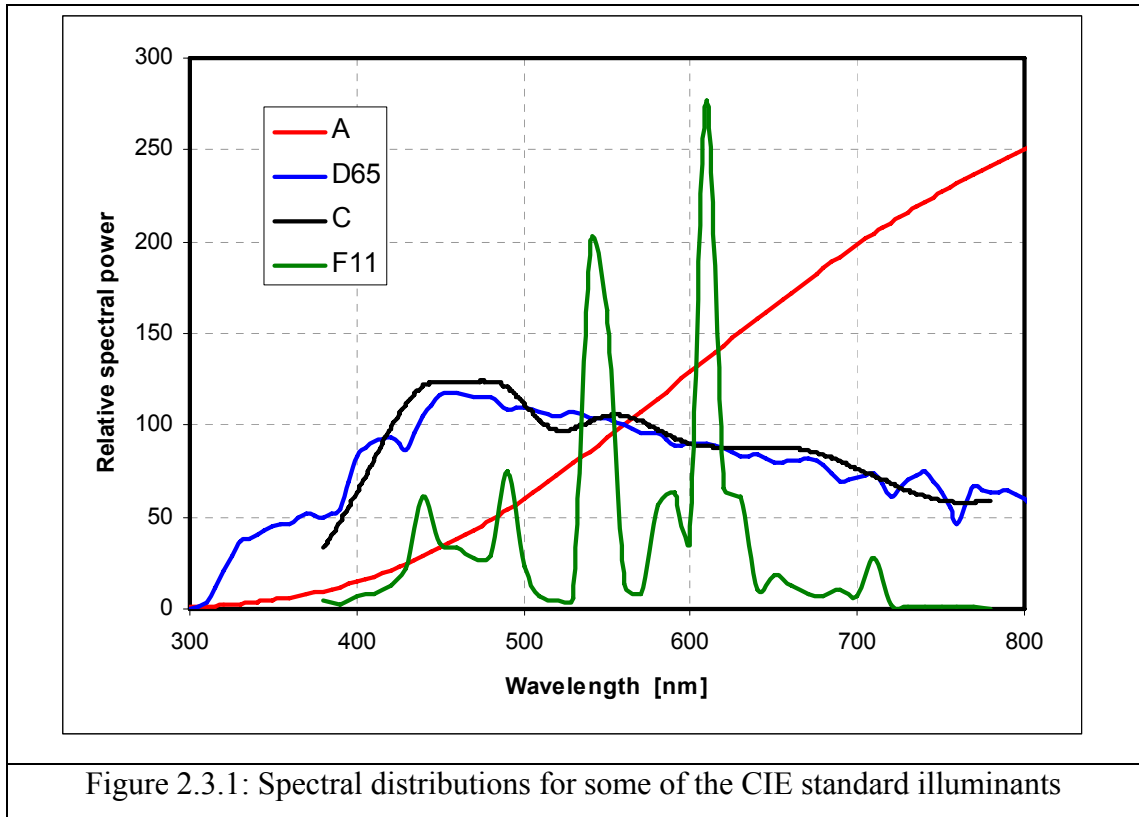
Figure 2.3.1: Spectral distributions for some of the CIE standard illuminants

The spectral composition of a light source may be described by the correlated colour temperature (CCT) and the general colour rendering index Ra. The CCT of a light source relates to the temperature of a Blackbody radiator emitting light of a similar spectral composition. The spectral radiant exitance $M(\lambda; T)$ of a Blackbody radiator as a function of the absolute temperature T in degree Kelvin (K) is given by Planck's formula [68; 69; 74]:

$$M(\lambda, T) = \frac{2hc^2}{\lambda^5} \frac{1}{e^{hc/\lambda kT} - 1}$$

(Eq. 2.3.1)

where $h = 6.625 \times 10^{-27}$ is Planck constant, $k = 1.38 \times 10^{-16}$ is the Boltzmann constant and c is the speed of light in vacuum.

A spectrum with a low CCT has a maximum in the radiant power distribution at long wavelengths, which gives a reddish appearance, for example low power electric light bulbs and the sunlight filtered by the atmosphere during sunset. A light source with a high CCT has a maximum in the radiant power distribution at short

wavelengths and has a bluish appearance, e.g., diffuse skylight and special fluorescent lamps.

2.3.2 Spectral Reflectance

Spectral reflectance is defined as light reflection at an object boundary or an interface between two media. Denoted by $R(\lambda)$, it is the fraction of incident radiation reflected by a surface.

$$R\left(\lambda\right) = \frac{I\left(\lambda\right)}{I_0\left(\lambda\right)} \qquad \text{(Eq. 2.3.2)}$$

where $I\left(\lambda\right)$ and $I_0\left(\lambda\right)$ are the reflected and incident intensities respectively. Spectral reflectances apply to boundaries of all kinds of materials, including those that are opaque, transparent and translucent.

In case of non-fluorescent materials, a spectral reflectance is independent of the intensity of the incident light and is an intrinsic property of the material. This property, which is referred to as the spectral linearity allows transformation of reflectance data to other illumination conditions. Measured data for many natural materials are available in the literature [63, 72, 68].

2.3.3 Spectral Transmittance

Spectral transmittance is the ratio between the transmitted and incident energies

$$T\left(\lambda\right) = \frac{I\left(\lambda\right)}{I_0\left(\lambda\right)} \qquad \text{(Eq. 2.3.3)}$$

where $I\left(\lambda\right)$ and $I_0(\lambda)$ are the intensities of the transmitted and incident lights. A spectral transmittance is also useful for prediction of the result after a light ray passes through a thin, transparent layer such as a filter [57, 68]. The following relationship may be used

$$I\left(\lambda\right) = I_0\left(\lambda\right) T\left(\lambda\right) \qquad \text{(Eq. 2.3.4)}$$

to compute the light intensity after the transmission. This interpretation allows the use of a similar equation for computing the spectral power distribution of reflected light based on spectral reflectance.

2.3.4 Spectral Absorptivity

Transmittance can be plotted against the concentration of an absorbing species, but the relationship is not linear. Spectral absorptivity is the part of light energy absorbed by a transparent or translucent material within a unit path length (l) of light propagation. General analytical description of spectral absorption is given by equation Eq. 2.3.5.:

$$a(\lambda,\mathbf{r}) = -\frac{1}{I(\lambda,\mathbf{r})}\frac{dI(\lambda,\mathbf{r})}{dl} \qquad \text{(Eq. 2.3.5)}$$

The spectral absorptivity depends not only on wavelength λ, but in case of not homogenous material also on spatial location $\mathbf{r}$. With respect of the spectral linearity, the SPD of a light after it travels from r_0 to r with l = [r_0 – r] can be calculated from

$$I(\lambda,\mathbf{r}) = I_0(\lambda,\mathbf{r_0})e^{-\int_0^l a(\lambda,\mathbf{r})dl} \qquad \text{(Eq. 2.3.6)}$$

where I_0 (λ,r_0) is the initial SPD. In the case of a homogenous material, the spectral absorptivity is independent of location, so the simplification $a(\lambda,r)=a(\lambda)$ can be used. Based on that Eq. 2.3.6 becomes:

$$I(\lambda) = I_0(\lambda)e^{-a(\lambda)l} \qquad \text{(Eq. 2.3.7)}$$

This equation is known as Bouguer's law. The other expression of Bouguer's law has a form

$$T_{\text{internal}}(\lambda) = \frac{I(\lambda)}{I_0(\lambda)} = e^{-a(\lambda)l} \qquad \text{(Eq. 2.3.8)}$$

where $T_{\text{internal}}(\lambda)$ is the internal spectral transmittance. Eq. 2.3.7 or 2.3.8 describes the optical effect of absorption, which depends on the thickness l. In the case of a homogeneous transparent solute material (ideal solution), absorption depends on the solute concentration. Finally, the Beer's law can by described by equation Eq. 2.3.9:

$$T_{\text{internal}}(\lambda) = e^{-\varepsilon(\lambda)cl} \qquad \text{(Eq. 2.3.9)}$$

where c is the concentration and ε(λ) is a spectral function, which is called absorption coefficient. Validity of the Beer's law is limited for low or moderate concentrations while Bouguer's law is rigorous for all conditions [68, 73], nevertheless both are valid for non-turbid media.

2.4 Colours

Colours are implicated in physics, chemistry, physiology and psychology, as well as in language and philosophy. Colours in design and clothing affect our senses and can create predetermined responses. For example, red is associated with danger, the red traffic light meaning "stop" to the road user, red is used as a symbol of guilt, sin and anger, often as connected with blood or sex.

Light can be described by wavelength and spectral distributions, but colour is the result of the interaction between light and the human eye, and the operation of the brain on signals obtained from the eye. Light enters the eye through the cornea, a transparent section of the sclera, which is kept moist and free from dust by the tear ducts and by blinking of the eyelids. The light passes through a transparent flexible lens, which acts to form an inverted image on the retina. The retina owes its photosensitivity to a mosaic of light sensitive cells known as rods and cones, which derive their names from their physical shape. Under ideal conditions, a normal observer can distinguish about 10 million individual colours. Three separate types of cone cells have been identified in the eye and the ability to distinguish colours is associated with the fact that each of the three types is sensitive to light of a particular range of wavelengths [63, 77]. The letters **L**, **M**, and **S** represent the three types of cones with their peak sensitivities in the long, middle, and short wavelength regions, respectively. Short cones are most sensitive to blue light, the maximum response being at a wavelength of about 440 nm. Medium cones are most sensitive to green light, the maximum response being at about wavelength of about 545 nm. Long cones are most sensitive to red light, the maximum response being at about 585 nm. **S** cones differ from **L** and **M** cones in morphology, neurochemistry, and spatial arrangement in the retina, i.e. inside specific area of retina, which is called fovea centralis (there is sharp central vision) are located **L** and **M** cones only.

The integration process of the three receptors reduces the entire spectrum to three signals, one for each cone type, resulting in trichromacy. Therefore, three signals are necessary and sufficient to describe any color.

The measurements and specifications of colours as well as transformations among different colour systems are topics within colour science. The following review focuses on the colour models most relevant to this thesis [68,71,78,79,80,81,82].

2.4.1 CIE COLORIMETRY

An international organization, the Commission International de L'Eclairage (CIE), worked in the first half of the 20th century developing a method for systematically measuring colour in relation to the wavelengths they contain [82]. This system became known as the CIE colour system. The model was originally developed based on the tristimulus theory of colour perception, which is known as the Young-Helmholtz theory [69]. The CIE colour model was developed to be completely independent of any device or other means of emission or reproduction and is based as closely as possible on how humans perceive colour. The key elements of the CIE model are the definitions of standard sources and the specifications for a standard observer. The colour-matching properties of the 1931 CIE standard colorimetry observer are defined as the colour-matching functions $\overline{x}(\lambda)$, $\overline{y}(\lambda)$ and $\overline{z}(\lambda)$, and today has two standardisation 2° (1931) and 10° (1964). Using these colour-matching functions, the tristimulus values X, Y, Z are

$$X = k \int_{\lambda_{min}}^{\lambda_{max}} E_\lambda R_\lambda \overline{x}_\lambda d\lambda$$

$$Y = k \int_{\lambda_{min}}^{\lambda_{max}} E_\lambda R_\lambda \overline{y}_\lambda d\lambda \qquad \text{Eq.2.4.1}$$

$$Z = k \int_{\lambda_{min}}^{\lambda_{max}} E_\lambda R_\lambda \overline{z}_\lambda d\lambda$$

where [λ_{min}, λ_{max}] defines the visible range (λ_{min} = 360nm, λ_{max} = 780nm), R_λ is reflectance, E_λ is spectral power distribution of used light source and k is a constant given by equation Eq. 2.4.2:

$$k = 100 \Bigg/ \int_{\lambda_{min}}^{\lambda_{max}} E_\lambda \bar{y}_\lambda d\lambda \qquad \text{Eq.2.4.2}$$

Setting the value of k to 100 makes for the perfect reflecting diffuser - ideal standard white [68,74]. The colour-matching function $\bar{y}(\lambda)$ is chosen to exactly match the luminous efficiency function $V(\lambda)$ for the human eye such that the Y value corresponds to the perceived luminance. For the three-dimensional Cartesian space where the tristimulus values X, Y, Z are its coordinates, every colour can be described as a vector

$$\mathbf{C} = X\mathbf{X} + Y\mathbf{Y} + Z\mathbf{Z} \qquad \text{Eq.2.4.3}$$

This equation may be interpreted as follows: Stimulus $\mathbf{C}$ is matched by X units of primary stimulus $\mathbf{X}$ mixed with Y units of primary stimulus $\mathbf{Y}$ and Z units of primary stimulus $\mathbf{Z}$. As before, the quantities X, Y, and Z are tristimulus values and provide a convenient way of describing the stimulus $\mathbf{C}$.

$$x = \frac{X}{X + Y + Z}$$

$$y = \frac{Y}{X + Y + Z} \qquad \text{Eq.2.4.4}$$

$$z = 1 - x - y$$

where x, y, z are coordinates in CIEXYZ space

To study the chromaticity of colours, it is adequate as well as convenient to use the relative coordinate values called the chromaticity coordinates, defined by Helmholtz [68].

These relative coordinates correspond to the tristimulus values on the $X + Y + Z = 1$ plane, unitary triangle respectively. Using the relative coordinates brings advantage in the separation of the chromaticity and luminance of any colour. For the specification of the chromacity the CIE coordinates x, y can be used and Y can be calculated for the

specification of the luminance. The tristimulus values can be calculated from CIE x, y, Y colour coordinates:

$$\begin{cases} X = \dfrac{x}{y}Y \\[2mm] Y = Y \\[2mm] Z = \dfrac{z}{y}Y = \dfrac{1-x-y}{y}Y \end{cases}$$

Eq.2.4.5

Figure 2.4.1 displays a chromaticity diagram in the two-dimensional space of *x* and *y*. The entire area of perceivable colours is divided into many regions corresponding to different descriptive terms of colour. The white colours are near the centre at x=0.33 and y=0.33. The colours for monochromatic lights are along the curved locus (called the spectral locus), where the marked values are the wavelengths in nm (10^{-9}m). A curve is demonstrated for blackbody radiation along with values of the colour temperatures [68].
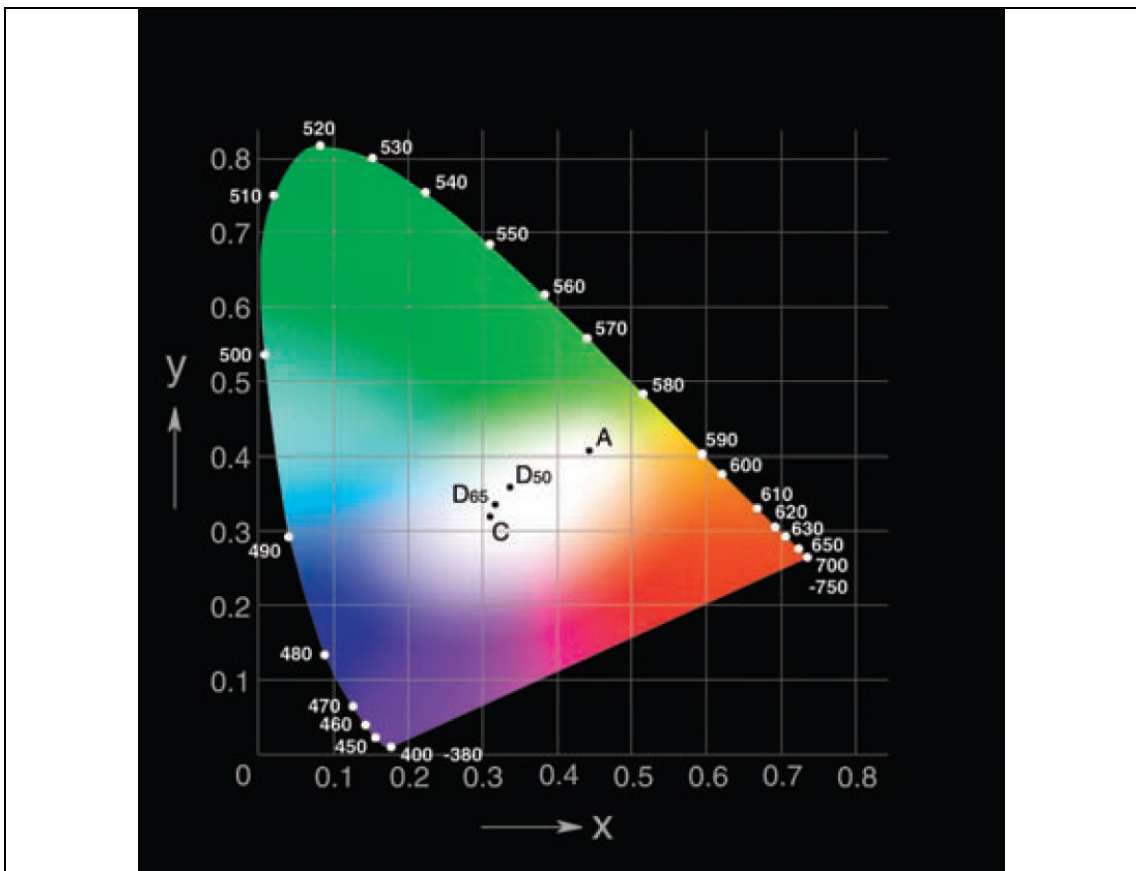

Fig. 2.4.1 CIE x,y diagram (from Lukac R., Plataniotis, K.N. Color Image Processing, Taylor and Francis, 2007)

The locations and chromaticity values for a number of standard CIE light sources are also shown in the diagram.

2.4.2 CIELAB and CIELUV

CIE colour space is not perceptually uniform. For many reasons, including evaluating colour differences, a perceptually uniform colour space is required. The CIELAB and CIELUV systems have improved the organization of colours so that a numeric difference between colours agree more consistently with human visual perceptions, and therefore, offers specific advantages over the 1931 CIE system.

The CIELUV colour space is a perpetually uniform derivation of the standard CIEXYZ space. It is based on a linear transformation of tristimulus values XYZ to a perceptually uniform chromacity plane with new coordinates u'and v' and on the nonlinear transformation of Y tristimulus value to a lightness axis L*.

The CIELAB colour space is based on the concept that colours can be considered as combinations of red and yellow, red and blue, green and yellow, and green and blue. To determine the exact combination of colours of a product, coordinates of a three dimensional colour space are assigned. The CIELAB space is related to CIEXYZ space via a nonlinear transformation based on Adams model of opponent colour vision [63,83,84,85,86,87,88,89,90].

$$
\begin{cases}
L^* = 116\left(\dfrac{Y}{Y_0}\right)^{1/3} - 16 & \text{if } Y/Y_0 > (24/116)^3 \\[2ex]
L^* = 903.3\left(\dfrac{Y}{Y_0}\right) & \text{if } Y/Y_0 \leq (24/116)^3 \\[3ex]
a^* = 500\left[f\left(\dfrac{X}{X_0}\right) - f\left(\dfrac{Y}{Y_0}\right) \right] \\[3ex]
b^* = 200\left[f\left(\dfrac{Y}{Y_0}\right) - f\left(\dfrac{Z}{Z_0}\right) \right]
\end{cases}
$$

(Eq. 2.4.12)

$$f(d) = \begin{cases} d^{1/3} & \text{if } d > (24/116)^3 \\ 7.787d + \dfrac{16}{116} & \text{if } d \le (24/116)^3 \end{cases} \qquad \text{(Eq. 2.4.13)}$$

where X_0, Y_0 and Z_0 are the CIE tristimulus values for the chosen standard illuminant and d is ratio of X/X_0 or Y/Y_0 or Z/Z_0.

The orthogonal L*a*b* colour system is easy to use, but does not always correspond to perception. For example, in the case of two orange colours where one is stronger than the other, the colour difference will not be described as redder and more yellow, but as stronger or weaker. For this reason the polar parameters hue h_{ab} and chroma C_{ab} are used that more closely match the visual experience of colours:

$$h_{ab} = \arctan\left(\frac{b*}{a*}\right) \qquad \text{(Eq. 2.4.14)}$$

and

$$C_{ab} = \sqrt{a*^2 + b*^2} \qquad \text{(Eq. 2.4.15)}$$
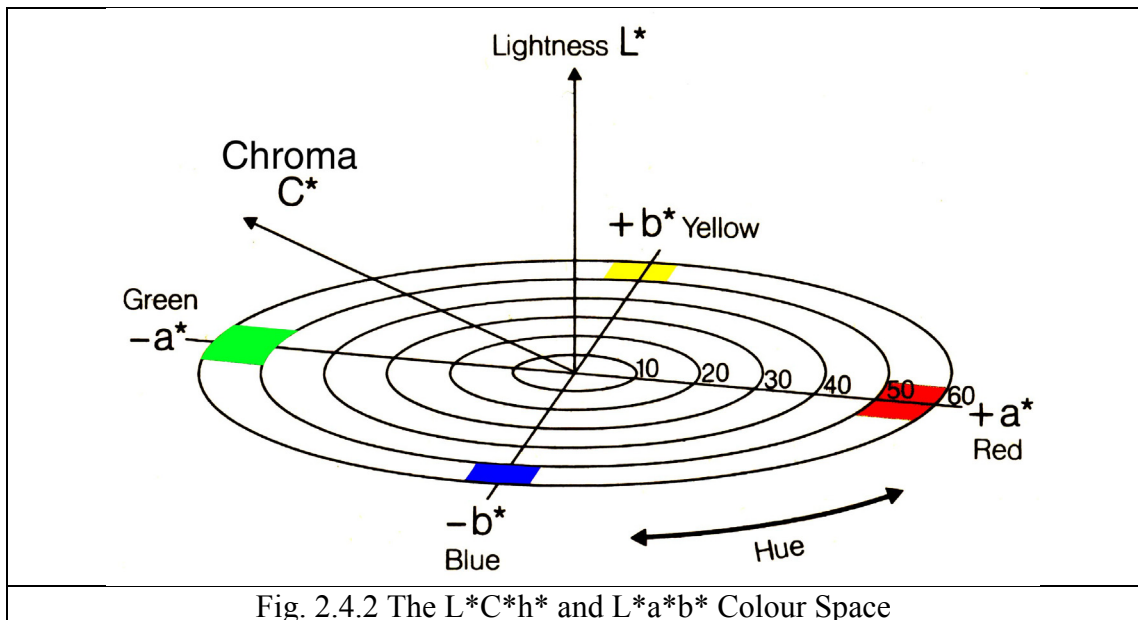
Fig. 2.4.2 The L*C*h* and L*a*b* Colour Space

In the CIELuv model, the definition of $L*$ is the same as in Eq. 2.4.12, but the other two coordinates are defined as:

$$\begin{cases} u^* = 13L^*(u'-u_0') \\ v^* = 13L^*(v'-v_0') \end{cases}$$

<div align="right">(Eq. 2.4.16)</div>

Where coordinates u´and v´are obtained from:

$$\begin{cases} u' = \dfrac{4X}{X+15Y+3Z} \\ v' = \dfrac{9Y}{X+15Y+3Z} \end{cases}$$

<div align="right">(Eq. 2.4.17)</div>

and u_0' and v_0' are the values for a standard white source. The values for hue and chroma are

$$h_{uv}^o = \arctan\left(\frac{v*}{u*}\right)$$

<div align="right">(Eq. 2.4.18)</div>

and

$$C_{uv}^* = \sqrt{u*^2 + v*^2}$$

<div align="right">(Eq.2.4.19)</div>

The colour difference between a batch and its standard is defined, in each space (CIELab or CIELuv), as the Euclidean distance between the points representing their colours in the relevant space. The formulae for the calculation of colour difference and its components in the two spaces are identical in all but the nomenclature of their variables. Two versions are defined, ΔE*uv for colours in CIEL*u*v* colour space and ΔE*ab for colours in CIEL*a*b*.

$$\Delta E^*_{uv} = \sqrt{\left(\Delta L^*\right)^2 + \left(\Delta u^*\right)^2 + \left(\Delta v^*\right)^2}$$

<div align="right">(Eq. 2.4.20)</div>

$$\Delta E^*_{ab} = \sqrt{\left(\Delta L^*\right)^2 + \left(\Delta a^*\right)^2 + \left(\Delta b^*\right)^2},$$

where $\Delta L^* = L^*_2 - L^*_1$ (1 – standard, 2 – batch) and similarly for the other terms.

It is well known, while the CIE 1976 recommendations were evolving, several colour-difference formulas were being developed outside the CIE. Nevertheless, in

case of measurement colorimetric properties of colour changeable materials give simple colour difference calculation based on CIELAB colour space sufficient reliability [118].

.

2.5 Optical models of translucent media

When a beam of light strikes a material medium, it is propagated through the thickness of the medium, where it experiences absorption while being transmitted according to the laws of geometrical optics. That is to say, the beam is deflected from the rectilinear path of light expected in a vacuum because of refraction, reflection, diffraction, and diffusion. This happens a number of times depending on the quality of the medium (homogeneous or not, transparent or opaque, smooth or rough). The beam is then deprived of absorbed parts at each wavelength and the resulting emitted spectrum constitutes the spectrum of reflectance.

Reflectance measures the capacity of a surface to reflect the incident energy flux, given that the medium beneath this surface can absorb photons and diffuse light once or many times. Reflectance is defined as the ratio of reflected to incident radiation energy flux for a given wavelength and is thus a dimensionless quantity, usually expressed as a percentage.

The reflectance spectrum consists of a plot of reflectance values R versus wavelength λ in the visible spectrum range (from 380 to 780 nm). One curve $R(\lambda)$ uniquely characterizes one colour: the reflectance spectrum objectively quantifies the colour itself.

When light impinges on dispersed particles, such as pigmented fibres, in addition to being partially absorbed, it is also scattered, changing its direction arbitrarily and several times in space. Light that passes through such a turbid media loses a considerable part of its intensity, and the relationship between the colorant concentration and the observed spectral response becomes more and more complicated. The analysis of light scattering in translucent, turbid media, such as clouds, ice structures, human tissues, food, paper and textiles is a wide and yet increasingly active research field. Hereafter, a few of the classical approaches are reviewed. An extended survey of the reflectance theories for the reflectance of diffusing media is given in reference [91].

2.5.1 Survey of fundamental light scattering theories

Rayleigh scattering is a fundamental theory that provides a tool to analyze the phenomenon of light scattered by air molecules [92]. According to this theory, the scattering power is strongly wavelength-dependent, which explains the blue appearance of the sky away from the sun. The theory can be extended to light scattered from particles with a diameter of up to a maximum of a tenth of the radiant wavelength. This restriction makes the theory impractical for analyzing the scattering of light in technical opaque or translucent media.

The Mie theory [92], on the other hand, describes the scattered light from a single spherical particle with a diameter that may be even larger than the scattered wavelength. Mie scattering is less wavelength-dependent than Rayleigh scattering and explains the almost white glare around the sun and the neutral colours of fog and clouds. It is a single scattering theory that ignores any rescattered light from neighbouring particles. Therefore, without being further extended, this approach does not strictly apply to light scattered from an assembly of particles.

To circumvent this disadvantage, the multiple scattering approaches are proposed for particle crowding with an average separation between particles greater than three particle diameters. However, when the particle crowding gets tighter, the problem of dependent scattering begins to increase as Mie scattering starts to fail, due to wavelength-dependent interference between the neighbouring scatterers. Nevertheless, most colorimetric problems do not require such elaborate handling and, in technology, more emphasis is placed on simpler calculation methods.

One of the most important simplified scattering approaches is based on a theory known in astrophysics as radiative transfer [93]. In its original form it studies the transmission of light through absorbing and scattering media such as stellar and planetary atmospheres. The radiative transfer equations are rather complex and the multichannel technique is a suitable approach that overcomes the imposed complexity. This technique subdivides the analyzed medium into as many channels as needed, each of them covering a different range of angles from the perpendicular to the horizontal [94]. Each channel is supplied with specific absorption and scattering coefficients, which determine how much light is being absorbed and scattered into other channels. The interesting aspect of this concept is its ability to connect the series of coefficients directly to Mie's theory. This helps to incorporate fundamental

properties of the scatterer into the model, such as the particle size and the refractive index.

Reducing the number of channels considered even further, one arrives at the case of two-flux models proposed by Schuster [95] and other authors. However, the Kubelka & Munk model, which is presented in the following section, is probably the most recognized approach and best suits the purpose of analyzing light scattered within textile fabrics and by colorant particles.

2.5.2 Kubelka-Munk's theory

The original theory of Kubelka and Munk [96] was developed for uniform colorant layers. Due to its simple use and its acceptable prediction accuracy, the model has become widely used in industrial applications [97,98]. It is suitable for turbid layered media. The expressive dimensionality of the scattering problem is reduced by assuming that light is being absorbed and scattered only in two directions, up and down. Thus, no special account needs to be taken of fluxes proceeding parallel to the boundaries, and only two vertical fluxes need to be considered. The illumination of the top face of the turbid medium is expected to be homogeneous and diffuse. Besides being infinitely extended, the concept assumes that the medium forms a plane layer of constant, generally finite thickness. The material is presumed to be homogeneous, i.e. the optical inhomogeneities are incomparably smaller than the thickness of the specimen and uniformly distributed in the material. Finally, the material is assumed to emit no fluorescent radiation. In addition, it is assumed to have the same refractive index as the medium from which the light comes [99,100].
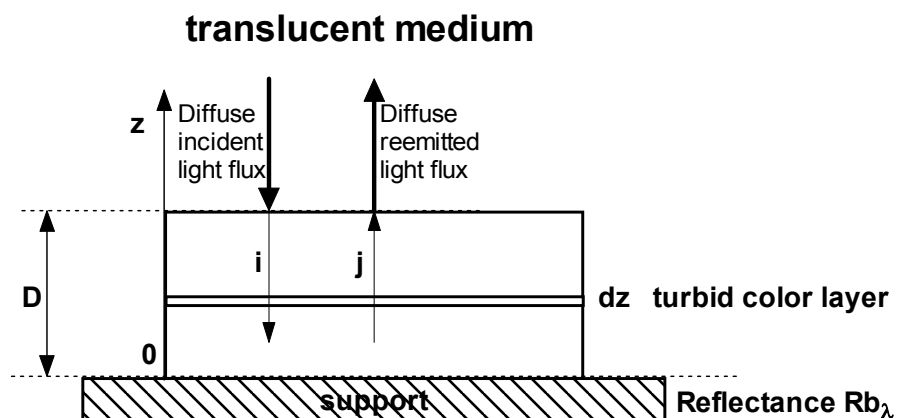

Fig.2.5.1 Scheme of Kubelka and Munk's theoretical model

As depicted in Figure 2.5.1 the colorant layer has a total thickness **D** and is in direct optical contact with a backing of reflectance Rb_λ. The model analyzes two fluxes through an elementary layer of thickness **dz**, the flux $i_\lambda(z)$ proceeding downward, and $j_\lambda(z)$ simultaneously upward. The depth parameter **z** is considered to be zero at the background of the layer and **D** at the illuminated interface of the layer.

During its passage through **dz**, the upward flux $j_\lambda(z)$ is attenuated by <u>absorption</u> $\alpha_\lambda \cdot$ **dz** and by <u>scattering</u> downwards $\sigma_\lambda \cdot$ **dz**. At the same time, $j_\lambda(z)$ gains by scattering from the opposed flux amount to $\sigma_\lambda \cdot$ **dz** yielding the flux variation $dj_\lambda(z)$ per thickness element **dz** :

$$\frac{dj_\lambda(z)}{dz} = \sigma_\lambda . i_\lambda(z) - (\alpha_\lambda + \sigma_\lambda). j_\lambda(z),$$

(Eq. 2.5.1)

The corresponding variation of the downward flux $i_\lambda(z)$ is derived in the same manner with the exception that **dz** is negative, as the process is occurring in the reverse direction,

$$-\frac{di_\lambda(z)}{dz} = \sigma_\lambda . j_\lambda(z) - (\alpha_\lambda + \sigma_\lambda). i_\lambda(z)$$

(Eq. 2.5.2)

The differential equations 2.5.1 and 2.5.2 obtained describe the net changes of both light fluxes, $i_\lambda(z)$ and $j_\lambda(z)$. The equations are classified as the two-constant theory, referring to the introduced colorant optical coefficients, absorption and scattering.

Kubelka and Munk solved this system of equations and obtained the reflectance value associated with a given wavelength in the case of an infinite $R_{\infty\lambda}$ or finite R_λ painted layer, in terms of the absorption and scattering coefficients and the reflectance of the support $R_{b\lambda}$, as expressed in Eq. 2.5.3:

$$R_{\infty\lambda} = \frac{\dfrac{R_{b\lambda} - R_{\infty\lambda}}{R_{\infty\lambda}} - R_{\infty\lambda}\left(R_{b\lambda} - \dfrac{1}{R_{\infty\lambda}}\right)\exp\left[\sigma_\lambda D\left(\dfrac{1}{R_{\infty\lambda}} - R_{\infty\lambda}\right)\right]}{R_{b\lambda} - R_{\infty\lambda} - \left(R_{b\lambda} - \dfrac{1}{R_{\infty\lambda}}\right)\exp\left[\sigma_\lambda D\left(\dfrac{1}{R_{\infty\lambda}} - R_{\infty\lambda}\right)\right]} .$$

(Eq. 2.5.3)

In practice, $R_{\infty\lambda}$ is the reflectance of a layer that is thick enough to completely hide the support [99], that is, the limiting reflectance that is not modified by any additional thickness of the same material [100]. Moreover, the calculation of $R_{\infty\lambda}$ allows the ratio $\alpha_\lambda/\sigma_\lambda$ to be obtained by inversion of equation 2.5.4:

$$R_{\infty\lambda} = 1 + \frac{\alpha_\lambda}{\sigma_\lambda} - \sqrt{\frac{\alpha_\lambda^{\,2}}{\sigma_\lambda^{\,2}} + 2\frac{\alpha_\lambda}{\sigma_\lambda}} \; . \qquad \text{(Eq. 2.5.4)}$$

$$\frac{\alpha_\lambda}{\sigma_\lambda} = \frac{(1 - R_{\infty\lambda})^2}{2R_{\infty\lambda}} = K/S \qquad \text{(Eq. 2.5.5)}$$

K/S function is the Kubelka-Munk function.

2.5.3 Colour Intensity

Considering that significant current and future research is directed towards the development of Smart textile sensors with photochromic pigments, which can react under UV irradiation, it is necessary for the purposes of their calibration to provide an objective description of visual colour change. The Kubelka – Munk function forms the basis of one possible solution for spectrophotometric description of colour appearance. In the case of photochromic pigments, the changes of spectral characteristic before and after illumination, expressed by the integral equation 2.5.6, can be considered [20,115]:

$$I = \int_{380}^{760} (K/S)_\lambda \, d\lambda \qquad \text{(Eq. 2.5.6)}$$

The value *I* represents shade intensity. In practice it is obtained by integration using equation 2.5.6 expressed by the sum in equation 2.5.7:

$$I = \sum_{i=380}^{760} (K/S)_i \, \Delta\lambda \qquad \text{(Eq. 2.5.7)}$$

$\Delta\lambda$ depends on the band pass of spectrophotometer (usually 10 nm).

In the case of photochromic substances, I depends on both time and intensity of illumination. For the purpose of the work, described in this thesis, the term I_t is the colour intensity developed by irradiation for time t.

2.5.4 Kinetic model of photochromic response during exposure

A first order kinetic model of photochromic response during exposure is proposed which describes simply the process of changes within a sample of an applied photochromic pigment from I_0 (colour intensity at time t_0, or sample without exposure) to I_∞ (colour intensity after infinite time t_∞) as illustrated in Fig. 2.5.2:
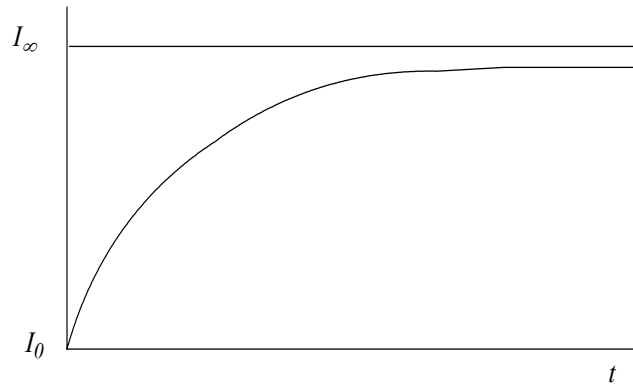
Fig. 2.5.2 Curve of colour intensity change for a photochromic dye during exposure with time

The proposed model is based on the view, that the process follows first order kinetics with the rate described by equation 2.5.8. The rate of colour intensity development dI/dt is directly proportional to the difference of colour intensity at time t and in equilibrium:

$$\frac{dI_t}{dt} = -k(I - I_\infty),$$

(Eq. 2.5.8)

For $t = 0$ $I = I_0$

Integration of this equation between the limits $(0,t)$ (I_0,I) leads to the exponential equation 2.5.9:

$$I_t = I_\infty + (I_0 - I_\infty)\, e^{-kt} \qquad\qquad \text{(Eq. 2.5.9)}$$

2.5.5 Kinetic model of the photochromic response during reversion

The kinetic model for relaxation and change of colour intensity I for the photochromic pigment (photochromic response during reversion) is based on fact that during reversion the change of colour intensity I_t reduces from I_∞ to I_0 (see Fig. 2.5.3):
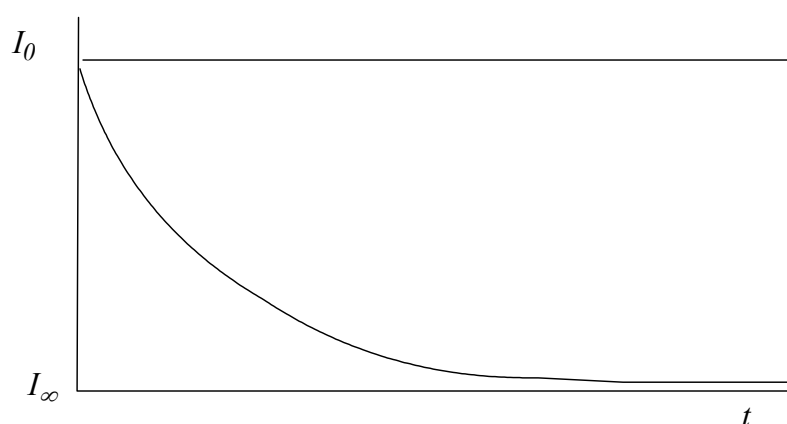
Fig. 2.5.3 Curve of colour intensity change for a photochromic dye during reversion with time

The basic presumption is again of first order kinetics as for exposure. The rate of colour intensity changes dI/dt is also directly proportional to the difference in colour intensity after time t and at equilibrium:

$$\frac{dI_t}{dt} = -k(I_\infty - I), \qquad\qquad \text{(Eq. 2.5.10)}$$

For $t = 0$ $I = I_\infty$

Again, through the integration, the solution of the differential equation within the limits $(0,t)$ (I_∞, I) gives the exponential equation :

$$I = I_0 + (I_\infty - I_0)\, e^{-kt} \qquad\qquad \text{(Eq. 2.5.11)}$$

2.6 Colorimetric measurement of photochromic samples

Colorimetric instruments can be divided into three basic types, these being the colorimeter, spectroradiometer and spectrophotometer, of which the most important is the spectrophotometer. The spectrophotometer mainly measures reflectance, transmittance, or absorbance at different wavelengths in the spectrum. The quantity of reflectance measured is referred to as the reflectance factor **RF**. This factor is defined as the reflectance of the sample at a specific wavelength, over a range of wavelengths, compared to the reflectance of the perfectly reflecting diffuse white measured under the same conditions. The mathematical expression is as follows

$$RF(\lambda) = \frac{R(\lambda)_{\text{sample}}}{R(\lambda)_{\text{standard (ideal white)}}} \qquad\qquad \textbf{(Eq. 2.6.1)}$$

2.6.1 Standard for the reflectance factor

The perfect reflecting diffuser was recommended as a reference standard in 1986 in the publication CIE Standard Colorimetric Observers [ISO/CIE 10527 – 1991: Colorimetric observers]. It is defined as the ideal isotropic diffuser with a reflectance equal to unity. Because a perfect reflecting diffuser does not exist in practice, durable reference standards must be calibrated by comparing the reflected radiation with incident radiation directly. Such calibrations are difficult to do accurately and, consequently, are usually performed only in selected national metrology institutes. Until the 1959 CIE Session [89] the colorimetric measurements of materials were referred not to the perfect reflecting diffuser but to smoked magnesium oxide, and its reflectance value was taken to be 100% for all wavelengths.

Values reported before 1969 must be corrected by multiplying the values by the absolute reflectance of MgO [88].

A secondary reference standard, such as pressed barium sulphate, smoked magnesium oxide and pressed powder of magnesium oxide, must be calibrated in terms of the perfect reflecting diffuser, and the absolute reflectance of these standards is used in present day measuring systems. These samples resemble more or less a Lambertian surface and thus can be used to transfer reflectance and reflectance factor data between different instruments. Their drawback is that they usually have a very fragile surface and have limited stability.

The calibration is carried out by a working transfer standard, which has calibration data specific to the standard, relating to the perfect reflecting diffuser. When an instrument is subjected to its calibration procedure, the transfer standard equation 2.6.1 is used to calibrate the photometric scale.

2.6.2 Illuminating and viewing conditions for a reflecting specimen

The CIE recommends the use of one of the following illuminating and viewing conditions: 45°/normal, normal/45°, diffuse/normal and normal/diffuse [89]. For these conditions the following symbols are used 45/0, 0/45, *d*/0 and 0/*d*, respectively. Now, there are eight recommended geometries - 45a:0, 0:45a, 45x:0, 0:45x, *di*:8, 8:*di, de*:8, 8:*de*. [90]

In the 45/0 geometry the sample is illuminated by one or more beams whose effective axes are at an angle of $45^o \pm 2^o$ from the normal to the sample surface. The viewing angle from the normal to the sample should be less than 10°. There is also a restriction in the viewing and illuminating beams: the angle between the axis and ray should not exceed 5° [89]. The reason is an overfilling of the sample area.

In the 0/45 geometry the illumination is in the direction normal to the sample, and the viewing angle is 45° from the normal. Now normal illumination is within 2°, and the angle between the axis and any ray should not exceed 8°. The same restriction should be observed in the viewing beam. The illuminating conditions 0/45 and 45/0 are shown in Fig. 2.6.1.
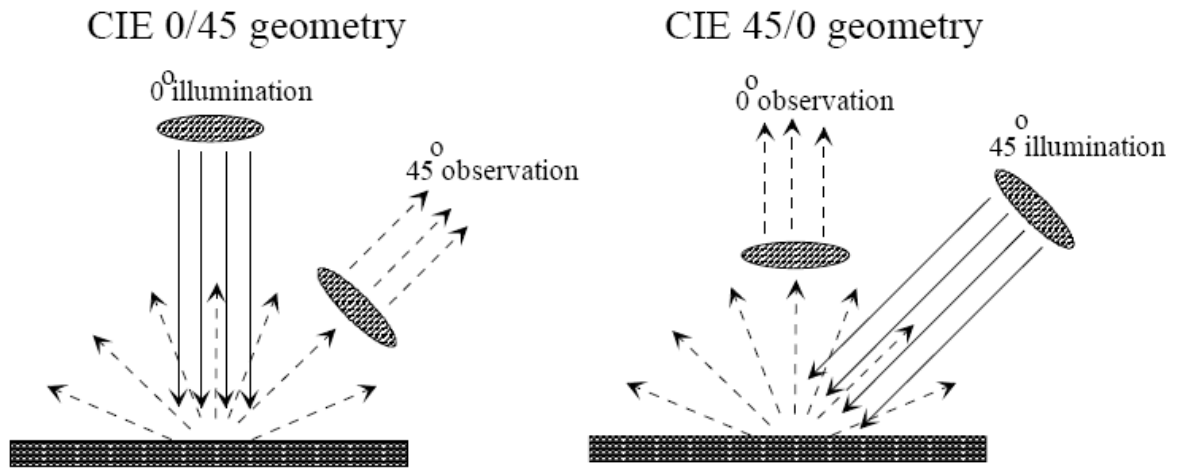
Figure 2.6.1 : Viewing geometries of 0/45 and 45/0.

If the sample is illuminated diffusely by an integrating sphere and the viewing angle does not exceed 10° from the direction normal to the surface of the sample, this refers to the *d/0* geometry. The integrating sphere may be of any diameter provided the total areas of the ports do not exceed 10 percent of the internal reflecting sphere area. The angle between the axis and arbitrary ray of the viewing beam should not exceed 5°. If the specimen is illuminated by a beam whose axis does not exceed 10° from the normal to the specimen, this refers to 0/*d* geometry. The reflected flux is collected by means of an integrating sphere. The angle between the axis and any ray of the illuminating beam should not exceed 5°. In Fig. 2.6.2, a typical setup of 0/*d* geometry is shown using an integrating sphere. When integrating spheres are used, they should be equipped with white coated baffles to prevent light passing directly between the sample and the spot of the sphere wall illuminated or viewed.

Figure 2.6.2: Integrating sphere.

In the 0/*d* and *d*/0 conditions, specular reflection can be excluded or included by the use of a gloss trap. In the 0/*d* condition, the sample should not be measured with a strictly norma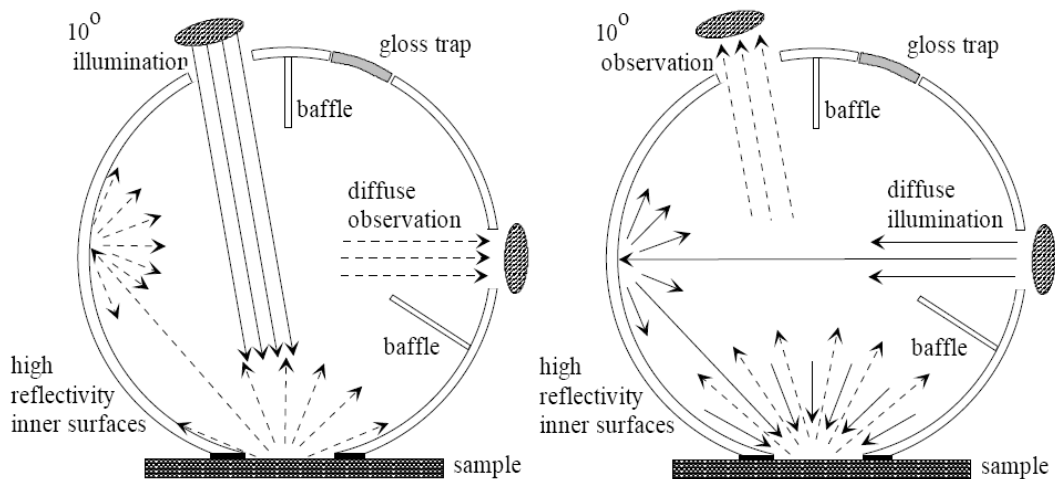l axis of illumination if it is required to include the regular component of reflection. It should be noted that only the 0/*d* geometry provides a spectral reflectance. The other conditions *d*/0, 0/45 and 45/0 give a specific radiance factor.

2.6.3 Illuminating and viewing conditions for transmitting specimens

It is recommended that the colorimetric specification of transmitting species corresponds to one of the following illuminating and viewing conditions: normal/normal, normal/diffuse and diffuse/diffuse. The following symbols are used 0/0, 0/*d* and *d*/*d*, respectively [89].

In the normal/normal (0/0) condition, the specimen is illuminated by a beam whose effective axis is at an angle not exceeding 5° from the normal to its surface and with the angle between the axis and any ray of the illuminating beam not exceeding 5°. The geometric arrangement of the viewing beam is the same as that of the illuminating beam. The specimen is positioned so that only the regularly transmitted flux reaches the detector. This condition gives the regular transmittance, τ_r.

In the normal/diffuse (0/*d*) condition, the specimen is illuminated by a beam whose effective axis is at an angle not exceeding 5° from the normal to its surface and with the angle between the axis and any ray of the illuminating beam not exceeding 5°. The hemispherical transmitted flux is usually measured with an integrating sphere. The reflectance of the reflecting surface of a sphere or other material at the point of impingement of the regularly transmitted beam, or at the point of impingement of the illuminating beam in the absence of a specimen, must be identical to the reflectance of the remainder of the internal reflecting sphere area. This condition gives the total transmittance, τ.

If the regularly transmitted flux is excluded, for example by the use of a light trap, it gives the diffuse transmittance, $\tau_{0/d}$. If the positions of the light source and detector are interchanged, the method gives the equivalent diffuse/normal (*d*/0) quantities. In the diffuse/diffuse (*d*/*d*) condition, the specimen is illuminated diffusely

with an integrating sphere and transmitted flux is collected using a second integrating sphere. This condition gives the double transmittance, τ_{dd}.

2.7. Conclusion

The principles of the photochromism of organic compounds, fundamental optical concepts, spectral functions, optical models of translucent media and colorimetric measurement of photochromic samples have been reviewed and discussed in this chapter. In order to inform the respect into aspects of the effectiveness of the production of photochromic textiles, which is the main subject in this thesis, four equally important set of principles require to be understood and considered:

1. The chemistry of photochromic colour change.

2. The use of the colorimetric values $L^*a^*b^*$ and the K/S function with colour change intensity I for the description of photochromic colour change phenomena.
3. A description and understanding of the geometry of spectrophotometers, leading to the possibility of spectrophotometer modification for the measurement of photochromic reactions in reflectance mode.

4. Basic optical concepts included in Maxwell`s equations allow a description of the relationships of electromagnetic radiation in the context of on photochromic transitions. Consequently, these principles will be used to exploit the photochromic system as a sensor of UV radiation.

The study of colour change phenomena of selected photochromic materials allows to deep understanding of the conformation changes induced by UV radiation, especially the pyrans and naphthooxazine dye types and their photochromic heterolytic cleavage reactions, used in the experimental work described in this thesis.

There are also many limitations encountered during measurement of photochromic materials in the application of the classical spectrophotometers. Therefore it is necessary also to study the geometry of spectrophotometers, to select

the right configuration together with factor such as thermal stabilisation, time sequenced individual measurements to allow a kinetic study of the photochromic reaction, and to define the kinetic model of photochromic reaction, which is well described by the Kubelka-Munk function.

Chapter 3
EXPERIMENTAL

In chapter 2 of this thesis, the important technical features of photochromic materials have been reviewed. The review was particularly oriented towards various features of transparent photochromic media (e.g., solution, glass, polymeric film etc.). In the case of the measurement of photochromic textiles, consideration is required of coloured surfaces with changeable features. This problem may be addressed with an approach involving time sequence measurement and with simultaneous control of UV exposure.

This experimental section contains two main parts: development of a measuring system for the evaluation of the kinetics of colour change and the testing of two types of photochromic textiles. Comparisons are made with photochromic solutions where appropriate.

3.1. Instrumentation

Humans can perceive two types of colour: the colour from a self-luminous object is referred to as self-luminous colour, and the colour of an illuminated object, referred to as object colour. A self-luminous object may be natural, such as the sun, or artificial, such as computer displays, incandescent light bulbs, mercury lamps, and the like. An object colour is the colour reflected from an illuminated object, and comprises both the light reflected from the object's surface as well as any light reflected and scattered from beneath the object's surface.

Instrumental colour measurement is now common practice in many situations requiring colour quality control owing to the high variability in visual assessment and the need for accurate colour assessment and communication. The interaction between observer, light and object form the basis for all instrumental methods for measurement of colour. Since direct measurement of colour perception is not possible, the measurement of factors related to colour perception can be used to numerically to describe colour. Colour measurement in practice does not necessarily eliminate the need for a visual evaluation of the standard and batch.

Devices for colour measurement date from as early as 1900 when they were originally known as absorptiometers. They were used to establish, by a visual inspection, whether two coloured solutions were equal in shade [103]. The first

device designed for colour measurement of opaque materials was developed in the period 1915-1920 and it was called a reflectometer. This device consisted of three coloured filters and the apparatus was used to directly measure reflectance factors relative to the amount of the three primaries contained in the measured sample. Following the development of the CIE 1931 standard observer, the tristimulus colorimeter was introduced. This device replaced the existing reflectometer [104].

The beginning of reflectance spectrophotometry dates back to 1928 when A.C. Hardy, Professor of Optics at the Massachusetts Institute of Technology, initiated a project to produce the first spectrophotometer specifically for the measurement of reflectance. Commercialization of Hardy's design began in 1935 when General Electric introduced the General Electric Recording Spectrophotometer. This instrument became the much needed reference spectrophotometer and provided the basis for the development of modern industrial colour measurement [105, 106].

3.1.1 Tristimulus colorimeters and spectrocolorimeters

Early spectrophotometers were expensive and required skilled technicians to run and maintain them. Colorimetric calculations had to be performed by hand or with mechanical calculating machines. Industrial colour measurement eventually became a common practice with the development of the colorimeter. Colorimeters were developed in the 1940s and, because of their lower cost and simplicity of operation, were in common use by the 1950s.

Colorimeters have been constructed using all eight CIE recommended geometries [90]. They use three or four broad response filters to modify their light source in an attempt to simulate a CIE illuminant and a standard observer combination. Sample measurements did not result in spectral reflectance readings but gave a direct conversion to either CIE tristimulus values or the coordinates of a uniform colour space, such as CIELAB.

The main problem with colorimeters is their inability to measure metamerism. Colorimeters generally allow for only one illuminant/observer combination and the determination of metamerism requires a minimum of two such combinations. Colorimeters using polychromatic illumination have been modified by filtering their light sources to provide two illuminant/observer combinations. Another problem with colorimeters is their lack of accuracy caused by the difficulty in finding filters

accurately to duplicate the CIE illuminant and observer functions. Colorimeters can determine the colour difference between two materials more accurately and are thus often referred to as colour difference meters.

As optics and computer technology progressed, spectrophotometers became much less expensive, faster and easier to operate. When the difference in cost between a spectrophotometer and a colorimeter narrowed, it appeared that spectrophotometers would entirely replace colorimeters. About the same time, portable colorimeters were developed. Portability allowed colour measurement to be taken directly to the shop floor or even to a remote location. The recent development of relatively inexpensive portable spectrophotometers makes them likely candidates to replace the portable colorimeters. This is especially true for spectrocolorimeters - a spectrophotometer that only outputs tristimulus values and/or uniform colour space coordinates. Spectrocolorimeters are less expensive than full function spectrophotometers, but can be used to determine metamerism.
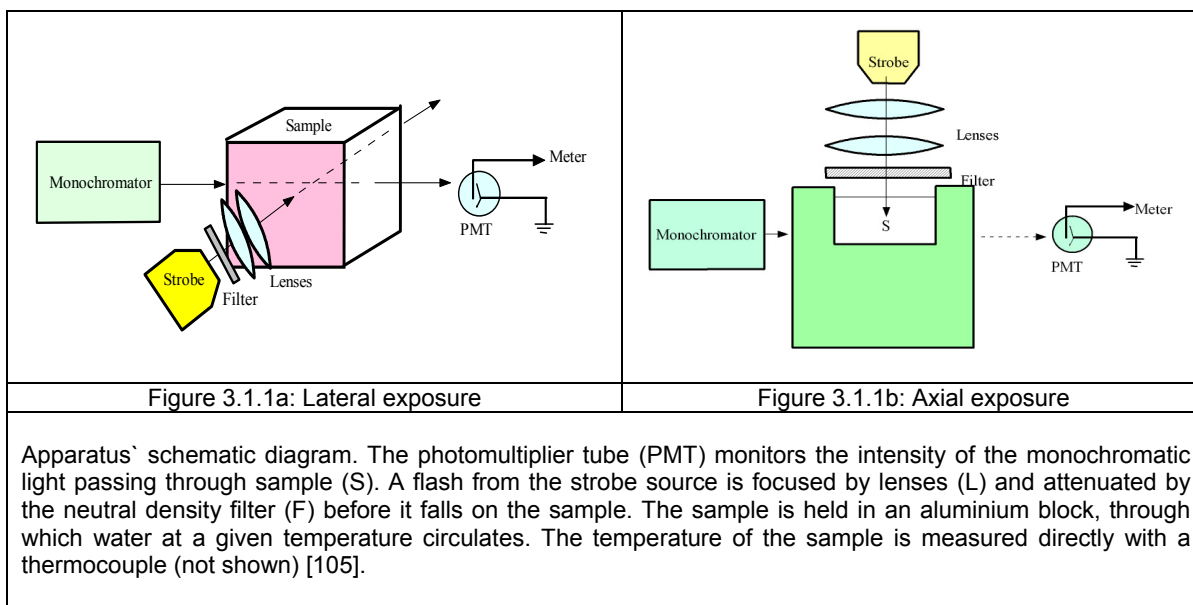
3.1.2. Spectrophotometers

Spectrophotometers are classified according to their area of application and according to whether polychromatic or monochromatic illumination is used. Analytical spectrophotometers use monochromatic illumination. Polychromatic illumination is used in certain new spectrophotometers, specifically spectrophotometers used to acquire spectral data in a short time. Unfortunately, these systems are limited in the width of the measured band pass in comparison to the systems with monochromatic illumination.

(a) Transmittance measurement of transparent media

In this case, the usual measurement method involves a solution in a cuvette, which allows either lateral or axial illumination of the sample, as shown in Figure 3.1.1a and Figure 3.1.1b, respectively. These diagrams show an experimental set-up for discontinuous irradiation with respect to time. It is evident that the same experimental set-up can be use for continuous irradiation. The light source for exposure can be, for example, a laser, discharge lamp, LED or other source. Analytical spectrophotometers typically measure only transparent liquids in transmission, as their 0°/0° measurement geometry makes them very sensitive to scattering when measuring hazy samples that

scatter light. The time resolution of modern diode array spectrophotometers is around 0.5 s for a completely scanned spectrum. The measurement time for most analytical spectrophotometers is much longer, typically about a minute, due to the extended scanning range and smaller scanning wavelength interval.

Figure 3.1.1a: Lateral exposure	Figure 3.1.1b: Axial exposure

Apparatus` schematic diagram. The photomultiplier tube (PMT) monitors the intensity of the monochromatic light passing through sample (S). A flash from the strobe source is focused by lenses (L) and attenuated by the neutral density filter (F) before it falls on the sample. The sample is held in an aluminium block, through which water at a given temperature circulates. The temperature of the sample is measured directly with a thermocouple (not shown) [105].

In the case of continuous irradiation experiments, the diode array spectrophotometer measuring system allows the study of photochromic systems, when the lifetime of colour change is longer than 50 ms. If systems with faster photochromic changes are to be studied, it is necessary to use the discontinuous (pulsed) irradiation measurement method. A typical example is a time resolved method using a femtosecond laser pumped probe technique [108,109]. If the set-up of the spectrophotometer also includes the irradiation monochromator or a system of band pass filters, it becomes possible to study the spectral sensitivity of the sample.

(b) Transmittance measurement of translucent media

The measurement of translucent media presents a specific problem that results from the combination of transmission and reflection of light. In translucent media, it is possible to measure in either transmission or reflection mode. In the case of the measurement of transmittance of light through translucent media, it is necessary to take in to consideration scattering caused by the turbidity of these media. In this case, when it is necessary to assume not only regular but also diffuse transmission, it is

necessary to use the integrating sphere for measurement. Usually an adaptation of analytical spectrophotometers is used, in which the integrating sphere is placed in the cuvette space as shown in Fig. 3.1.2a. Hazemeters for the measurement of opacity have similar construction. For measurement of the data from the complete spectral range, it is necessary to equip the spectrophotometer with a photodiode array detector or other type of linear sensor. In this way, the spectrophotometers are equipped for measurement of coloured surfaces and therefore the inverted adjustment can be used as the variation, when the sample is illuminated diffusely from the integrating sphere as described in Fig. 3.1.2b.

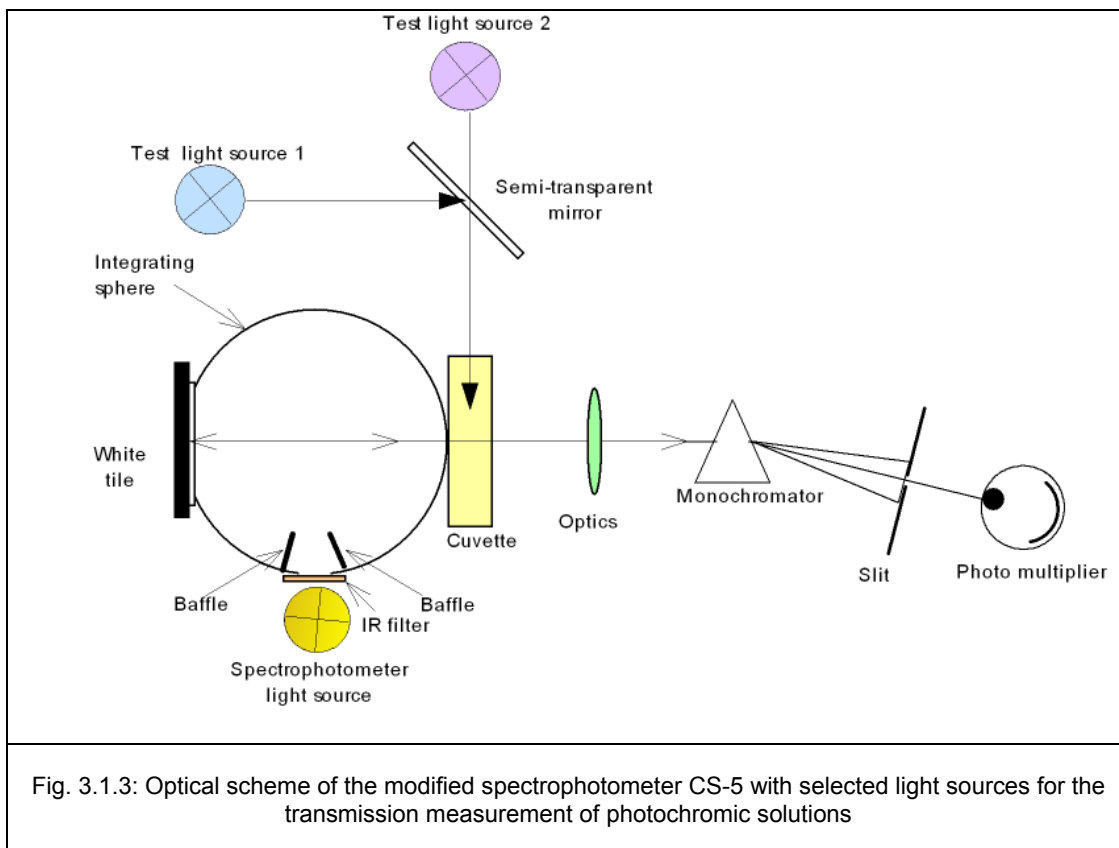| Fig. 3.1.2a: Direct measurement of total transmission	Fig.3.1.2b: Inverted measurement of total transmission
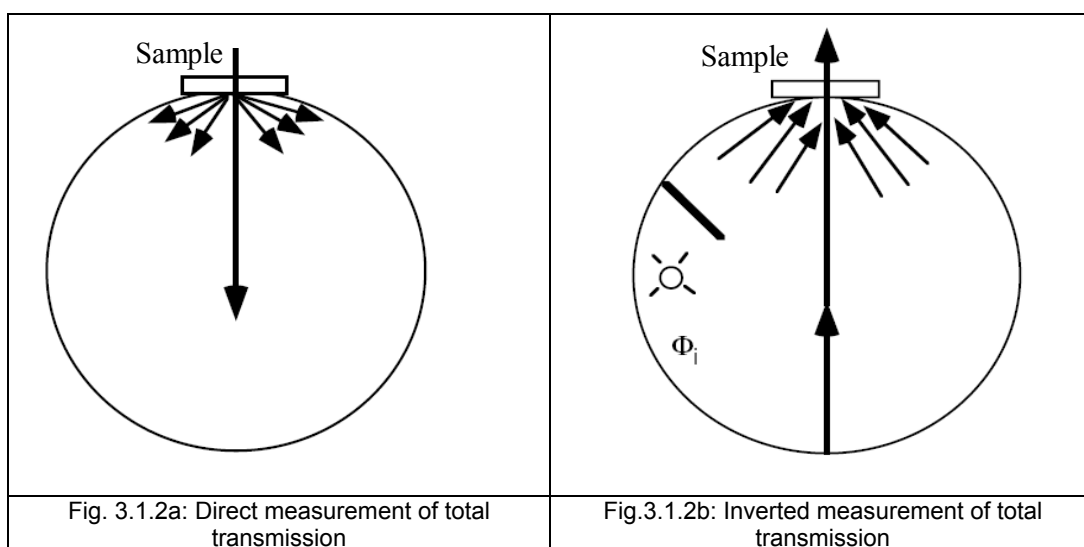
On the basis of these reasons, for this part of the experimental work described in this thesis, a solution spectrophotometer ACS ChromaSensor CS-5 with spherical measuring geometry was adapted for measurement. The instrument was placed in a dark room to eliminate luminous irradiation from other light sources. Fig. 3.1.3 shows the arrangement.

Usually the concentration in solution is roughly100 times lower than that used in this work. In the research described in this thesis such a high concentration was used to provide the possibility to compare the behaviour of photochromic pigments under conditions similar to those given by the pigments inside the polymer, as in the case of mass dyeing.

As discussed above, it is necessary to use a source of excitation to allow measurement of photochromic materials. The main target was experimental work

involving continuous illumination of the measured sample using sources operating in the UV-visible region. Suitable sources are those involving continuous discharge.

Fig. 3.1.3: Optical scheme of the modified spectrophotometer CS-5 with selected light sources for the transmission measurement of photochromic solutions

These light sources have their own individual characteristics of spectral power distribution and thus have abilities to evoke different intensities of the photochromic effect. Most discharge lamps have a bright-line spectrum and in their spectrum there are characteristic spectral gaps. As shown in Fig. 3.1.3, the measuring system is equipped with two test light sources. The experimental set-ups were selected from the range of available light sources, the UV lamp, Deuterium lamp, Germicid lamp and Xenon discharge lamp. Their spectral characteristics are illustrated in the Fig. 3.1.4.

In a test of the spectral sensitivity of photochromic pigments, two independent test light sources were used. This design of this measuring system allows the use of light sources independently or in combination.
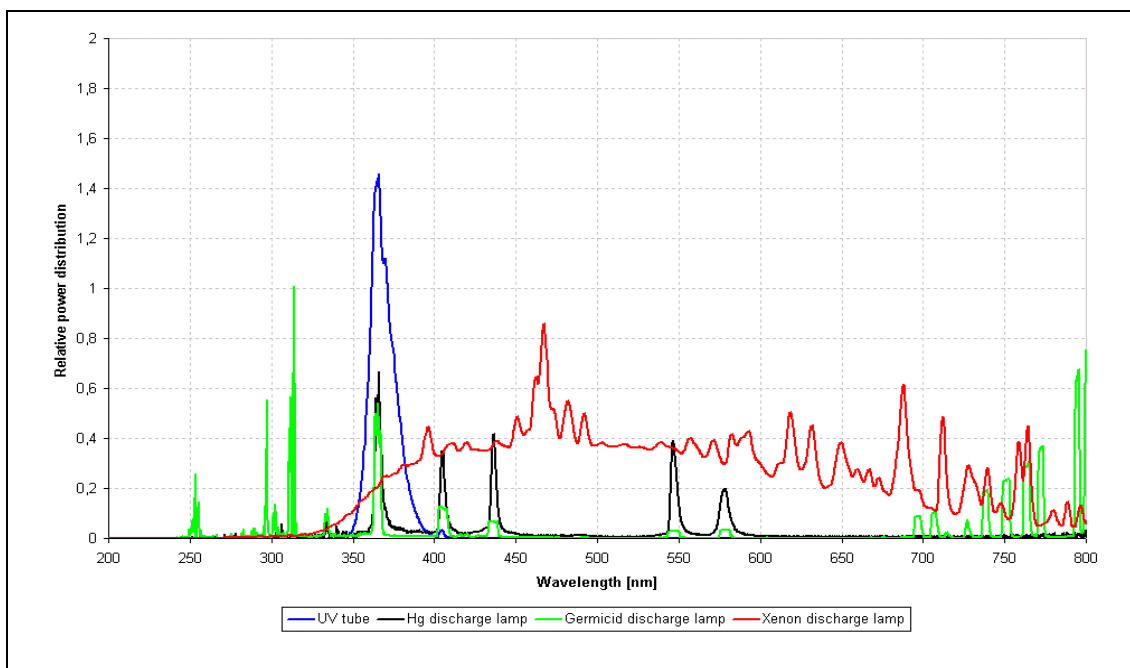
Fig. 3.1.4:   Spectral characteristics of tested exciting light sources

During the measurement of photochromic solutions an interesting problem was observed, which can be described as non-uniform coloration. As shown in Fig. 3.1.3 lateral illumination was used for the excitation. It was observed that only the upper surface was fully coloured while the rest of sample did not develop colour. It appears that the coloured upper surface acts as a UV filter inhibiting photochromic conversion further into the sample.
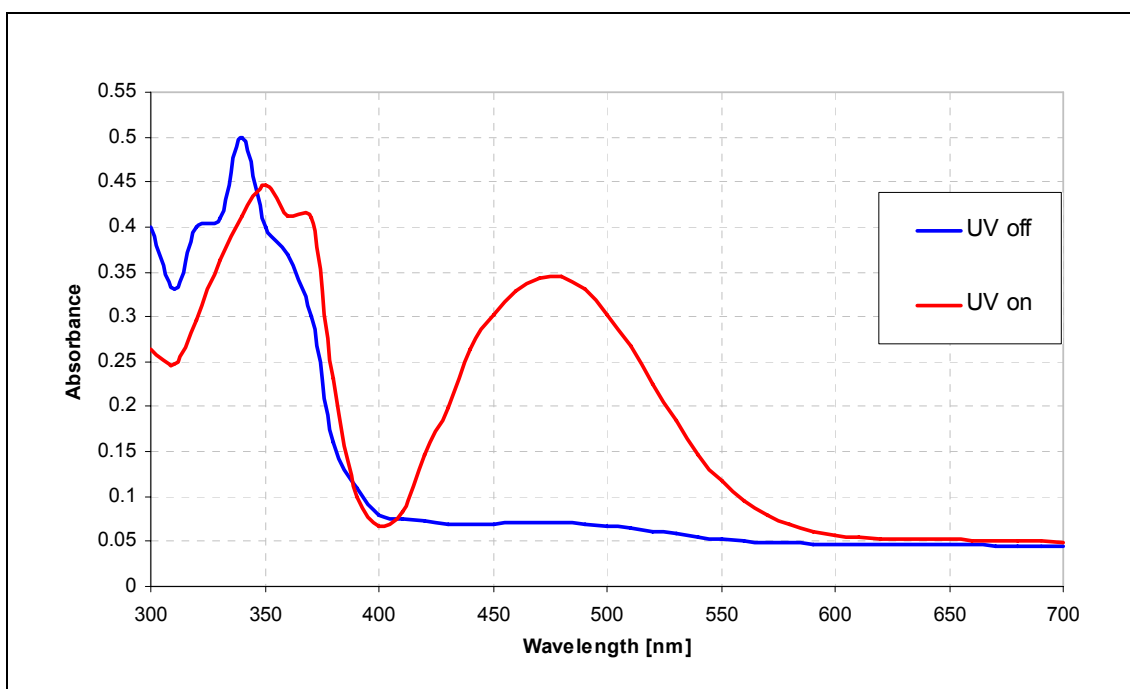

Fig. 3.1.5: Spectral characteristics a of photochromic compound in photostationary state (PS), before and after irradiation (methyl 2,2-bis(4-methoxyphenyl)-6-acetoxy-2H-naphtho-[1,2-b]pyran-5-carboxylate – pigment P3)

As illustrated in Fig. 3.1.5, photochromic materials usually give rise to significant changes in spectral features in the visible and UV regions of the electromagnetic spectrum when irradiated by UV light. However, in the UV region, as the spectra reveal, only a small change in absorption intensity and shift of the absorption maximum is observed as a result of the change in the molecular conformation, which accompanies UV irradiation. From this, it follows that the higher concentration of photochromic compounds has an influence on effectively blocking UV irradiation during transmission.
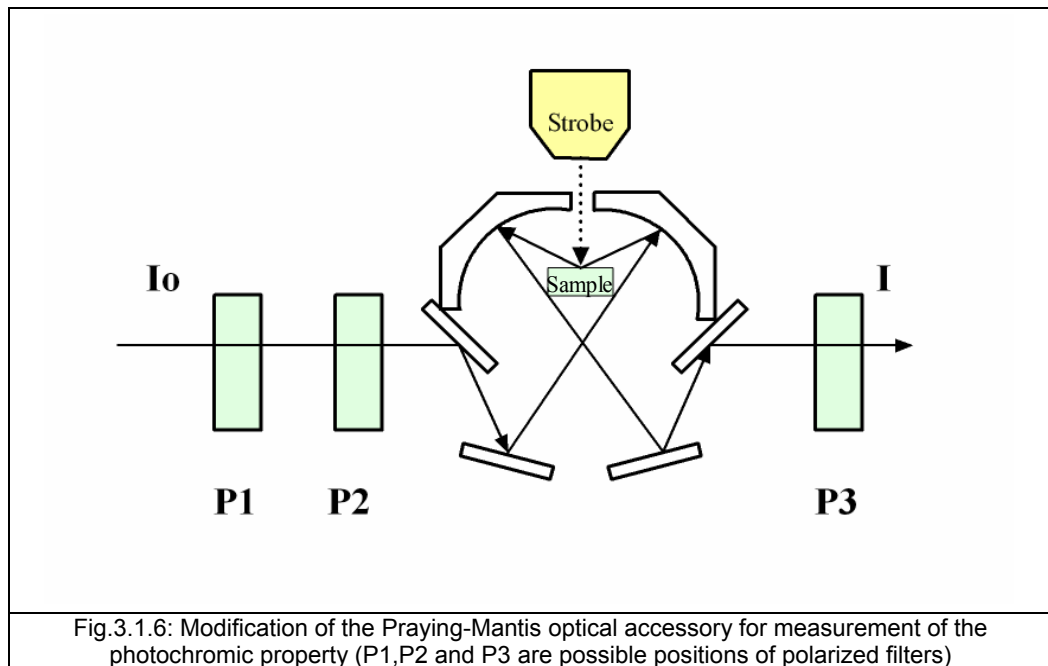
As observed in this experiment, some product at the beginning of the measurement is formed in a thin upper layer of solvent, which separates from the rest of the solution in the cuvette. This results in insufficient homogenization of concentrated, saturated solutions. To eliminate this effect, a hot homogenization process was used, in which the solvent (cyclohexane, C_6H_{12}) was heated to a maximum temperature of 60 ^{o}C. After heating, the photochromic solution was slowly chilled to 25 ^{o}C with continuous mixing. With this technique, sedimentation was eliminated. Together with sedimentation compensation, the set-up for illumination contains excitation together with lateral and axial illumination of the sample with the help of optical mirrors.

(c) Measurement of translucent media by reflectance

In measuring coloured surfaces, the basic problem with a photochromic system becomes the controlled exposure by the selected irradiation. As follows from the previously discussed description of the basic systems of illumination and observation in colorimetric devices, these systems are not usually designed for the incorporation of other light sources. In the case of the analytical spectrophotometer, it is possible to use a simple adaptation of a Praying-Mantis accessory [110,111], which is presented in Fig. 3.1.6. This system allows the incorporation of a light source for irradiation in the measurement of photochromic surfaces. A disadvantage of this system is the reality that only a small area is measured and this configuration can be used only for homogenous smooth surfaces.

Based on this knowledge, the measuring system constructed contains an Avantes USB 2000 spectrometer. This spectrometer was coupled to the measuring

probe by an optical cable 200μm in diameter. The illumination used for excitation was the same combination of light sources as for the measurement of concentrated solutions. There were two exciting sources.

Fig.3.1.6: Modification of the Praying-Mantis optical accessory for measurement of the photochromic property (P1,P2 and P3 are possible positions of polarized filters)

Because the spectrophotometric measurements are based on a comparison of incident and transmitted (reflected) light at individual wavelengths in the visible region of the spectrum, it is necessary to use a special stabilised light source. This light source has added a special cut-off filter GG395, which blocks the radiation of wavelengths lower than 395nm, to eliminate initiation of the photochromic effect by the light source of the spectrophotometer. The optical scheme of the spectrophotometer is shown in Fig. 3.1.7a and Fig. 3.1.7b which also show the detail of the measuring probe.
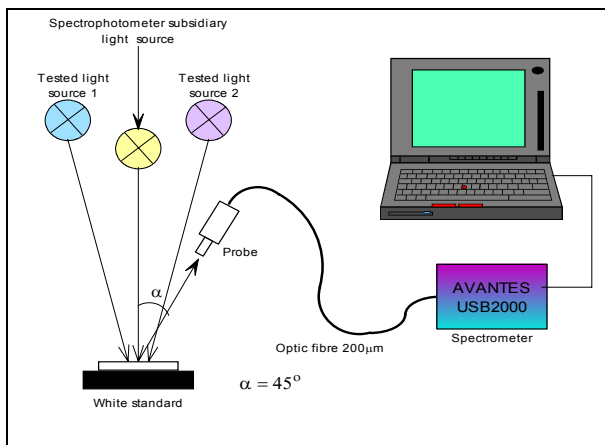

Fig. 3.1.7a: Optical scheme of the measuring system "Photochrom I" for remission measurement of textiles with photochromic prints and mass dyed non woven

Fig. 3.1.7b: Detail of the measuring probe

During the testing of this system, it was observed that for measurement of textile samples it is not suitable to use the angle viewing geometry. This means that in the case where illumination is realised only from one side, the reproducibility is relatively low.

Many commercially available spectrophotometers and colorimeters have cylindrical illumination, in which the illumination is realised by optical fibres or a cylindrical mirror. Nevertheless, the compact construction of the measuring head does not permit simple inclusion of an excitation light source. Optical fibres, which are used for illumination, are not suitable for excitation. A standard optical fibre causes a large reduction in intensity of UV irradiation. In these fibres, the limitations for UV light transmission are the intrinsic attenuation (in dB/m) and additional losses (in dB) due to UV-defects. The intrinsic attenuation is given by Rayleigh-scattering, electronic transitions and a non-structured OH-absorption tail below 200 nm. Most spectroscopic applications with fibre optics have been restricted to wavelength ranges above 230 nm, because standard silica fibres with an undoped core and fluorine doped cladding are frequently damaged by exposure to deep-UV light (below 230 nm). This solarisation effect is induced by the formation of "colour centres" with an absorption band at 214 nm. These colour centres are formed when impurities (such as Cl) exist in the core fibre material and form unbound electron pairs on the Si atom, which are affected by the deep UV radiation. Solarisation resistant fibres use a modified core preform that protects the fibre from the damaging effects of deep UV. These fibres have excellent performance and long-term stability at 30 to 40% transmission (for 215nm). Nevertheless, commercially available solarisation resistant optical fibres are limited in diameter to 1000 μm [112]. The result of a small diameter of the optical fibre is a small area of measured sample, which is irradiated by the excitation irradiation. This problem may be solved by a multi fibre irradiation design. Nevertheless, as was mentioned above, an insufficient space in the measuring head of commercially available spectrophotometers makes this impossible.

Based on this experience, the research described in this thesis employed commercial reflectance spectrophotometers as used by the textile industry. Two spectrophotometers were tested, which were both available at our laboratory:

- Spectraflash SF 300 – geometry d/8, measuring aperture 20mm in SCI mode

- Microflash 200 d – geometry d/8, measuring aperture 5 mm also in SCI mode

Both spectrophotometers have the same diameter of integrating sphere (66mm) and they allow the measurement in both modes SCI (specular component included) and SCE (specular component excluded).

Fig. 3.1.8a: Spectraflash SF 300	Fig. 3.1.8b Microflash 200 d
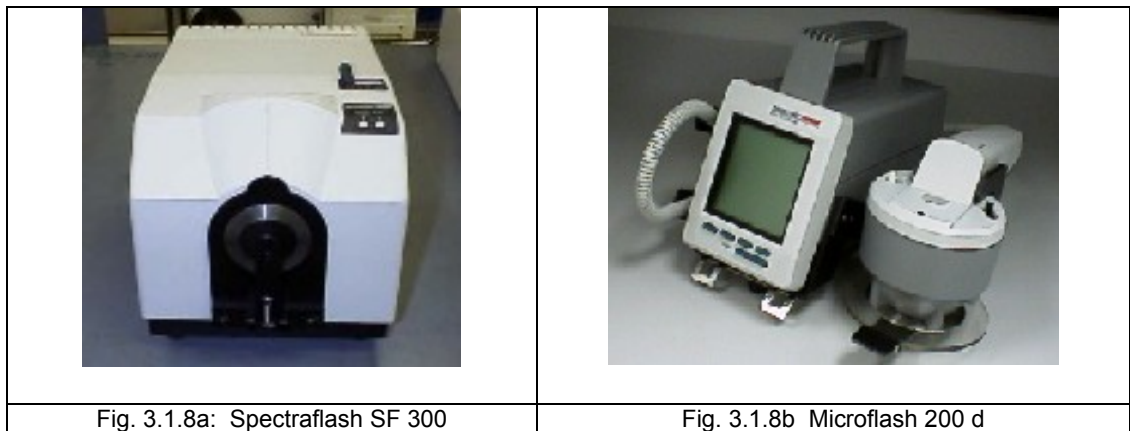
These spectrophotometers are equipped with Xenon lamps as the light source and therefore it was necessary to stop the excitation of the photochromic solution during measurement of spectral and colorimetric characteristics. Similarly, as previously described for this purpose cut-off filters GG395 were used. The cut-off filters were placed between the Xenon lamp and the measuring integrating sphere, to eliminate UV irradiation and the influence on the calibration of the measuring system. The placement of cut-off filter between the sample and aperture of the device presented some problems, such as for example the uncontrolled light outlet in different directions, not only perpendicular to the sample. This type of measurement did not influence the sample during the excitation. There was also the need to solve the issue of the excitation light used to initiate the photochromism.

The first experiment with photochromic pigments applied onto a textile substrate showed that exposure and reversal is relatively long (minutes). The experimentation can be realised as an off-line system, with the exposure first controlled followed by quick measurement of the exposed sample in a stationary exposed state - in equilibrium. For initiation of a photochromic effect, a viewing box JUDGE II (Gretag Macbeth, USA) was used. To increase the effect of UV irradiation, a combination of a D65 simulator and a UV fluorescent tube was used. For illustration of the system used, the configuration of a light box is shown in Fig. 3.1.9a, and the spectral power distribution of the experimental illumination arrangement used is given in Fig. 3.1.9b.
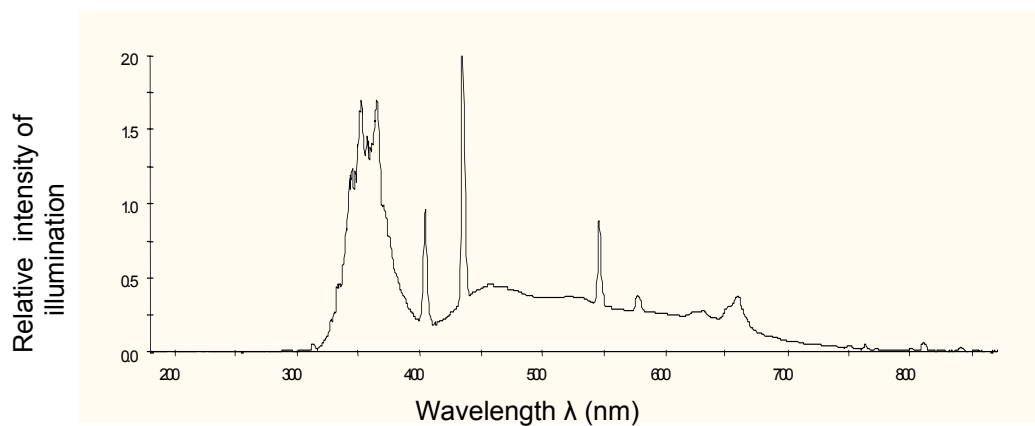
Fig. 3.1.9a: Light box JUDGE II

Fig. 3.1.9b: Spectral characteristic of illumination used (UV fluorescent tube + D65 simulator)

The irradiance or illuminance falling on any surface varies as the cosine of the incident angle, θ. The perceived measurement area orthogonal to the incident flux is reduced at oblique angles, causing light to spread out over a wider area than it would if perpendicular to the measurement plane. For example to measure the amount of light falling on human skin, it is necessary to mimic the skin's cosine response. Since filter rings restrict off-angle light, a cosine diffuser must be used to correct the spatial responsivity. In full immersion applications, such as the phototherapy booth, off angle light is significant, requiring accurate cosine correction optics. The cosine correctors involve spectroradiometric sampling optics, designed to collect radiation (light) over 180°, thus eliminating optical interface problems associated with the light collection sampling geometry inherent in other sampling devices Therefore, the Avantes USB2000 fibre optic spectrometer with cosine corrector was used for measurement of the spectral power distribution of the light sources used. The CC-UV/VIS cosine corrector has an active area of 3.9 mm, with a Teflon® diffusing material and is

optimized for applications from 200-800 nm. These cosine correctors can be used to measure UV-A and UV-B[1] solar radiation, environmental light, lamps and other emission sources.

Besides the cosine corrector, a solarisation resistant optical fibre was used with a diameter of 200 μm. This was necessary to control the spectrometer sensitivity by a calibrated light source, which was also produced by the Avantes company. The AvaLight-DH-CAL is a calibrated light source for the UV/VIS/NIR spectral range (205-1095 nm). This National Institute of Standards and Technology - traceable calibrated light source was developed for use with all AvaSpec spectrometers to be used in measuring absolute spectral intensity. The AvaLight-DH-CAL comes with a cosine corrector with a SMA 905 (SubMiniature version A) connector, which has screw, ferulle diameter is 3.14 mm and usually is used for industrial lasers, military and telecom multimode.
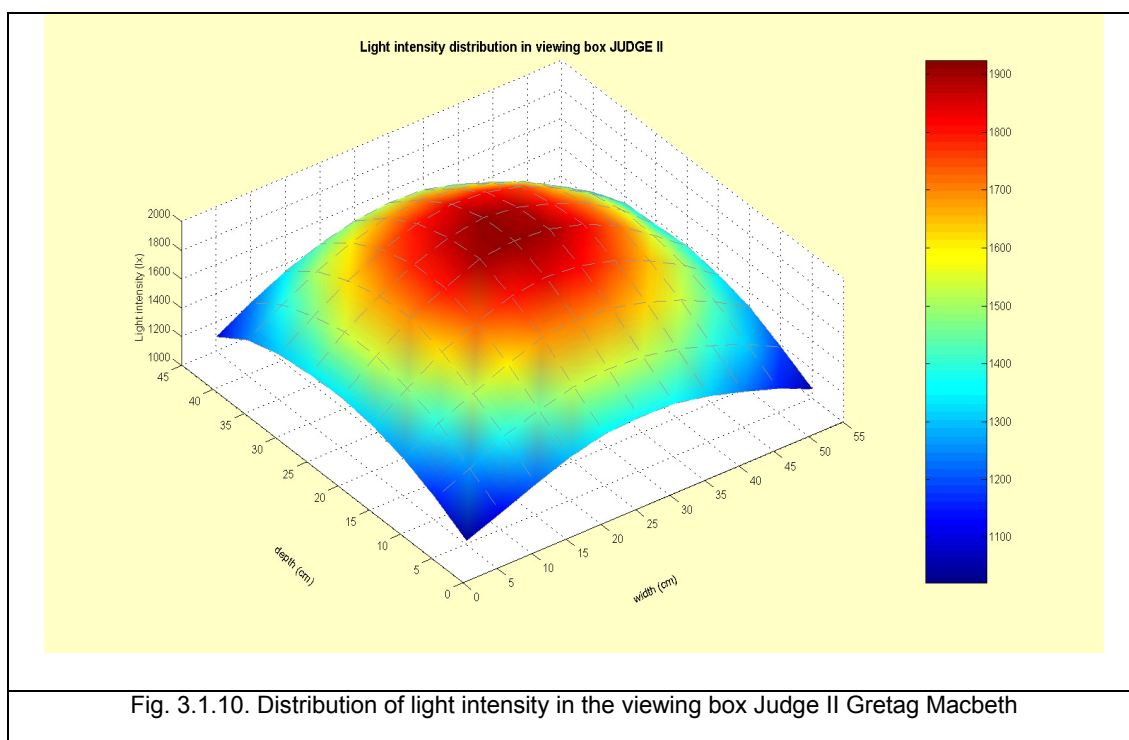
In addition, lighting parameters were measured in the viewing box Judge II Gretag Macbeth, as given in Table 3.1.1. Because the experiment has been realised in the standard viewing box, it was also necessary to establish irradiance intensity and whether, the intensity is constant in all areas of the viewing box. Thus for measurement of illuminance, the illuminance meter Minolta IT10 was used. For measurement of UV-A radiation intensity, an MIT Goldilux Radiometer was used. Illuminance and irradiance results are given in Fig. 3.1.10, where the distribution of light intensity in the viewing box is documented.

Table 3.1.1.: Parameters of light involved in viewing with Judge II Gretag Macbeth

Distance between light source and sample	Illuminance E lx	Irradiance F_e μWcm^{-2}	Irradiance dose H_e μJcm^{-2}	Colour temperature T_C K	Luminous flux Φ lm	Radiant flux Φ_e μW	Radiant energy Q_e μJ
45 cm	979.3	714.6	10.00	6649.4	0.0117	85.37	1.20
31 cm	1754.2	1149.7	16.10	6664.6	0.021	137.3	1.92
21 cm	2631.5	1750.4	24.51	6693.9	0.0314	209.1	2.93
17 cm	3406.7	2077.6	29.09	6713.1	0.0407	248.2	3.47
13.5 cm	4138.3	2436.7	34.11	6743.7	0.0494	291.1	4.08
10 cm	5152.5	2895.0	40.53	6742.8	0.0616	345.8	4.84
6.5 cm	6693.8	3522.5	49.32	6769.7	0.080	420.8	5.89
3 cm	9651.0	4621.7	64.70	6760.2	0.115	552.1	7.73

---

[1] UV-A: 400 – 315 nm, UV-B: 315- 280 nm and UV-C: 280-100 nm [67]

Fig. 3.1.10 illustrates that the maximum of illuminance *E* was in a central position of the viewing box and the area with maximum of illuminance *E* was approximately a rectangle, 5 x 10 cm. These measurements were made after 15 min warm up time. The ratio E_{min}/E_{max} was in a chosen area 0.964.

Fig. 3.1.10. Distribution of light intensity in the viewing box Judge II Gretag Macbeth

The central position with maximum of illuminance *E* was hence used as the target for every exposed sample to obtain the same radiation level during each experiment for each sample.

Table 3.1.1 also documents the changes in exposure dependent on the distance of the sample from the light sources in the viewing box. To obtain constant conditions of exposure for every sample a calibrated telescopic table was used, which was placed inside on the bottom of the viewing box. Every sample was placed on the upper desk of the table, where the distance between the front layer of the sample and the light source used was controlled. This system allowed the use of different distances of sample from light source repeatable way, because the precision of the telescopic table was 10μm.

Measurements of the photochromic substrates were carried out by separate exposure and measurement. Illumination inside the commercial reflectance spectrophotometers was modified by cut-off filter GG395, because it was necessary

to minimize the influence of the spectrophotometer light source on the photochromic effect. On the other side, it was necessary to use external exposure by the selected light source, because these spectrophotometers do not allow simple incorporation of an external light source as an accessory.
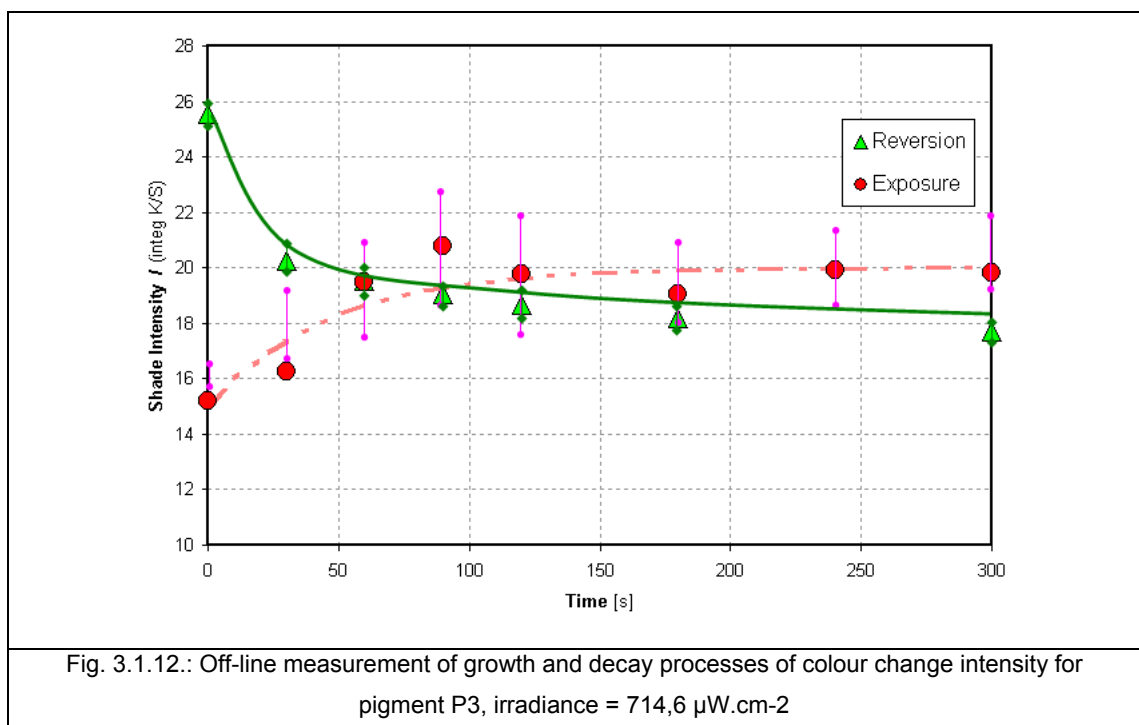
A method where the sample is exposed in one place and after exposure moved to an other place for measurement of actual colour, causes a time delay that is dependent on movement velocity between the place of exposure and the place of measurement. In such methodology, the results show poor reproducibility of measurement of the exposure phase of the photochromic colour change.

Fig. 3.1.11 illustrates the result for 3,3,5,6-tetramethyl-1-propylspiro[indoline-2,3'[3H]pyrido[3,2-f][1,4]benzoxazine] (pigment P1), which was obtained as an average of the ten measurements of both phases. The measured error was less than 1.3% in the reversion phase. This explains, why in the graph given in Fig. 3.1.11, the decay curve errors bars are practically invisible in comparison with those for the exposure curve.

Fig.3.1.11. Off-line measurement of growth and decay processes of colour change intensity for 3,3,5,6-tetramethyl-1-propylspiro [indoline-2,3'[3H] pyrido [3,2-f][1,4]benzoxazine] (pigment P1), irradiance = 714,6 µW.cm^{-2}
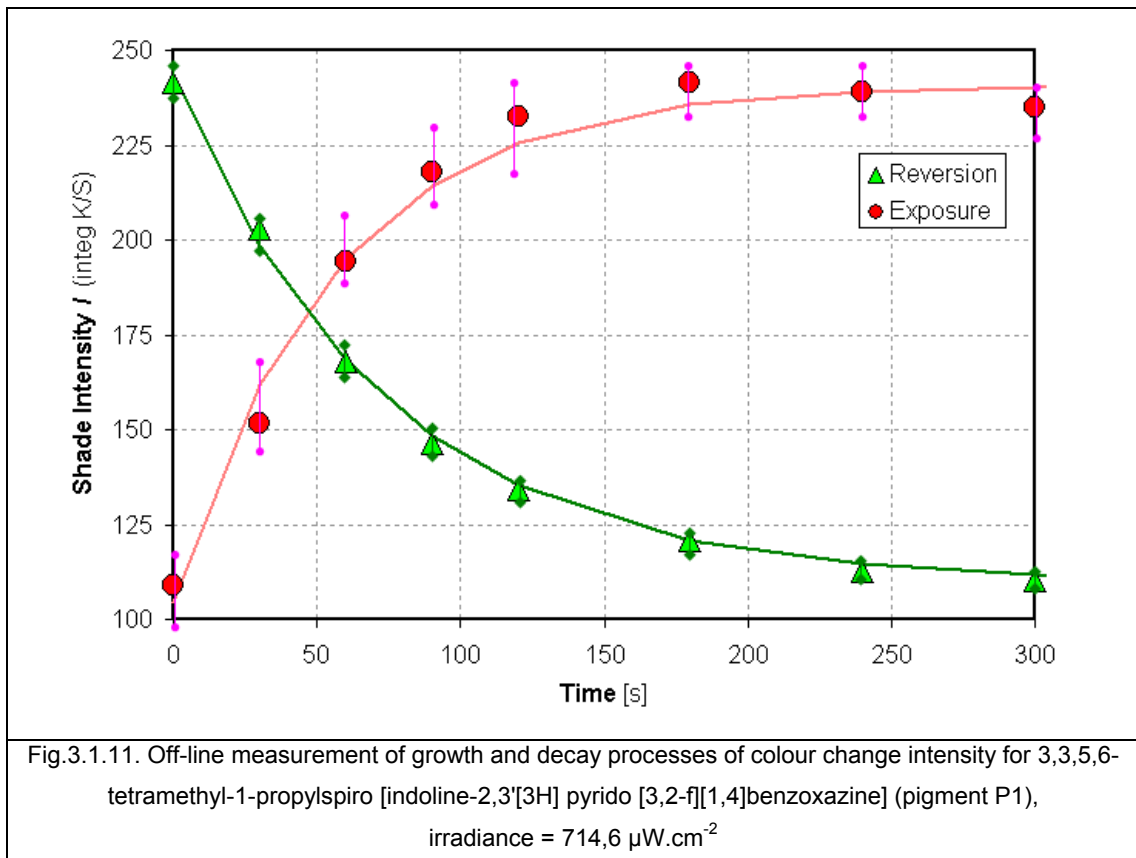
It is evident that the variability of measurement in the decay phase from the maximum from which the decay phase starts is lower. The lower variability during

the decay phase documents that the problem of high variability during the exposure phase is caused by the variability of the time delay between exposure and colour measurement, because the sample is moved from one place to another place. The variation of the measured data set for exposure is dependent also on the rate of photochromic colour change as Fig. 3.1.12 documents. There is higher variance for a sample with the pigment based on the chromene system, [34] - methyl 2,2-bis(4-methoxyphenyl)-6-acetoxy-2H-naphtho-[1,2-b]pyran-5-carboxylate (pigment P3). It is possible to use the model of first order kinetics in the case of this data set, but the precision of measurement is lower. The maximum of photochromic colour intensity is lower in the case of exposure than the maximum from which the decay phase starts. The reason in the case of the measurement of the sample with pigment P3 is associated with the methodology of measurement. The problem is the impossibility of exposure of the photochromic sample during measurement using a standard commercial spectrophotometer.

Fig. 3.1.12.: Off-line measurement of growth and decay processes of colour change intensity for pigment P3, irradiance = 714,6 µW.cm-2

The procedure for obtaining the data set was as follows. First, the data set in the decay phase for individual time cycles was obtained. This means that the sample was exposed for 15 minutes and then was removed from the place of exposure directly to the measuring aperture of the spectrophotometer. Measurement of shade intensity I was conducted at 0, 30, 60, 90, 120, 180, 240, 300 and 600 second intervals. The data set for exposure was obtained via exposure of the sample followed

by immediate measurement of colorimetric parameters.   After exposure, the relaxation phase of the sample was continued in a black box. The time of relaxation was constant at 15 minutes. The time scale for the exposure phase was the same as for reversion phase, ie., 0, 60, 90, 120, 180, 240, 300 and 600 seconds.

The method for obtaining the data set for photochromic colour change on exposure is similar to the fatigue test and does not involve continuous exposure. From the above-mentioned description, it is evident that instead of cyclic exposure this method has the problem of scattering due to the time delay between the exposure and the measurement. Effort was made to minimize the delay (there was a team) but it was not possible to minimize this problem for a "quicker speed" system.

Based on this, there was a necessity to develop a special measuring system, which allowed the measurement of a textured photochromic colour surface. In the case of textured photochromic surfaces, it was necessary to use the adaptation of a hemispherical illumination in the integrating sphere, so that it was possible to include another aperture for irradiation [113,114,115]. The optical scheme of the system, now patented, is given in Fig. 3.1.13.

Fig. 3.1.13: Optical scheme of LCAM PHOTOCHROM2 measuring system
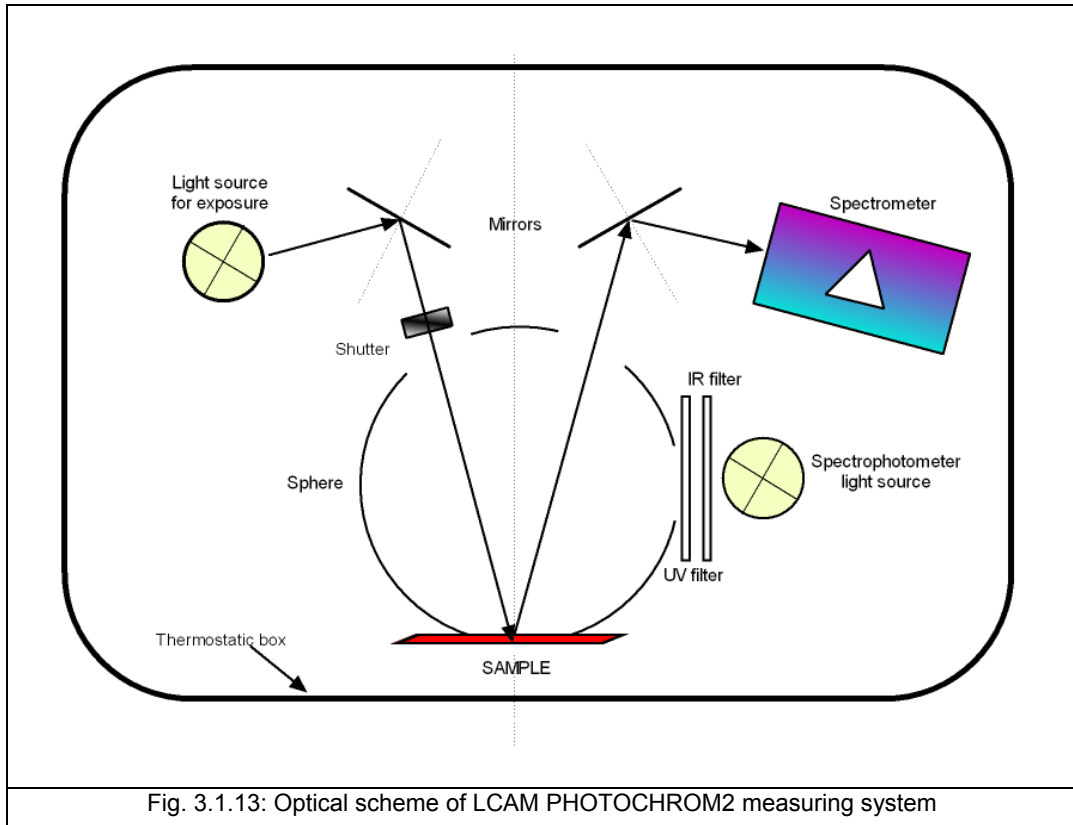
Due to the hemispherical illumination, the problem of the texture of the textile samples was eliminated. Because the reversion from the coloured form to the colourless form is promoted thermally, the photochromic structure will achieve lower saturated absorbance at higher temperatures than at lower temperatures. This phenomenon is known as *temperature dependency* and for example, oxazine structures are more sensitive in comparison to naphthopyrans [116]. Fig. 3.1.14 shows the temperature dependence of three photochromic pigments based on Photopia® AQ Ink systems in which the yellow and blue dyes are structures based on naphthopyrans [117] and purple (purpur) dyes on the oxazine structure in which K/S values were calculated at the appropriate absorption maximum.

Fig. 3.1.14: Temperature dependence of three photochromic pigments in Photopia® AQ Ink (Matsui, Int. Comp., Inc. Japan) on textile substrate [116]
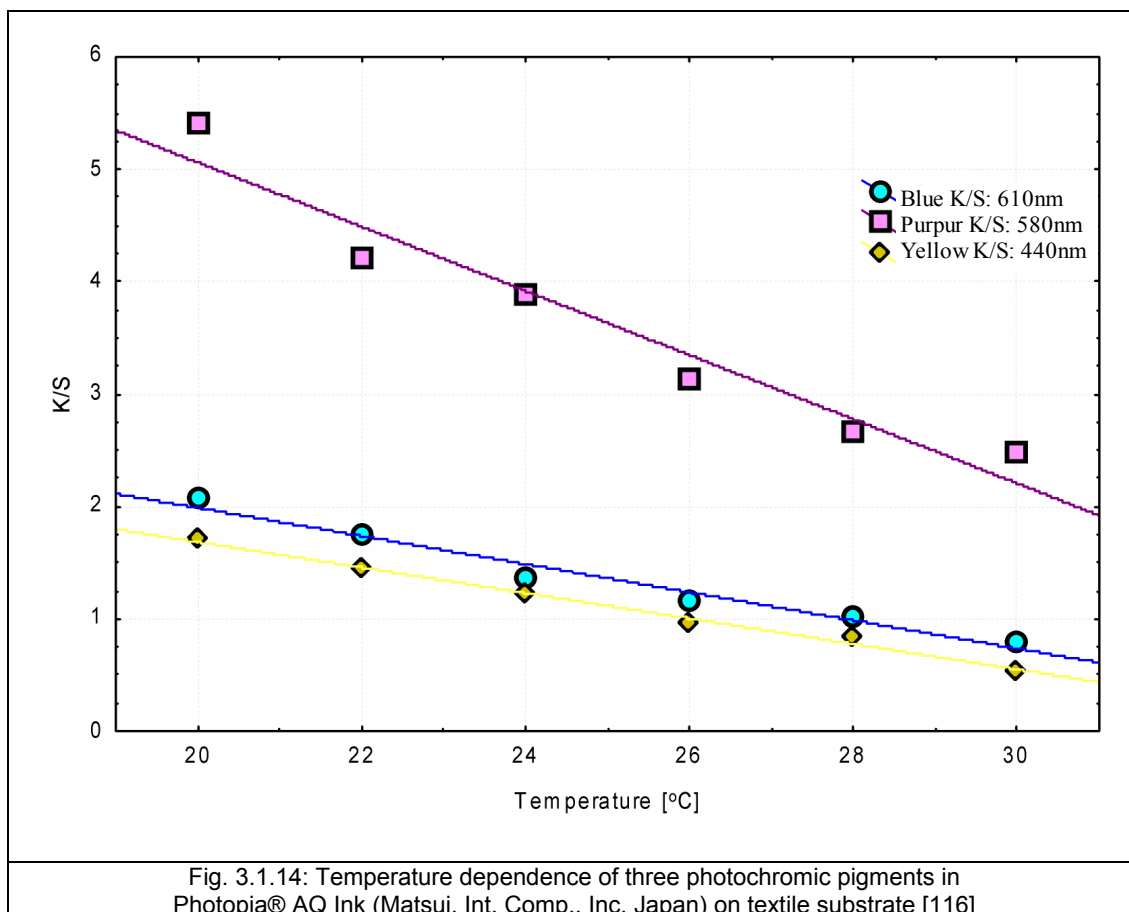
Recognising that photochromic colour change is affected by temperature, there was a necessity to carefully stabilize the temperature of the sample during measurement. If the temperature is not stabilized, it is possible to observe local fading of colour during exposure. This phenomenon is illustrated in Fig. 3.1.15a and 3.1.15b. Local fading can be influenced by increasing the temperature of the measured sample

or by photobleaching of the photochromic pigment. Nevertheless, for the measured samples after thermal stabilization this phenomenon was not observed.
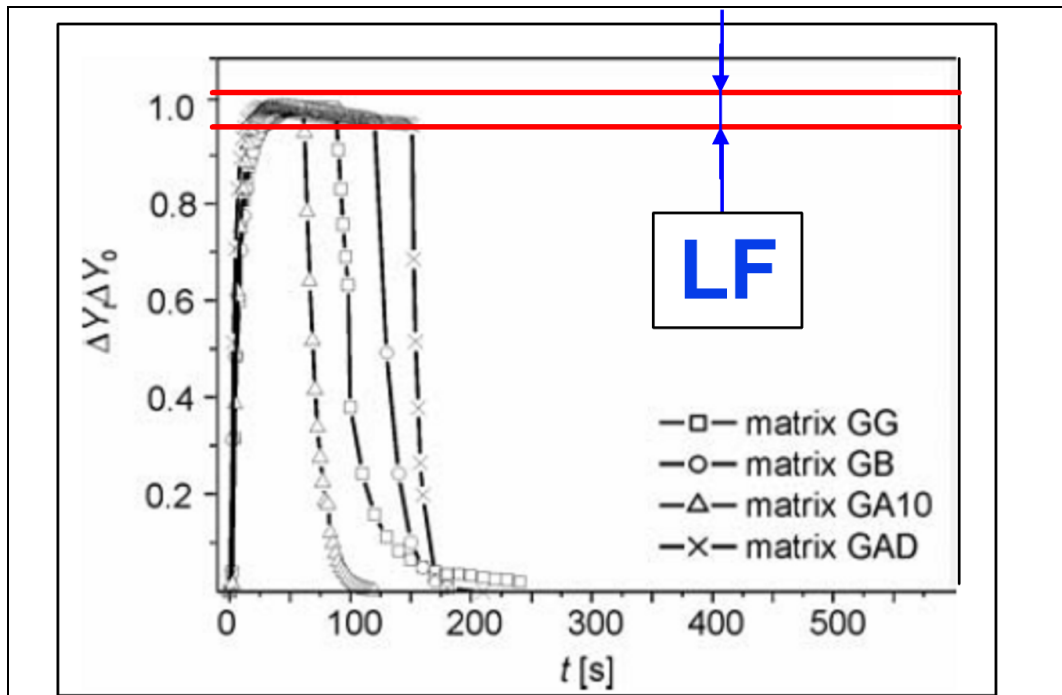

Fig. 3.1.15a: On/off kinetics of spirooxazines entrapped in the four hybrid polymer matrices [119], where ΔYt – change of luminous transmittance after irradiation for a given time t, ΔY0 – change of luminous transmittance at maximum colouration (photochromic activity) and LF – local fading effect
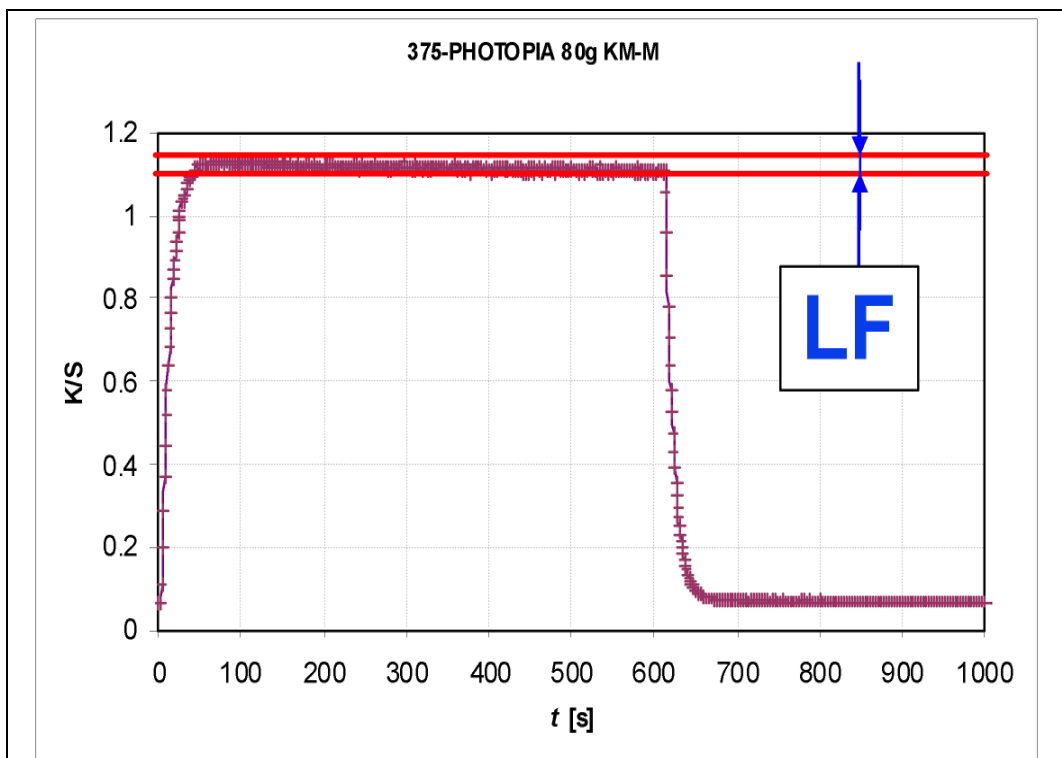

Fig. 3.1.15b: On/off kinetics of Photopia® AQ Ink Blue [118] (LF – local fading effect)

A final problem that needed to be solved in the construction of the unique spectrophotometer was the question of spectral sensitivity of the selected samples of photochromic textile materials. The light sources selected in the first part of the development of a system for measurement of colorimetric and spectrophotometric data for photochromic textiles were tested. Except for the Xenon lamp, all sources had spectral lines. This is evident also for the UV lamp, which is a short band pass light source. The disadvantage of this source is the presence of many gaps in the spectrum and these gaps can negatively influence measurement results. The absorption spectra of the photochromic systems examined are quite different and thus the monochromatic stimulation at specific wavelengths based on the light source affects the response obtained from the photochromic systems. In section 4.5 the spectral sensitivity of the photochromic systems tested based on a bi-spectral type of measurement is illustrated, demonstrating where the relative visible spectral sensitivity of the photochromic systems is different.

In the second part of the construction and adaptation of the measuring system, which allows the measurement of spectral sensitivity, the interference filters were used. These filters can be used as a Mercury line set at a 10nm band pass in combination with the Xenon lamp 100W. The main aim was to find out the wavelength where the pigments have highest sensitivity (i.e. the shade is the deepest) and other set up parameters are constant. After the first tests, it was evident that the intensity of transmitted light was not sufficient for excitation of the photochromic effect and the intensity of developed shade was low. From this consideration, a Xe lamp 450W was used as excitation light source with sufficient amount of radiance. Therefore, it was decided to use a monochromator based on a diffraction grating and a 450W Xe lamp. This monochromator has the advantage that the intensity of excitation illumination may also be modulated by the size of slit.

The final system, LCAM Photochrom 3 shown in Fig. 3.1.17b, is a system which allows the study of photochromism kinetics, the influence of exposure time, the thermal sensitivity, and in this case includes a test for the spectral sensitivity of the photochromic samples via an excitation monochromator [120]. The dual light source construction of the spectrophotometer with the shutter over the exciting light source makes possible continuous measurement of photochromic colour change during exposure and reversion after the shutdown of the exciting light source. A Xenon discharge lamp with continuous discharge was used. Pulsed discharge lamps

allow using such system as a fatigue tester for photochromic systems with a halflife of the photochromic colour change around 500 ms. For textile samples, which are frequently slower, it is advantageous to use an electronic shutter and a continuous discharge lamp for fatigue tests.
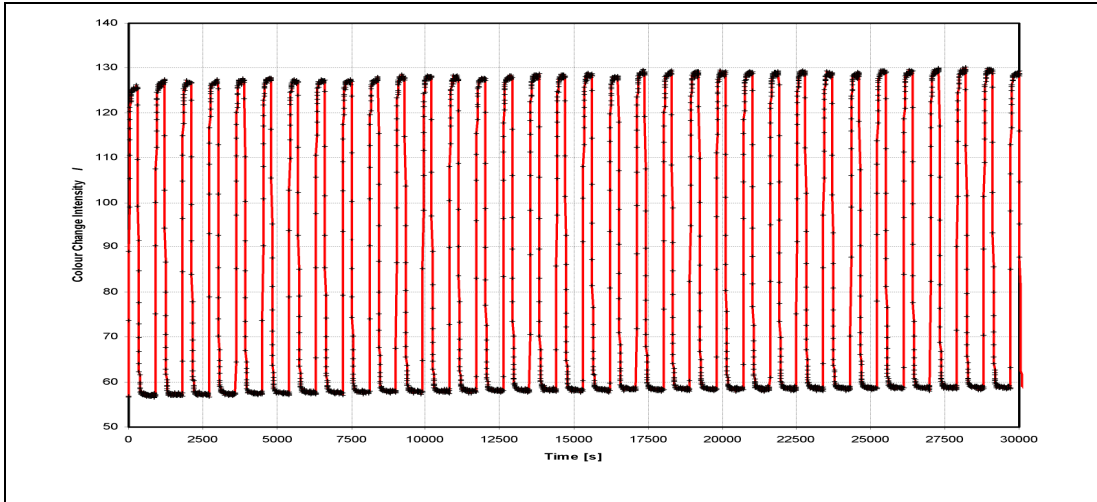

Fig. 3.1.16: Selected part of a cyclic fatigue test on a photochromic textile sensor of UV-A radiation

The basic difference between the "LCAM-Photochrom 3" system which is shown on Fig. 3.1.17b and a standard spectrophotometer is in the continuous illumination of the sample against a flash source that is used as standard. In such a measuring system, it is possible to use a flash discharge lamp. The reflectance values obtained are independent of whether it is a Xenon, Mercury or other strobe source. This construction allows measurement of the colour change of the sample in fast scans without disturbing the drift of the light source. The system developed allows 5ms intervals between each measuring scan. Nevertheless, it was found that 5 seconds was a sufficient interval for the above-mentioned samples (see Fig. 3.1.17a).
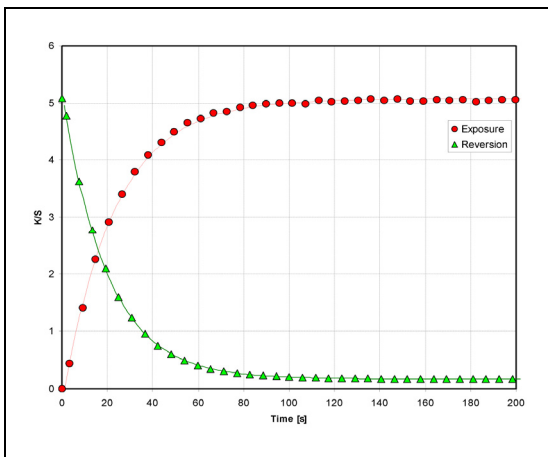

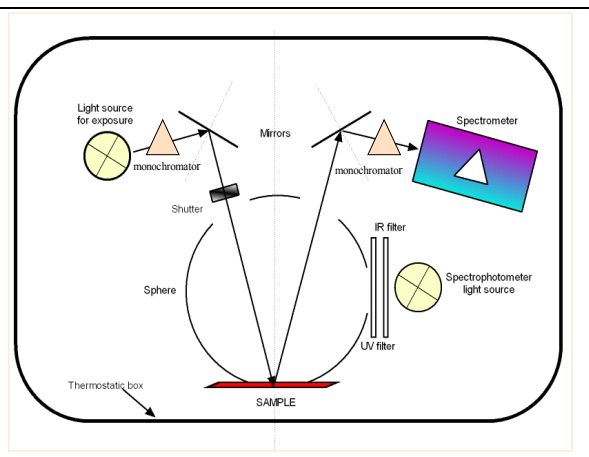| Fig. 3.1.17a: On/off kinetics of Photopia® AQ Ink Purpur	Fig. 3.1.17b: Prototype of measuring system PHOTOCHROM3

A demonstration of the reproducibility of the Photochrom3 system is given in Table 3.1.3 and Fig. 3.1.18. In this case, data sets are for 10 different individual samples. The results show the presence of experimental errors, which are due to the measuring system, are together with the influence of the method of preparation of individual samples. In the case of the repeatability of device Photochrom 3, the data in Table 3.1.2 are presented. These data result from the short-term drift test procedure, when the white tile from the BCRA set was measured 20 times with 30s delay between each measurement. These data allow the calculation of the total colour difference for the short time drift test.

Table 3.1.2.: Results of short-term drift test of Photochrom 3 at selected wavelengths

Wavelength /nm/	Max.	Dev.	Var.	Avg.	Min.
400	82.924	0.019676	0.000387	82.889	82.853
410	85.292	0.013793	0.00019	85.269	85.248
420	86.399	0.012472	0.000156	86.379	86.358
430	87.258	0.011302	0.000128	87.238	87.208
440	87.639	0.013204	0.000174	87.61	87.585
450	87.997	0.012006	0.000144	87.968	87.944
460	88.518	0.008822	7.78E-05	88.503	88.483
470	88.933	0.011291	0.000127	88.912	88.893
480	89.277	0.011487	0.000132	89.248	89.228
490	89.408	0.010947	0.00012	89.388	89.372
500	89.648	0.010547	0.000111	89.633	89.613
510	89.776	0.010234	0.000105	89.759	89.737
520	89.844	0.008499	7.22E-05	89.826	89.81
530	89.96	0.009867	9.73E-05	89.939	89.918
540	90.026	0.008814	7.77E-05	90.009	89.995
550	90.097	0.009828	9.66E-05	90.079	90.06
560	90.109	0.010585	0.000112	90.093	90.074
570	90.043	0.009835	9.67E-05	90.023	90.007
580	90.001	0.01206	0.000145	89.973	89.955
590	90.084	0.01413	0.0002	90.056	90.032
600	90.208	0.012253	0.00015	90.186	90.165
610	90.271	0.010178	0.000104	90.254	90.235
620	90.299	0.009605	9.22E-05	90.278	90.263
630	90.3	0.011661	0.000136	90.277	90.254
640	90.317	0.010453	0.000109	90.298	90.279
650	90.404	0.008649	7.48E-05	90.379	90.365
660	90.483	0.00923	8.52E-05	90.461	90.446
670	90.55	0.00773	5.97E-05	90.536	90.518
680	90.69	0.010254	0.000105	90.671	90.642
690	90.761	0.009345	8.73E-05	90.742	90.719
700	90.812	0.009195	8.45E-05	90.793	90.773

Table 3.1.3.: Parameters of measured reproducibility K/S function for sample
Photopia Blue , t=20^{0}C, no. of samples 10

| Time (s)	Avg.	Dev.	Var.	Min.	Max.
0.73	0.27764	0.009866	9.73324E-05	0.258303	0.296977
6.53	0.60607	0.102576	0.010521842	0.405021	0.807119
12.31	1.30319	0.058624	0.003436765	1.188287	1.418093
17.39	1.67229	0.040243	0.001619483	1.593414	1.751166
22.54	1.86343	0.038791	0.001504776	1.787399	1.939461
28.2	1.9707	0.039743	0.001579528	1.892803	2.048597
33.99	2.03093	0.039798	0.00158387	1.952926	2.108934
39.48	2.06344	0.040655	0.001652806	1.983757	2.143123
44.74	2.0828	0.042192	0.001780148	2.000104	2.165496
50.37	2.09062	0.044602	0.001989348	2.0032	2.17804
55.65	2.10021	0.046383	0.002151409	2.009299	2.191121
61.05	2.10499	0.0445	0.001980291	2.017769	2.192211
66.23	2.10937	0.042407	0.001798344	2.026253	2.192487
71.55	2.10994	0.043612	0.001902002	2.024461	2.195419
76.68	2.11581	0.042303	0.001789523	2.032897	2.198723
82.07	2.11694	0.042731	0.001825916	2.033188	2.200692
87.41	2.12045	0.047027	0.002211554	2.028277	2.212623
92.72	2.1215	0.0433	0.00187493	2.036631	2.206369
97.73	2.12006	0.044299	0.00196244	2.033233	2.206887
103.13	2.11952	0.045088	0.002032948	2.031147	2.207893
108.82	2.1228	0.047632	0.002268794	2.029442	2.216158
114.05	2.12144	0.044026	0.001938322	2.035148	2.207732
119.17	2.12385	0.0456	0.002079338	2.034474	2.213226
124.64	2.11964	0.047705	0.002275802	2.026137	2.213143
129.9	2.12185	0.051068	0.002607929	2.021757	2.221943
135	2.1197	0.048493	0.002351562	2.024654	2.214746
140.08	2.12063	0.052327	0.002738164	2.018068	2.223192
145.13	2.12228	0.051864	0.002689864	2.020627	2.223933
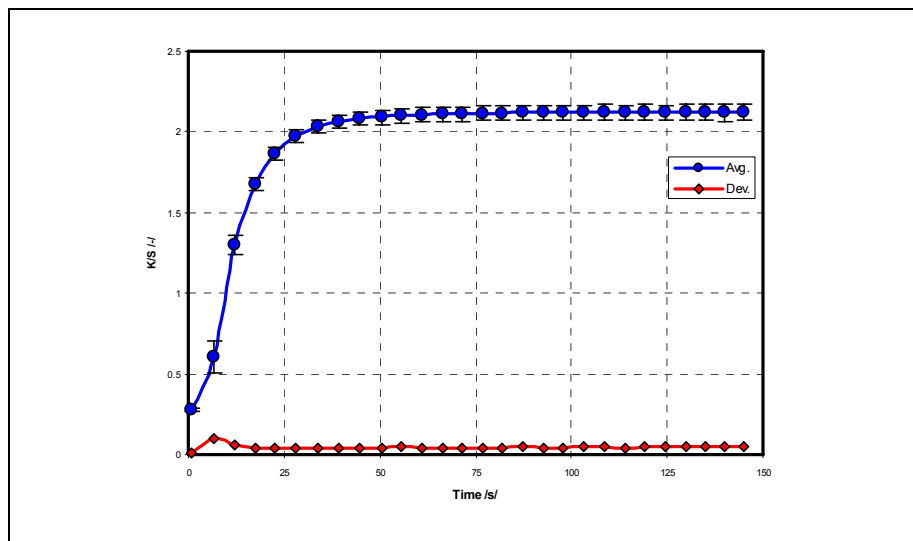
Fig. 3.1.18: Reproducibility of the measurement the K/S function for Photopia Blue, t=20^{0}C

75

3.1.3. Light fastness tests

In the case of photochromic materials, the assessment of lightfastness has its own particular specificity. Standard light fastness tests have been devised for traditional dyes and pigments. In the case of photochromic materials, because of their dynamic colour change properties fatigue tests are relevant.

Standard light fastness tests may use outdoor exposure in selected locations or exposure devices, which use artificial illumination. The standard ISO 105-B02 describes the test with artificial illumination [121]. In this thesis, a Xenotest 450 LF test apparatus has been used modified to provide colorimetric measurement of photochromic samples. The spectral response of photochromic samples is measured before and after the light fastness test. Spectral properties were measured 15 minutes after exposure in a viewing box. Based on the information it was possible to compare two parameters – the colour change of photochromic samples after the lightfastness test and the decrease of the extent of the photochromic colour change. Because photochromic materials do not have high light fastness, the light fastness test was arranged involving 10 cycles with 1 hour exposure in the Xenotest apparatus. It was found that some of the samples have a stepwise reversion phase of the photochromic cycle – the samples have a quick and slow part of the reversion phase. The total number of exposure cycles was 10 with 24 hours relaxation before re-measurement. After every hour the reflectance characteristics of all samples were measured by the spectrophotometer. Because some pigments had a residual coloration from previous illumination, similar measurements were also arranged after 24-hour relaxation. From the observation, if the samples gave a photochromic response, the samples were exposed and once again measured.
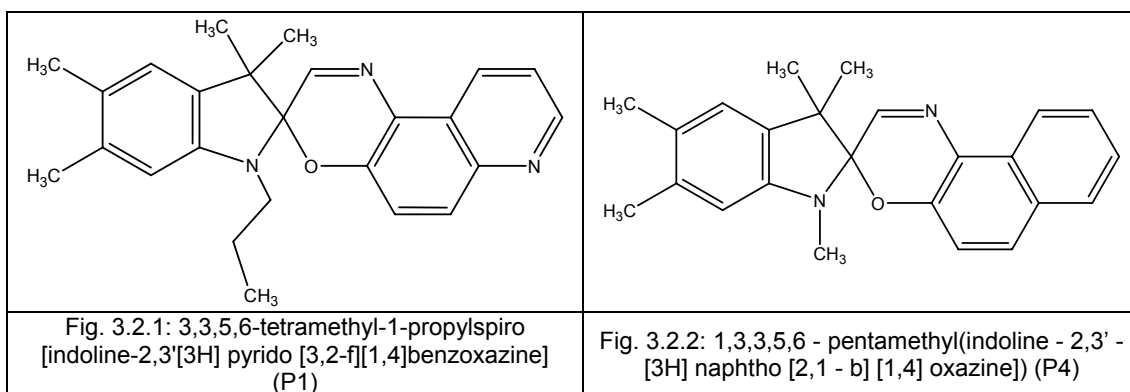
As discussed in the case of photochromic textiles, instead of the resistance against continuous exposure to a light source containing UV irradiation, it is also necessary to study the number of cycles, which the photochromic system can realize.

The number of possible cycles can theoretically be infinite. Therefore, the limitation was used involving a 50% reduction in the photochromic response (50% intensity of coloration).
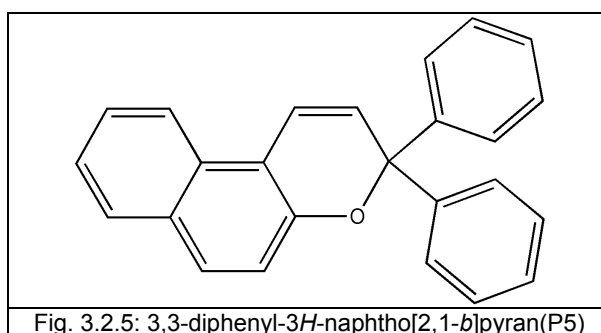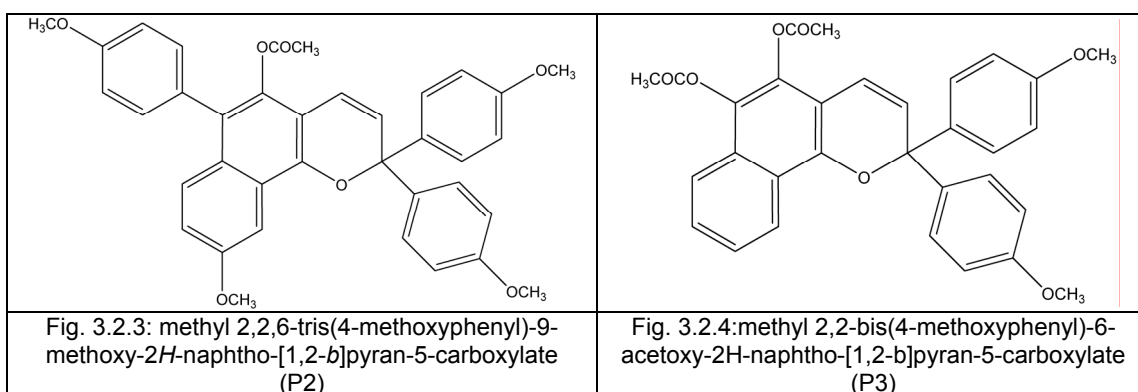
Based on discussion with the dye manufacturer, the number of cycles was limited to 200. The exposure was for 5 minutes and relaxation was for 10 minutes before repetitions of exposure.
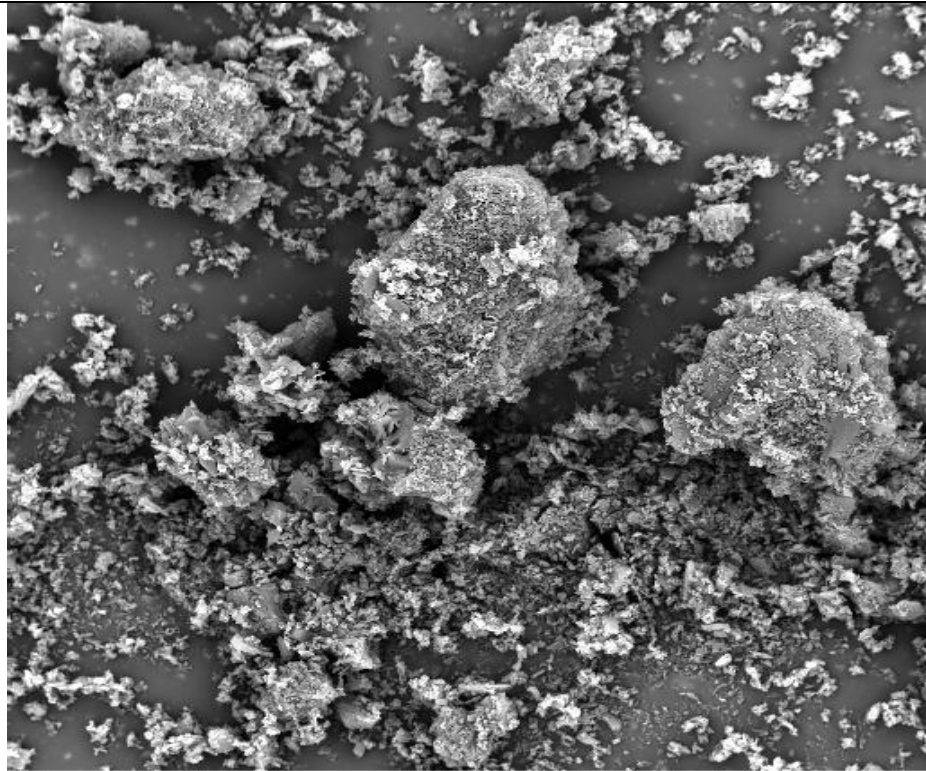
3.2 Materials

The main aim of this thesis is the examination of the kinetic behaviour of photochromic pigments applied onto a textile substrate. It was decided to use commercial photochromic pigments, from which two oxazine structures – P1 and P4 were selected. Figs. 3.2.1 and 3.2.2 show their chemical structures. A description of the properties of the pigments is given in Table 6(Appendix A).

Fig. 3.2.1: 3,3,5,6-tetramethyl-1-propylspiro [indoline-2,3'[3H] pyrido [3,2-f][1,4]benzoxazine] (P1)

Fig. 3.2.2: 1,3,3,5,6 - pentamethyl(indoline - 2,3' - [3H] naphtho [2,1 - b] [1,4] oxazine]) (P4)

Also 3 chromene structures were selected – two 1,2-b pyrans and one 2,1-b pyran.

Fig. 3.2.3: methyl 2,2,6-tris(4-methoxyphenyl)-9-methoxy-2H-naphtho-[1,2-b]pyran-5-carboxylate (P2)

Fig. 3.2.4:methyl 2,2-bis(4-methoxyphenyl)-6-acetoxy-2H-naphtho-[1,2-b]pyran-5-carboxylate (P3)

Fig. 3.2.5: 3,3-diphenyl-3H-naphtho[2,1-b]pyran(P5)

None of the pigments used were soluble in water. Four pigments were delivered as powders with different fineness of particles and pigment P4 was delivered as a granulate. This situation is documented from scanning electron microscope (SEM) photomicrographs as illustrated in Figs. 3.2.6.a-e.
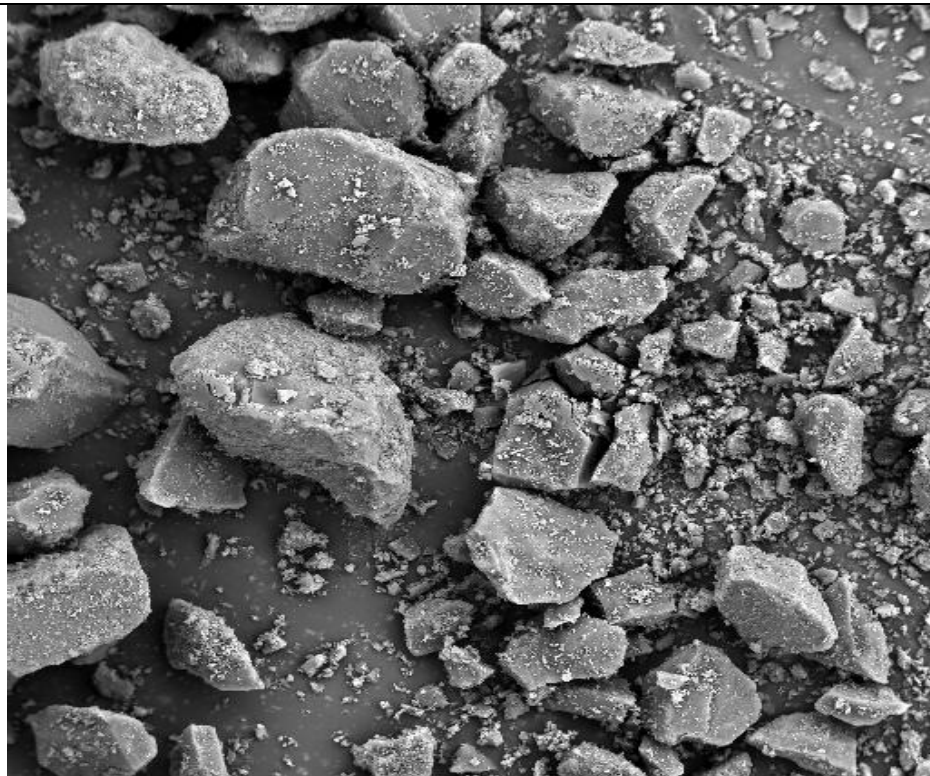
SEM MAG: 300 x DET: BE Detector 200 µm Vega ©Tescan
HV: 30.0 kV DATE: 01/19/04 TU Liberec

Fig. 3.2.6a: SEM pigment P1

SEM MAG: 150 x DET: BE Detector 200 µm Vega ©Tescan
HV: 30.0 kV DATE: 01/19/04 TU Liberec

Fig. 3.2.6b: SEM pigment P2
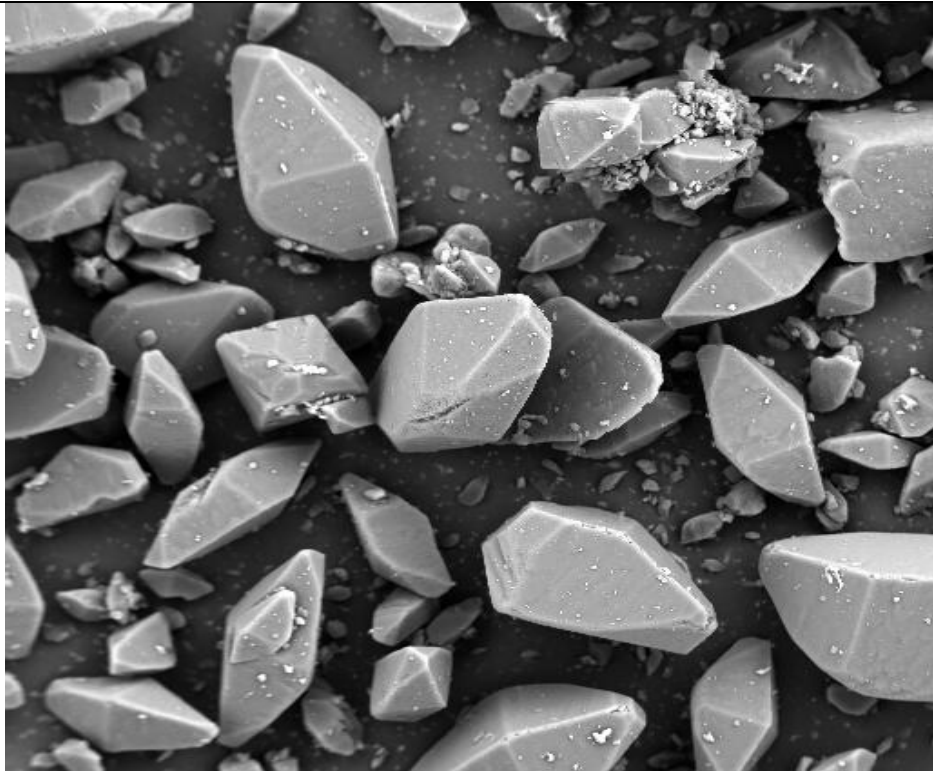
SEM MAG: 150 x   DET: BE Detector
HV: 30.0 kV   DATE: 01/19/04   200 µm   Vega ©Tescan TU Liberec
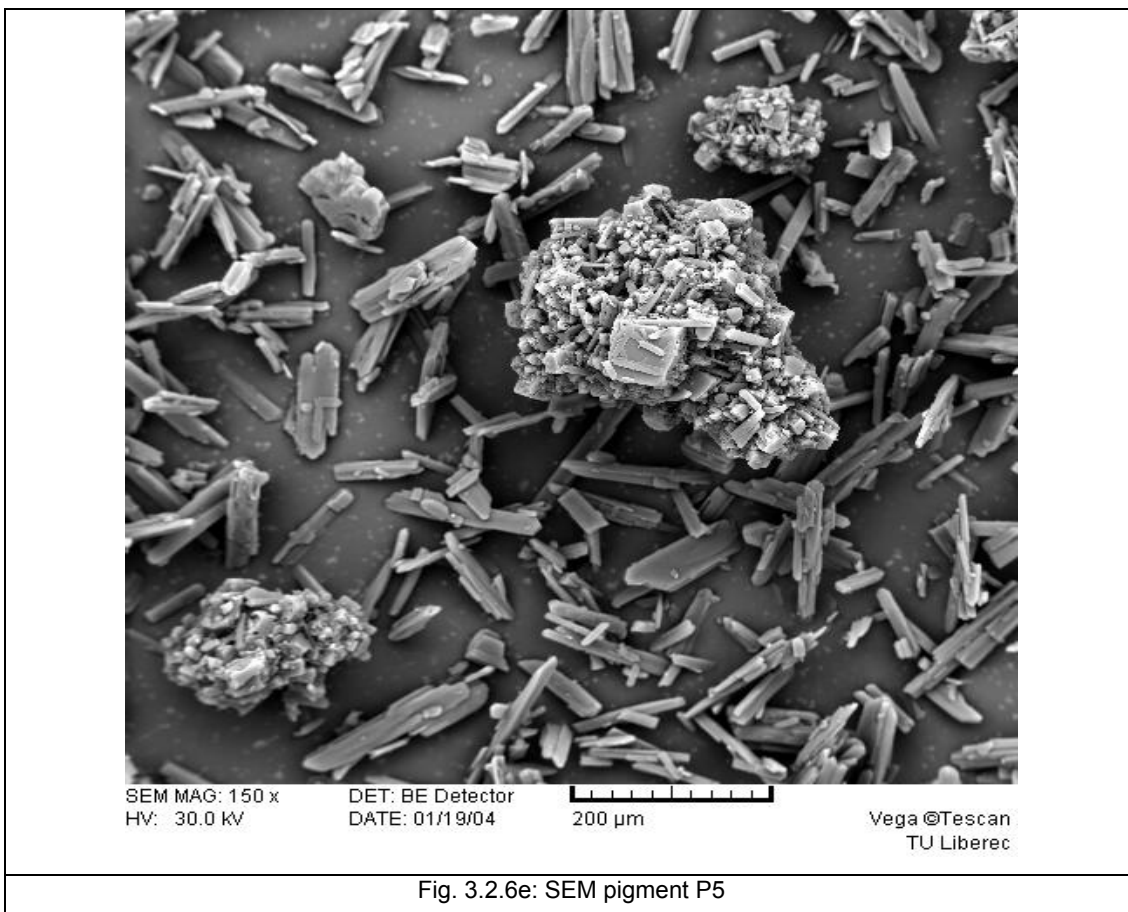
Fig. 3.2.6c: SEM pigment P3

SEM MAG: 80 x   DET: BE Detector
HV: 30.0 kV   DATE: 01/19/04   500 µm   Vega ©Tescan TU Liberec

Fig. 3.2.6d: SEM pigment P4

| SEM MAG: 150 x | DET: BE Detector | | Vega ©Tescan |
| HV: 30.0 KV | DATE: 01/19/04 | 200 µm | TU Liberec |

Fig. 3.2.6e: SEM pigment P5

Experimental technologies were investigated which allowed application of the pigment onto the textile substrate or inside the fibres and which allowed the optical effect of the photochromic pigments to be observed. The technology of dyeing from organic solvent was rejected due to ecological reasons and dyeing in supercritical carbon dioxide was also discounted on the basis of the high costs of machinery. It is possible to use padding as for vat dyes, but in this case, powders are needed with submicron dimensions. In our case, pigments were used where the average dimension was around 150 µm and pigment P4 existed as granules of length up to 0.5mm.

From the other technologies available, only screen-printing, stencil printing and mass dyeing appeared applicable. From a consideration that stencil printing and screen-printing are similar from the point of view of the fixation of pigment onto the textile substrate, it was decided to use the screen-printing laboratory equipment.
As a second method of application, mass dyeing was used. This technology allows fixation of the pigment inside the man made fibre during production of the fibres. Because the photochromic pigments do not have high thermal resistance,

polypropylene with a lower melting temperature was selected. A method of mass dyeing used the experimental laboratory equipment for Melt – Blown technology.

Many reported studies and articles in the area of photochromic pigments allude to photochromic solutions and the application of photochromic pigments in polymeric matrixes [119,143,142]. In the case of fibres dyed in mass, it is likely that solid solutions of the photochromic pigment form in the polymer fibre. Therefore, the solutions in organic solvents, which were also investigated experimentally, had similar concentrations as fibres dyed in mass, to follow similar conditions. The experimental part of this thesis contains three main sections directed to a comparison of the three main methods used for photochromic pigment applications:

  a) Screen printing

  b) Mass dyeing

  c) Solution

3.2.1 Screen printing

In order to develop a simple textile based photosensor for UV irradiation the main attention was directed to the possibility of application of photochromic pigments by screen-printing. This experimental work was supplemented by a study of the influence of UV absorbers for modification of sensor properties to alter their sensitivity to an external UV stimulus. The influence of the shade intensity *I* on the concentration of photochromic pigment was studied. To complete the study an experimental investigation was also carried out of the dependence of the fatigue resistance on the intensity of the illumination *E* of the source, time of exposure and the classical tests of lightfastness and rubbing, to explore the application limitations of the sensors developed.

A PET substrate was used according to standard ISO 105-F04:2001 for photochromic screen-printing. Samples were prepared for the purpose of the study of photochromic behaviour and a description of the kinetic model, as follows:

- Range of pigment concentration– g/30 g acrylate paste:

0.25 ;	0.5 ;	1.0 ;	1.5 ;	2.0 ;	2.5 ;	3.0

- concentration UV absorber – 1.5, 3% by weight of material

The concentration was selected on the basis of the visual assessment of the strongest colour change. As discussed, five different pigments were used. The photochromic pigments were applied as PTP – photochromic textile prints. For printing, a standard printing composition, TF (acrylate paste), which is frequently used in standard textile pigment printing was used as given in Table 3.2.1:

Table 3.2.1 – Composition of complex paste TF

Water	818 g
Glycerin	20 g
Lukosan S (antifoamer)	2 g
Sokrat 4924 (acrylate binder)	70 g
Acramin BA (butadiene binder)	70 g
Ammonia	5 g
Lambicol L 90 S (thickener)	15 g
Total	1000 g

In accordance with the manufacturer's recommendation, a drying temperature of $75^{o}C$ and time of drying of 5 min was selected. The photochromic prints were fixed by ironing at a temperature a $190^{o}C$ for a time of 20 sec. These parameters were followed to limit thermal degradation of the photochromic pigments [120].

The intensity of colour change usually depends on the concentration of photochromic pigment and on the intensity of UV irradiation. The intensity of UV irradiation may be controlled by UV absorbers, but only in the case when the spectral absorption spectra of the UV absorbers and photochromic pigments are similar. This means that the UV absorber and the photochromic pigment absorb in the same wavelength ranges. In this case, an influence on the depth of colour photochromic change was expected.

In this investigation UV absorbers Cibatex APS and Cibafast HLF from CIBA Specialty Chemicals, Switzerland were applied. Both UV absorbers were applied by screen-printing. As a comparison, a control print was arranged with only the acrylate paste to eliminate the influence of the complex paste on the photochromic effect. The concentrations used were 1.5 % and 3 % of UV absorber by weight of materials only for the sample with a concentration of 0.25g/30g complex paste.

3.2.2 Non - woven samples produced by Melt Blown technology

In this part of the investigation, the photochromic properties of textiles produced by Melt blown technology (mass dyeing) were studied.

Non-woven textiles were used involving a PP polymeric matrix as the carrier of photochromic pigments using mass dyeing technology. This technology was used from the point of view of its availability and relative simplicity of production in comparison to classical methods of fibre production. First, a masterbatch was prepared, containing a maximally technically useable concentration of pigment in the PP granulate (20%).

The measurement of the granulate was arranged in a sample cup, as shown in the photograph in Fig. 3.2.7.

Fig. 3.2.7: Sample cup for measurement of granulate reflectance parameters

The sample cup shown permits fibres and non-compressible powder to be reproducibly presented to the measuring instrument. The material to be tested is filled into this sample cup and pressed against the inside of the cover glass by a plate. The small radial play of the plate in the cylinder prevents even the finest powder from falling through between the plate and the cylinder wall. The diameter of the other plate is 0.6 mm smaller and should be used for fibre-like material. The greater radial play of this plate prevents jamming of the plate caused by fibres getting between the plate and the cylinder wall. The masterbatch was mixed during production with clear PP granulate. For all pigments NW was produced with two fineness of fibres (T1 and T2 providing the distributions as given in Fig. 3.2.8 – histograms of fibre diameter

frequency) with three different concentrations of photochromic pigment (1.0%, 1.8% a 2.6%). The production of non-woven textiles by Melt – Blown technology was carried out using the following climatic conditions:

1. Temperatures in heated areas of the extruder: Z1: 180 $^{\circ}$C

Z2: 204 $^{\circ}$C

Z3: 232 $^{\circ}$C

2. F-(flange) temperature of heating against extruder and nozzles: 232 $^{\circ}$C.

D- (die) temperature of heating in nozzle: 260 $^{\circ}$C.

A_h- (air heater) temperature of air forming fibres: 260 $^{\circ}$C.

Number of nozzles – 60/10 cm, width of nozzle 15 cm, pressure of air – 0.1 MPa. Distance from collector 0.06mm, surface speed of collector – 60m min^{-1}, diameter of collector – 0.56m, circumference of collector –1.76 m and taxi speed of collector – 0.78 m min^{-1}.

During the experimental work, several difficult technological problems were encountered. First was the production of the master batch. During dissolving of the photochromic pigments in PP it was necessary to expose the photochromic pigment to a temperature of 130°C for 3 minutes.

Melting of PP during fibre production may have caused the degradation of pigment P1, because this pigment has a melting point between 125-130 $^{\circ}$C, in comparison to the rest of the pigments tested, which have higher melting temperatures [120], [see Table 6 in Appendix]. The result of mass dyeing with PP fibre using pigment P1 was slightly coloured fibres, which were inactive during UV exposure. Similar results were observed for pigment P4, which is also an oxazine-based structure. The melting temperature of pigment P4 is between 143-145 $^{\circ}$C and therefore during NW production pigment P4 probably melted similarly to pigment P1.

Based on the problem with homogenisation of a mixture of pure PP with masterbatch in the extruder, with weight uniformity, two different finenesses (T1 and T2) were used.

It was evaluated whether the fineness on fibres in non-woven textiles has an influence on the shade intensity on photochromic reaction. The weight of NW is given in Tables. 3.2.2a–c:

Table 3.2.2a			Table 3.2.2b			Table 3.2.2c		
NT-P2 weight g m^{-2}			NT- P3 weight g m^{-2}			NT- P5 weight g m^{-2}		
Conc.	T1	T2	Conc.	T1	T2	Conc.	T1	T2
1%	26.1	21.8	1%	41.4	18.5	1%	38.6	19.4
1.8%	13.7	10.4	1.8%	15.9	14.7	2.6%	36.9	19.6
2.6%	22.8	13.7	2.6%	61.5	30.2	4.6%	58.4	12.1
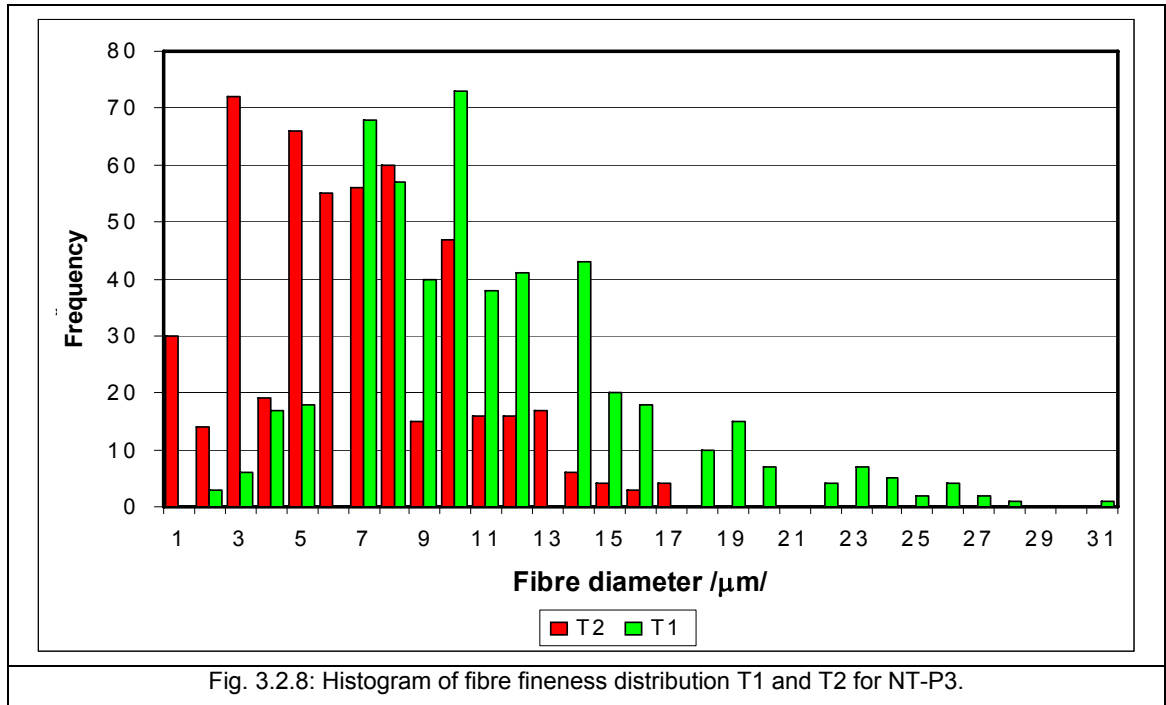
Fig. 3.2.8: Histogram of fibre fineness distribution T1 and T2 for NT-P3.

The next problem met during Melt-Blown non-woven production was the presence of agglomerates in fibres and villuses with a high concentration of photochromic pigment. This problem was influenced by the changes in rheology of the masterbatch in comparison with pure PP granulate. Huge problems with agglomeration were observed when a masterbatch, which was available on the market, was used. This master batch contained a polystyrene base and the sample is referred to as S1.

From Fig. 3.2.10d major problems are evident with fibre fineness distribution and with creation of significant villuses. Attempts were made to use a compatibilizer based on a copolymer of ethylene, vinyl acetate and sodium oleates that alter the rheological properties and improve the spinnability of the melt blend. Nevertheless, a final solution was not found. It is possible to observe from Fig. 3.2.9a–b, the existence of non-uniformity in certain of the colour change textiles.
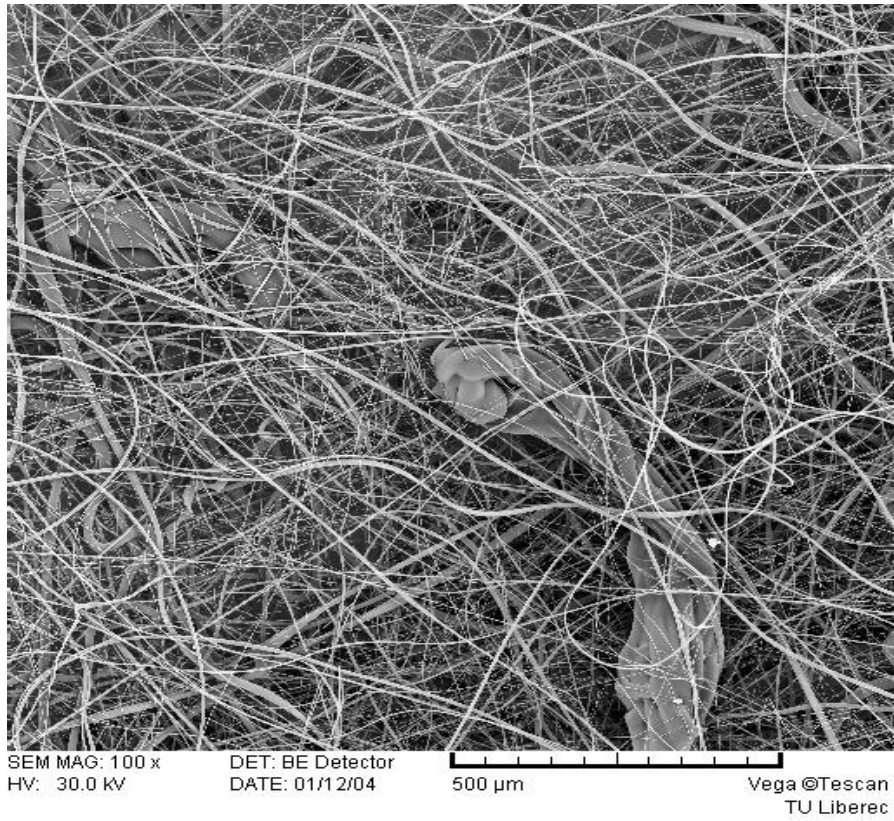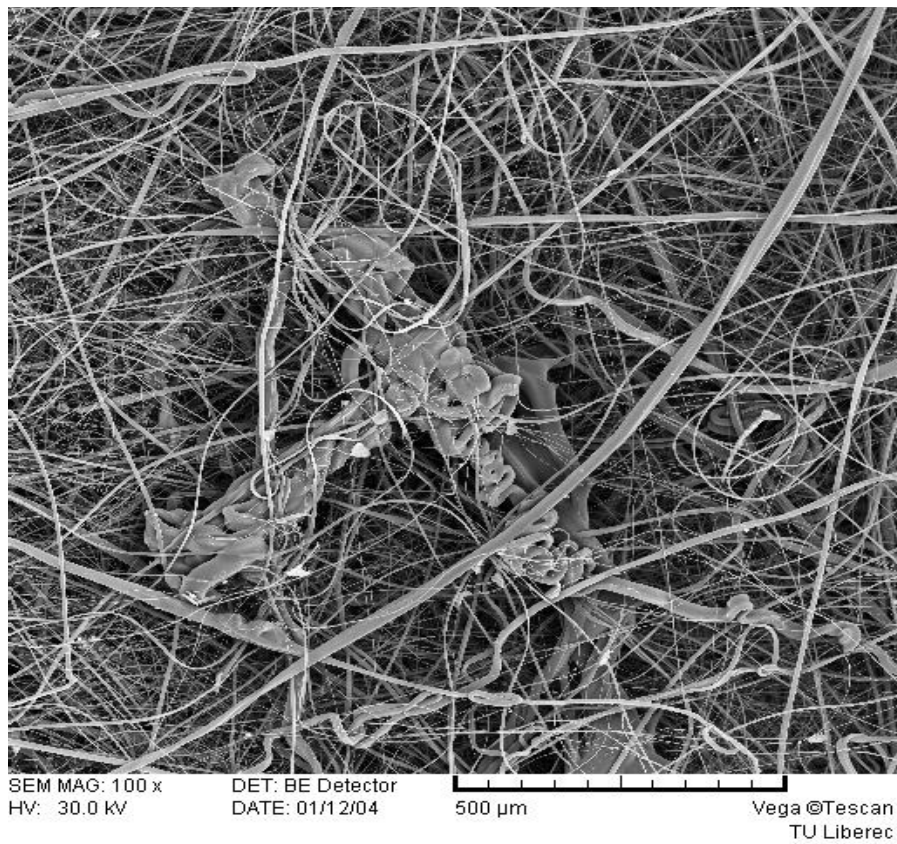
SEM MAG: 100 x   DET: BE Detector
HV: 30.0 kV   DATE: 01/12/04   500 µm   Vega ©Tescan
                                                    TU Liberec

Fig. 3.2.9a: SEM NW-P2 T1

SEM MAG: 100 x   DET: BE Detector
HV: 30.0 kV   DATE: 01/12/04   500 µm   Vega ©Tescan
                                                    TU Liberec

Fig. 3.2.9b: SEM NW- P2 T2

86

SEM MAG: 100 x — DET: BE Detector — 500 µm — Vega ©Tescan
HV: 30.0 kV — DATE: 01/12/04 — TU Liberec

Fig. 3.2.9c: SEM NW-P3 T1

SEM MAG: 100 x — DET: BE Detector — 500 µm — Vega ©Tescan
HV: 30.0 kV — DATE: 01/12/04 — TU Liberec
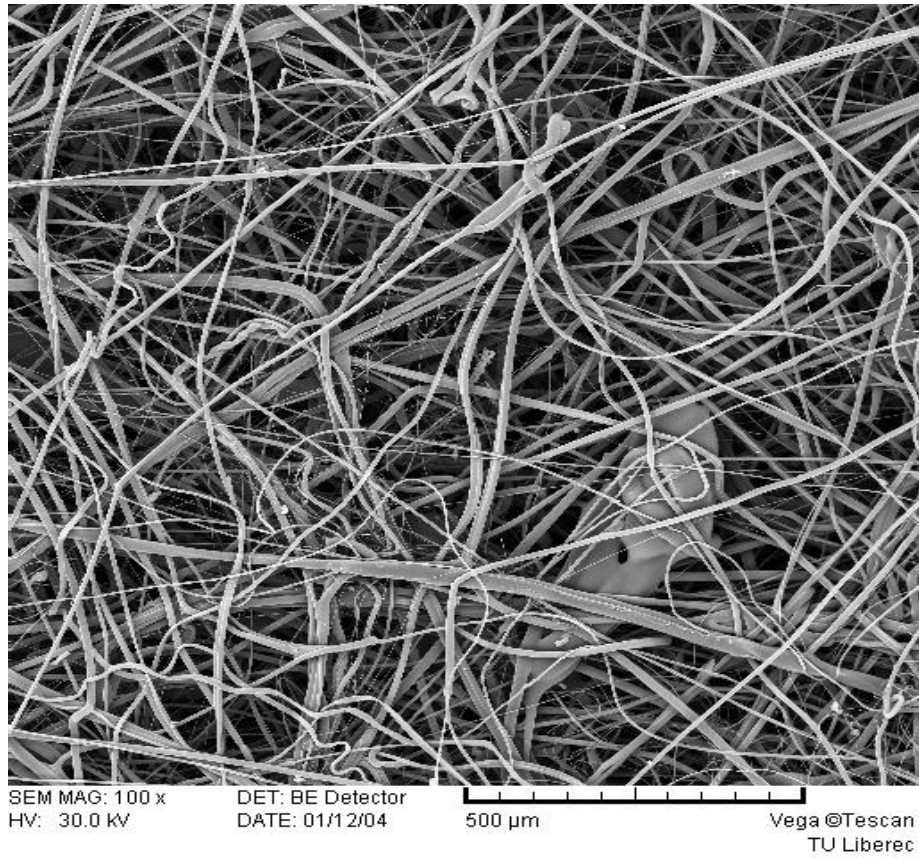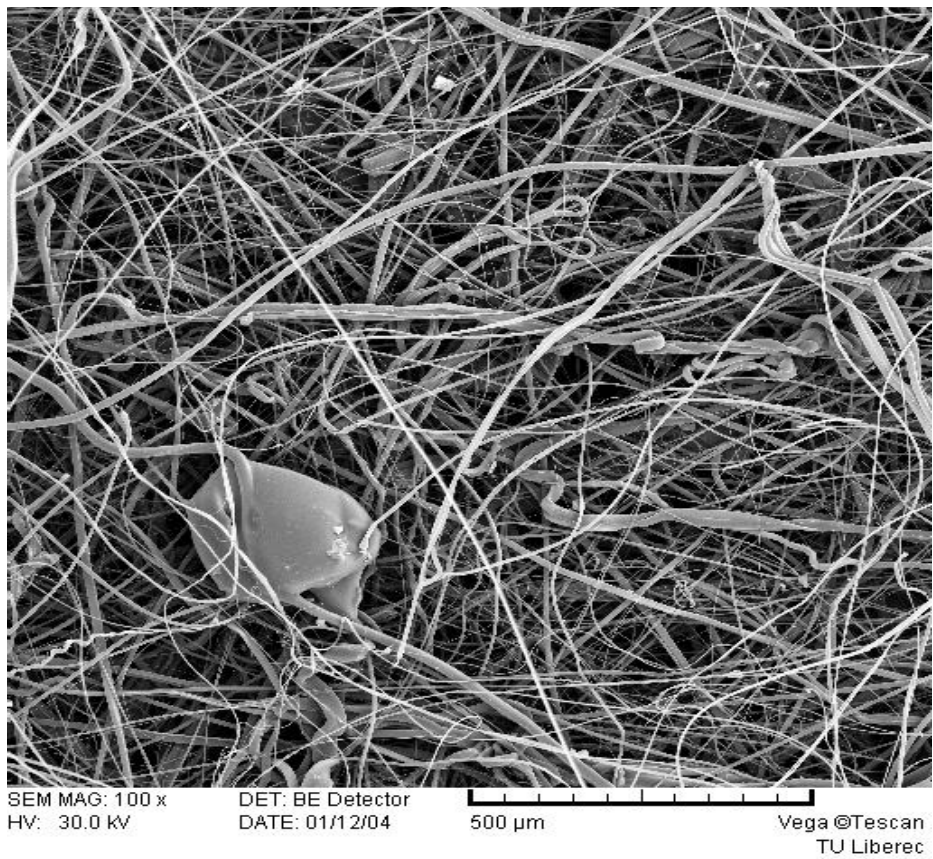
Fig. 3.2.9d: SEM NW-P3 T2

Fig. 3.2.10a: OM NW-P3 T1 k= 2,6 % exposure
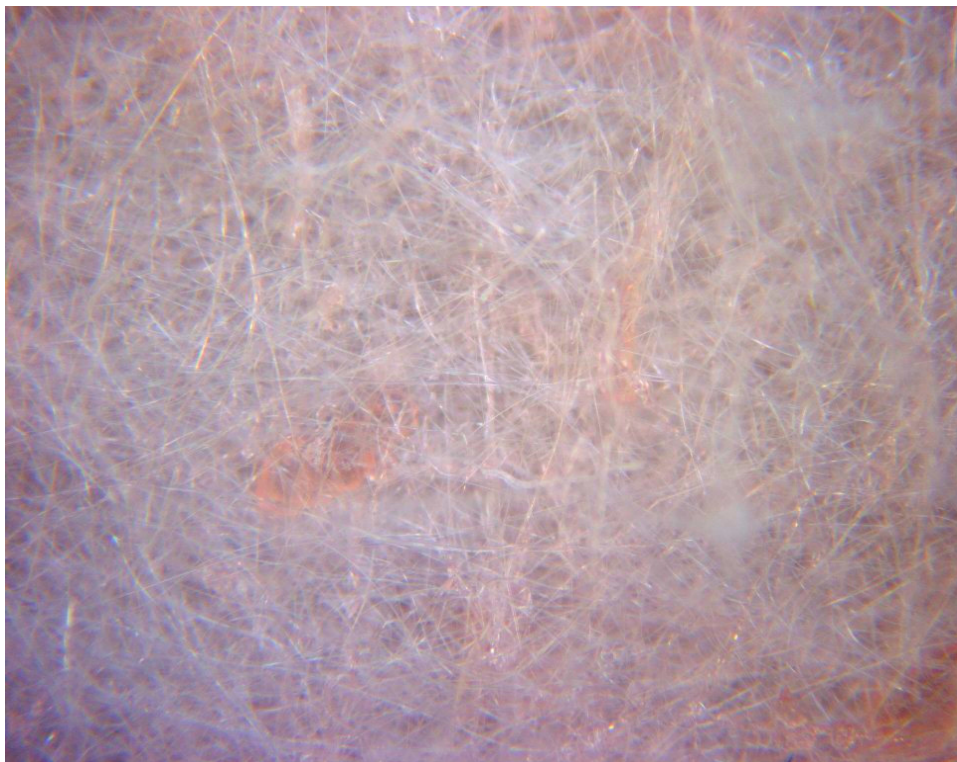
Fig. 3.2.10b: OM NW -P3 T2 k= 2,6 % exposure
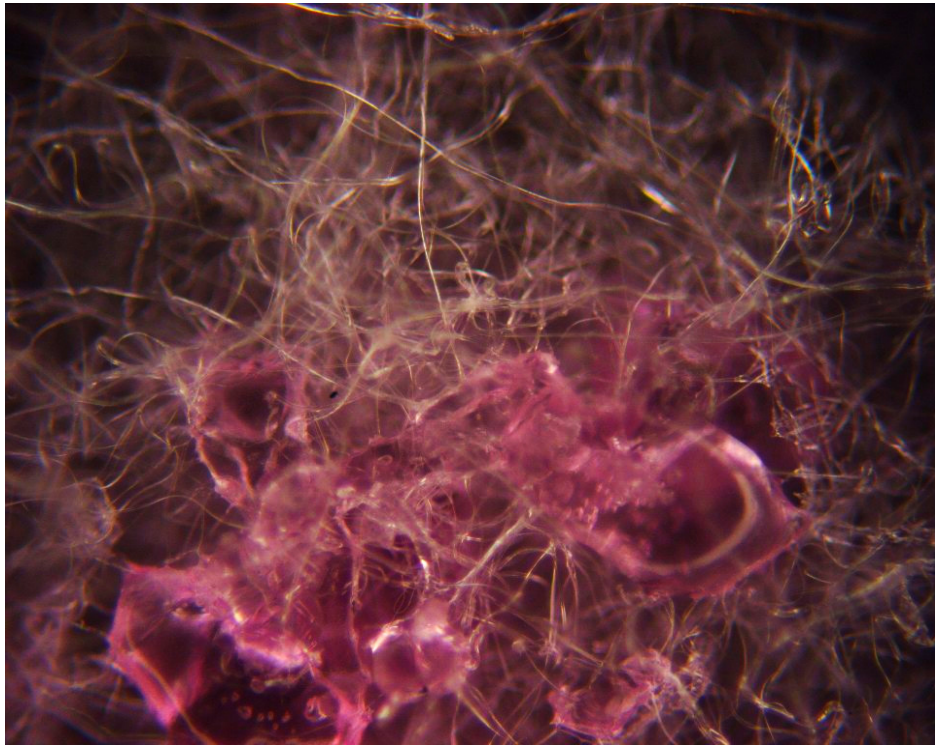
Fig. 3.2.10c: OM NW- S1 T2 k= 2,6 % exposure - master batch on PST base
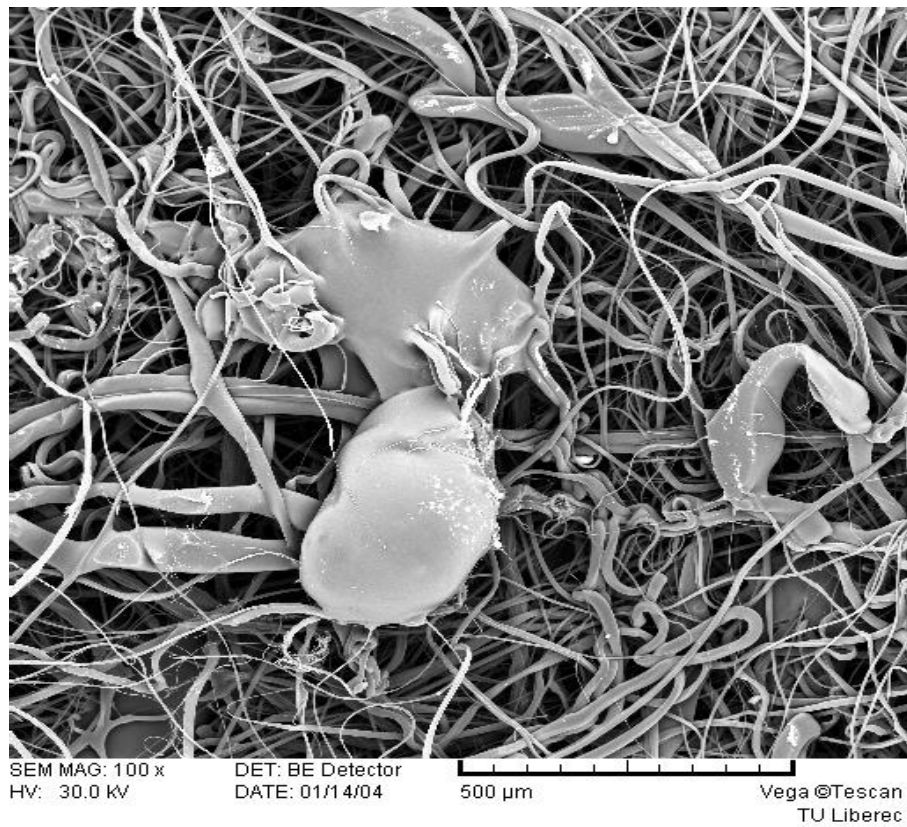
Fig. 3.2.10d: SEM NW- S1 T1 k= 2,6 % exposure - master batch on PST base

3.2.3 Photochromic solution

This investigation evaluated the behaviour of photochromic pigments in solution, in terms of their transmission characteristics, to complement the study of application in screen-printing and mass dyeing.

The photochromic pigments are not soluble in water. Therefore, it was necessary to find optimal solvents suitable for measurement of transmittance characteristics in the UV part of the spectrum. This means that the solvent must not absorb radiation in the measured UV region. On this basis the solvents in Table 3.2.3 were selected. For a determination of solubility limits of selected solvents, an analysis by the Lambert-Beer law was used [123]. If a genuine solution changed to a colloid solution, the linear relation of the L-B law is no longer followed. In the literature it is recommended to use toluene as a solvent [122, 34]. Tests showed that toluene is not suitable for high concentrations of the photochromic pigment. Finally, cyclohexane C_6H_{12} was selected for the measurement of photochromic solutions as the basis of good transmissibility at 220 nm (80%). Based on discussion with the manufacturer a temperature of $60^{\circ}C$ was selected, because it was necessary to heat some of the solutions [120].

Tab. 3.2.3: Organic solvents with transmissibility 80-100% at wavelength 220nm

Solvent	Transmissivity at 220	
acetonitrile far UV	98	
acetonitrile super grade [HPLC]	95	
cyclohexane	80	
Heptane fraction	80	
methanol	70	
n-heptane	80	
n-hexane	80	
n-pentane	90	
petrol ether	90	
toluene	*99	*till 340 nm

For solutions, a similar concentration range was selected as for photochromic printed textiles:

1.4g/l;	2.1g/l;	2.8g/l;	3.5g/l;	4.2g/l

This concentration range was selected to compare differences in the dependence of the photochromic reaction on the application medium of the photochromic pigments. The solutions were prepared one or two days before measurement in a dark room due to time demands on dissolving. The solutions were stored in a dark box to prevent their exposure to UV irradiation. In section 3.1.2, it was discussed that in the case of higher concentrations a separation of a thin layer from the rest of the solution was visible. An electromagnetic mixer with controlled heating solved the problem of photochromic solution non-homogeneity.

Chapter 4
Results and discussion

4.1 Screen-printed photochromic textiles
4.1.1 Dependence of colour change on irradiance

The main aim of this part of the investigation was to investigate the five photochromic pigments according to their kinetic behaviour in relation to the irradiance. Figs. 4.1.1 - 4.1.5 illustrate the photochromic changes in reflectance spectra for individual pigments at various concentrations (for example ratio 1/30 means 1g of photochromic pigment per 30 g of printing paste). Each sample was exposed in the viewing box for 15 minutes using a combination of UV tube and fluorescent tube F7 (daylight simulator).

The upper row of the samples represents the situation before UV illumination (see Figs. 4.1.1–4.1.5) and the lower row illustrates the situation after UV illumination. From Fig. 4.1.1–4.1.5, the differences in shade intensity (decreasing of the reflectance minimum) are evident. Spectral characteristics were measured after 15 minutes exposure time with an intensity of illumination $E = 979.3$ lx. Spectral curves of pigments P4 and P5 show a spectral shift and a smaller change of shade intensity. Pigment P2 has a slight yellowish shade before irradiation and this shade is more intense at the higher concentrations of the pigment. The yellowish background colour has an influence on the colour change of the pigments during UV exposure and this is evident from the reflectance minimum obtained during excitation (see Fig. 4.1.2)

The shape of the K/S curves for pigment P1 as shown in Figures 4.1.8 and 4.1.9 show the changes in the shade depth, corresponding with a decreasing of the minimum reflectance with increasing concentration. It is necessary to understand that small spectral minima shifts are better described by colorimetric values, as discussed in subsequent chapters. The colorimetric explanation of hue colour change allows a better understanding of the spectral shift of measured samples. The spectral power distribution of a daylight simulator and UV fluorescent tube in a viewing box by Gretag Macbeth - Judge II, as discussed in chapter 3.1.2, was used to carry out the exposure. Spectral characteristics were measured after 15 minutes exposure with intensity of illumination $E = 979.3$ lx (distance from light source was 45cm) and for a pigment concentration of 0.25g.

In this thesis the parameter *Shade Intensity I* is primarily used, which is defined as the area under the Kubelka-Munk function. There are also graphs presented of the Kubelka –Munk function for the photochromic reaction curve. From the graphs in Fig. 4.1.6 and 4.1.8 it is evident that K/S is approximately inverted in value compared to reflectance. There is a similar relation between absorption and transmission. The dependence of the K/S function on exposure and reversion is documented in the graphs given in Fig. 4.1.8 and 4.1.9.
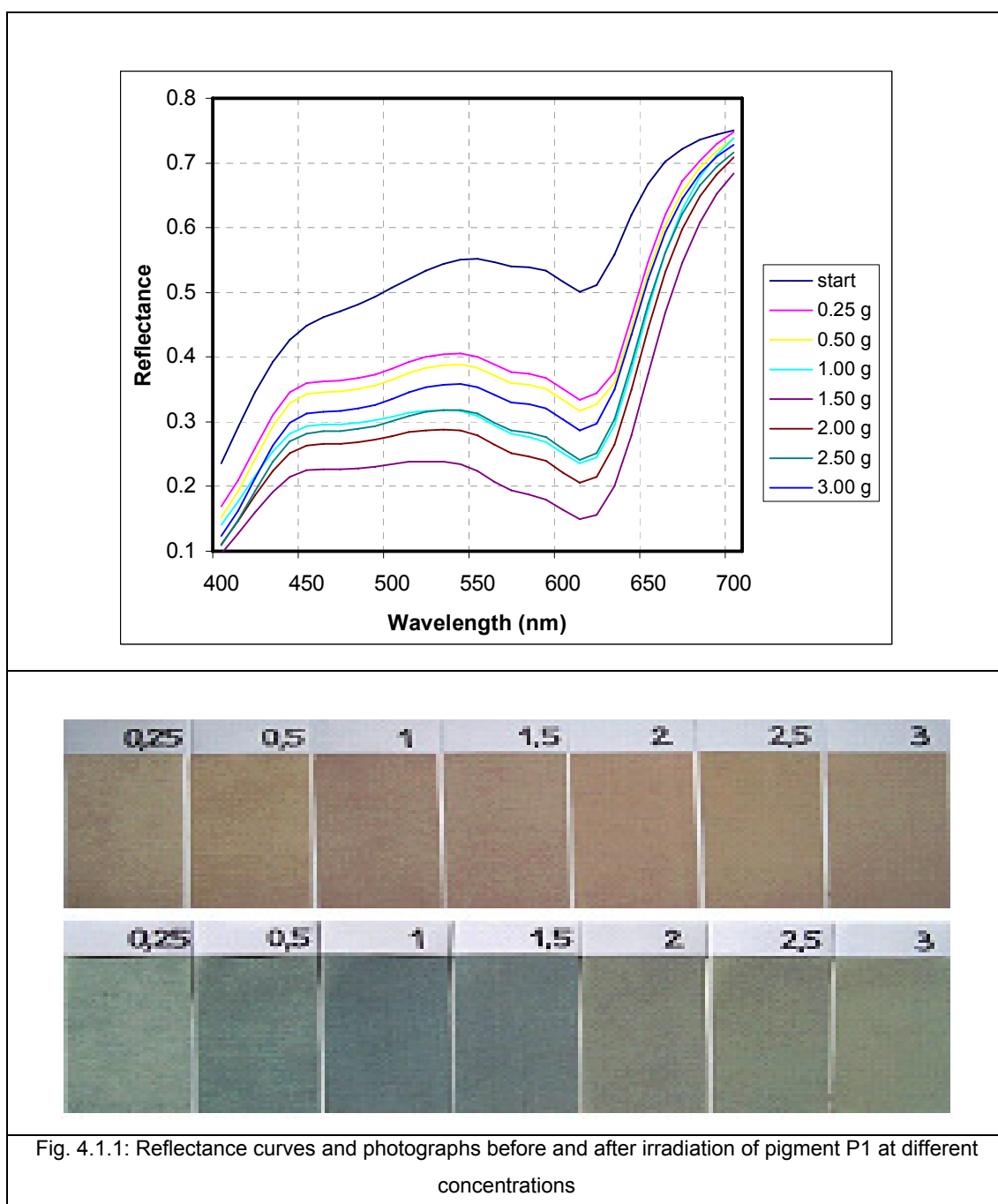
Fig. 4.1.1: Reflectance curves and photographs before and after irradiation of pigment P1 at different concentrations
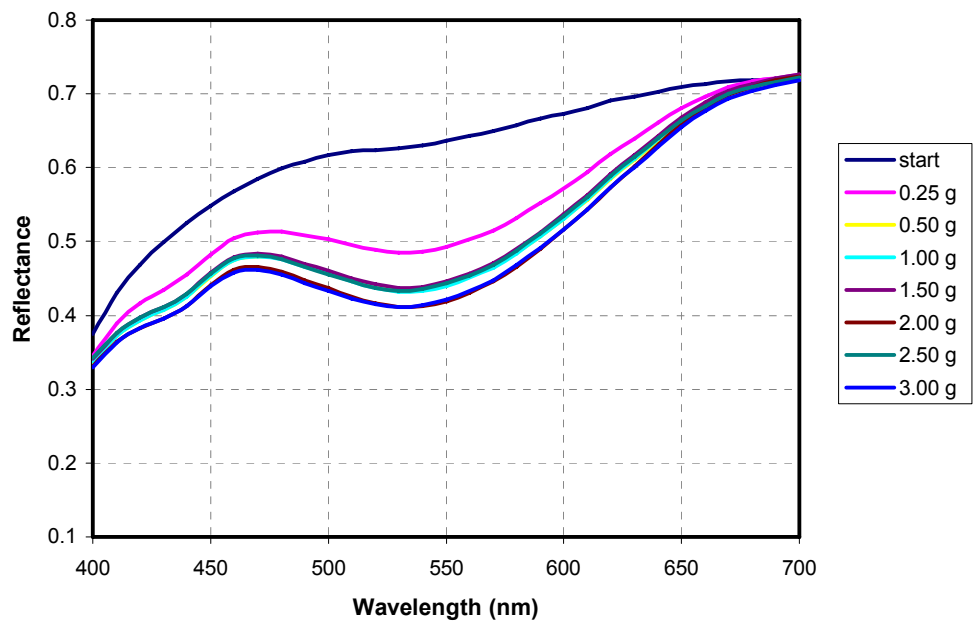
Fig. 4.1.2: Reflectance curves and photographs before and after irradiation of pigment P2 at different concentrations
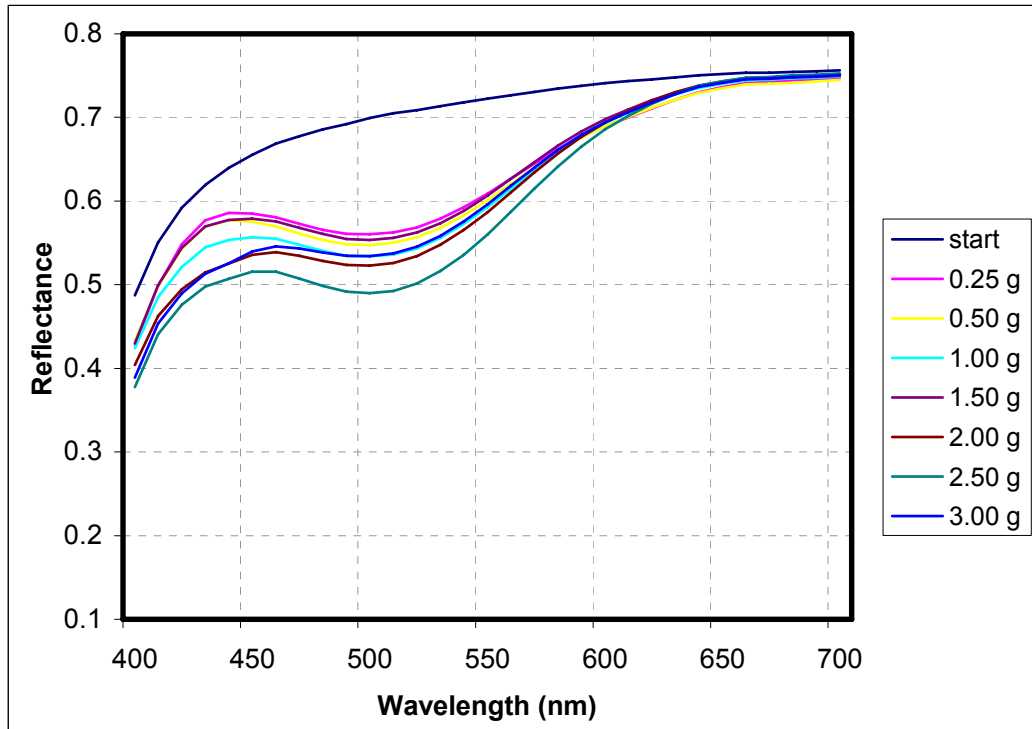
Fig. 4.1.3: Reflectance curves and photographs before and after irradiation of pigment P3 at different concentrations
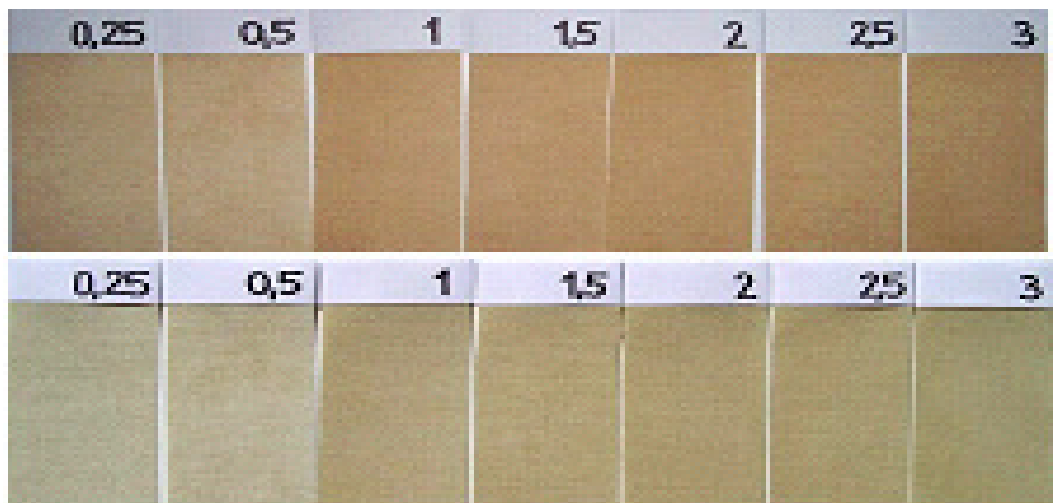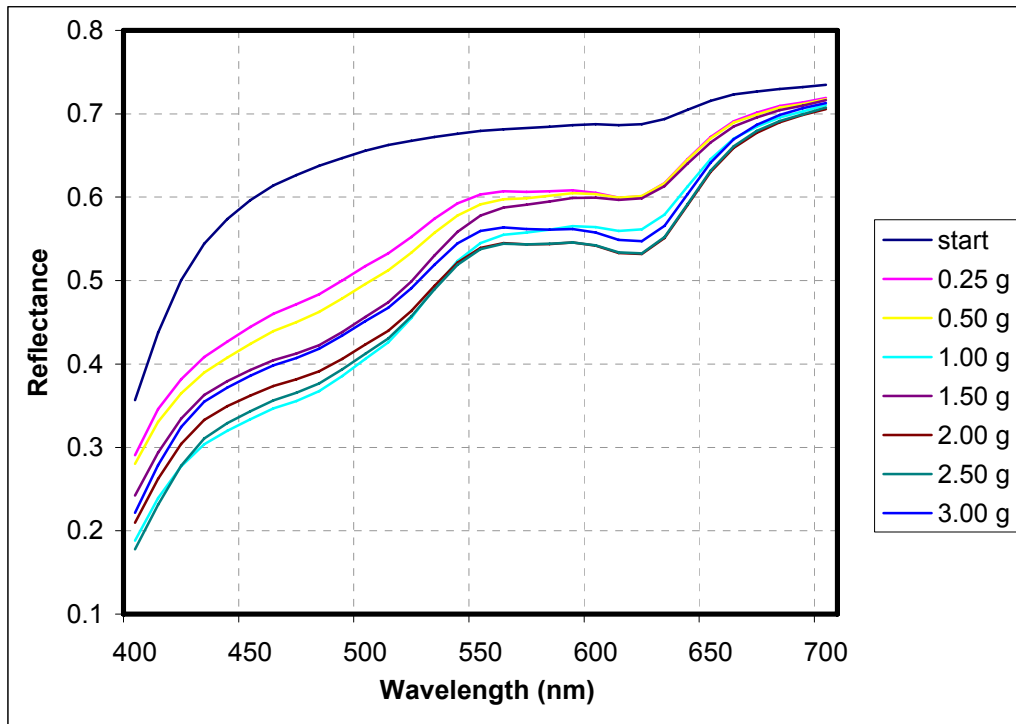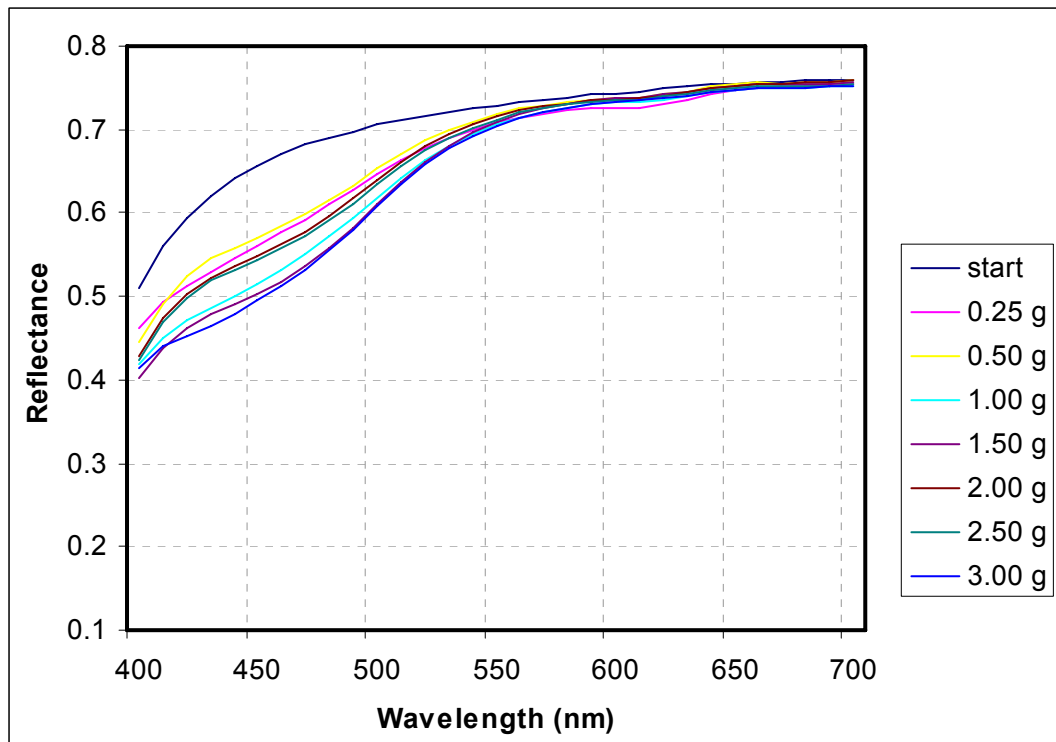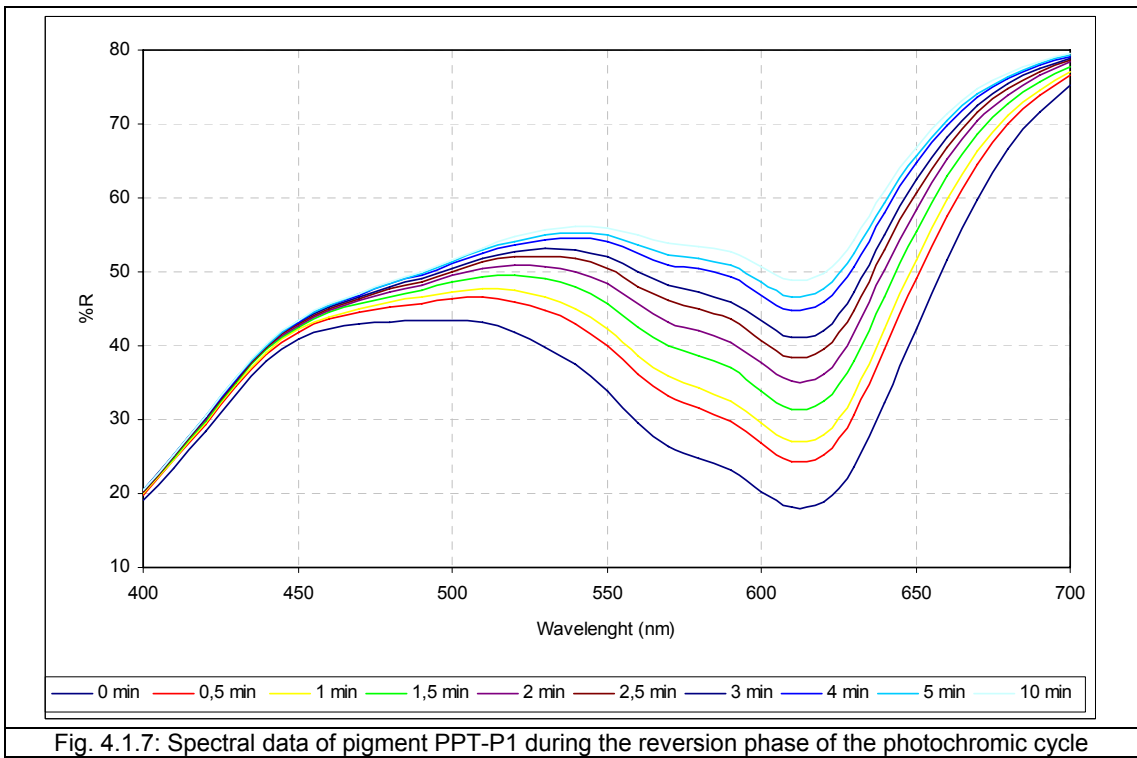
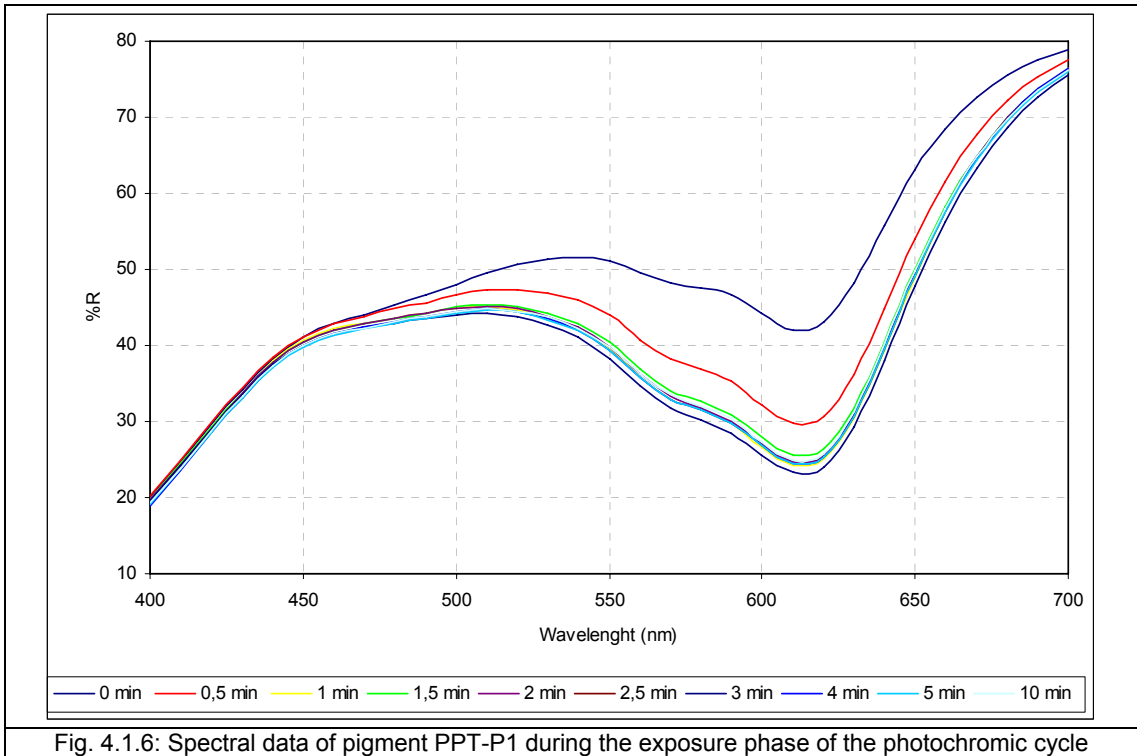Fig. 4.1.4: Reflectance curves and photographs before and after irradiation of pigment P4 at different concentrations
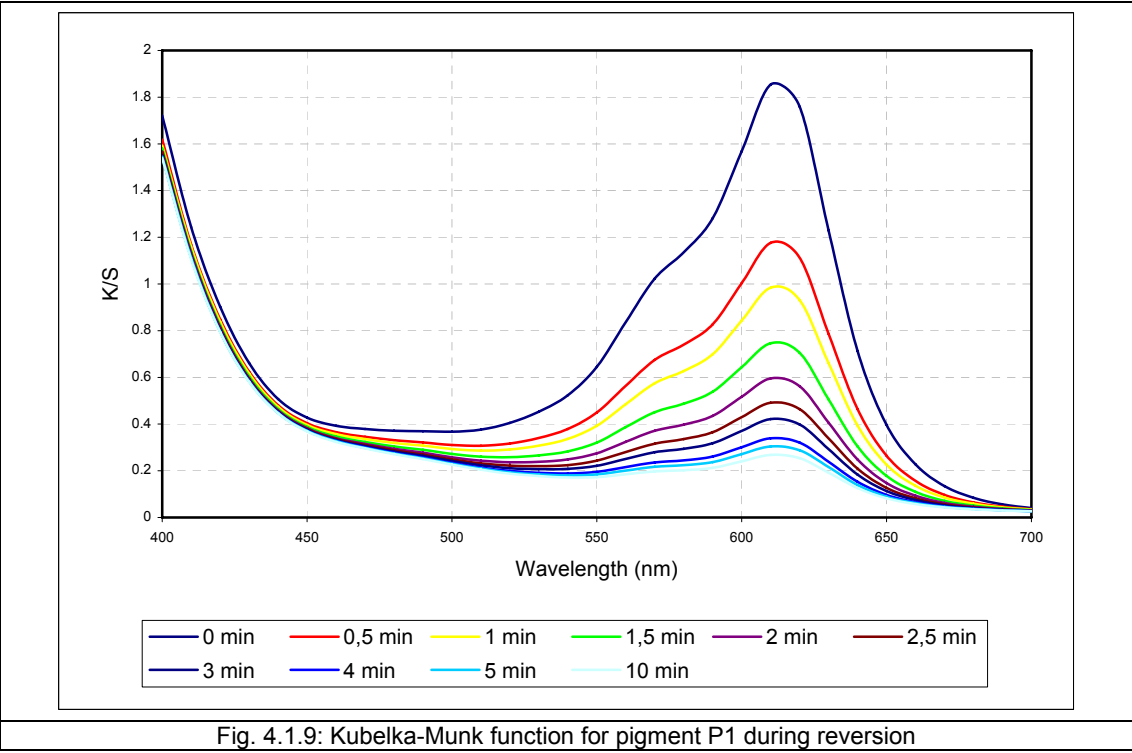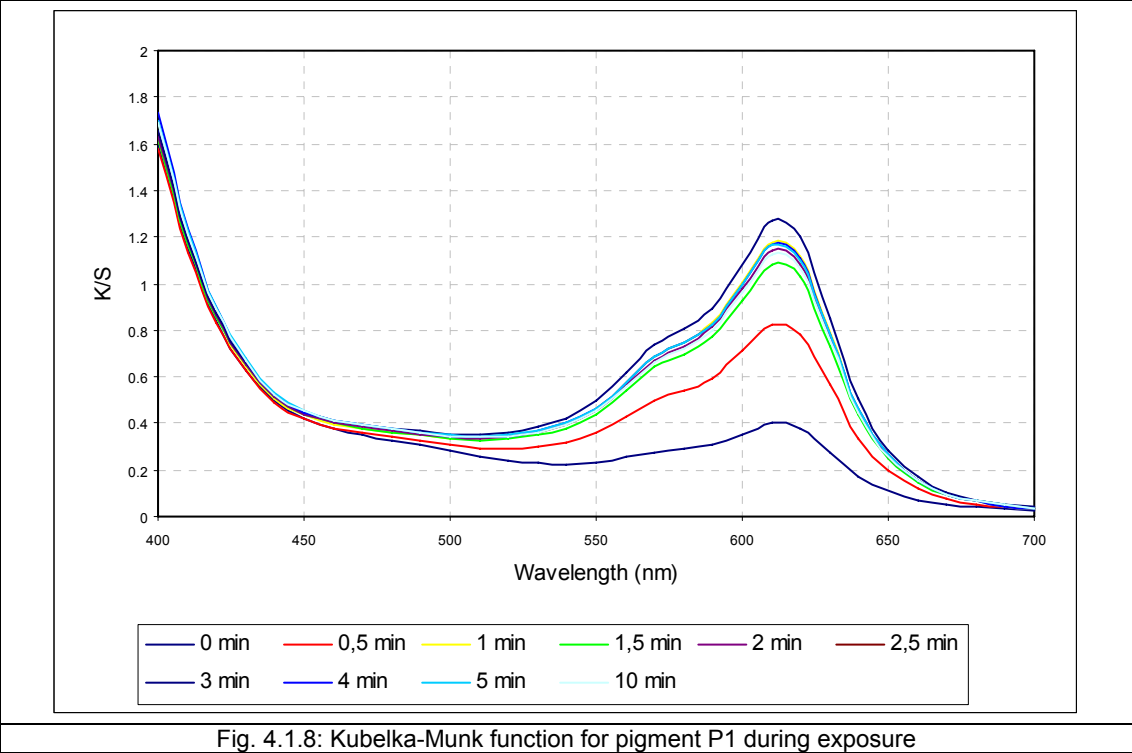
Fig. 4.1.5: Reflectance curves and photographs before and after irradiation of pigment P5 at different concentrations

Fig. 4.1.6: Spectral data of pigment PPT-P1 during the exposure phase of the photochromic cycle

Fig. 4.1.7: Spectral data of pigment PPT-P1 during the reversion phase of the photochromic cycle

Fig. 4.1.8: Kubelka-Munk function for pigment P1 during exposure

Fig. 4.1.9: Kubelka-Munk function for pigment P1 during reversion

Figs. 4.1.6 and 4.1.7 document the situation for reflectance and Figs. 4.1.8 and 4.1.9 for the K/S function using pigment P1. The figures show a good separation of individual spectral curves during the reversion period in comparison to an overlapping of some curves during exposure. This problem is due to several reasons, which are discussed in section 3.1.2. One reason is the difference between the rate of colour change (shade intensity) during exposure and reversion. During exposure the rate of colour change is obviously higher. A consequent problem is caused by the measuring technique. As discussed in chapter 3.1.3, measurement by commercial reflectance spectrophotometers is influenced by variability of the time delay between the time of photochromic sample exposure and the time of measurement. Other sources of spectral curves confusion are local fading, which is caused by changing of environmental temperature, and bleaching effects.

Fig. 4.1.10 shows experimental data incorporating a first order kinetic model according to equation 2.5.9 for the exposure and 2.5.11 for the reversion. It is evident that the proposed model functions fit the experimental data well [124, 125]. Statistical criteria such as those resulting from the t-test and others, which are used to evaluate the model parameters, are presented in the Tables 4.1.1 and 4.1.2. These tables, which also document the influence of UV absorbers Cibafast HLF and Cibatex APS (together with the graph in Fig. 4.1.14 a,b). In Fig.4.1.10, the main levels of shade intensity (I_0, I_∞, $I_{1/2}$) are shown. Special attention is given to the half shade intensity $I_{1/2}$, because this value is related to the half-life of the photochromic reaction, the half-life of photochromic colour change $t_{1/2}$. The half-life of photochromic colour change $t_{1/2}$ is a measured of the rate of the colour change and is calculated based on equation:

$$t_{1/2} = \frac{\ln 2}{k} \qquad , \qquad (4.1.1)$$

where k is the rate constant which is calculated from equations 2.5.9 or 2.5.11.

When the relationship between the half-life of colour change $t_{1/2}$ and the effect of pigment concentration is tested, the result is a practically independent linear relation for the exposure period of photochromic colour change as shown in Fig. 4.1.11. This means that the time of colour change during exposure is not influenced by increased concentration of the pigments (a virtually constant value of $t_{1/2}$)
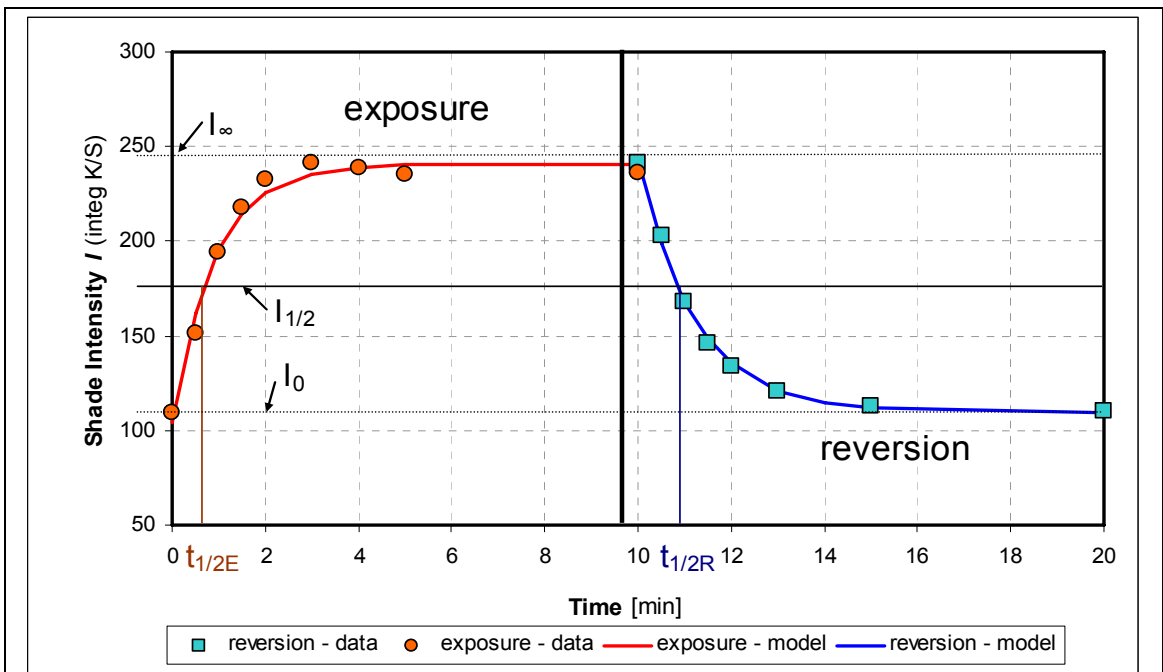
Fig. 4.1.10: Typical growth and decay processes of shade intensity for a sample of pigment P1 in concentration 3g/30g UV-A irradiance = 714,6 µW.cm-2 power (979,3 lx)

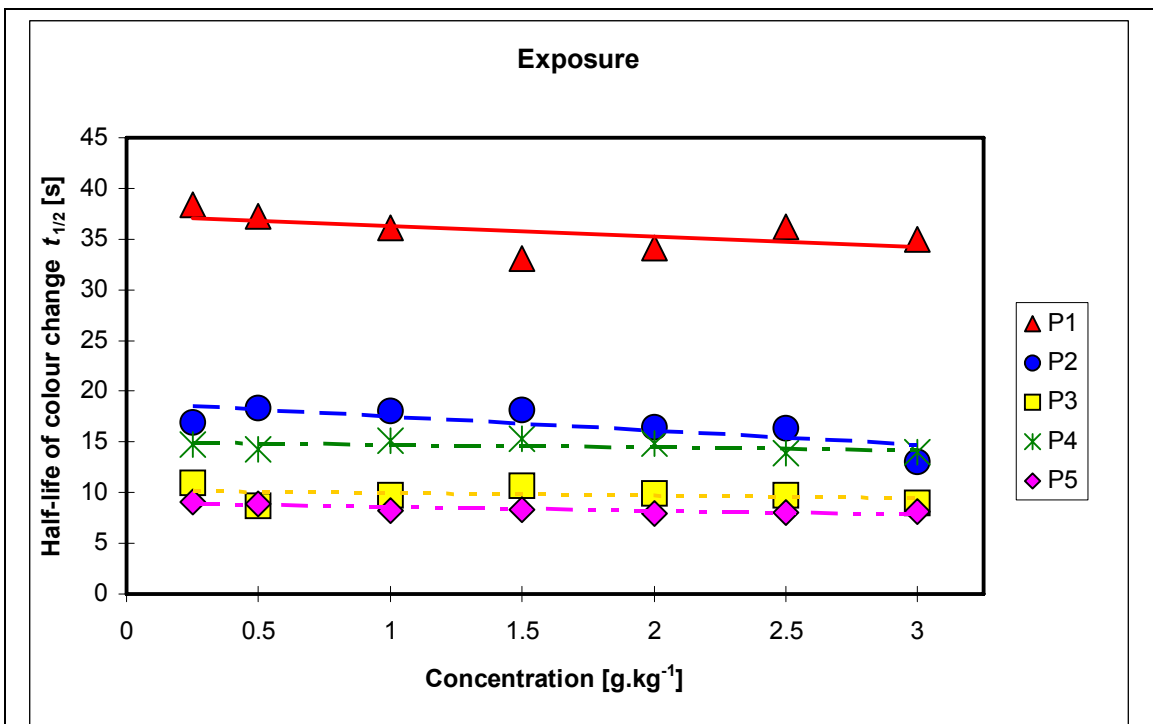Fig. 4.1.11: Dependence of Half-life of colour change on concentration of pigments, UV-A irradiance = 714,6 µW.cm^{-2} – exposure (growth phase)

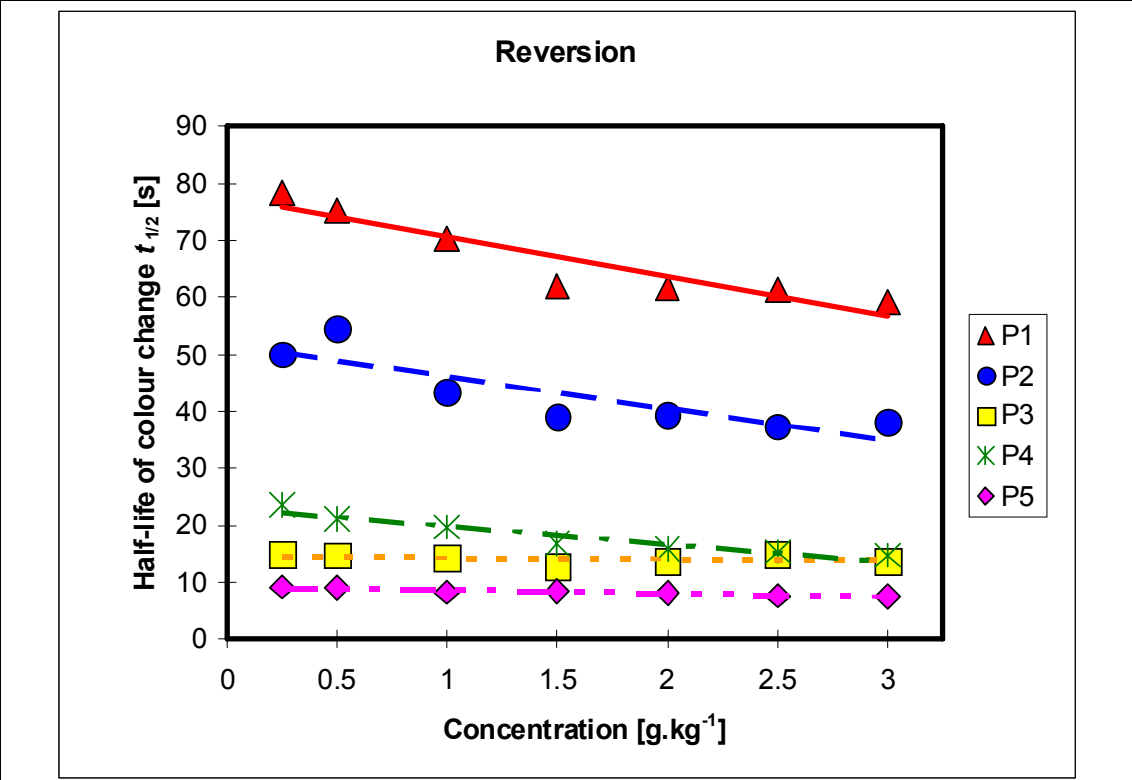Fig. 4.1.12: Dependence of Half-life of colour change on concentration of pigments, UV-A irradiance = 714,6 µW.cm-2 – reversion (decay phase)
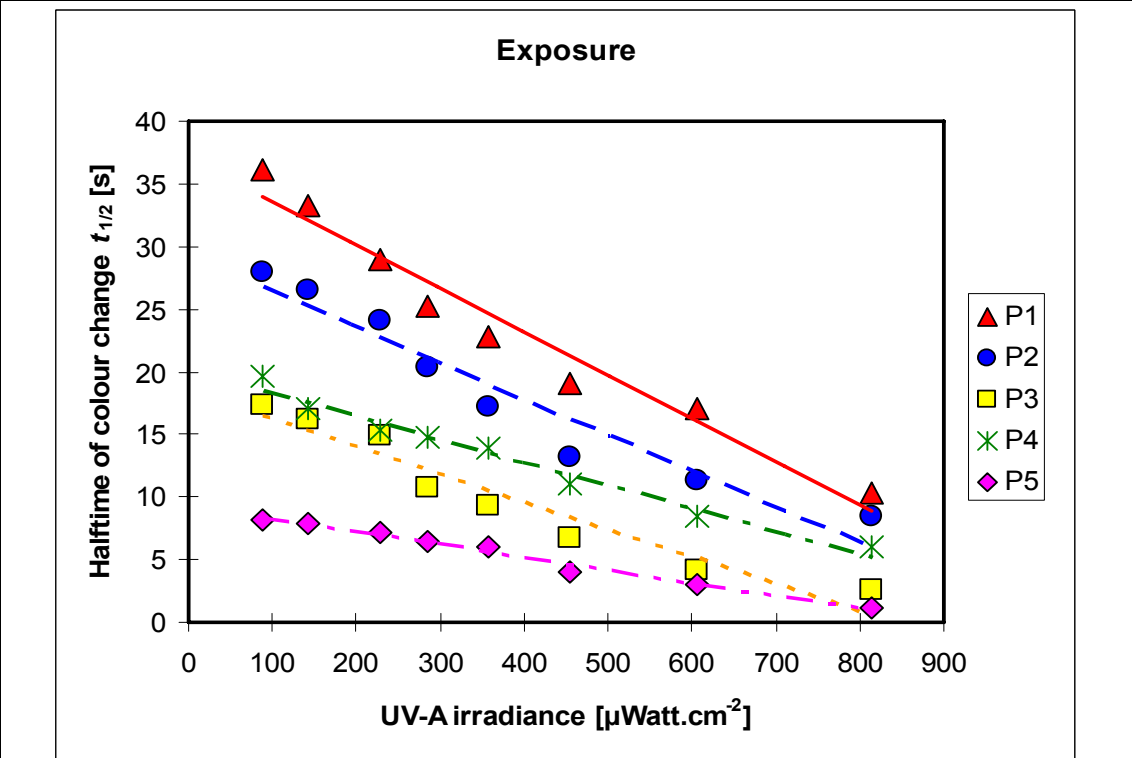

Fig. 4.1.13: Dependence of half-life of colour change $t_{1/2}$ in relation to irradiance E

It can be seen from Fig. 4.1.12 that the rate of the colour change during the reversion phase is slightly dependent on pigment concentration, mainly for the two pigments with a slow rate of colour change. Thus, it is possible to conclude that the half-life of colour change is, for the exposure period of colour change, practically independent of concentration. On the other hand, for the reversion period it can seen that there is a decrease of $t_{1/2}$ with increasing concentration. One explanation, which may be proposed, is that this relationship is based on a faster reconversion to the original chemical structure of the photochromic pigment at higher concentration. Fig. 4.1.13 shows that an increased intensity of illumination affects a linear decrease of $t_{1/2}$ (halftime of colour change).

The optical yield O_y of photochromic colour change is calculated based on equation (4.1.2).

$$O_y = \int_0^{t_1} I_{\infty,e} + \left(I_{0,e} - I_{\infty,e}\right)e^{-k_e t}dt - \int_{t_1}^{t_2} I_{0,r} + \left(I_{\infty,r} - I_{0,r}\right)e^{-k_r t}dt \qquad (4.1.2)$$

where I_∞ is the intensity of coloration at infinite time, I_0 is the intensity of coloration at the start of experiment, k_e is the rate constant during exposure and k_r is the rate constant during reversion for time t. For this purpose, exposure and reversion are independent processes. The intensity of coloration at infinite time I_∞ is described by two values. For the meaning of shade intensity I subscripts $(0,\infty)$ are used, which are related to the actual stage of the process. In the case of exposure, $I_{\infty,e}$ is practically the maximum intensity obtained and in the case of reversion. The shade intensity $I_{\infty,r}$ is equal to the shade intensity $I_{0,e}$ from exposure, because reversion starts at the shade intensity, when exposure is finished, and reversion ends ideally at the same intensity of shade as exposure starts.

As observed from equation (4.1.2) it is evident that the Optical yield O_y is based on the colour hysteresis area. Usually in the literature [126], this type of equation involving a bi-exponential function is used to represent the photochromic reaction. For the purpose of this work not only a bi-exponential function but also the area under the bi-exponential function was used, where t_1 is the time of maximal

shade intensity during exposure and t_2 is the time of maximum relaxation of the sample with minimum shade intensity.

In balanced systems, usually the relationship between intensity I, as K/S value, and optical yield O_y is linear as shown in Fig. 4.1.14a. The balanced photochromic systems referred to in this work are systems, where the ratio between half-life of exposure and half-life of reversion is maximally 1:3. The ratio between half-lives of photochromic reaction may be used as the criterion of photochromic system quality as illustrated in the graph given in Fig. 4.1.14b. If the half-life ratio is lower than 1:3, it is possible to approximate the relationship via linear regression. Therefore we can define the ideal system, where the half-lives are fully balanced (the ratio is 1:1).

Fig:4.1.14a: Relationship between optical yield O_y and shade intensity I	Fig:4.1.14b: Relationship between optical yield O_y and half-lives ratio
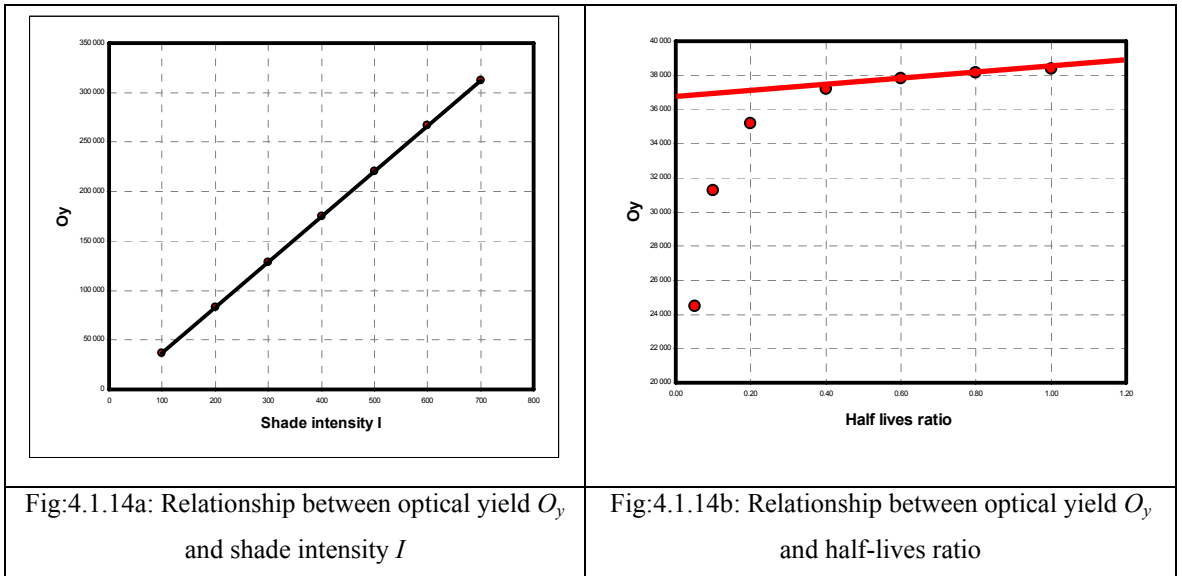
The equations 2.5.9 and 2.5.11 describe the kinetics of colour change during exposure and reversion and the area under both curves defines the total colour change during the entire photochromic cycle. In CIE L*a*b* colour space a photochromic cycle is characterized by hysteresis and this area corresponds also to the optical yield.

In Tables 4.1.1a and 4.1.1b parameters of a linear regression model for the relationship between O_y and irradiance E are given. A linear regression model fits a linear function to a set of data points. The general form of the function is:

$$Oy = A0 + A1*X1 + A2*X2 + \ldots + An*Xn$$

Where Oy is the target variable, X1, X2, … Xn are the predictor variables (irradiance E), and A1, A2, … An are coefficients that multiply the predictor variables. A0 is a constant. In this work a simplified variant of linear model is used:

$$Oy = A0 + A1*X.$$

Together with these regression model coefficients, "t" statistics are also computed. The "t" statistic is computed by dividing the estimated value of the β coefficient by its standard error. This statistic is a measure of the likelihood that the actual value of the parameter is not zero. The larger the absolute value of t, the less likely that the actual value of the parameter could be zero. The "t"statistic probability is computed using a two-sided test.

From Fig. 4.1.15 a-b, it is evident that optical yield O_y depends on irradiance E. This Figure also shows that a higher UV absorber concentration leads to a lower optical yield of photochromic reaction O_y. Nevertheless, Tables 4.1.1 a-b shows that the computed constant A0 of the regression model are insignificant in case when UV absorbers are used. This result is affected by experimental errors, because in this experiment a line method for measurement of colorimetric properties was used.

Table 4.1.1 a: Coefficients for model O_y=A0+A1*X for Cibafast HLF

Concentration of UV absorber (%)	A0	standard deviation	t-criterion	Decision	A1	standard deviation	t-criterion	Decision
0.0	849.658	216.731	3.920	significant	1.041	0.046	22.669	significant
1.5	190.334	194.905	0.561	insignificant	1.026	0.041	24.856	significant
3.0	109.324	157.070	1.212	insignificant	0.905	0.033	27.190	significant

Table 4.1.1 b: Coefficients for model O_y=A0+A1*X for Cibatex APS

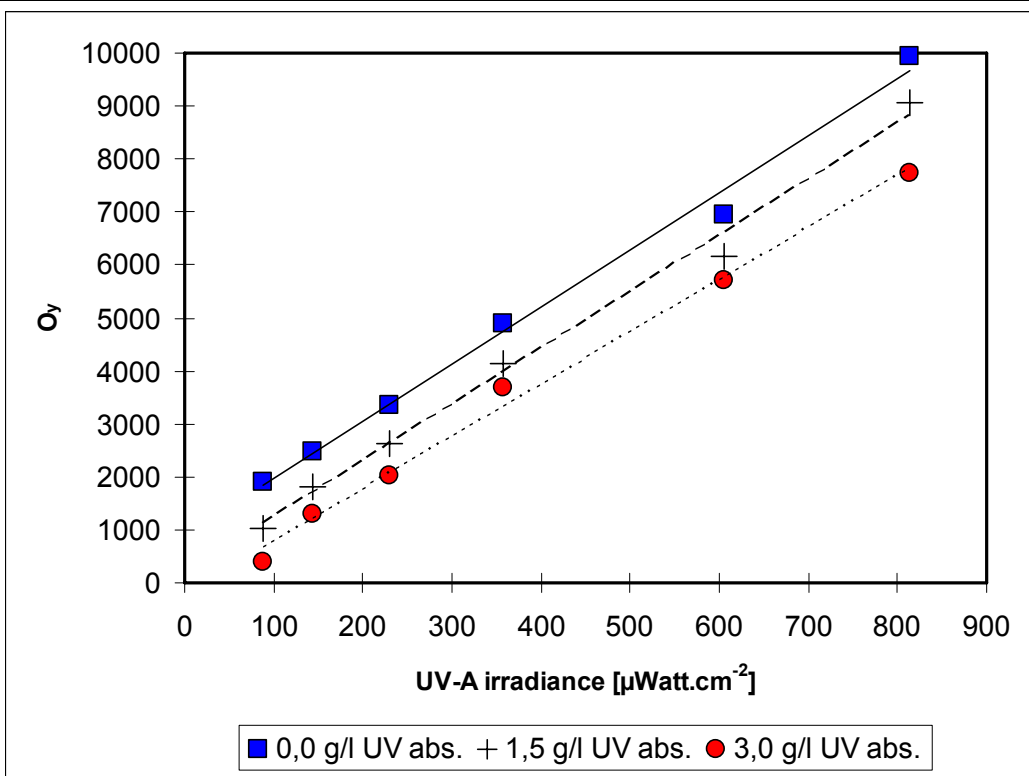| Concentration of UV absorber (%)	A0	standard deviation	t-criterion	Decision	A1	standard deviation	t-criterion	Decision
0.0	849.658	216.731	3.920	significant	1.041	0.046	22.669	significant
1.5	177.764	199.640	0.890	insignificant	1.087	0.042	25.704	significant
3.0	173.313	202.833	0.854	insignificant	1.019	0.043	23.723	significant

Fig. 4.1.15 a: Dependency of Oy on irradiance for different concentrations of UV absorber Cibafast HLF - pigment P1
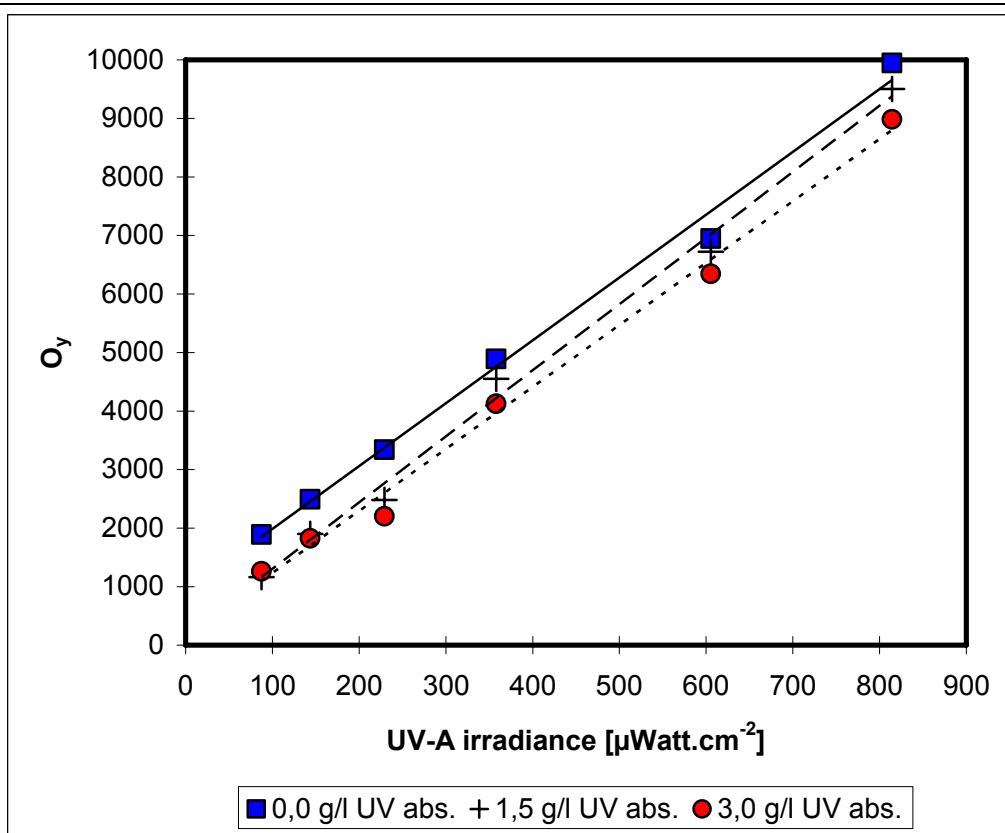

Fig.4.1.15 b: Dependency of Oy on irradiance for different concentrations of UV absorber Cibatex APS - pigment P1

The Tables 4.1.1c-d show the rate constants, half-life and the % extension of half-life provided by the use of UV absorbers. From Tables 4.1.1c-d decrease of half-life extension with increasing irradiance is evident.

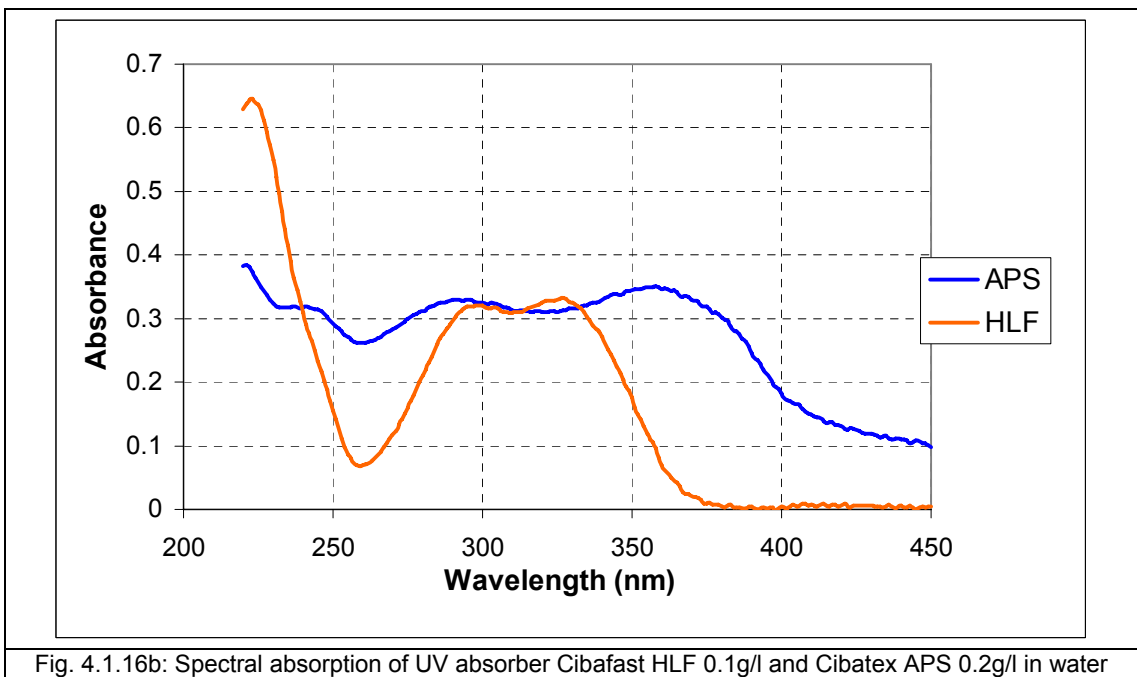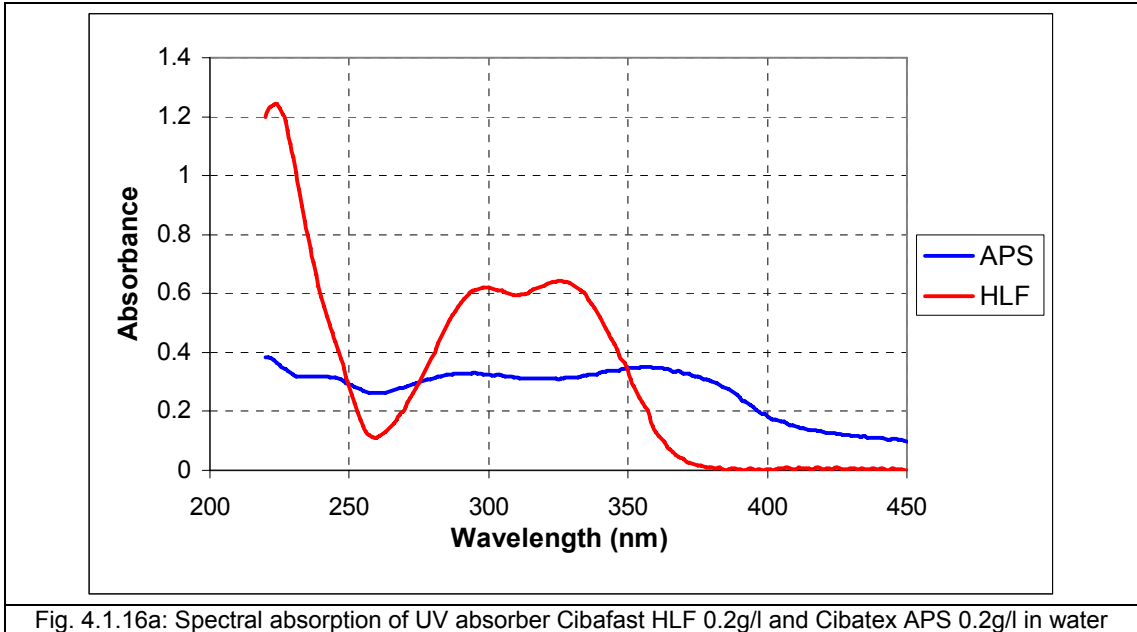Table 4.1.1 c: First order kinetic parameters for Cibafast HLF

Irradiance E [μW.cm^{-2}]	0% HLF		1.5% HLF			3.0% HLF		
	Rate constant k	Half life $t_{1/2}$ [s]	Rate constant k	Half-life $t_{1/2}$ [s]	Extension of Half-life %	Rate constant k	Half-life $t_{1/2}$ [s]	Extension of Half-life %
87.60	0.0191	36.09	0.0161	42.96	19.01	0.0136	50.77	40.66
143.43	0.0235	29.50	0.0203	33.96	15.12	0.0186	37.03	25.52
229.11	0.0278	24.96	0.0255	27.18	8.89	0.0220	31.47	26.08
358.10	0.0355	19.50	0.0320	21.65	11.00	0.0301	23.07	18.30
605.50	0.0495	14.01	0.0470	14.72	5.06	0.0436	15.90	13.48
814.39	0.0666	10.39	0.0606	11.43	10.06	0.0551	12.58	21.09

Table 4.1.1 d: First order kinetic parameters for Cibatex APS

Irradiance E [μW.cm^{-2}]	0% APS		1.5% APS			3.0% APS		
	Rate constant k	Half life $t_{1/2}$ [s]	Rate constant k	Half-life $t_{1/2}$ [s]	Extension of Half-life %	Rate constant k	Half-life $t_{1/2}$ [s]	Extension of Half-life %
87.60	0.0191	36.09	0.0140	49.52	37.20	0.0150	46.03	27.54
143.43	0.0235	29.50	0.0201	34.28	16.19	0.0193	35.71	21.04
229.11	0.0278	24.96	0.0233	29.66	18.82	0.0213	32.56	30.44
358.10	0.0355	19.50	0.0340	20.41	4.65	0.0310	22.37	14.73
605.50	0.0495	14.01	0.0473	14.65	4.52	0.0466	14.86	6.02
814.39	0.0666	10.39	0.0636	10.90	4.94	0.0605	11.45	10.27

These values also demonstrate the UV absorber efficiency. The efficiency of Cibatex APS is approximately a factor of two times lower in comparison to Cibafast HLF. The reason for this phenomenon is probably associated with different absorptions in the UV part of the spectrum and different absorbances at the same concentration, as is documented in Fig. 4.1.16a. In Fig. 4.1.16b normalised absorption curves are shown, where similar values of absorbance are obtained by the use of different concentrations of UV absorbers. In the case of Cibatex APS it is necessary to use double the concentration. This result correlates with the result obtained for UV absorbers efficiency – the extension of half-life, as documented in Table. 4.1.1c-d. In section 4.5 the influence of different wavelength of UV radiation on final shade

intensity is discussed. It is thus necessary to select UV absorbers with specific UV absorbance character.

Fig. 4.1.16a: Spectral absorption of UV absorber Cibafast HLF 0.2g/l and Cibatex APS 0.2g/l in water

Fig. 4.1.16b: Spectral absorption of UV absorber Cibafast HLF 0.1g/l and Cibatex APS 0.2g/l in water

4.1.2 Dependence of colour change on pigment concentration

In addition to the influence of intensity of illumination, the influence of concentration of the photochromic pigments on the optical yield of the photochromic reaction was also studied. Figs. 4.1.17a–c document the dependence of O_y on the distance from the exciting source and on concentration. The systems studied have the maximum sensitivity in the concentration range from 0.5 to 1.5g. An exception is the photochromic pigment P3, which has a local maximum also at a concentration of 2.5g (the test was repeated three times to ensure the same result [127]).

Similar results are evident from Figs. 4.1.18a-e. In the range of concentrations 0.5 − 1.5g there is not only a higher O_y value, but also there is a difference in directions of the linear regression model for these concentrations. This effect is more significant for pigment P2.
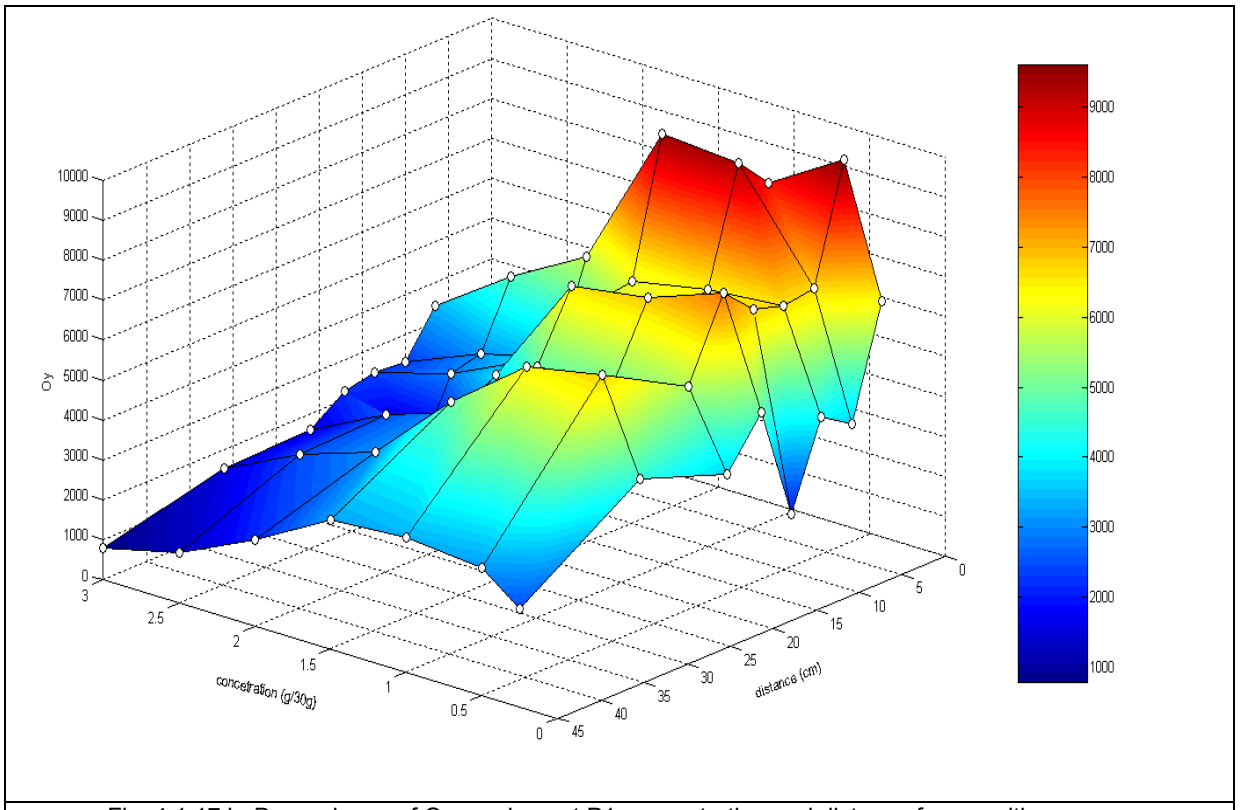

Fig. 4.1.17a: Dependence of Oy on pigment P3 concentration and distance from exciting source
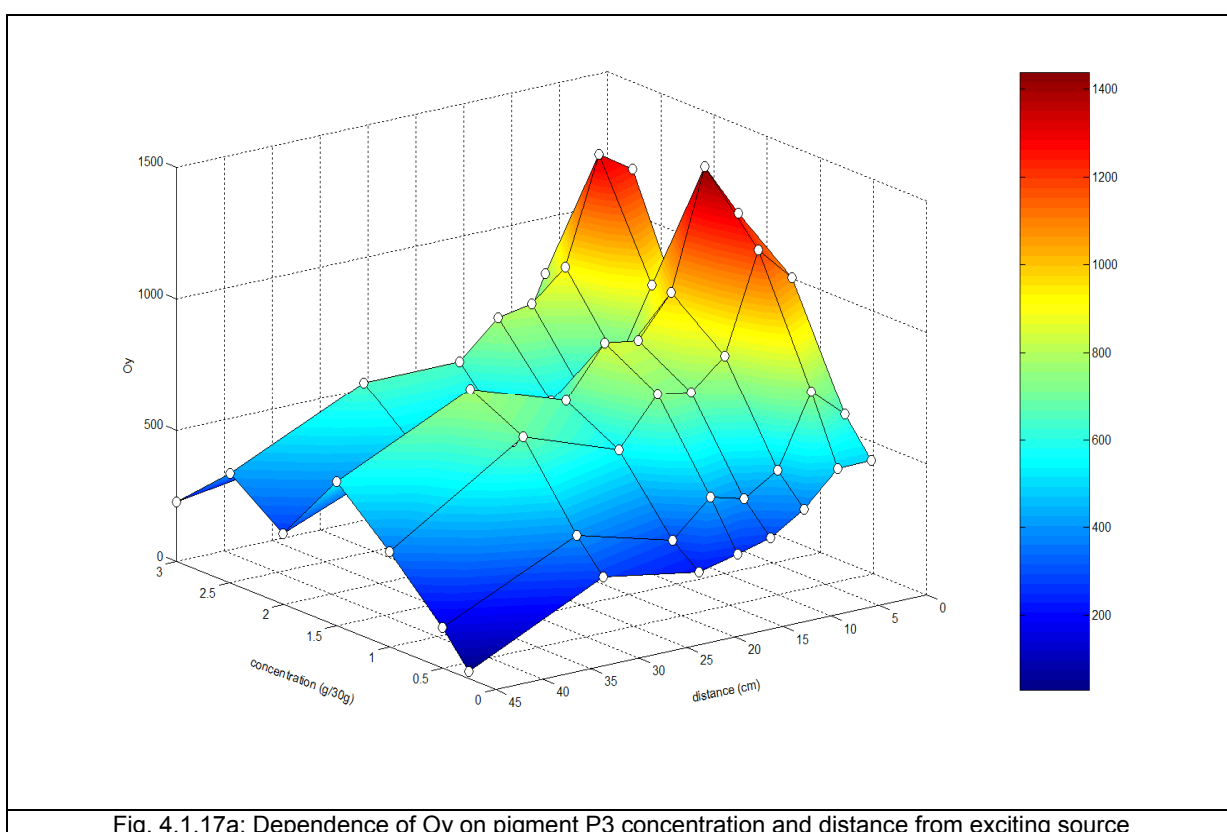
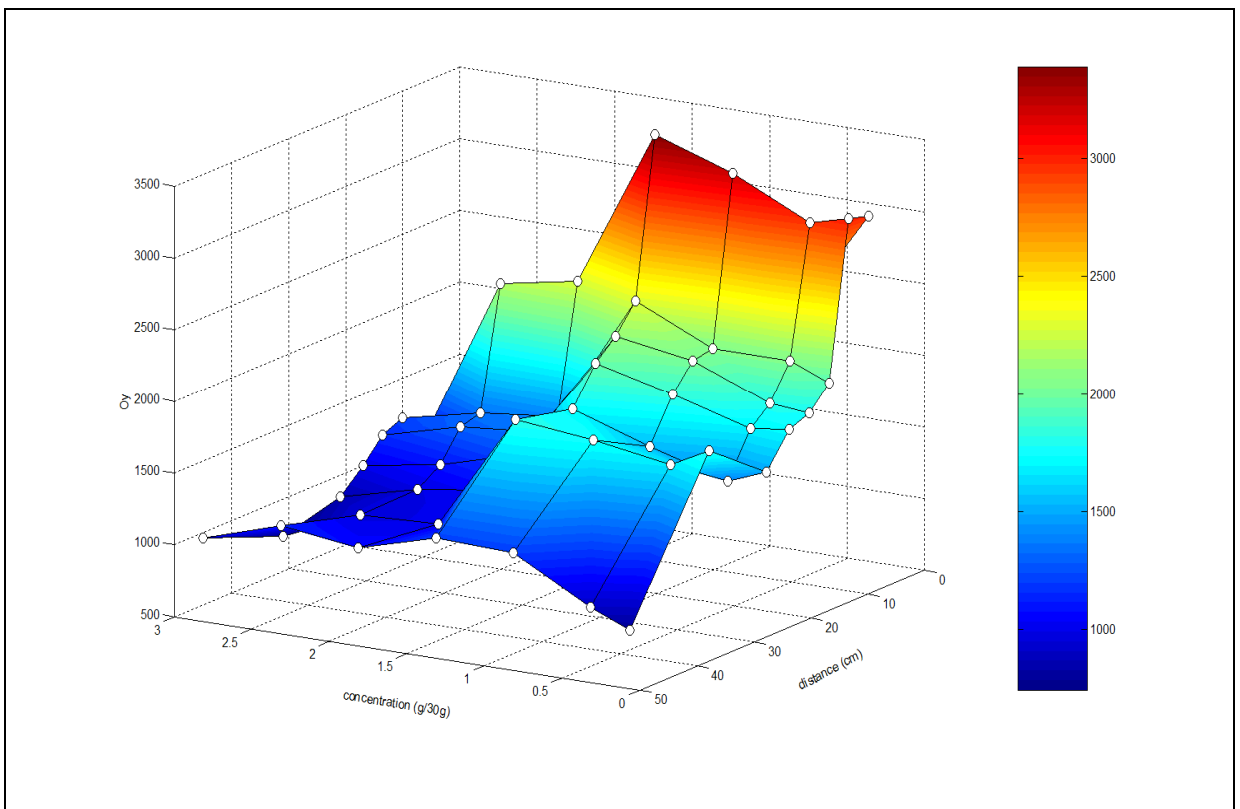Fig. 4.1.17 b: Dependence of Oy on pigment P1 concentration and distance from exciting source

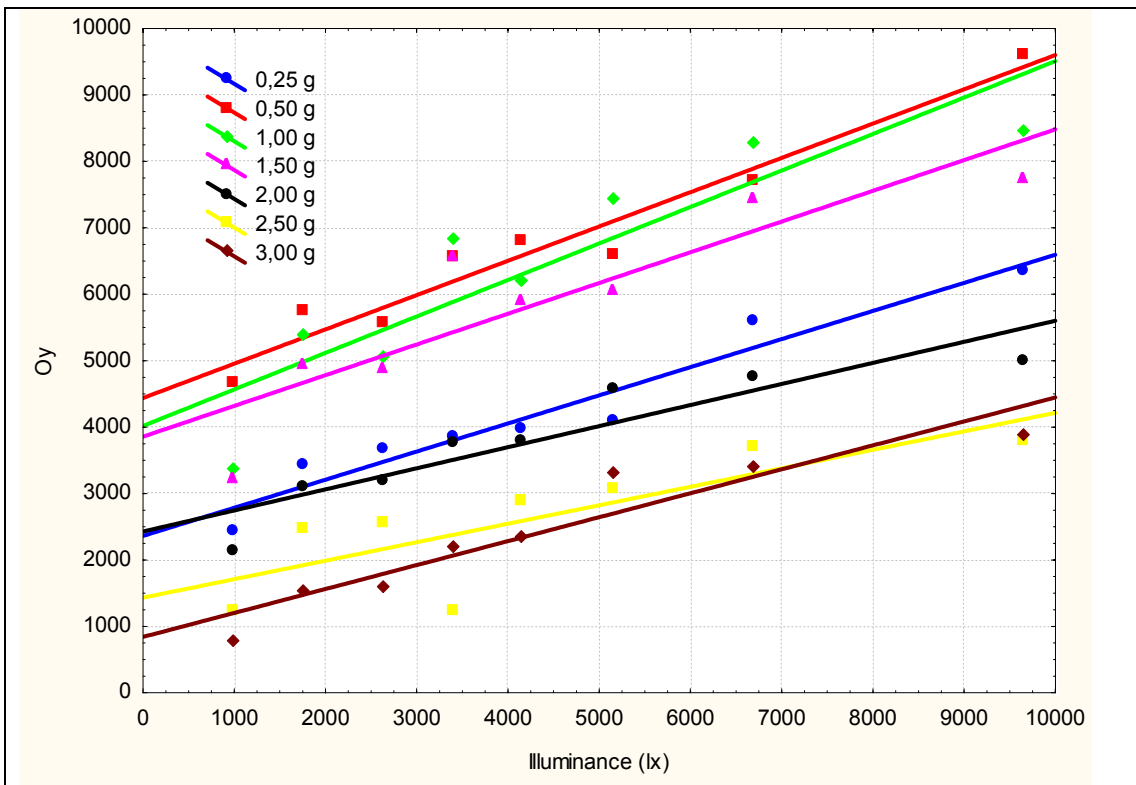Fig. 4.1.17 c: Dependence of Oy on pigment P2 concentration and distance from exciting source

Fig. 4.1.18a :Dependence of Oy on illuminance E for different concentrations of P1
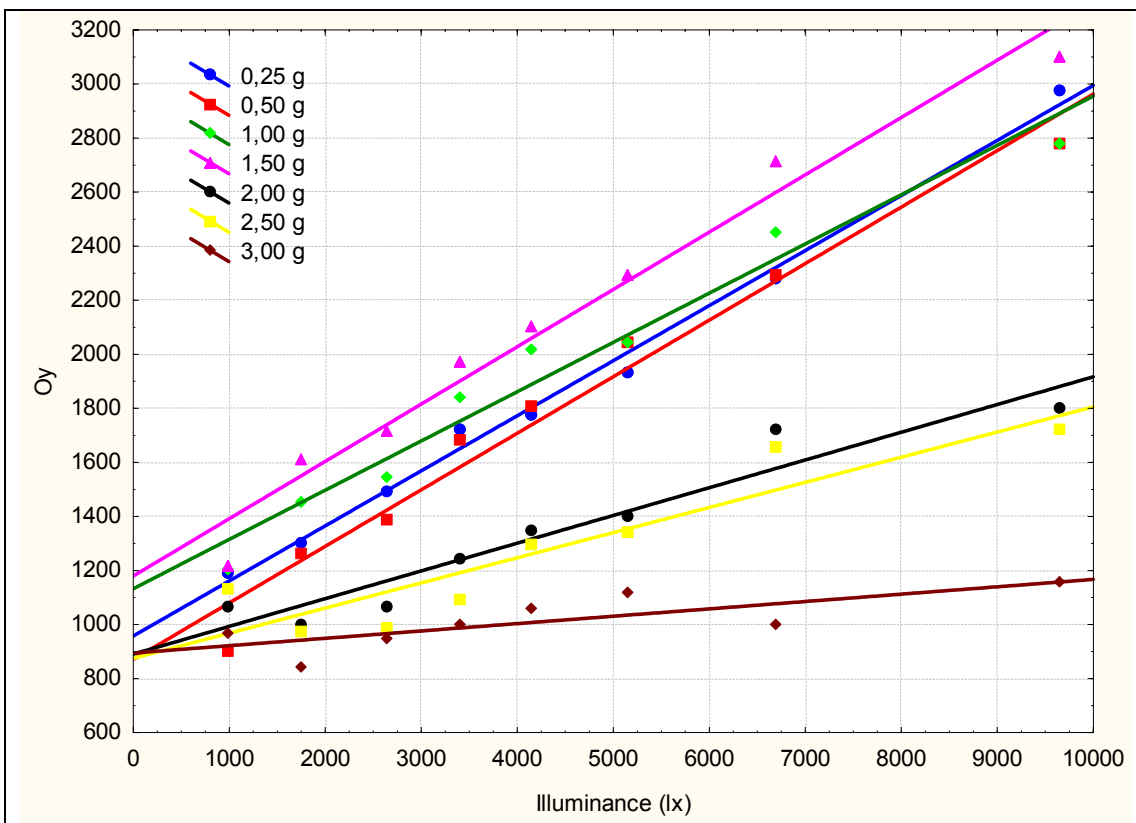

Fig. 4.1.18b: Dependence of Oy on illuminance E for different concentrations of P2
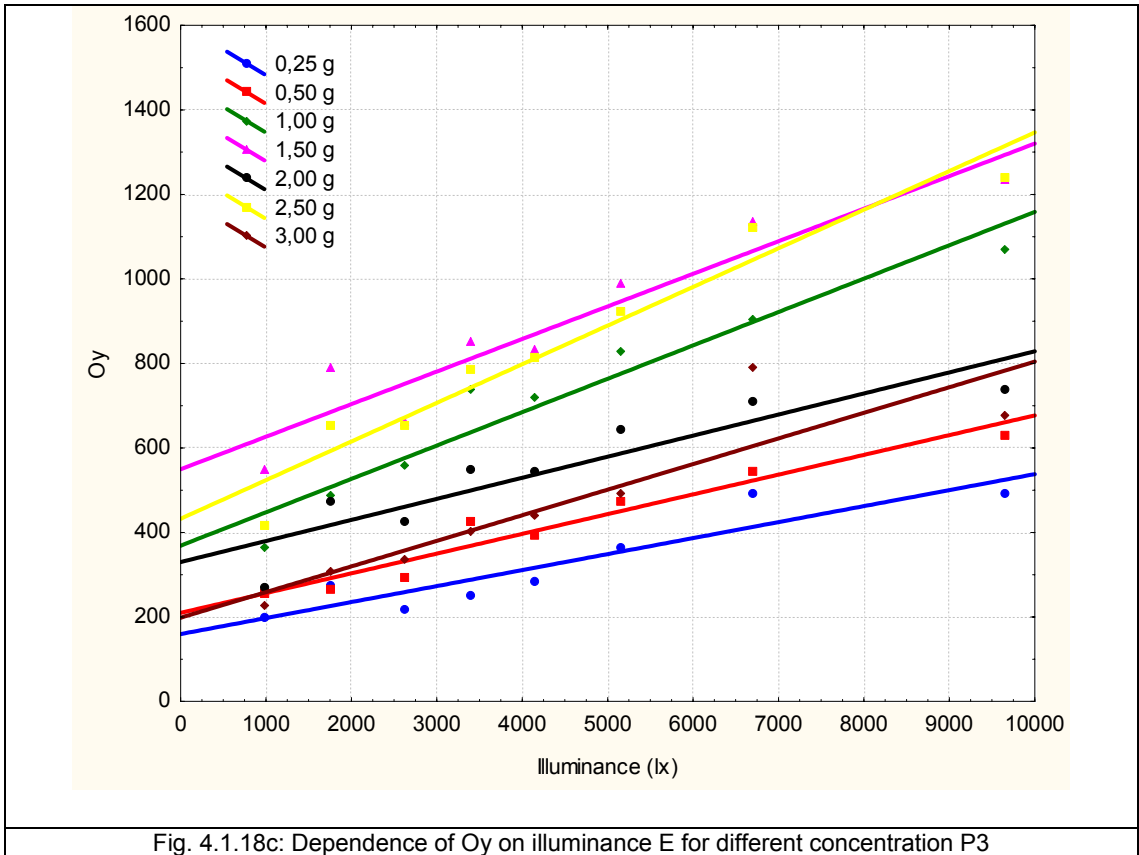
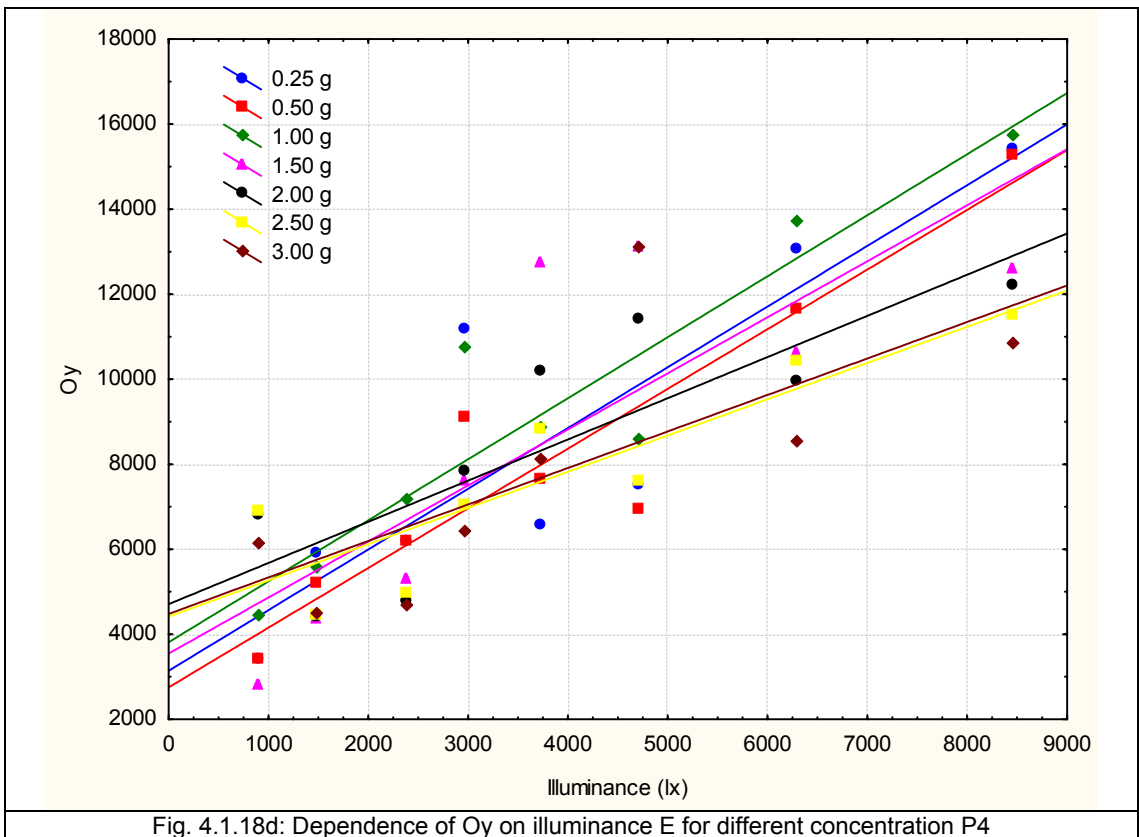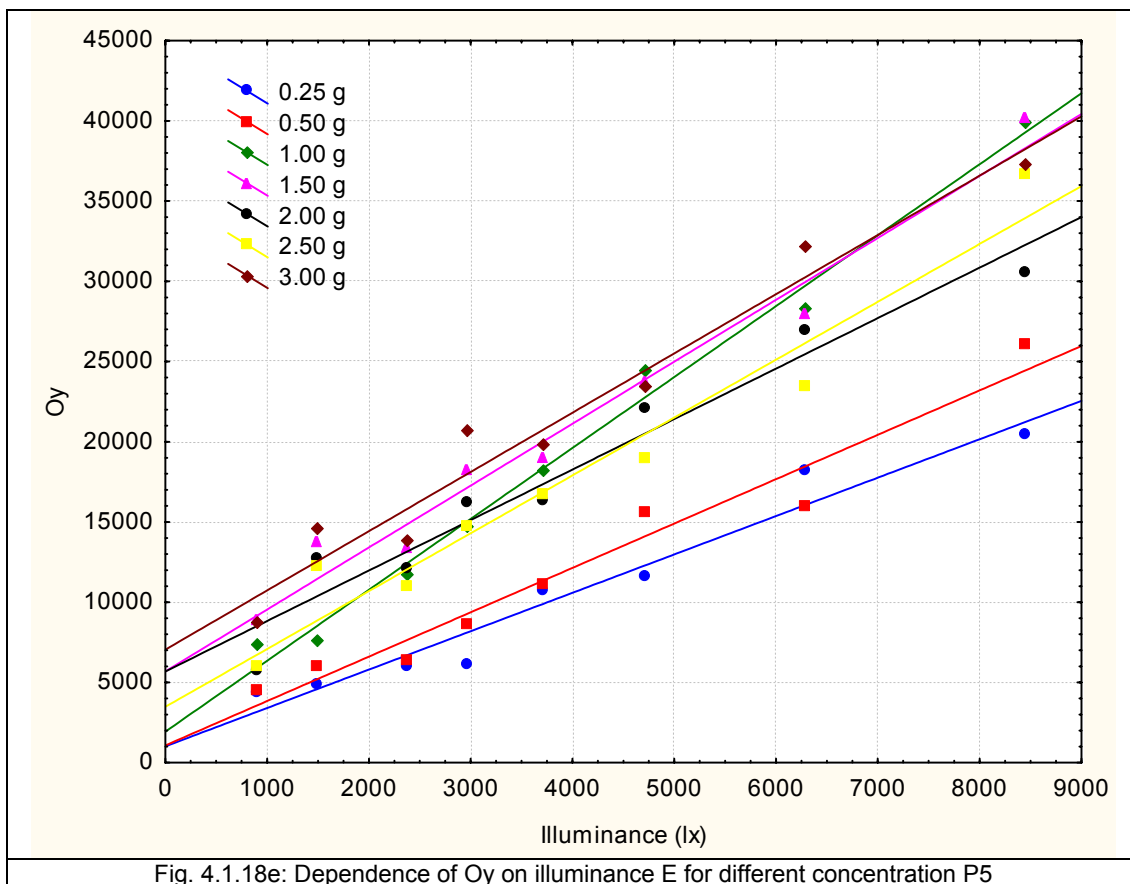Fig. 4.1.18c: Dependence of Oy on illuminance E for different concentration P3

Fig. 4.1.18d: Dependence of Oy on illuminance E for different concentration P4

Fig. 4.1.18e: Dependence of Oy on illuminance E for different concentration P5

From the graphs presented in Figs.4.1.17a-c and Figs.4.1.18a-e it is evident that concentrations above 2g/30g provide lower optical yields than at concentration 0.25g/30g. This phenomenon is probably caused by the higher concentration of pigment on the textile substrate. Pure photochromic pigment powder is not sensitive to UV radiation in day light. After irradiation, the photochromic pigment in powder form does not change colour. Concentrations of photochromic pigment above 50g/kg of printing paste may well cause crystallization of photochromic pigment into the solid-state form. The microscopic pictures in Fig. 4.1.19 a-b support this concept. In Fig. 4.1.19b there is visible crystallization of pigment P1 at a concentration of 3g/30g.
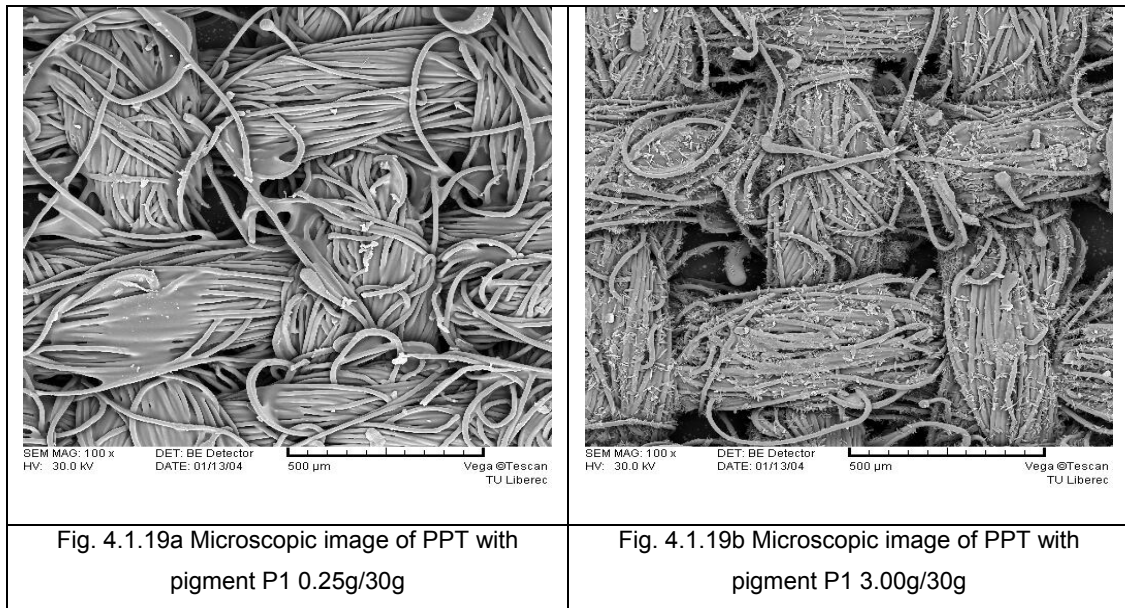
Fig. 4.1.19a Microscopic image of PPT with pigment P1 0.25g/30g	Fig. 4.1.19b Microscopic image of PPT with pigment P1 3.00g/30g

Table 4.1.2 a Coefficients of model O_y=A0+A1*X for pigment P1

Concentration of pigment (%)	A0	standard deviation	t-criterion	Decision	A1	standard deviation	t-criterion	Decision
0.25	3106.470	620.549	5.006	significant	0.292	0.136	2.133	insignificant
0.50	4497.949	853.349	5.271	significant	0.543	0.188	2.887	significant
1.00	4187.523	751.610	5.571	significant	0.600	0.165	3.619	significant
1.50	3680.316	753.990	4.881	significant	0.625	0.166	3.760	significant
2.00	2277.973	398.043	5.723	significant	0.392	0.087	4.467	significant
2.50	1325.447	522.783	2.535	significant	0.369	0.115	3.206	significant
3.00	960.411	245.838	3.907	significant	0.315	0.054	5.815	significant

Table 4.1.2b Coefficients of model O_y =A0+A1*X for pigment P2

Concentration of pigment (%)	A0	standard deviation	t-criterion	Decision	A1	standard deviation	t-criterion	Decision
0.25	910.751	226.404	4.023	significant	0.266	0.265	5.328	significant
0.50	998.408	215.916	4.624	significant	0.227	0.047	4.778	significant
1.00	1217.997	240.769	5.059	significant	0.208	0.053	3.924	significant
1.50	1452.587	342.614	4.239	significant	0.161	0.075	2.136	insignificant
2.00	838.037	172.988	4.844	significant	0.146	0.038	3.827	significant
2.50	824.409	177.516	4.644	significant	0.134	0.039	3.417	significant
3.00	855.648	91.941	9.307	significant	0.040	0.020	1.991	insignificant

Table 4.1.2c Coefficients of model $O_y =$A0+A1*X for pigment P3

Concentration of pigment (%)	A0	standard deviation	t-criterion	Decision	A1	standard deviation	t-criterion	Decision
0.25	92.536	47.957	1.929	insignificant	0.053	0.010	5.103	significant
0.50	196.711	67.741	2.904	significant	0.062	0.014	4.205	significant
1.00	408.247	89.587	4.557	significant	0.093	0.019	4.751	significant
1.50	522.347	99.935	5.227	significant	0.102	0.022	4.652	significant
2.00	311.226	72.688	4.282	significant	0.066	0.016	4.167	significant
2.50	412.818	75.567	5.463	significant	0.113	0.016	6.798	significant
3.00	191.667	54.228	3.534	significant	0.069	0.011	5.783	significant

Table 4.1.2d Coefficients of model $O_y =$A0+A1*X for pigment P4

Concentration of pigment (%)	A0	standard deviation	t-criterion	Decision	A1	standard deviation	t-criterion	Decision
0.25	4692.527	1679.749	2.793	significant	0.839	0.370	2.267	significant
0.50	4299.297	1170.593	3.672	significant	0.817	0.258	3.167	significant
1.00	5365.986	1482.266	3.620	significant	0.845	0.326	2.588	significant
1.50	5099.068	2470.676	2.063	insignificant	0.729	0.544	1.339	insignificant
2.00	6261.331	1755.921	3.565	significant	0.380	0.387	0.981	insignificant
2.50	5960.627	1355.697	4.396	significant	0.266	0.299	0.890	insignificant
3.00	6020.265	2020.713	2.979	significant	0.274	0.445	0.615	insignificant

Table 4.1.2e Coefficients of model $O_y =$A0+A1*X for pigment P5

Concentration of pigment (%)	A0	standard deviation	t-criterion	Decision	A1	standard deviation	t-criterion	Decision
0.25	1013.825	981.984	1.032	insignificant	2.393	0.216	11.055	significant
0.50	1074.193	1050.624	1.022	insignificant	2.766	0.232	11.944	significant
1.00	1929.984	812.450	2.375	significant	4.421	0.179	24.688	significant
1.50	5686.607	1157.188	4.914	significant	3.860	0.255	15.135	significant
2.00	5680.506	1373.826	4.134	significant	3.147	0.303	10.392	significant
2.50	3477.345	1524.665	2.280	significant	3.606	0.336	10.732	significant
3.00	7038.975	1362.153	5.167	significant	3.693	0.300	12.301	significant

Table 4.1.3 c: First order kinetic parameters for pigment P1

Irradiance E [μW.cm-2]	0.25%		0.50%		1.00%		1.50%	
	Rate constant k	Half life $t_{1/2}$ [s]	Rate constant k	Half life $t_{1/2}$ [s]	Rate constant k	Half life $t_{1/2}$ [s]	Rate constant k	Half life $t_{1/2}$ [s]
87.6	0.0183	37.73	0.0182	37.96	0.0168	41.09	0.0209	33.15
143.4	0.0229	30.19	0.0227	30.40	0.0236	29.32	0.0255	27.11
229.1	0.0249	27.77	0.0236	29.31	0.0277	24.97	0.0236	29.31
285.9	0.0242	28.57	0.0188	36.77	0.0275	25.18	0.0232	29.82
358.1	0.0275	25.19	0.0202	34.21	0.0369	18.76	0.0231	29.90
453.4	0.0563	12.31	0.0471	14.71	0.0460	15.06	0.0438	15.82
605.5	0.0581	11.91	0.0542	12.77	0.0462	14.99	0.0348	19.90
814.4	0.0718	9.64	0.0623	11.12	0.0667	10.38	0.0654	10.59

Irradiance E [μW.cm-2]	2.00%		2.50%		3.00%	
	Rate constant k	Half life $t_{1/2}$ [s]	Rate constant k	Half life $t_{1/2}$ [s]	Rate constant k Half life	$t_{1/2}$ [s]
87.6	0.0211	32.73	0.0177	39.09	0.0169	40.82
143.4	0.0233	29.62	0.0249	27.73	0.0304	22.77
229.1	0.0223	30.99	0.0218	31.78	0.0213	32.40
285.9	0.0192	35.97	0.0239	28.98	0.0236	29.35
358.1	0.0218	31.70	0.0203	34.08	0.0167	41.28
453.4	0.0434	15.95	0.0386	17.93	0.0344	20.13
605.5	0.0301	23.03	0.0364	19.01	0.0289	23.90
814.4	0.0598	11.58	0.0613	11.30	0.0581	11.93

Table 4.1.3 d: First order kinetic parameters for pigment P2

Irradiance E [μW.cm-2]	0.25%		0.50%		1.00%		1.50%	
	Rate constant k	Half life $t_{1/2}$ [s]	Rate constant k	Half life $t_{1/2}$ [s]	Rate constant k	Half life $t_{1/2}$ [s]	Rate constant k	Half life $t_{1/2}$ [s]
87.6	0.0321	21.56	0.0139	49.67	0.0198	34.94	0.0221	31.22
143.4	0.0246	28.10	0.0264	26.19	0.0261	26.53	0.0264	26.20
229.1	0.0484	14.32	0.0377	18.36	0.0266	26.02	0.0284	24.40
285.9	0.0602	11.49	0.0404	17.13	0.0341	20.28	0.0353	19.62
358.1	0.0526	13.15	0.0359	19.30	0.0298	23.20	0.0270	25.62
453.4	0.0729	9.50	0.0589	11.76	0.0528	13.12	0.0521	13.29
605.5	0.0767	9.03	0.0566	12.24	0.0521	13.31	0.0448	15.47
814.4	0.0852	8.12	0.0896	7.73	0.0727	9.52	0.0955	7.25

Irradiance E [μW.cm-2]	2.00%		2.50%		3.00%	
	Rate constant k	Half life $t_{1/2}$ [s]	Rate constant k	Half life $t_{1/2}$ [s]	Rate constant k Half life	$t_{1/2}$ [s]
87.6	0.0273	25.33	0.0166	41.56	0.0389	17.80
143.4	0.0266	26.02	0.0290	23.88	0.0314	22.06
229.1	0.0273	25.30	0.0304	22.79	0.0290	23.82
285.9	0.0321	21.54	0.0350	19.77	0.0291	23.86
358.1	0.0242	28.56	0.0267	25.90	0.0260	26.65
453.4	0.0488	14.18	0.0432	16.02	0.0432	16.02
605.5	0.0339	20.43	0.0337	20.55	0.0389	17.77
814.4	0.0741	9.35	0.0632	10.95	0.0711	9.76

Table 4.1.3 c: First order kinetic parameters for pigment P3

Irradiance E [μW.cm-2]	0.25%		0.50%		1.00%		1.50%	
	Rate constant k	Half life t1/2 [s]	Rate constant k	Half life t1/2 [s]	Rate constant k	Half life t1/2 [s]	Rate constant k	Half life t1/2 [s]
87.6	0.0321	21.62	0.0617	11.21	0.0468	14.81	0.0369	18.75
143.4	0.0847	8.18	0.0612	11.31	0.0707	9.79	0.0582	11.90
229.1	0.1985	3.49	0.1155	5.99	0.0946	7.32	0.1024	6.76
285.9	0.0967	7.17	0.0816	8.48	0.0679	10.19	0.0826	8.38
358.1	0.0923	7.50	0.0833	8.31	0.0564	12.28	0.0759	9.13
453.4	0.1585	4.37	0.1803	3.84	0.1212	5.71	0.1193	5.81
605.5	0.1968	3.52	0.1964	3.52	0.1229	5.63	0.1372	5.05
814.4	0.2472	2.80	0.2516	2.75	0.1872	3.70	0.2318	2.99

Irradiance E [μW.cm-2]	2.00%		2.50%		3.00%	
	Rate constant k	Half life t1/2 [s]	Rate constant k	Half life t1/2 [s]	Rate constant k Half life	t1/2 [s]
87.6	0.0426	16.26	0.0468	14.81	0.0471	14.69
143.4	0.0583	11.88	0.0707	9.79	0.0854	8.11
229.1	0.0798	8.68	0.0946	7.32	0.0826	8.39
285.9	0.0706	9.81	0.0679	10.19	0.0377	18.37
358.1	0.0647	10.69	0.0564	12.28	0.0559	12.38
453.4	0.1254	5.52	0.1212	5.72	0.1148	6.03
605.5	0.1457	4.75	0.1229	5.64	0.0958	7.23
814.4	0.2045	3.38	0.1872	3.70	0.2213	3.13

Table 4.1.3 d: First order kinetic parameters for pigment P4

Irradiance E [μW.cm^{-2}]	0.25%		0.50%		1.00%		1.50%	
	Rate constant k	Half life t$_{1/2}$ [s]	Rate constant k	Half life t$_{1/2}$ [s]	Rate constant k	Half life t$_{1/2}$ [s]	Rate constant k	Half life t$_{1/2}$ [s]
87.6	0.0326	21.26	0.0340	20.33	0.0327	21.16	0.0358	19.32
143.4	0.0345	20.08	0.0360	19.21	0.0349	19.80	0.0370	18.68
229.1	0.0379	18.28	0.0396	17.48	0.0384	18.02	0.0407	17.01
285.9	0.0405	17.08	0.0424	16.34	0.0411	16.85	0.0435	15.89
358.1	0.0445	15.56	0.0465	14.89	0.0451	15.35	0.0489	14.14
453.4	0.0511	13.56	0.0534	12.97	0.0518	13.37	0.0562	12.32
605.5	0.0668	10.36	0.0699	9.91	0.0671	10.31	0.0736	9.41
814.4	0.1161	5.96	0.1214	5.70	0.1178	5.88	0.1278	5.42

Irradiance E [μW.cm^{-2}]	2.00%		2.50%		3.00%	
	Rate constant k	Half life t$_{1/2}$ [s]	Rate constant k	Half life t$_{1/2}$ [s]	Rate constant k Half life	t$_{1/2}$ [s]
87.6	0.0363	19.04	0.0358	19.32	0.0363	19.04
143.4	0.0385	17.99	0.0370	18.68	0.0385	17.99
229.1	0.0423	16.37	0.0407	17.01	0.0423	16.37
285.9	0.0485	14.26	0.0435	15.89	0.0485	14.26
358.1	0.0533	12.99	0.0489	14.14	0.0533	12.99
453.4	0.0523	13.24	0.0562	12.32	0.0523	13.24
605.5	0.0684	10.11	0.0736	9.41	0.0684	10.11
814.4	0.1391	4.98	0.1278	5.42	0.1391	4.98

Table 4.1.3 e: First order kinetic parameters for pigment P5

Irradiance E [μW.cm^{-2}]	0.25%		0.50%		1.00%		1.50%	
	Rate constant k	Half life t1/2 [s]	Rate constant k	Half life t1/2 [s]	Rate constant k	Half life t1/2 [s]	Rate constant k	Half life t1/2 [s]
87.6	0.0435	15.91	0.0579	11.95	0.0665	10.42	0.0601	11.54
143.4	0.0523	13.23	0.0628	11.04	0.0651	10.65	0.0654	10.59
229.1	0.0577	11.99	0.0698	9.92	0.0726	9.55	0.0739	9.37
285.9	0.0578	11.98	0.0806	8.60	0.0806	8.59	0.0823	8.41
358.1	0.0759	9.12	0.0806	8.59	0.0858	8.07	0.0811	8.54
453.4	0.0558	12.41	0.0882	7.85	0.0897	7.72	0.0885	7.83
605.5	0.0781	8.87	0.0975	7.10	0.1183	5.86	0.1148	6.03
814.4	0.1751	3.95	0.1745	3.97	0.1756	3.94	0.1776	3.90

Irradiance E [μW.cm^{-2}]	2.00%		2.50%		3.00%	
	Rate constant k	Half life t1/2 [s]	Rate constant k	Half life t1/2 [s]	Rate constant k Half life	t1/2 [s]
87.6	0.0569	12.16	0.0604	11.46	0.0674	10.28
143.4	0.0668	10.37	0.0704	9.83	0.0695	9.96
229.1	0.0757	9.15	0.0729	9.51	0.0742	9.33
285.9	0.0845	8.20	0.0744	9.31	0.0794	8.72
358.1	0.0783	8.85	0.0815	8.49	0.0804	8.61
453.4	0.0883	7.84	0.0862	8.03	0.0869	7.97
605.5	0.1122	6.17	0.1044	6.63	0.1142	6.06
814.4	0.1514	4.57	0.2059	3.36	0.1162	5.96

Tables 4.1.2a-e summarize the results of the statistic parameters obtained for photochromic pigment prints and Table 4.1.3 a-e summarize the kinetic parameters. The calculated statistic and kinetic parameters show that increasing the irradiance caused a decrease in the half-life of colour change for every pigment. Only pigment P5 has a coefficient A1 higher than 2 units. This effect is caused by absolute values of *Oy*, which for pigment P5 is approximately 4-times larger in comparison to the other pigments. Tables 4.1.3 a-e show the variability of half-life from the point of view of the tested concentrations. This effect had an influence on the experimental error due to the off-line system of measurement, which was used for this experiment. The reason for using the off-line method for this experiment was relatively low ratio between lower and higher irradiance, which is 1:3 for on-line measurement in comparison to the off-line method, where the ratio is approximately 1:10. From point of view of colour change performance, pigments P1 and P2 have approximately 2 times longer half-life than the rest of the pigments and pigments P4, P5 have higher the optical yield *Oy* than the rest of the pigments.

4.2 Non-woven textiles containing the photochromic pigments

In addition to the kinetic study of the change of shade intensity for photochromic printed textiles, a study was also carried out with non-woven textiles, dope dyed with photochromic pigment, which were produced by Melt blown technology. As examples data are documented for pigments P2 and P3 in Tables 4.2.1a-e and Tables 4.2.2 a-e together with models derived from equations 2.5.9 and 2.5.11. There are documented data sets of first order kinetic parameters and model coefficients only for pigment P2 and P3, since it was not possible to produce all textiles (prints and non-woven) and comparative concentrations in solution with the other pigments. Fig. 4.2.1 illustrates a higher shade intensity of photochromic reaction for higher concentrations.

Fig. 4.2.1: Dependency of shade intensity *I* on concentration of photochromic pigment NW-P3 and irradiance E= 8460 lx
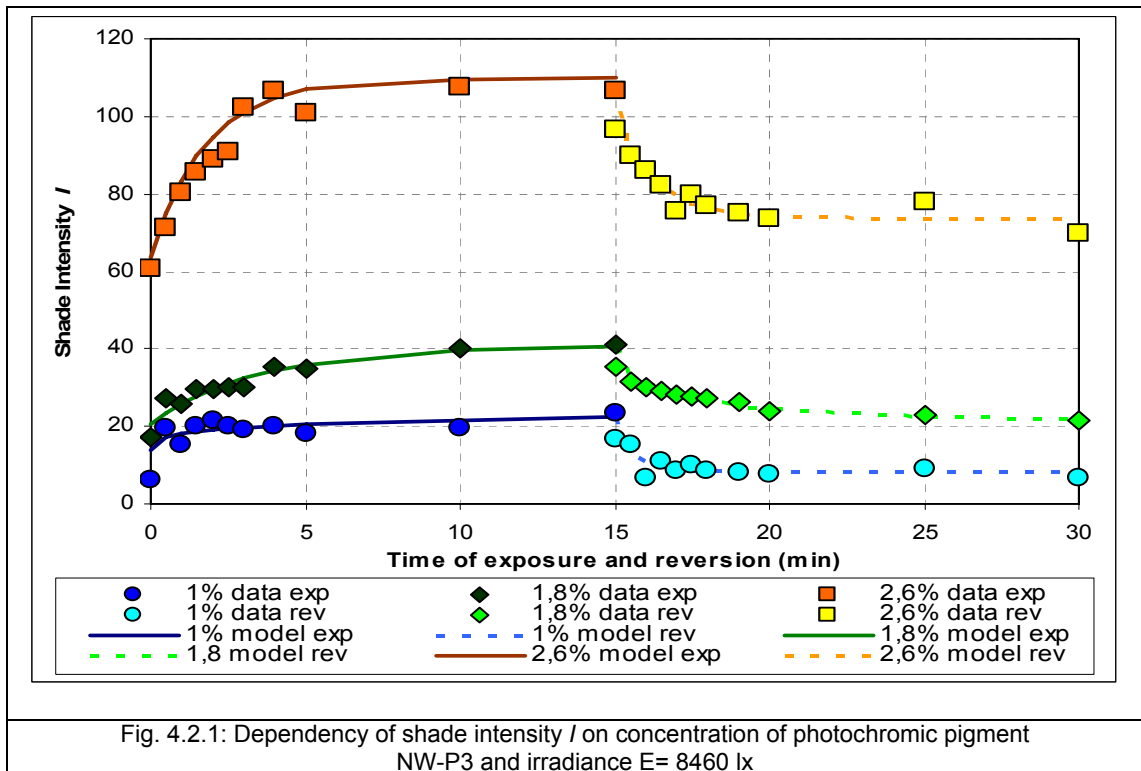
During the production of the non-woven samples it was necessary to solve several difficult technological problems, as discussed in section 3.2.2. From Figs. 3.2.9 and 3.2.10 it was shown that using the master batch with photochromic pigments effected the creation of villuses. Due to this problem, it was impossible with accessible devices to create non-woven textiles with a high concentration of photochromic pigment.

This feature limited the amount of experimental samples and influenced a detailed test of the relationship between O_y and concentration of photochromic pigment.

Nevertheless, from Figs. 4.2.2a–b and Figs. 4.2.3a–b a linear reasonable relation between O_y and irradiance E is observed. This trend is similar to that shown by the textiles with photochromic prints.

Table 4.2.1 a Coefficients of model $O_y=A0+A1*X$ for pigment NW-P3 f. T1

Concentration of pigment (%)	A0	Standard deviation	t-criterion	Decision	A1	Standard deviation	t-criterion	Decision
1.0	134.525	27.958	4.812	significant	0.020	0.006	3.316	significant
1.8	64.334	28.147	2.286	insignificant	0.034	0.006	5.492	significant
2.6	384.883	53.033	7.257	significant	0.041	0.011	3.559	significant

Table 4.2.1b Coefficients of model $O_y=A0+A1*X$ for pigment NW-P3 f. T2

Concentration of pigment (%)	A0	Standard deviation	t-criterion	Decision	A1	Standard deviation	t-criterion	Decision
1.0	21.649	4.459	4.854	significant	0.003	0.001	0.033	insignificant
1.8	32.055	24.468	1.310	insignificant	0.018	0.005	3.453	significant
2.6	120.046	45.065	2.664	significant	0.079	0.009	7.977	significant

Table 4.2.1c Coefficients of model $O_y=A0+A1*X$ for pigment NW-P2 f. T1

Concentration of pigment (%)	A0	Standard deviation	t-criterion	Decision	A1	Standard deviation	t-criterion	Decision
1.0	289.477	90.825	3.187	significant	0.099	0.020	4.967	significant
1.8	115.994	104.479	1.110	insignificant	0.068	0.023	2.986	significant
2.6	217.337	60.215	3.609	significant	0.070	0.013	5.340	significant

Table 4.2.1d Coefficients of model $O_y=A0+A1*X$ for pigment NW-P2 f. T2

Concentration of pigment (%)	A0	Standard deviation	t-criterion	Decision	A1	Standard deviation	t-criterion	Decision
1.0	143.994	61.065	2.358	significant	0.086	0.013	6.435	significant
1.8	167.231	40.487	4.130	significant	0.067	0.008	7.615	significant
2.6	167.453	47.373	3.535	significant	0.077	0.010	7.468	significant
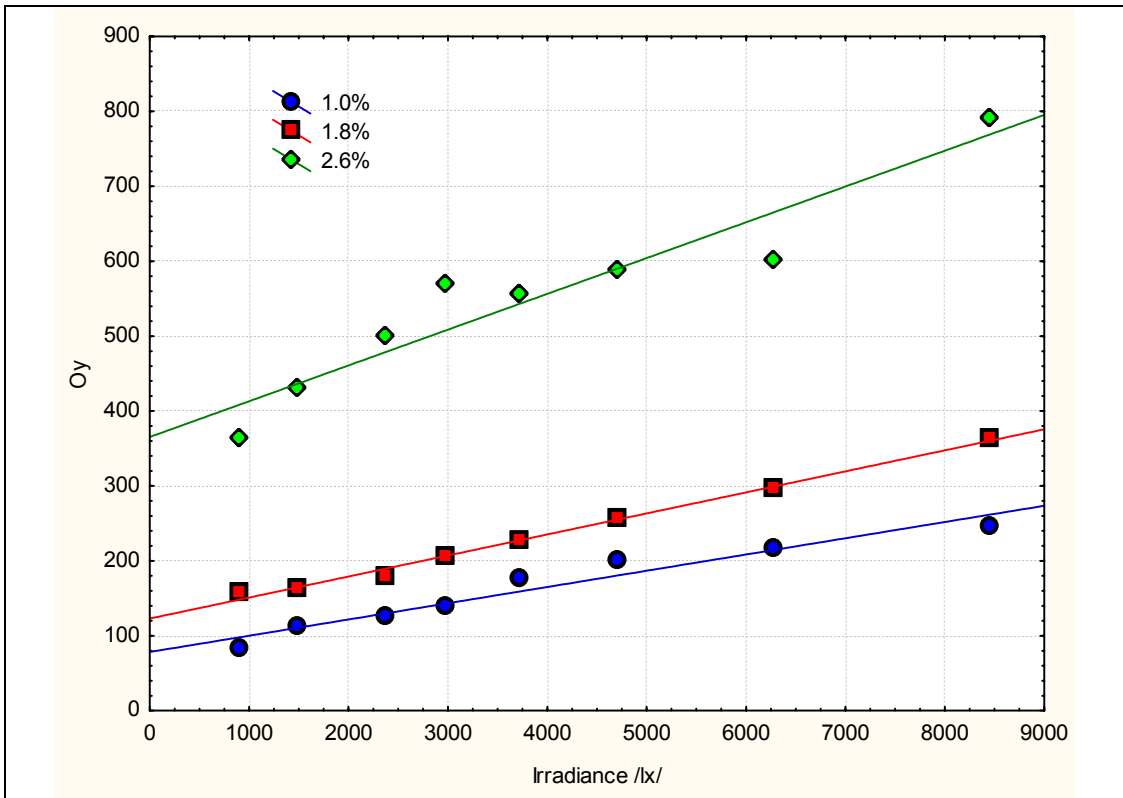
Fig. 4.2.2 a: Dependence of Oy on irradiance E for different concentrations of NW-P3 fineness T1
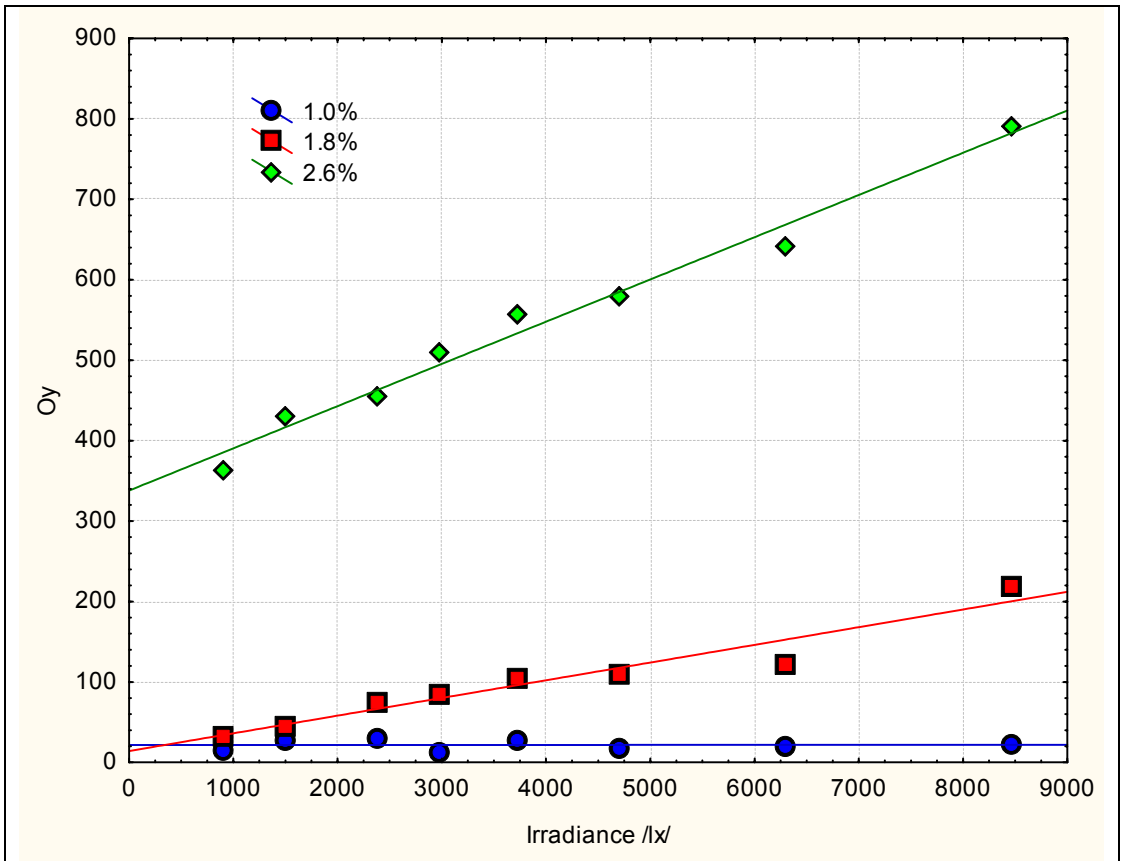
Fig. 4.2.2 b: Dependence of Oy on irradiance E for different concentrations of NW-P3 fineness T2

121
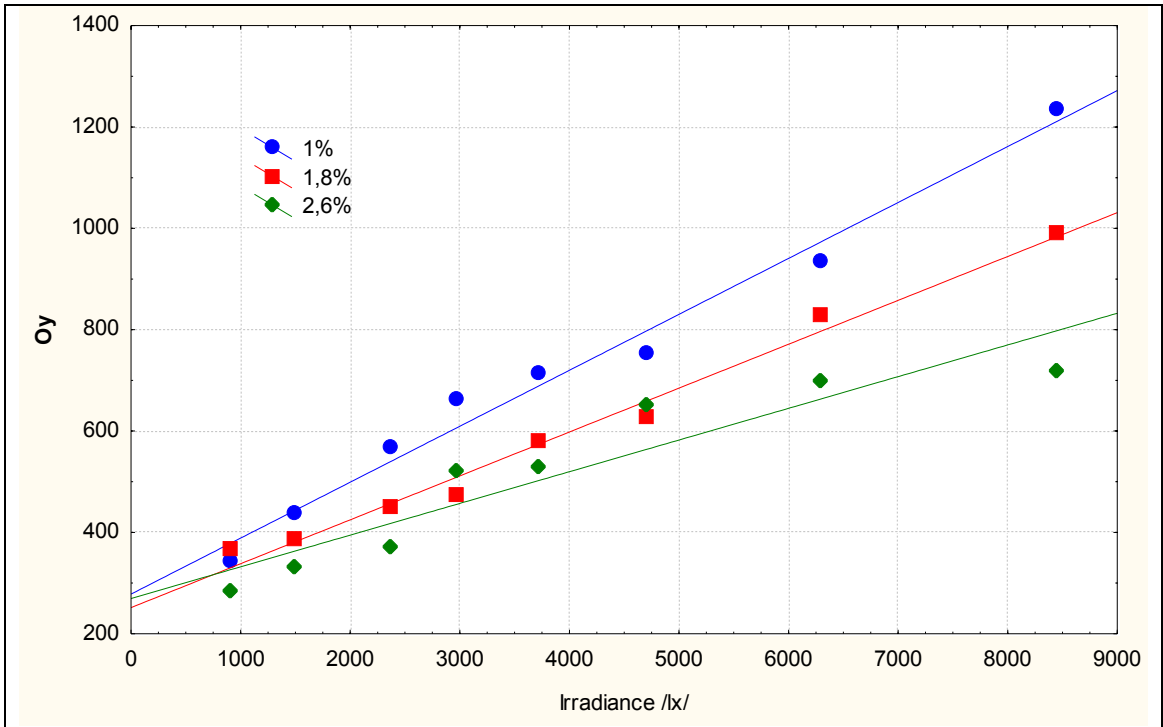
Fig. 4.2.3a: Dependence of Oy on irradiance E for different concentrations of NW-P2 fineness T1
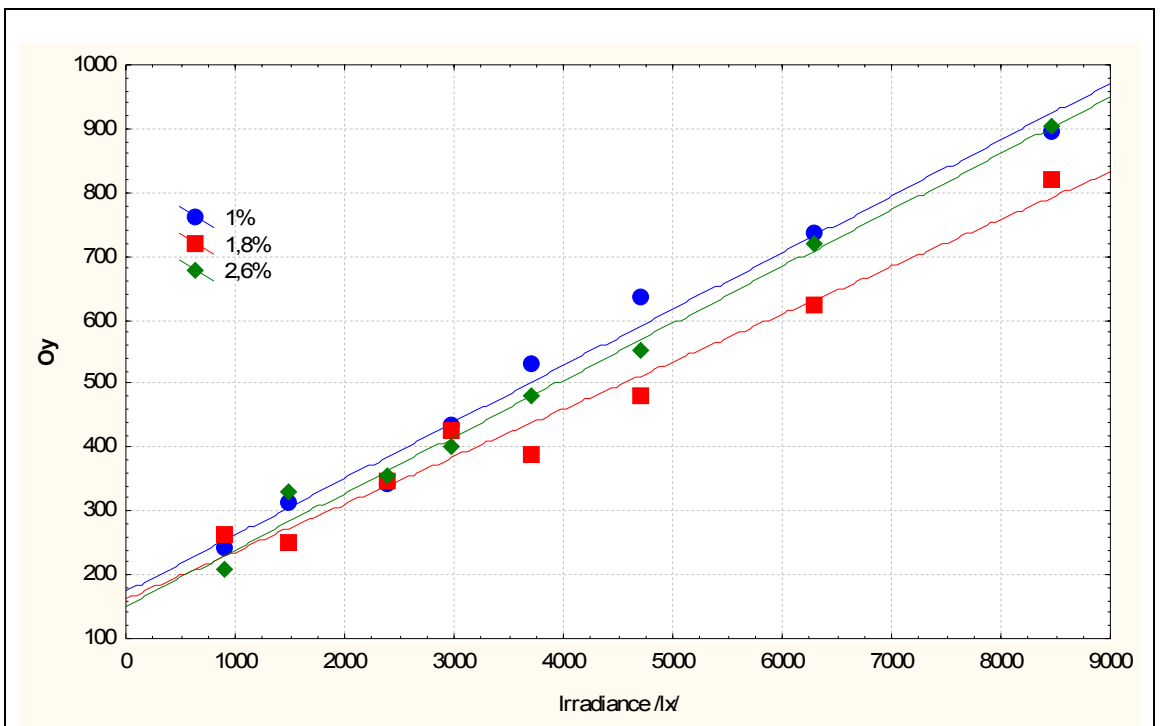
Fig. 4.2.3b: Dependence of Oy on irradiance E for different concentrations of NW-P2 fineness T2

Table 4.2.2 a: First order kinetic parameters for pigment P2 fineness T1

Irradiance E [μW.cm⁻²]	1.0%		1.8%		2.6%	
	Rate constant k	Half life t1/2 [s]	Rate constant k	Half-life t1/2 [s]	Rate constant k	Half-life t1/2 [s]
87.6	0.0051	136.76	0.0055	127.04	0.0059	117.67
143.4	0.0054	128.48	0.0058	119.25	0.0060	115.86
229.1	0.0060	115.85	0.0062	112.42	0.0065	106.36
285.9	0.0062	111.87	0.0063	110.56	0.0066	105.44
358.1	0.0070	98.50	0.0068	102.65	0.0070	98.74
453.4	0.0073	94.72	0.0069	100.17	0.0077	90.50
605.4	0.0093	74.86	0.0080	86.83	0.0079	87.98
814.3	0.0108	64.21	0.0087	79.62	0.0089	77.89

Table 4.2.2 b: First order kinetic parameters for pigment P2 fineness T2

Irradiance E [μW.cm⁻²]	1.0%		1.8%		2.6%	
	Rate constant k	Half life t1/2 [s]	Rate constant k	Half-life t1/2 [s]	Rate constant k	Half-life t1/2 [s]
87.6	0.0055	126.14	0.0054	127.85	0.0056	123.25
143.4	0.0057	122.22	0.0057	120.91	0.0058	119.96
229.1	0.0062	111.55	0.0058	120.15	0.0061	114.36
285.9	0.0064	108.57	0.0061	114.17	0.0061	112.99
358.1	0.0071	97.03	0.0065	107.13	0.0069	100.43
453.4	0.0075	92.71	0.0071	97.46	0.0071	97.09
605.4	0.0089	78.20	0.0077	90.05	0.0085	81.38
814.3	0.0098	71.03	0.0080	86.97	0.0095	73.29

Table 4.2.2 c: First order kinetic parameters for pigment P3 fineness T1

Irradiance E [μW.cm⁻²]	1.0%		1.8%		2.6%	
	Rate constant k	Half life t1/2 [s]	Rate constant k	Half-life t1/2 [s]	Rate constant k	Half-life t1/2 [s]
87.6	0.0245	28.25	0.0157	44.02	0.0172	40.41
143.4	0.0246	28.13	0.0161	43.12	0.0165	42.12
229.1	0.0284	24.42	0.0186	37.21	0.0195	35.61
285.9	0.0264	26.28	0.0191	36.28	0.0202	34.28
358.1	0.0333	20.84	0.0188	36.82	0.0229	30.32
453.4	0.0331	20.93	0.0227	30.58	0.0253	27.41
605.4	0.0410	16.89	0.0244	28.41	0.0327	21.17
814.3	0.0471	14.71	0.0341	20.31	0.0474	14.61

Table 4.2.2 d: First order kinetic parameters for pigment P3 fineness T2

Irradiance E [μW.cm⁻²]	1.0%		1.8%		2.6%	
	Rate constant k	Half life t1/2 [s]	Rate constant k	Half-life t1/2 [s]	Rate constant k	Half-life t1/2 [s]
87.6	0.0233	29.74	0.0163	42.42	0.0151	45.80
143.4	0.0220	31.57	0.0176	39.42	0.0150	46.12
229.1	0.0196	35.31	0.0174	39.88	0.0165	42.00
285.9	0.0223	31.14	0.0174	39.85	0.0172	40.28
358.1	0.0217	31.93	0.0195	35.55	0.0199	34.81
453.4	0.0206	33.64	0.0199	34.84	0.0209	33.24
605.4	0.0246	28.18	0.0230	30.10	0.0257	26.94
814.3	0.0227	30.56	0.0236	29.34	0.0387	17.91

Fig. 4.2.2.a-c shows another interesting fact that the fineness of fibres has an influence on shade intensity *I*. It is visible that the non-woven textile with 1% of pigment P3 is inactive. Fig. 4.2.4. shows that thicker fibres have an approximately 20% higher absorption of UV radiation. Nevertheless, this difference has less importance, because for exposure of non-woven textiles a UV fluorescent tube was used with radiance maximum at 365 nm, where there is insignificant absorption of UV radiation by PP fibres. Investigation of the absorption of the PP fibres used related to the thickness determined by micro-densitometry technique. Fibres were placed individually into the microscope connected to the Avantes USB 2000 spectrometer. A continuous discharge Xe lamp was used as light source.

The influence of the medium used is demonstrated in Fig 4.2.5. The transmission spectrum for the photochromic pigment in solution is described in the graph. In the case of NW and photochromic printed textiles it is evident that a bathochromic shift of 30 nm in the reflectance minimum is caused by the influence of the textile substrate. Besides, there is evidence also for a difference between the spectral reflectance shapes of the PET fabric used and the PP non-woven textiles, which is associated with the different reflectance properties of these substrates (as shown in Fig. 4.2.6).

Fig. 4.2.4: Comparison of absorption characteristics PP fibres in dependence on their fineness

Fig. 4.2.5: Spectral shift of reflectance (β) or transmittance (τ) minima based on the different applications (NWT-PP non-woven textile, PTP-screen printed photochromic textile, PPS- photochromic solution)

Fig. 4.2.6: Spectral reflectance of pure PP NW and PET fabric
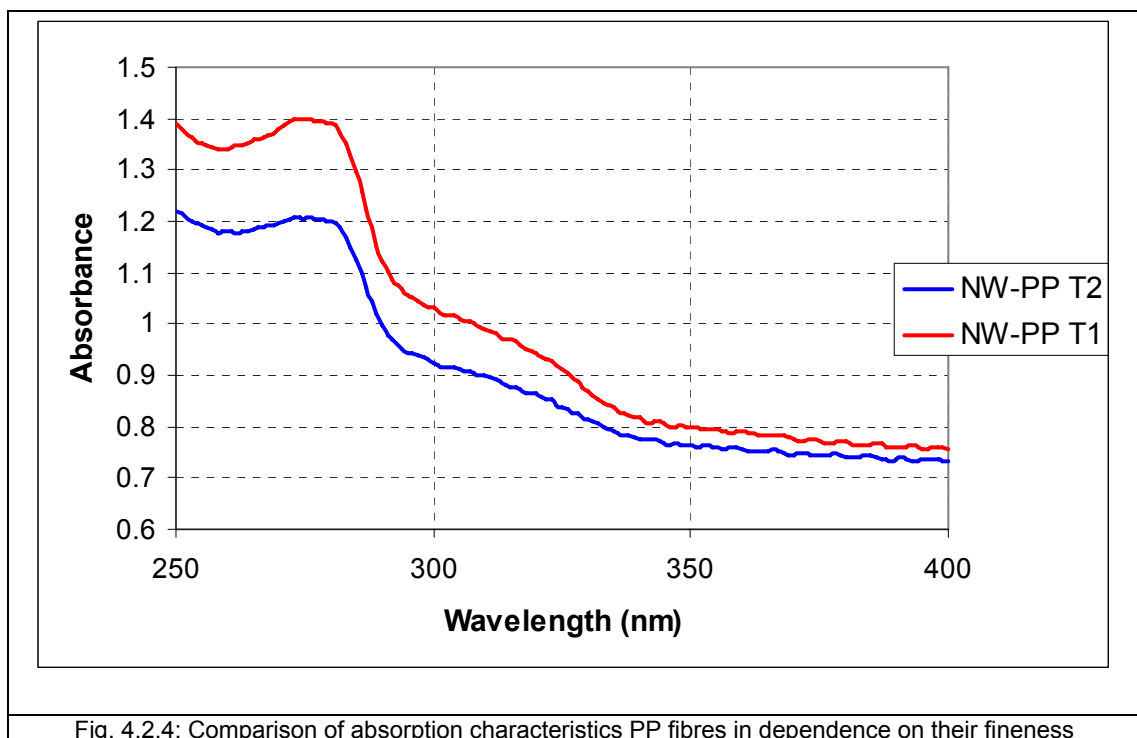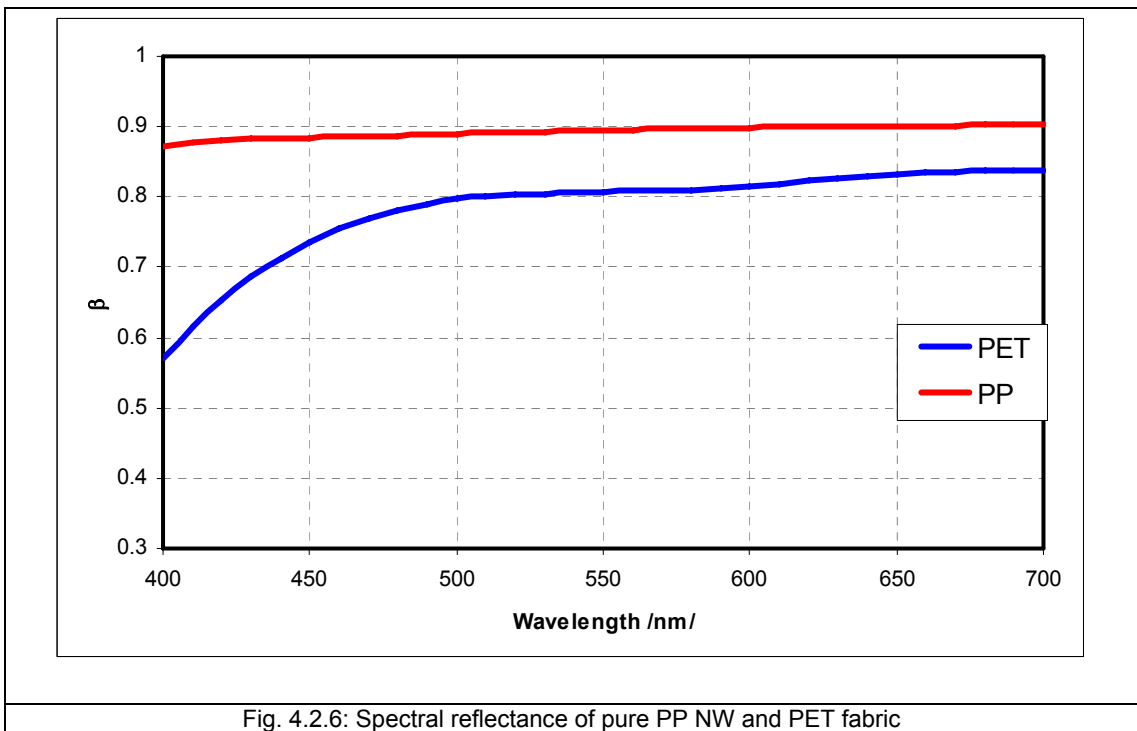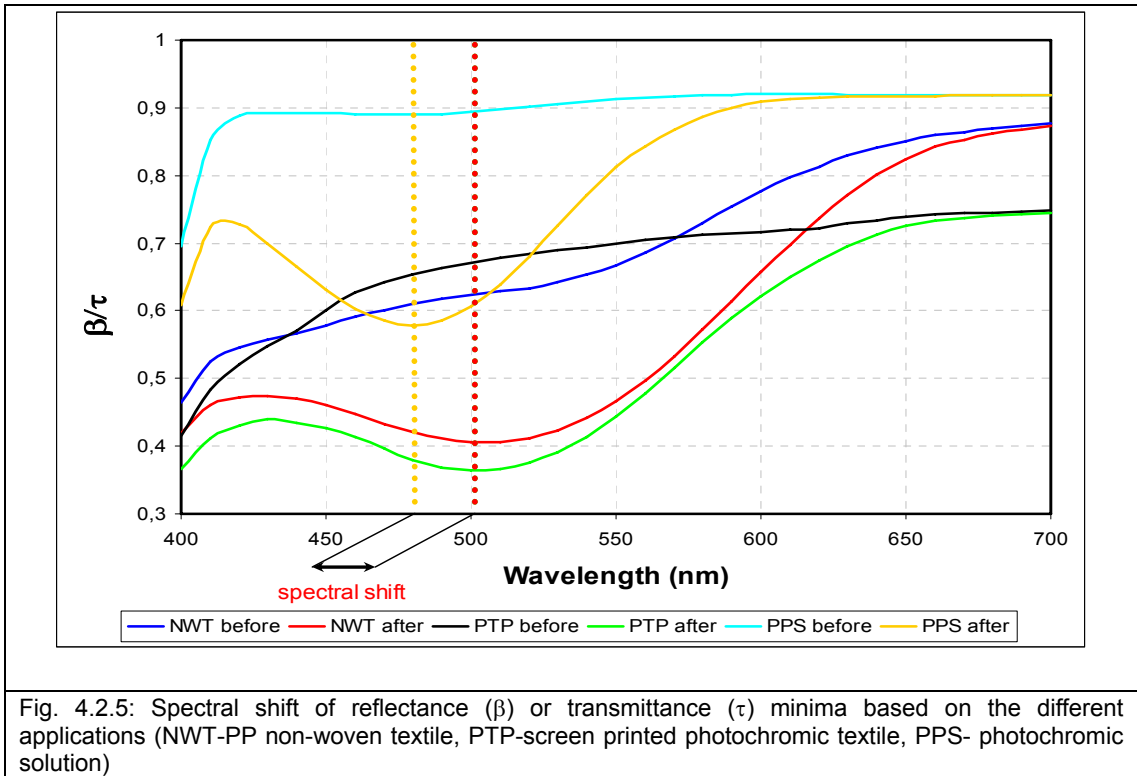
4.3 Photochromic pigments in solution

4.3.1 Influence of spectral power distribution of light sources

The spectral power distribution of the artificial light sources used for excitation was one of the factors which influenced the shade intensity of the photochromic systems. Because the main target was experiments with continuous illumination of the measured sample, sources were used throughout the range from UV to visible regions. As discussed, suitable sources involve continual discharge. UV visible light sources have their own characteristics of spectral power distribution and they have also different abilities to evoke different intensities of the photochromic effect. Most discharge lamps have a bright-line spectrum and in their spectrum there are characteristic spectral gaps. Adaptation of the CS-5 spectrophotometer, as discussed in section 3.1.2., allows irradiation with two independent light sources to be combined. For the experimental work described in this thesis, from the light sources available the UV lamp, Deuterium lamp, Germicid lamp and Xenon discharge lamps were selected. Irradiation by all light sources was measured by the Avantes spectrometer, in which case spectrometer sensitivity was checked using a calibrated light source with traceability to the primary standard of the National Institute of Standards and Technology, no. 0402004-CC-UV VIS. Irradiation by all light sources was controlled by a reduction diaphragm to provide similar intensities.

Due to irregularities in the distribution of the photochromic pigment in the non-woven samples and considering that the state of photochromic pigments inside PP fibres is similar to that in solution, a series of experiments were prepared with photochromic pigment solutions - PPS. The results obtained were compared with photochromic prints. The results are summarized in Fig. 4.3.1, 4.3.2 and Fig. 4.3.3a-e for pigments in solution and Fig. 4.3.3f-j, where the sensitivity of the printed photochromic textiles is documented – PPT. A high sensitivity of photochromic solutions to the spectral power distribution of the irradiating sources was obtained for pigments P3 (mean ΔE^* was 10.46) and P2 (mean ΔE^* was 14.74) – Fig. 4.3.1, where it is possible to observe significant differences in lightness and chroma based on changing the light sources. This finding is in agreement with a literature report [34], where different spectral sensitivity was mentioned. The other photochromic pigments in solution were essentially not sensitive to a change in the light source – movement of the final shade point for these pigments in CIELAB colour space was

minimal. The mean ΔE* was 3.84 for pigment P5, for P4 was 0.61 and 2.49 for P1. Similar results were observed for photochromic prints, where ΔE* was 1.38 for P4 and P5 was mean ΔE*= 3.43.

Fig. 4.3.1: Change of PPS colour position dependent on different light sources in CIEL*a*b* colour space

Fig. 4.3.2: Change of PPT colour position dependent on different light sources in CIEL*a*b* colour space
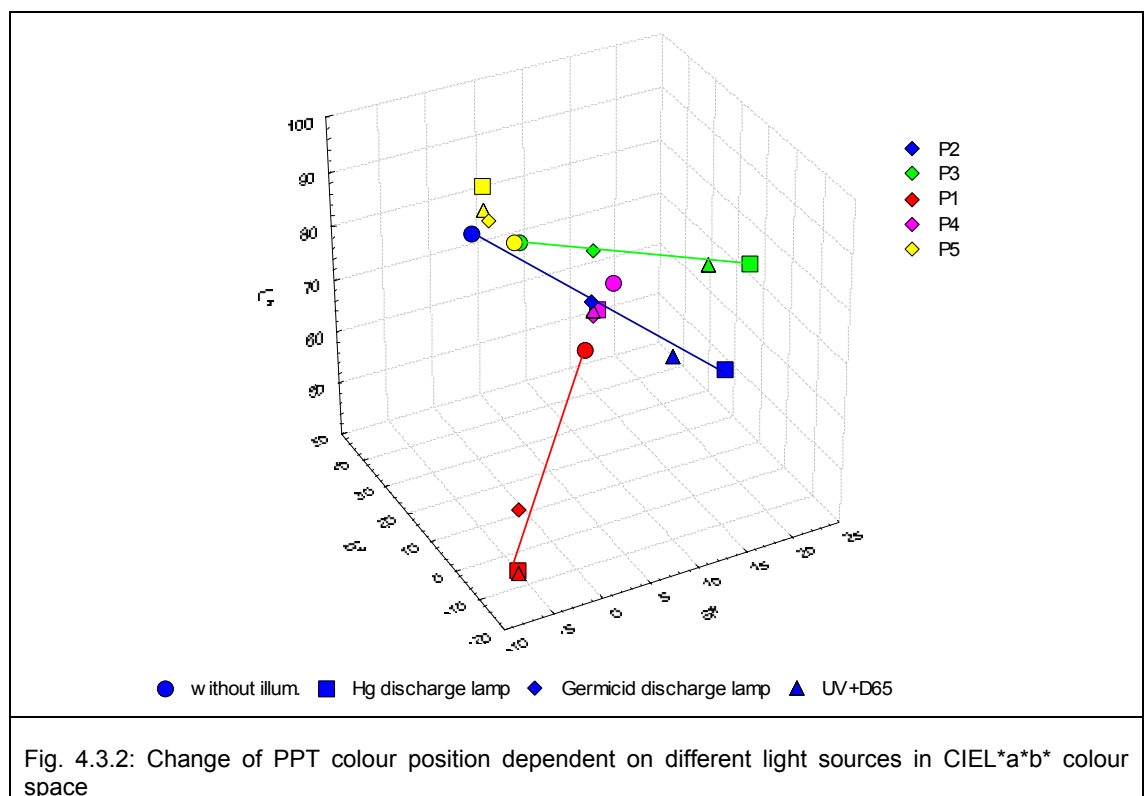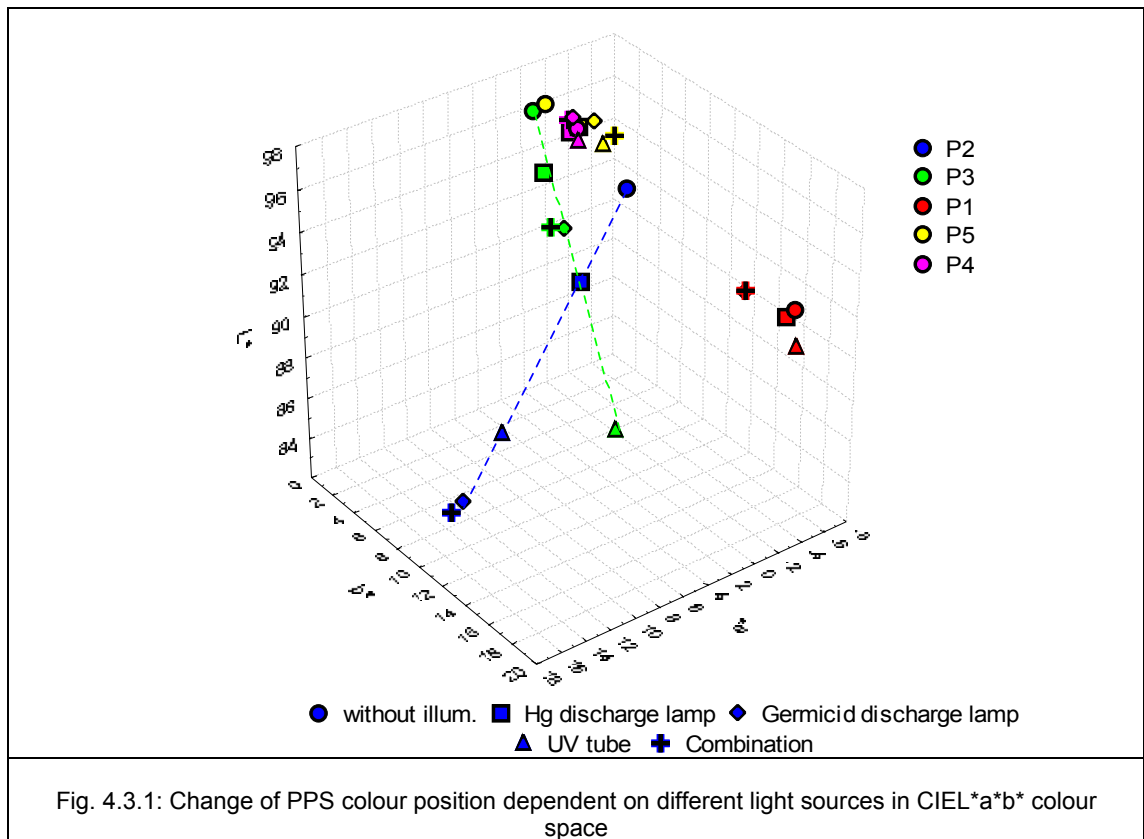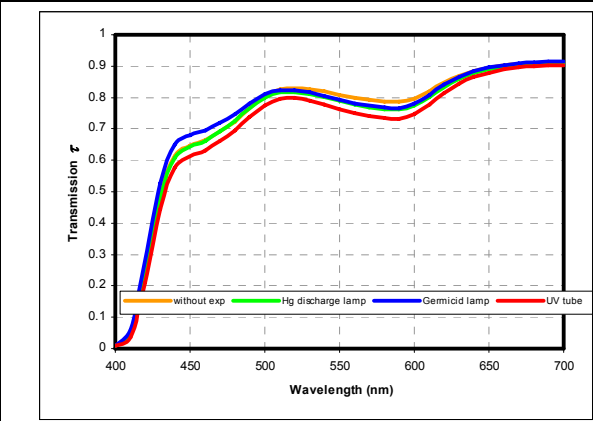
Fig. 4.3.3a: PPS-P1 4.2g/l
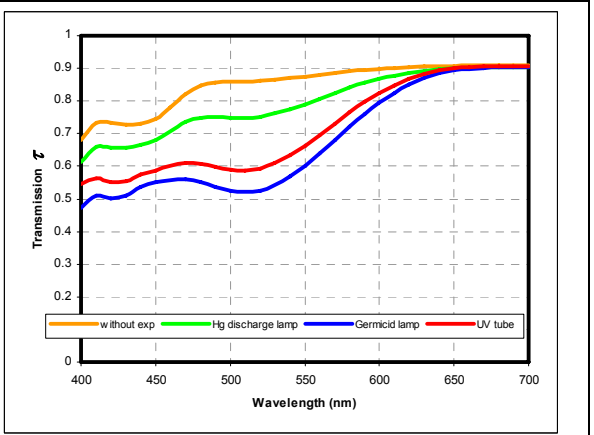
Fig. 4.3.3b: PPS-P2 4.2 g/l
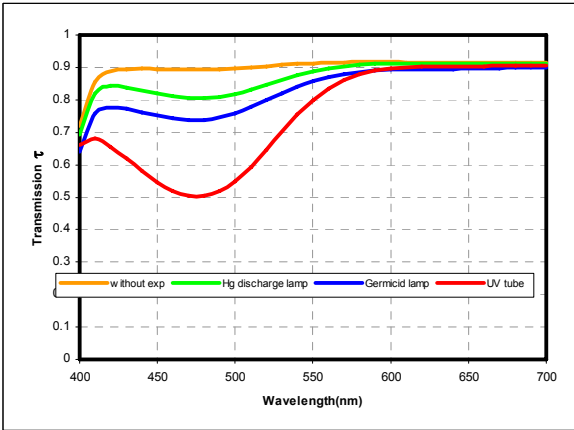
Fig. 4.3.3c: PPS-P3 4.2g/l
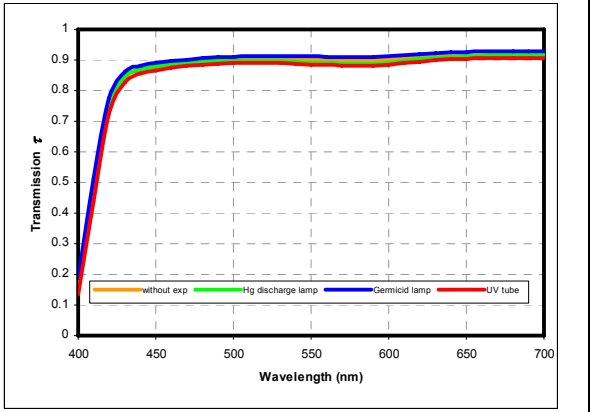
Fig. 4.3.3d: PPS-P4 4.2g/l
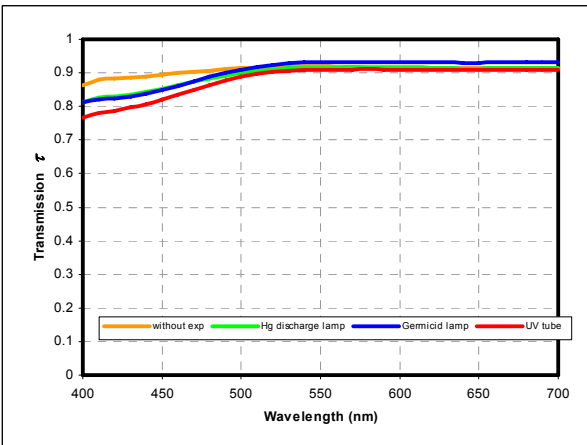
Fig. 4.3.3e: PPS-P5 4.2g/l

Fig. 4.3.3 a-e: Influence of light source used on spectral data of photochromic solutions

Fig. 4.3.3f: PPT-P1 1g/30g

Fig. 4.3.3g: PPT-P2 1g/30g

Fig. 4.3.3h: PPT-P3 1g/30g

Fig. 4.3.3i: PPT-P4 1g/30g

Fig. 4.3.3j: PPT-P5 1g/30g
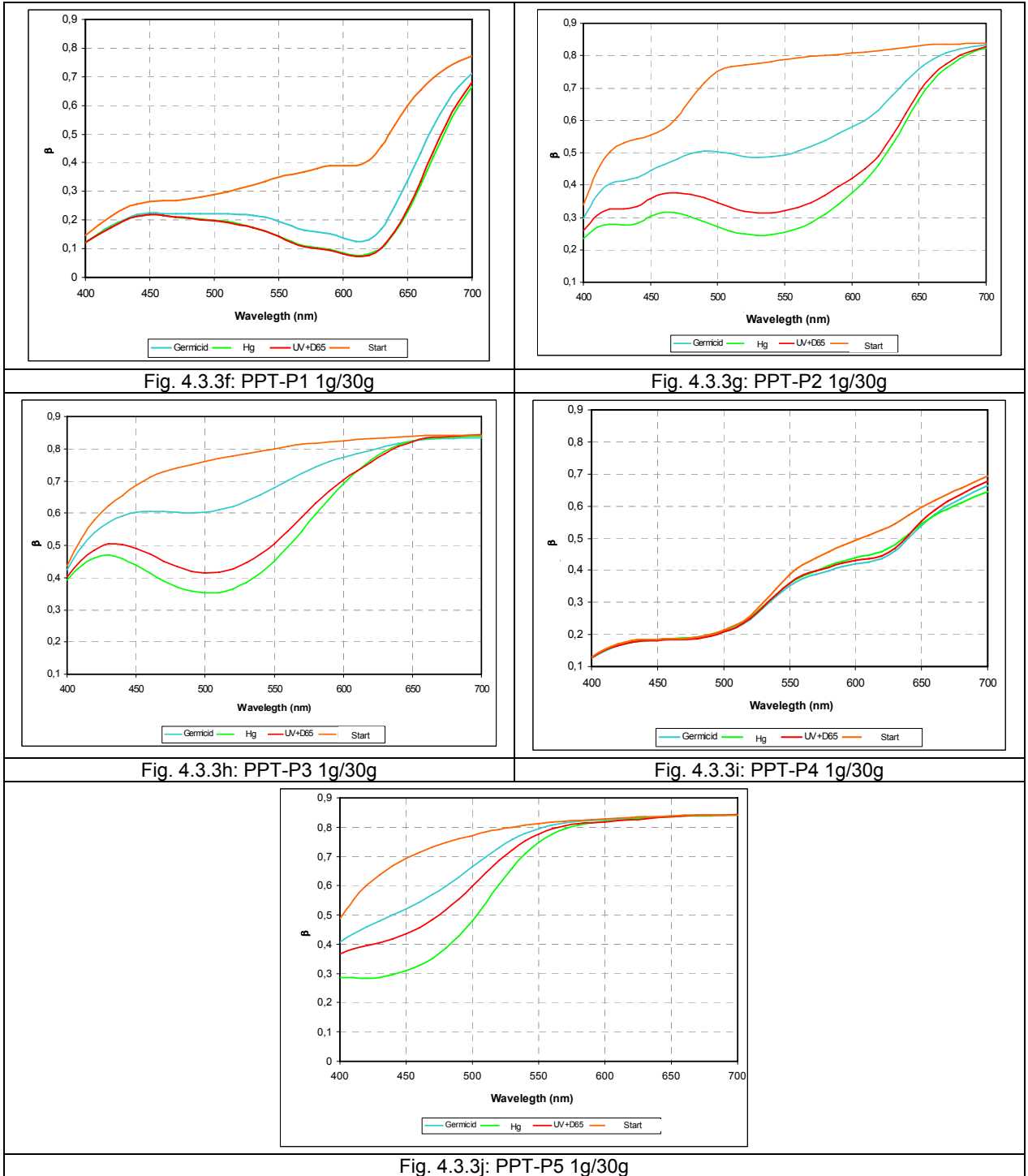
Fig. 4.3.3f-j: Influence of light source used on spectral data of photochromic textile prints

4.3.2 Influence of pigment concentration in solution on shade intensity

A spectral data set was measured for every concentration to provide graphs, which document the dependence of absorption on exposure time, to as certain kinetic behaviour of photochromic pigment in solvents. From Fig. 4.3.4a it is evident that during exposure the value of the half life is slightly decreased with increasing concentration for all pigments with the exception of pigment P4. During reversion Fig. 4.3.4 b shows that a linear decrease of the half life is significant, and in many cases this half life is approximately two times longer than half life of colour change during exposure. Fig. 4.3.5 documents the dependence of absorbance on wavelength and time of exposure for pigment P3 and for a concentration of 3.5 g/l (for other concentrations similar results were obtained). Pigment P3 was chosen for a comparative study because a full set of data on the different textile substrates at the same concentration levels was available only for this pigment.

From Fig. 4.3.6, which shows the reversion of photochromic change in solution there is rapid change of phases, initially showing the spectral characteristics of the exposed sample, processing through a phase of "transition" shade, which very slowly returns to the original shade of the photochromic solution before exposure. Fig. 4.3.7 documents the dependence of shade intensity I on concentration and time of reversion. A steady state of absorbance is evident for all concentrations after 1 minute of the reversion phase. This feature is observable only for a relatively short time of reversion because in Fig. 4.3.7 data are shown for only 20 minutes. Fig. 4.3.8 shows a much longer period of measured data of reversion. A significant increase of the time necessary for reversion based on increased concentration is observed for a concentration of 4.2 g/l. Complete reversion of the irradiated photochromic pigment required 48 hours for concentrations 1.4, 2.1 and 2.8g/l. Complete relaxation for concentration 3.5g/l occurred after 72 hours. In the case of concentration 4.2g/l there was a visible shift of absorbance back to similar values as for concentration 1.4g/l but there was a residual absorbance after 72 hours. Because the same absorbance was measured after one-week relaxation of the photochromic pigment in a light resistant black box, it is possible to speculate that there is situation at concentrations over 4 g/l where complete photochromic colour reversion becomes impossible. Possibly, the steric barriers caused by the clustering effect at high concentrations, blocking the re-locking of the open form of naphthopyrans back to the closed pyran ring form. It is

necessary to understand that the concentrations studied were approx. 1000-times higher than previously studied concentrations [37,139,140,141].

The results are also consistent with the product fatigue theory, which is discussed in the next section. The fatigue product theory suggests that the decay phase proceeds via a fatigue product (M), where the change from coloured form B→M proceeds relatively quickly in comparison to the slow change from M→A (colourless form).
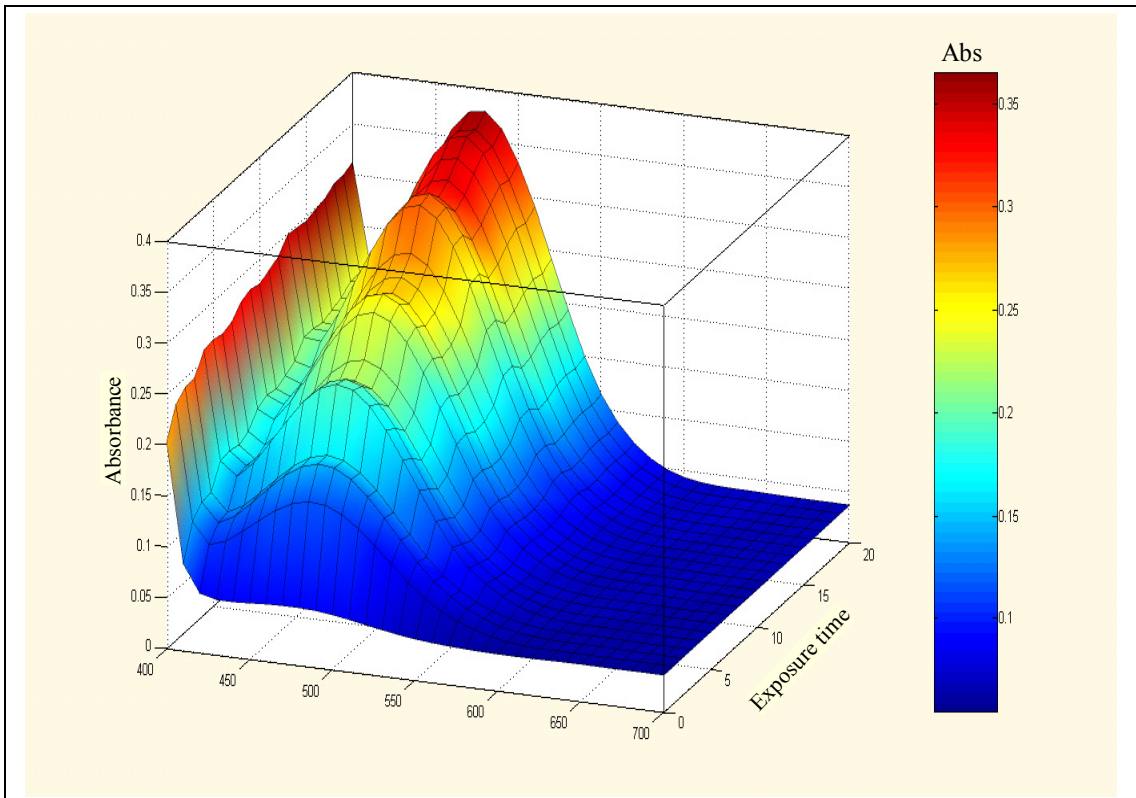

Fig 4.3.4a – Relationship between colour change half-life $t_{1/2}$ on concentration (PPS)

Fig. 4.3.4b – Relationship between colour change half-life $t_{1/2}$ and concentration (PPS)
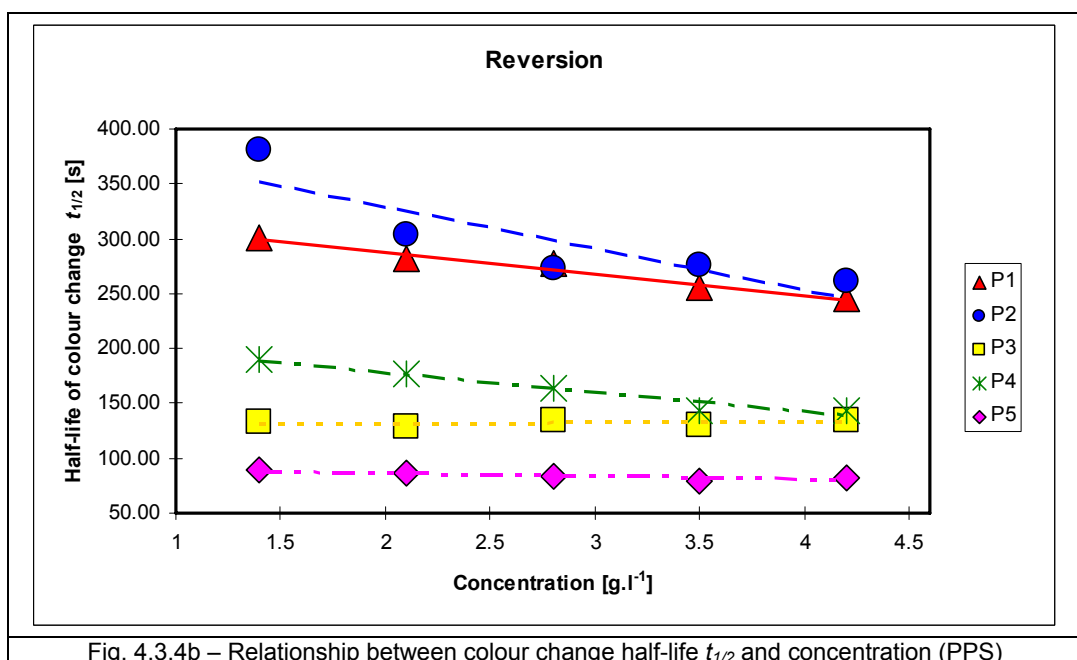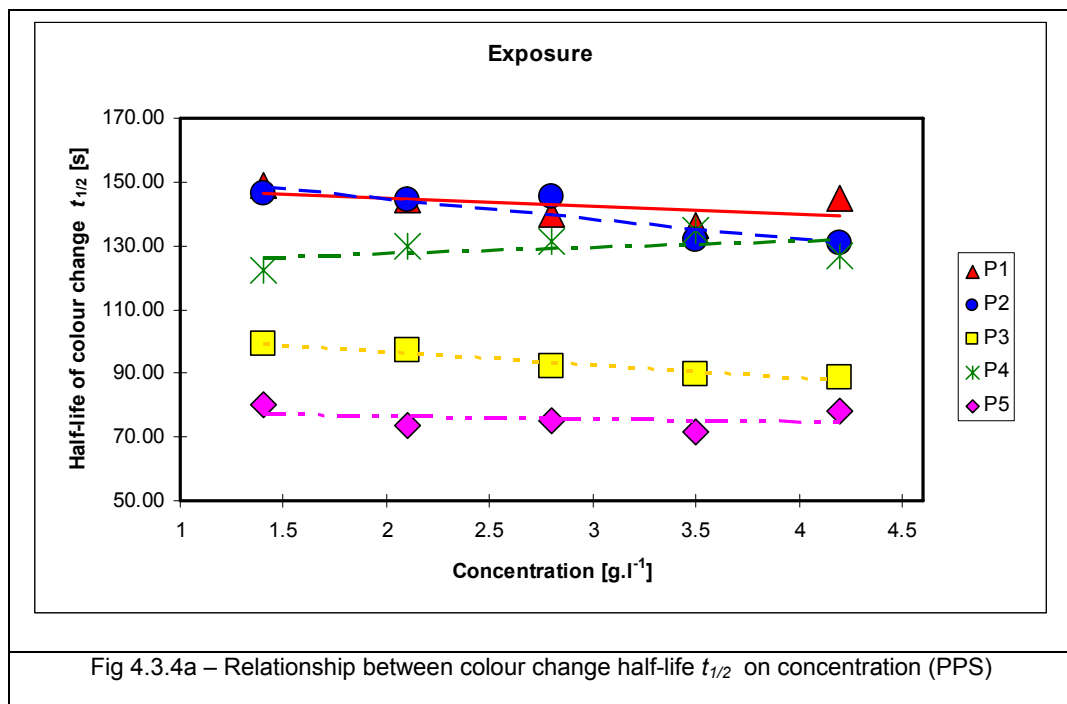
Fig. 4.3.5: PPS-P3 concentration 3.5 g/l – Dependence of absorption on time of exposure
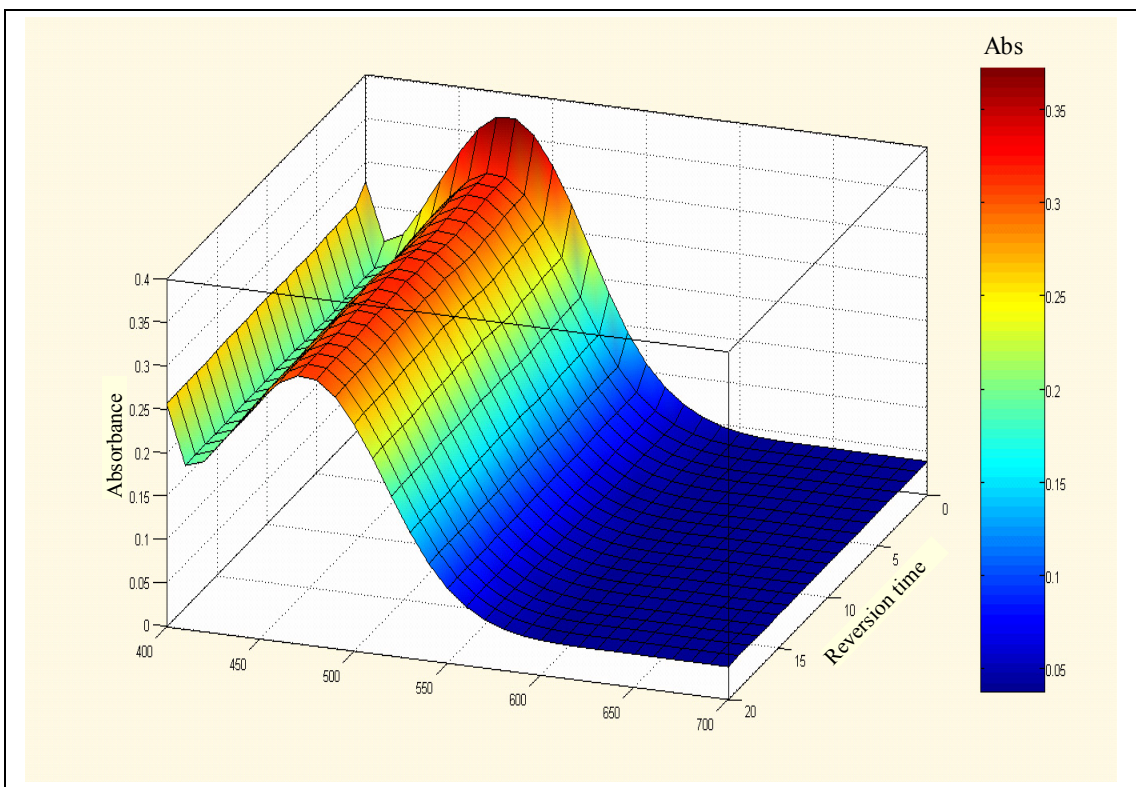
Fig. 4.3.6: PPS- P3 concentration 3.5 g/l – Dependence of absorption on time of reversion
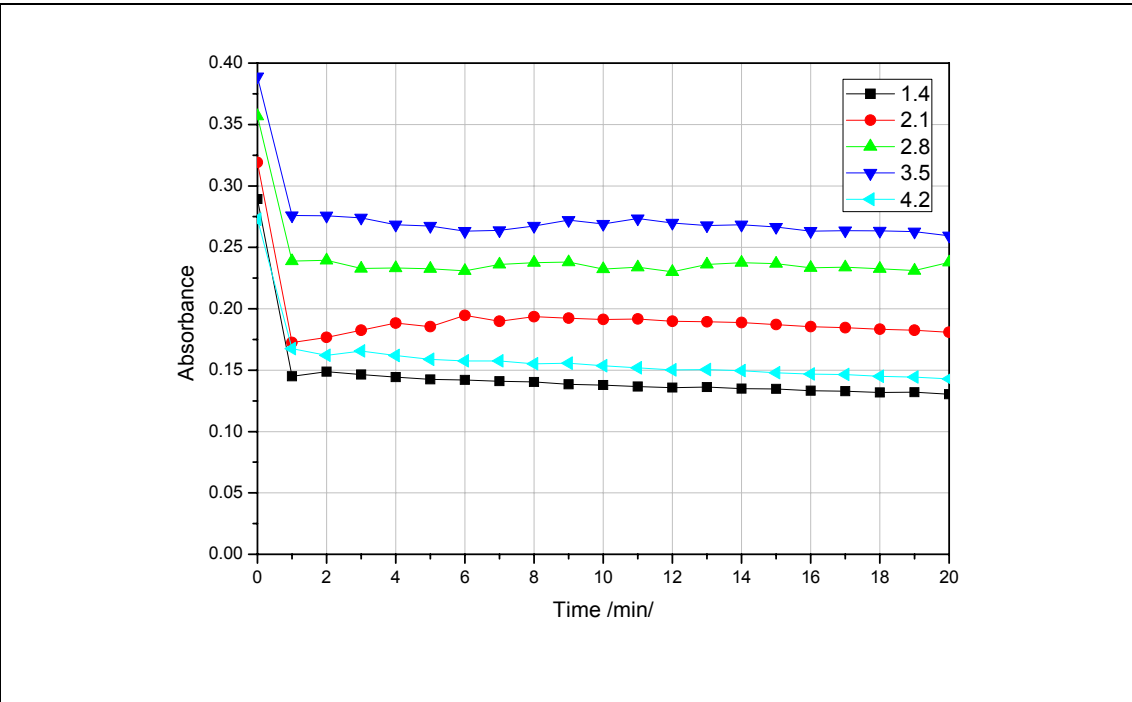
Fig. 4.3.7 – Dependence of absorbance on time of reversion and concentration PPS- P3
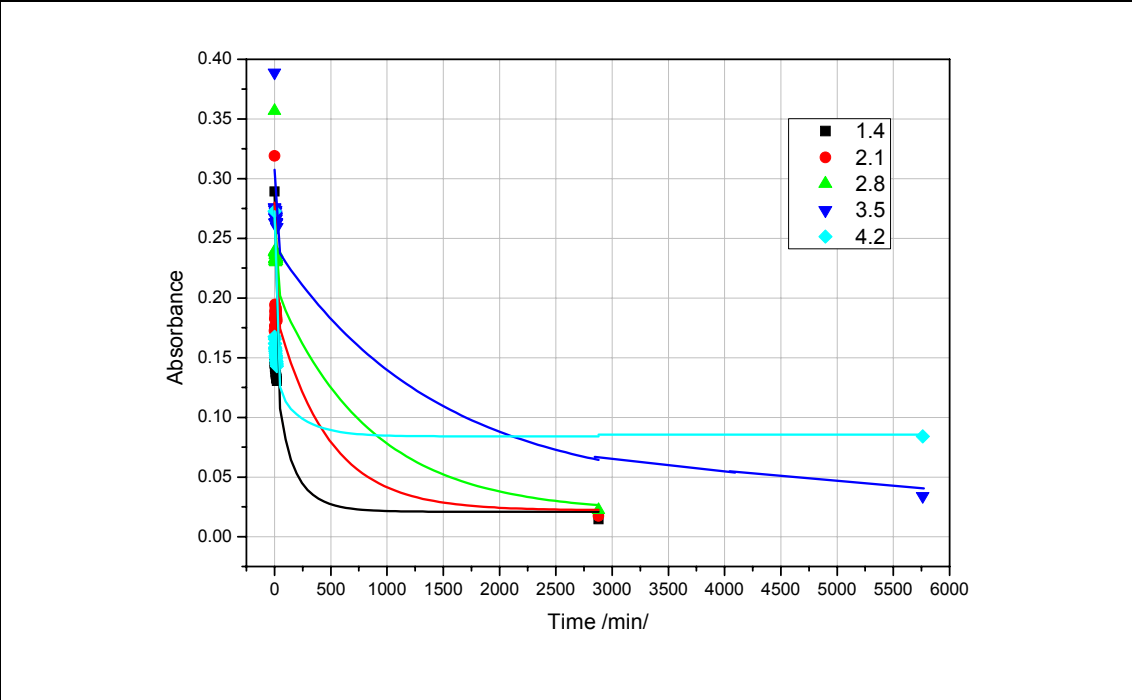
Fig. 4.3.8 – Dependence of absorbance on time of reversion and concentration PPS- P3

4.3.3 Colour shift in CIE L*a*b* space for solutions and photochromic prints

The description of colour change of photochromic pigments in CIE L*a*b* colour space provides the next possibility for the study of photochromic colour change. Fig. 4.3.9 shows that the photochromic colour change follows an approximately linear trend in the colour space. These properties are very interesting, but such graphs are not capable of informing us about the kinetic behaviour of colour change. The linearity of photochromic colour change illustrates only an increasing or decreasing colour strength of photochromic samples during exposure or reversion. The direction of this trend depends only on the specific colour of the photochromic pigment.

Fig.4.3.9: Colour change PPT-P2 during exposure and reversion in CIEL*a*b*
(Elementary numerous document position of points in time sequence – exposure and reversion)
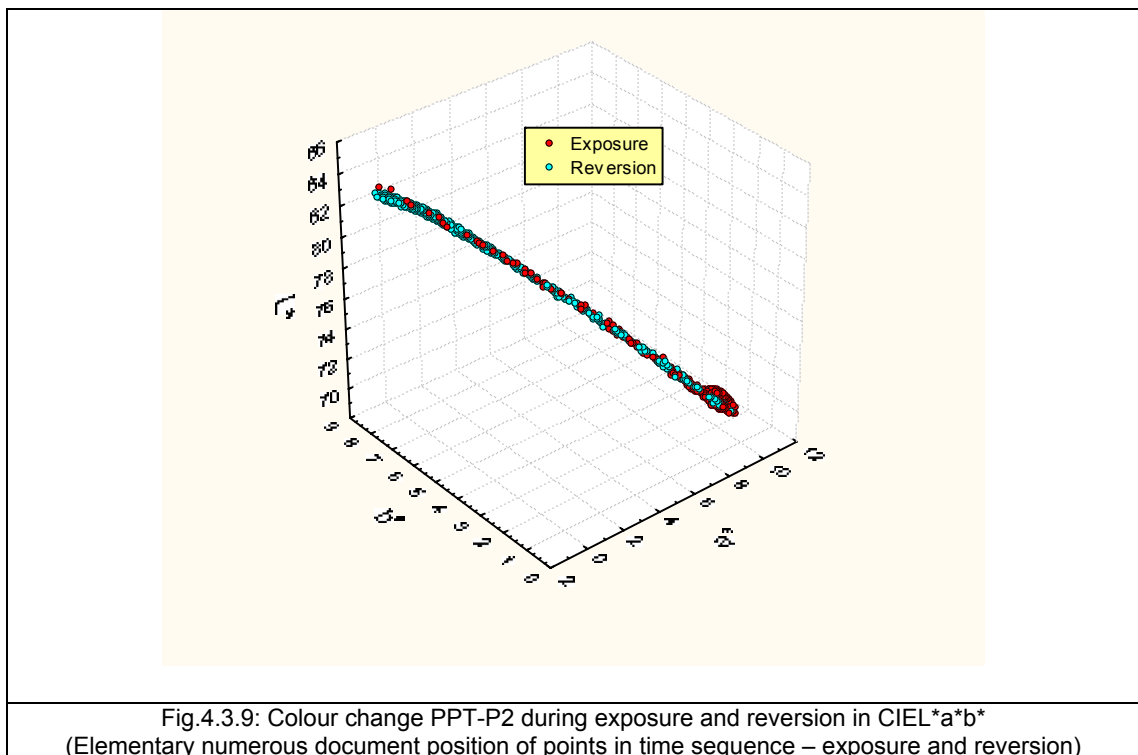
From Figs. 4.3.10a and b, a difference between exposure and reversion phase of colour data of the tested specimen on the chromatic L*a*and L*C* planes of CIEL*a*b* colour space is observed. This difference is caused by insufficient relaxation of the photochromic pigment during 15 minutes of the reversion phase. Arrows, which explain direction of relaxation shift, shows especially in graph 4.3.10.b, that lightness parameter of sample during relaxation is 1.75 unit darker than sample on the start of photochromic colour change – relaxation of 15 minutes was insufficient.
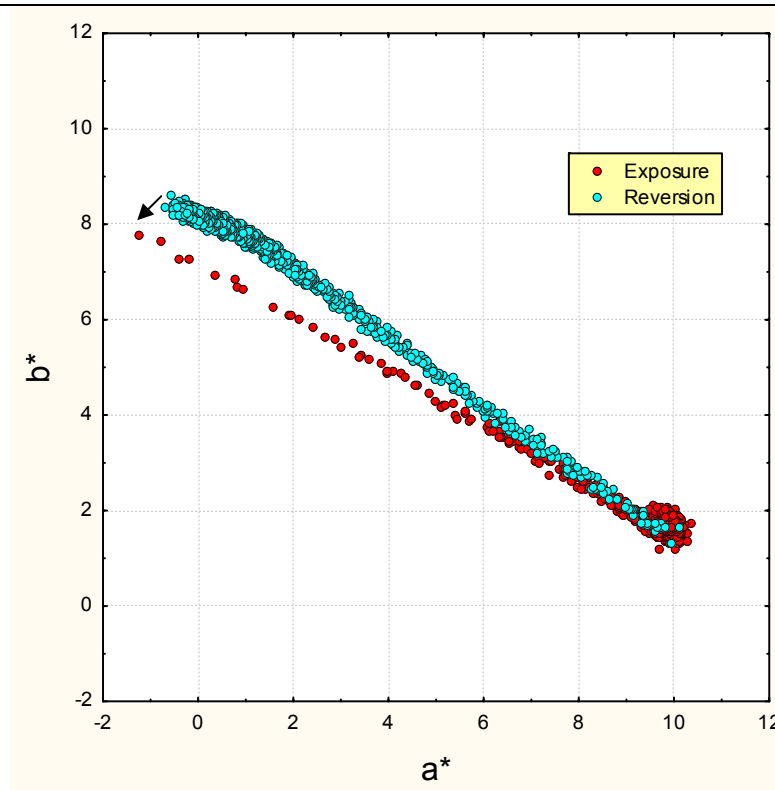
Fig. 4.3.10 a: PPT-P2 Description of shade intensity for exposure and reversion on the chromatic plane of colour space CIEL*a*b*
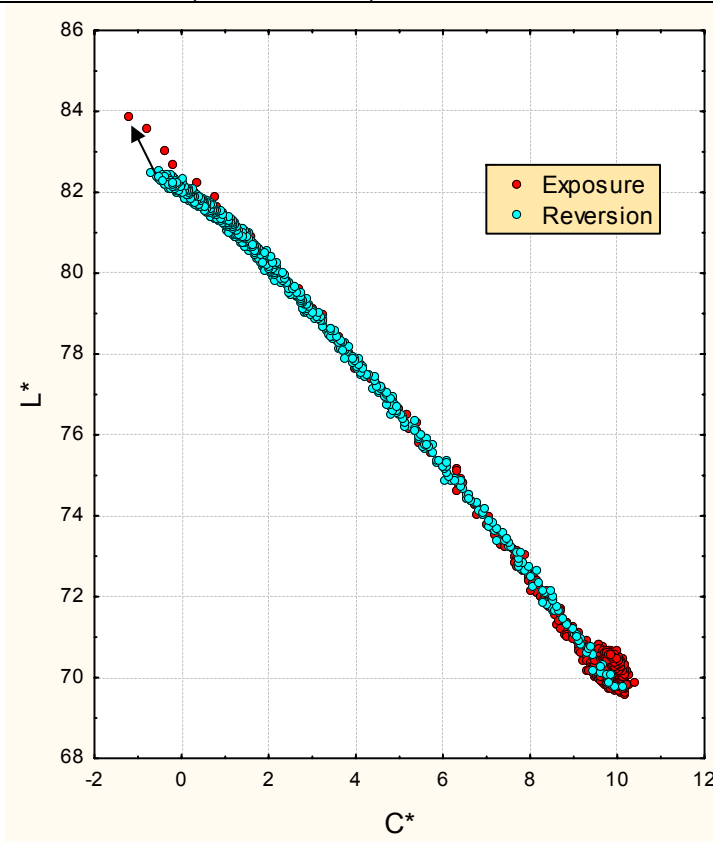
Fig.4.3.10b: PPT-P1 Description of shade intensity for exposure and reversion on the L*C* plane of colour space CIEL*a*b*

In section 4.3.2, a "transition" shade formation during reversion was discussed for photochromic pigments in proceeding from exposed to relaxation phase in solution. First of all in the case of chromenes – concretely in the case of methyl 2,2-bis(4-methoxyphenyl)-6-acetoxy-2H-naphtho-[1,2-b]pyran-5-carboxylate (P3) at a higher concentration a slower reversion (decay) phase was observed. For higher concentrations the time of reversion was more than 4 days and the time was not sufficient for the return to the original colourless form.

Chromenes are reported to photoproduce an open-structured species upon UV irradiation [128-132] as a consequence of C–O bond breakage. The metastable photoproduct(s) is (are) generally coloured (transition shade), due to increased electronic delocalisation, and reconvert thermally and/or photochemically to the starting material. This is the explanation for why chromenes are photochromic compounds [9]. The structure of a metastable species is supported by chemical evidence from similar compounds [131]. Its lifetime is strongly influenced by the nature of the substituents and the position of the condensed benzene rings [128]. Previous studies on the photochemistry and photophysics of this class of molecules were carried out in rigid matrices [128,130,133,134] and in fluid solution [135-138] by using both pulsed and continuous irradiation.

From the results of the measurement it is proposed, that the decay phase occurs via the fatigue product (M), with the change from B→M proceeding relatively quickly in comparison to the change from M→A that was slow, (see scheme below).

A - closed (colourless) form ⇄ **B** - open (coloured) form

M - fatigue product
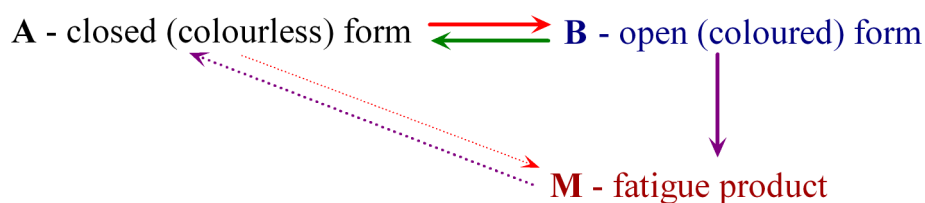
The issue of a fast colour change from B→M was discussed in section 4.3.2., where the measured parameter was the optical yield O_y of photochromic colour change. The graphs in Figs 4.3.6 and 4.3.8 document only part of photochromic colour change – fast conversion from B→M. The change from M→A is too slow and complete conversion is out with the graphs.

Agglomeration of elementary experimental points for two thirds of the distance between the B and A forms of the measured photochromic pigment is visible on the chromatic plane of CIELAB colour space (see Fig. 4.3.11). These points represent the position of the transition shade, or fatigue product (M) on the chromatic plane of CIELAB colour space. From Fig. 4.3.11a-b it is evident that with increasing concentration the rate of relaxation of photochromic solution decreases. Critical from this point of view are concentrations above 4.0 g/l, because 4 days relaxation in a dark box does not lead to the full relaxation and reversion to the original colourless form. It is probable that there is some retardation influenced by agglomeration and aggregation of the photochromic pigments, which are at their solubility limit. This phenomenon has not been previously reported, because most experiments were realized on dilute solutions with approximately 1000 times smaller concentration of photochromic pigment (see for example [139-140]).

In comparison to the application by textile printing, if elementary points are connected, colour hysteresis of the photochromic reaction in solution on the chromatic plane CIE L*a*b*space (see Fig. 4.3.11a and 4.3.11b) is observed.
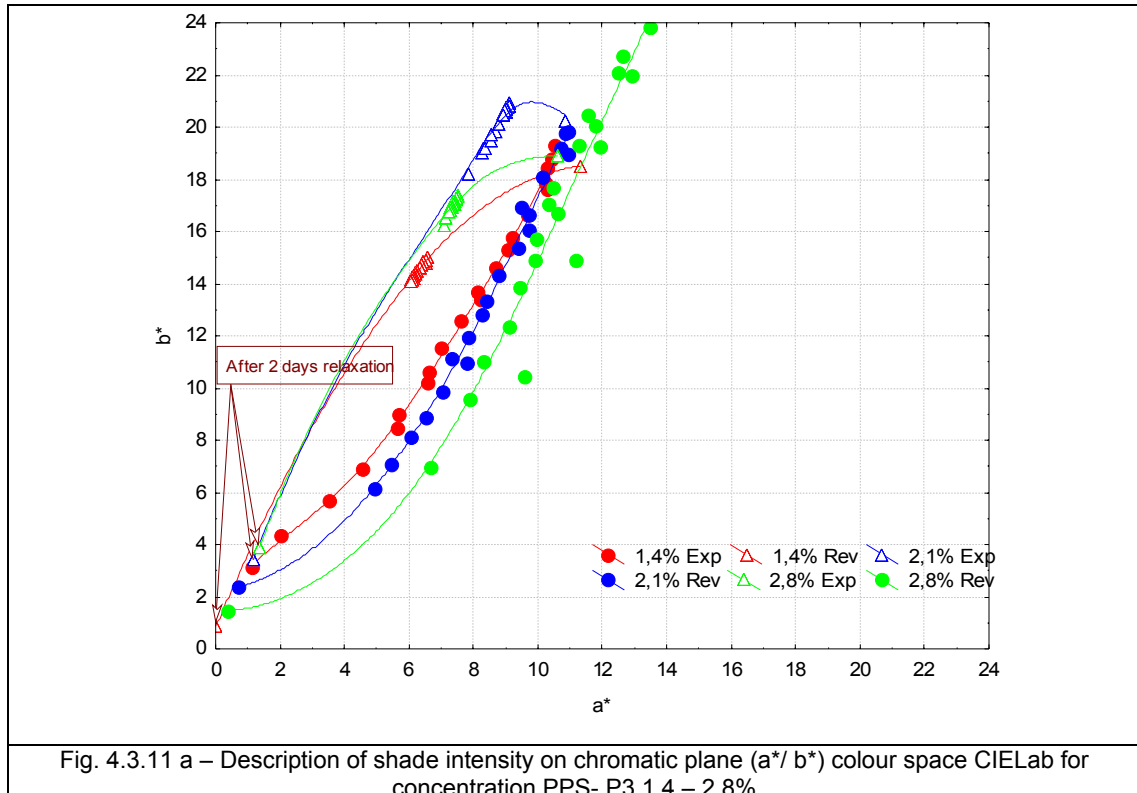
Fig. 4.3.11 a – Description of shade intensity on chromatic plane (a*/ b*) colour space CIELab for concentration PPS- P3 1.4 – 2.8%

Fig. 4.3.11 b – Description of shade intensity on chromatic plane (a*/ b*) colour space CIELab for concentration PPS - P3 3.5 – 4.2 g/l
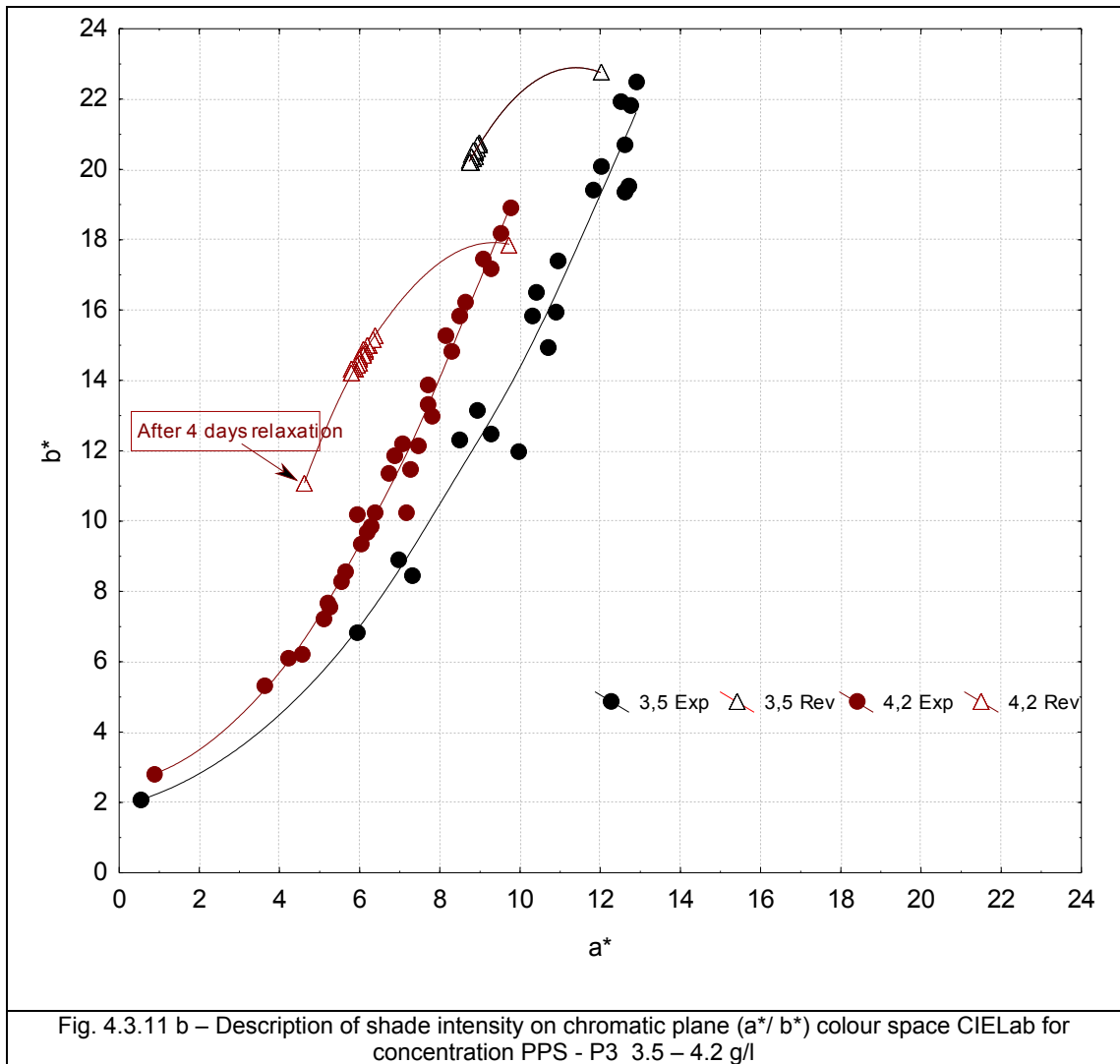
4.3.4 Dependence of the kinetics of photochromic change on applied media

The kinetic behaviour of the photochromic pigments in the different applications was tested following the development of the unique measuring system. Figs. 4.3.12a, b describe kinetic data for PPT, NW and PPS for pigments P2 and P3. The absorbance values for solution were recalculated to provide shade intensity I from the standard equation for K/S values by replacement of reflectance R with transmittance T in equation 2.5.5 as given in chapter 2.5.2.
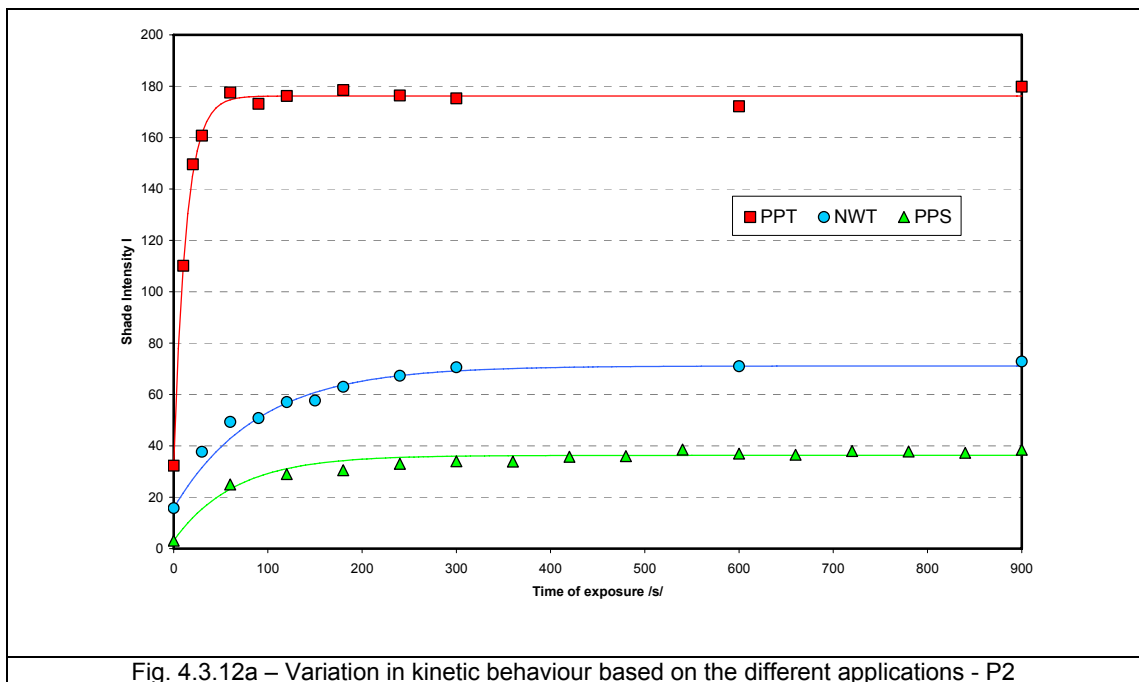
Fig. 4.3.12a – Variation in kinetic behaviour based on the different applications - P2
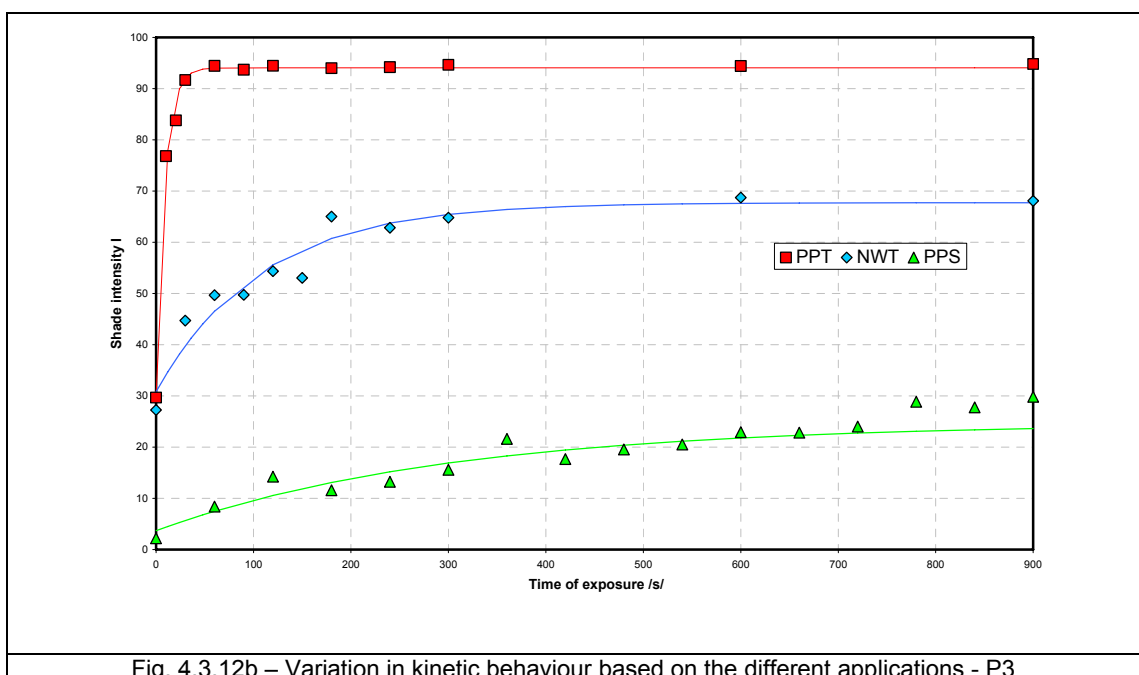
Fig. 4.3.12b – Variation in kinetic behaviour based on the different applications - P3

From Figs. 4.3.12a and b, a difference in the rate of photochromic colour change (shade intensity) is evident. Fig. 4.3.13 also illustrates previous observations in which the rate constants k for the individual application media are described and calculated from equation 4.1.1. as given in section 4.1.1.

Fig. 4.3.13 – Rate constant for exposure – pigment P3 - PPT (2.5%), NW Melt-Blown (2.6%) and PPS (2.8%)
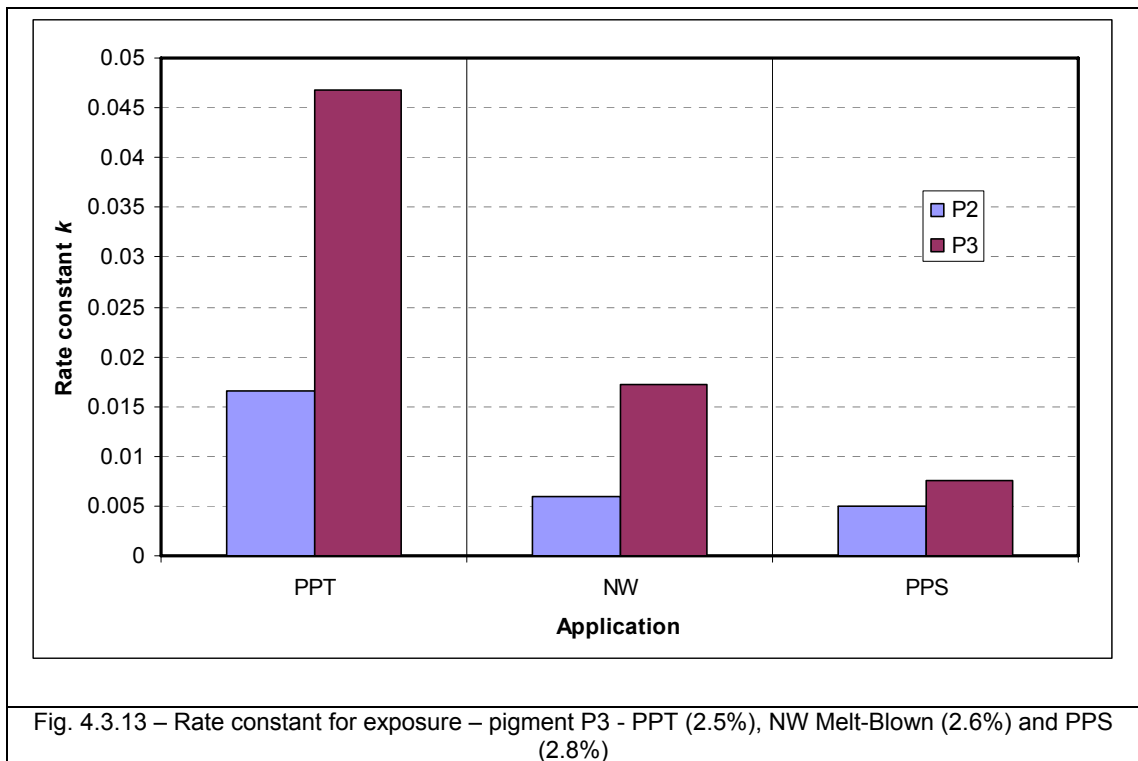
Both graphs are consistent with the pigment in the fibre mass being in a similar state as in a solution. In both cases, the pigment is encased inside a solvent mass and therefore values of the rate constants are similar. Also it is evident, that at the same concentration of pigments, the shade intensity is higher by about 50% in printed textiles as against application in non-woven textiles. The reason is probably scattering of light by fibres of non-woven textiles containing photochromic pigments.

Figs. 4.3.12 a, b shows approximately 30 units difference in shade intensity at the start of photochromic colour change between solution and photochromic print. This effect is caused by the inherent colour of the printed textile substrate. For non-wovens, two values of shade intensity were obtained, because mass dyeing technology influences the inherent colour of PP fibres due to incorporation of particles of photochromic pigment, which are slightly coloured.

4.4 Fatigue test of photochromic prints

4.4.1 Fatigue of the photochromic reaction – exposure D65 + UV fluorescent tube

A study was also conducted of fatigue resistance, as an indication of the effect of the concentration, to complete the kinetic study of the photochromic reaction. In the following graphs given in Figs. 4.4.1a – 4.4.1c the results of these experiments are documented, in which textile samples with photochromic prints were repeatedly exposed for 15 minute cycles with constant irradiance 979.3 lx and with 30 minutes relaxation between cycles. According to the recommendation of the manufacturer of the photochromic pigments [144], the number of cycles was 1 – 200. An evaluation of the experimental results is provided by Fig. 4.4.1a-c and Fig. 4.4.2a-c, where a comparison of the measured experimental data sets is shown for selected concentrations for pigment P1. The results for pigment P1 are presented due to its reasonable fatigue resistance, stability and providing constant values over all 200 cycles. Similar results were obtained for all pigments. The results given in the graph presented in Fig. 4.4.2d is for concentration of photochromic pigments of 0.25g/30g. Evaluation was carried out using total colour difference measurement, the colour difference (ΔE^*) in comparison to the initial shade intensity of PPT.

During measurement of fatigue resistance assessed as total colour difference ΔE^* against initial shade intensity of PPT, it was found that photochromic samples show two phases of colour change. The first is relatively short and represents a fast change of the measured sample. This phase is referred to as "seasoning" of the PPT samples, because after that follows a phase with a relatively small change of colour in the photochromic colour change process.

The second possibility for fatigue resistance evaluation involves measuring the shade intensity of an individual photochromic cycle. The results obtained show that both parameters, total colour difference ΔE^* and shade intensity I, may be expressed as a linear relationship with the number of exposure cycles:

$$\Delta E^* = a_i + b_i.x \tag{14}$$

$$I = c_i + d_i x, \tag{15}$$

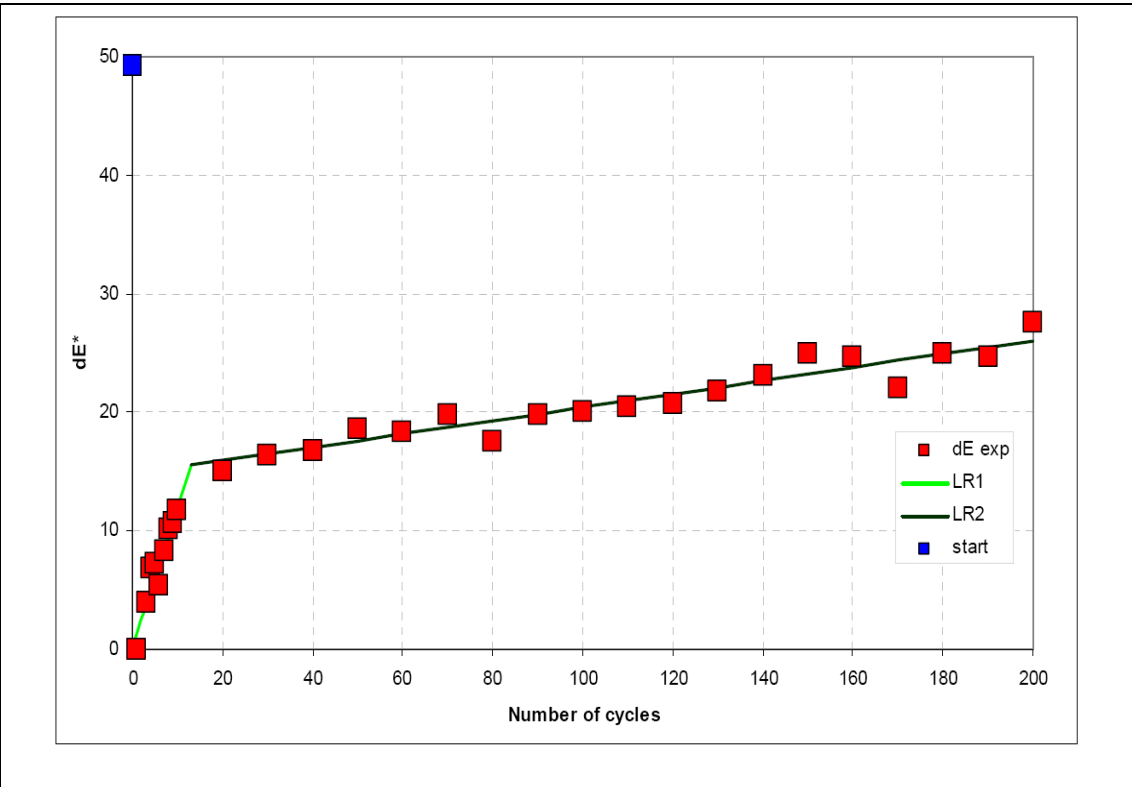where x is the number of exposure cycles.

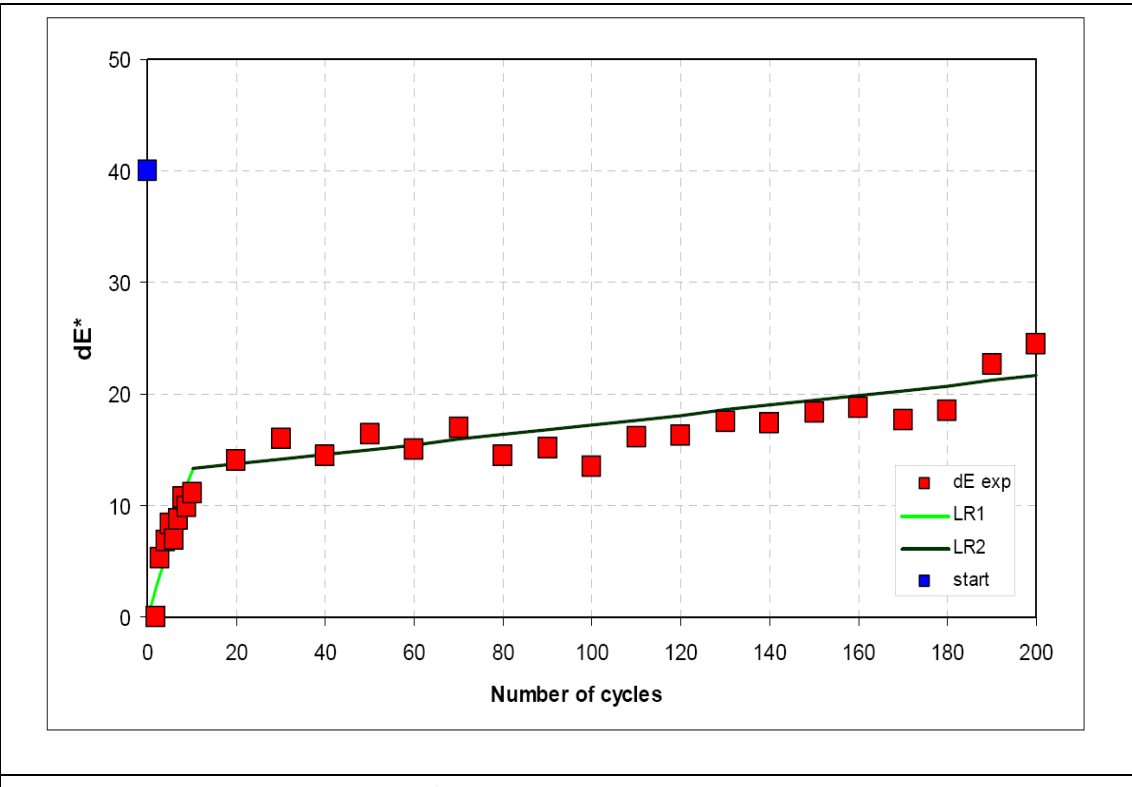Fig. 4.4.1 a – Dependence of ΔE* on the number of exposure cycles PPT-P1 0.25 g/30g

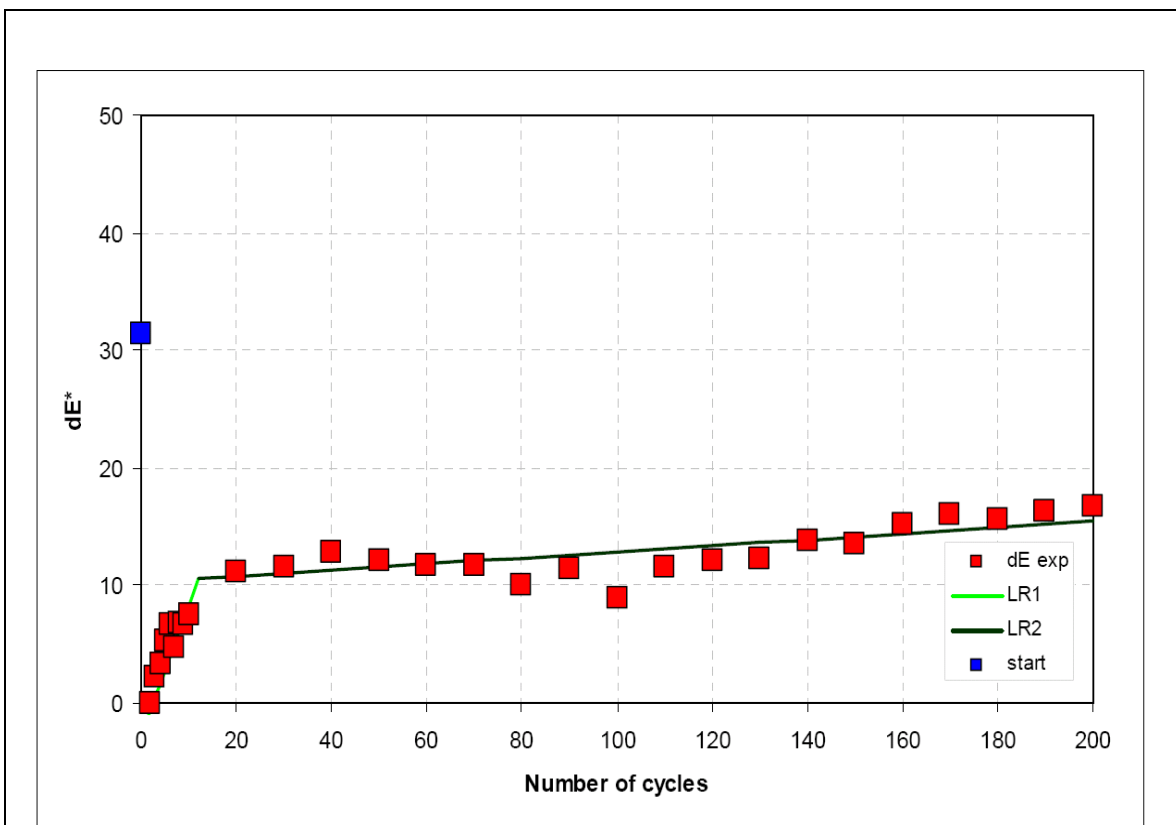Fig. 4.4.1 b – Dependence of ΔE* on the number of exposure cycles PPT-P1 1.5 g/30g

Fig. 4.4.1c - Dependence of ΔE* on number of exposure cycles PPT-P1 3.0 g/30g

Table 4.4.1 Coefficients of regression model - ΔE* for PPT-P1

Pigment concentration (g/30g)	a_1	b_1	a_2	b_2	Theoretical break point
0.25	0.200	1.168	14.801	0.056	12.997
0.50	0.093	1.223	13.936	0.049	12.002
1.00	-0.088	1.130	12.836	0.044	11.998
1.50	-0.075	1.330	12.765	0.045	10.131
2.00	-2.878	1.128	11.479	0.026	13.044
2.50	-2.133	1.130	10.670	0.025	12.004
3.00	-1.452	1.132	10.278	0.023	12.079

($\Delta E^* = a_1 + b_1.x$ is the model before the break point, $\Delta E^* = a_2 + b_2.x$ is the model after the break point)

Table 4.4.2 Coefficients of regression model - shade intensity I for PPT-P1

Pigment concentration (g/30g)	c_1	d_1	c_2	d_2	Theoretical break point
0.25	650.000	-34.690	276.233	-0.130	10.711
0.50	1026.691	-48.792	525.289	-0.211	10.303
1.00	938.001	-40.003	477.601	-0.031	11.498
1.50	937.092	-48.990	497.976	-0.029	8.997
2.00	588.115	-20.012	380.001	-0.003	10.426
2.50	505.990	-14.500	338.766	-0.001	10.937
3.00	466.783	-15.721	322.780	0.039	9.110

($I = c_1 + d_1.x$ is model before break point, $I = c_2 + d_2.x$ is model after break point)

Tables 4.4.1 and 4.4.2 show that the photochromic fatigue test is characterised by a break point, which occurs between 10–13 cycles (this is approximately 2.5 hours) from 200 cycles, where every cycle involves 5 minutes exposure and 10 minutes reversion. In the case of photochromic pigments applied by printing there is an evident rapid decay of shade intensity and this is followed by a relatively constant level of colour difference and shade intensity.

Fig.4.4.2 a – Dependence of shade intensity I on number of exposure cycles PPT-P1 0.25g/30g
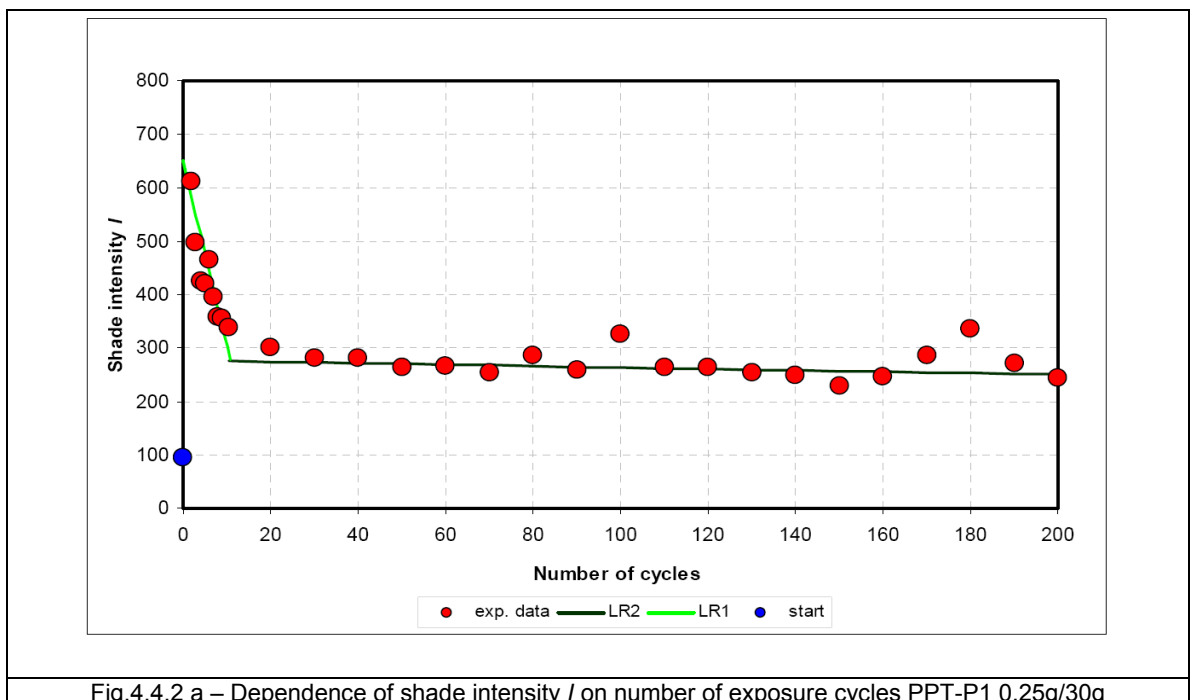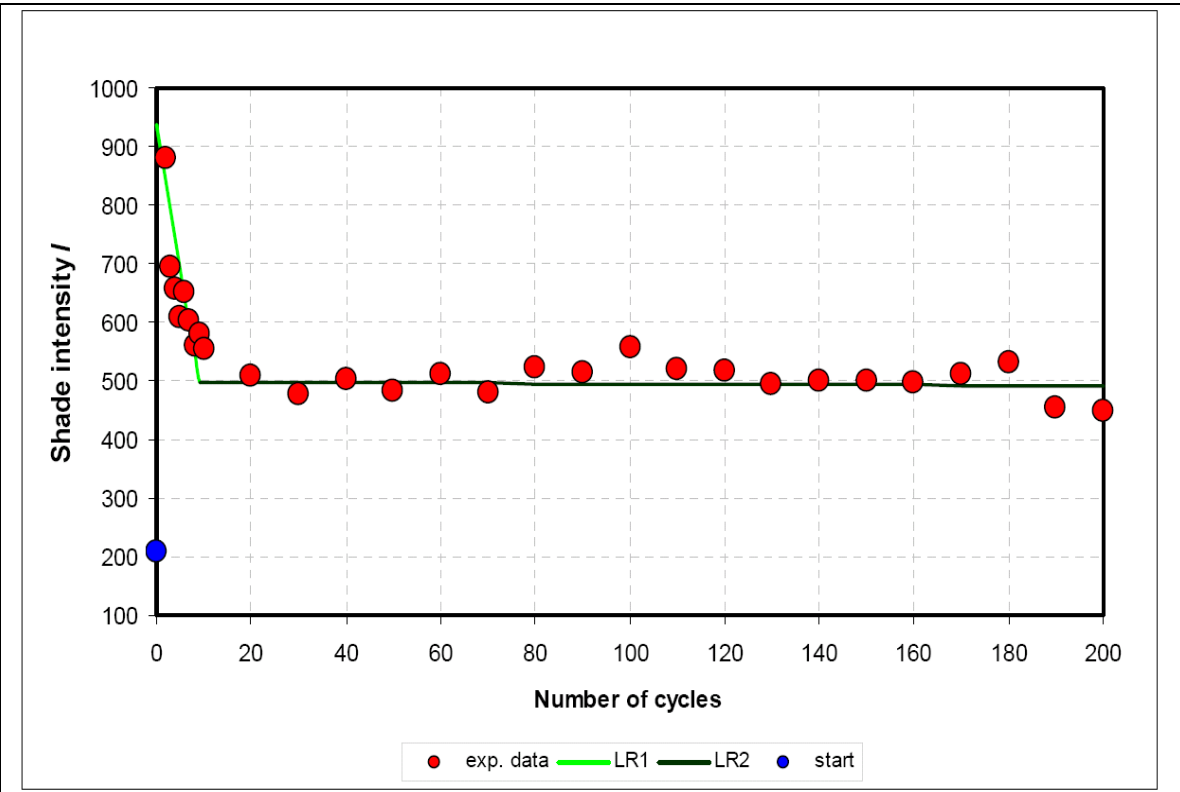
Fig.4.4.2 b – Dependence of shade intensity I on number of exposure cycles PPT-P1 1,5g/30g
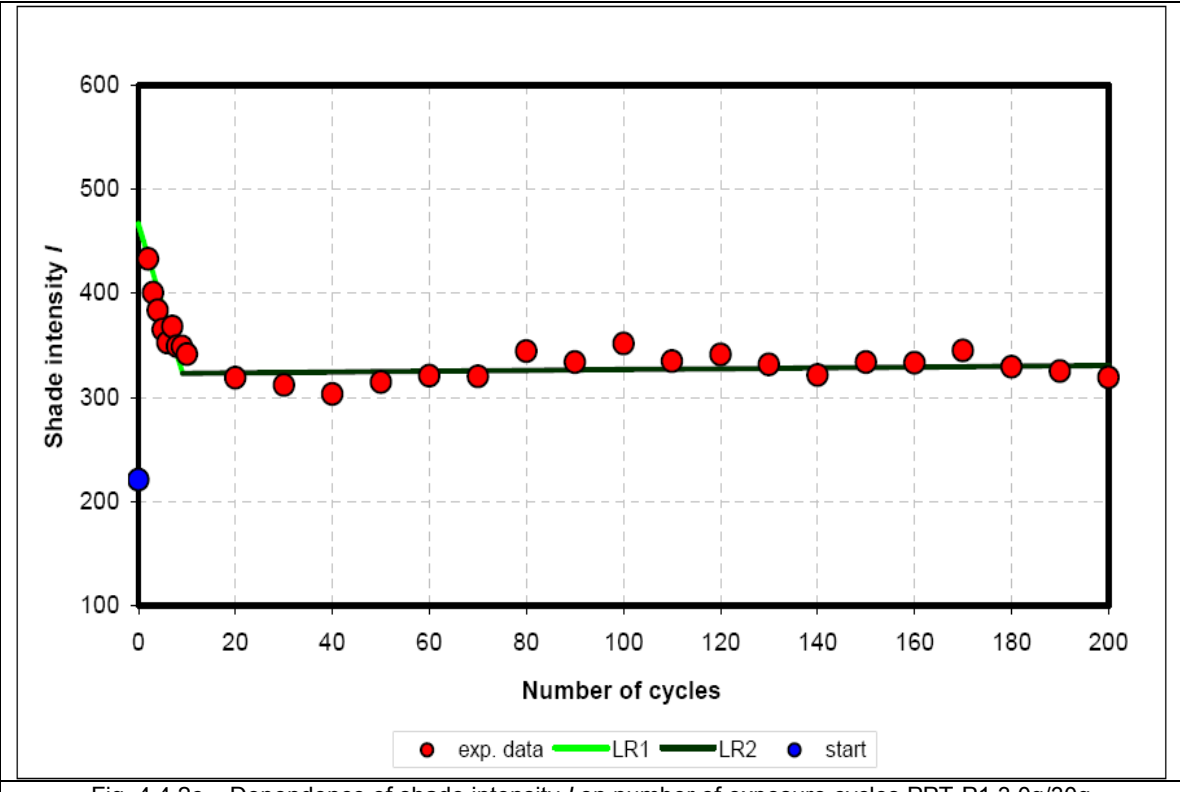
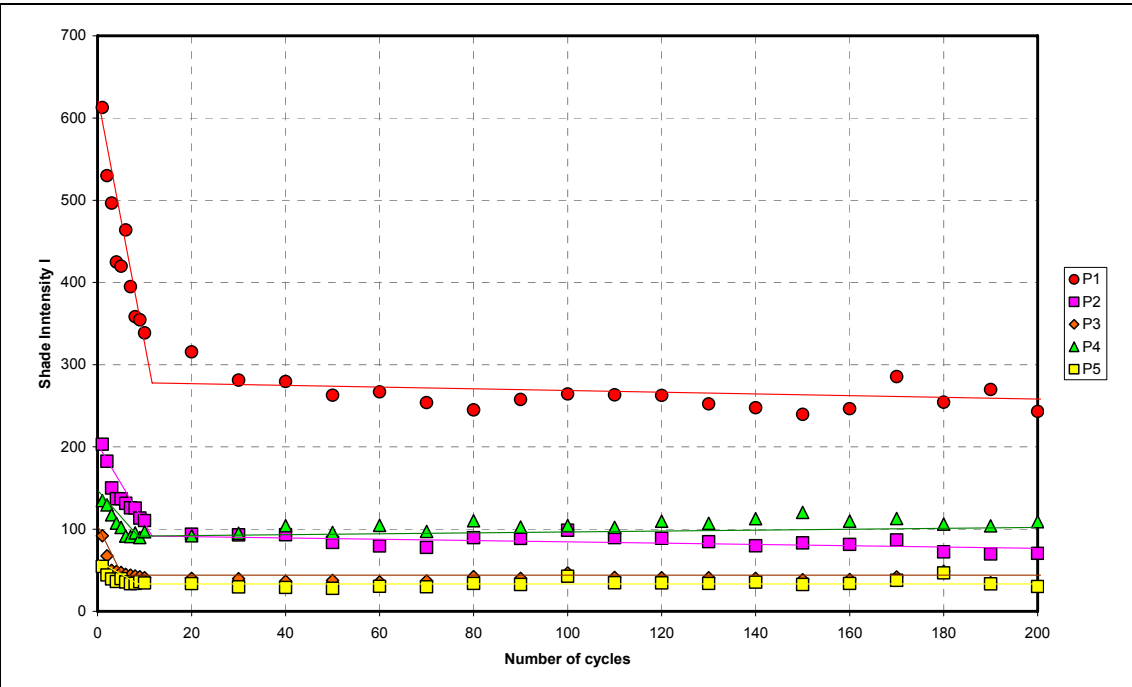Fig. 4.4.2c – Dependence of shade intensity *I* on number of exposure cycles PPT-P1 3.0g/30g

Fig. 4.4.2d – Dependence of shade intensity *I* on number of exposure cycles PPT with all tested photochromic pigments at concentration 0.25g/30g

4.4.2 Fatigue resistance - XENOTEST

When photochromic pigments are in use, typical quality characteristics such as colour fastness or strength parameters may change due to the effect of long-term exposure. Sunlight can cause a considerable rise in temperature in some cases. The sun radiates a continuous spectrum ranging from UV radiation (Wavelengths < 380 nm), through visible (wavelengths 380–780 nm) to infrared heat radiation (wavelengths > 780 nm). Radiation meeting the earth includes wavelengths ranging from approx. 300–3000 nm which corresponds in part to direct solar radiation and in part to diffuse celestial radiation (solar and sky radiation). The latter is not constant but varies according to position, time of day and time of year. Seasonal changes and changes throughout the day are significant and vary from year to year. These fluctuations are greater the shorter the wavelength. Outside weathering at different locations or different times cannot therefore be compared.

In the dyestuff industry and consequently in textile and other industries accelerated lightfastness tests based on artificial light sources are used. Typical examples are the XENOTEST fadeometer or ATLAS Weather-Ometer,in which Xe-discharge lamps are used as light sources.

The photochromic pigments were exposed to artificial sunlight for several hours with a XENOTEST 450 xenon arc lamp equipped with an optical filter system, which cuts off the wavelengths below 310 nm to follow standard BS EN ISO 105-B02:1999. Test chamber settings were 172 $W.m^{-2}$ for illuminance and 63°C for black standard temperature (BST) in every test. According to the data for test chamber conditions, the test chamber temperature CST remained fairly constant throughout the exposure periods, but the BST tended to rise towards the end of the runs. Relative humidity and temperature in the test chamber cannot be adjusted in this test set-up. Hence, they are determined by the predominating conditions of the measurement room (RH 35%, temperature 24°C).

Figs. 4.4.3 and Fig. 4.4.4 demonstrate the bleaching effect of the xenon light source on PPT and NW samples with photochromic pigments P2 and P3, as examples of similar results obtained for the other photochromic pigments P1,P4 and P5. Both graphs show, besides a bleaching effect, also a colour change of the exposed PPT samples. Nevertheless, for a study of fatigue resistance, graphs were used, which

illustrate the dependence of the shade intensity on time of exposure, because this allows a simple understanding of the fatigue process.
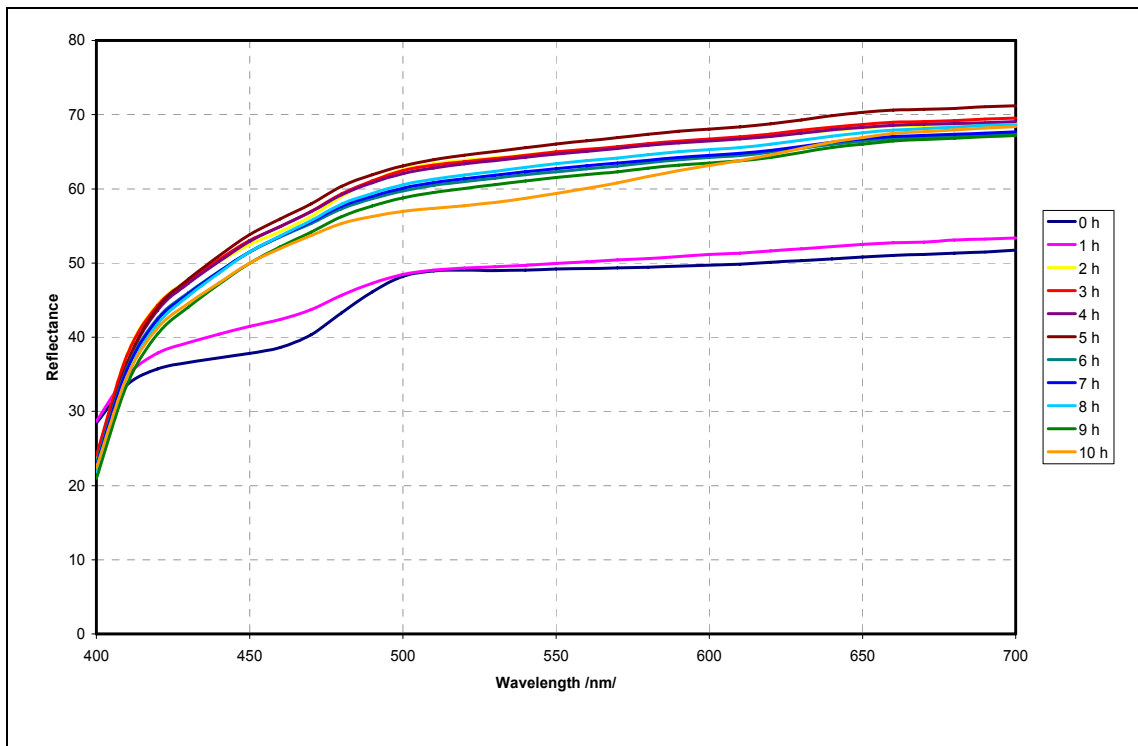

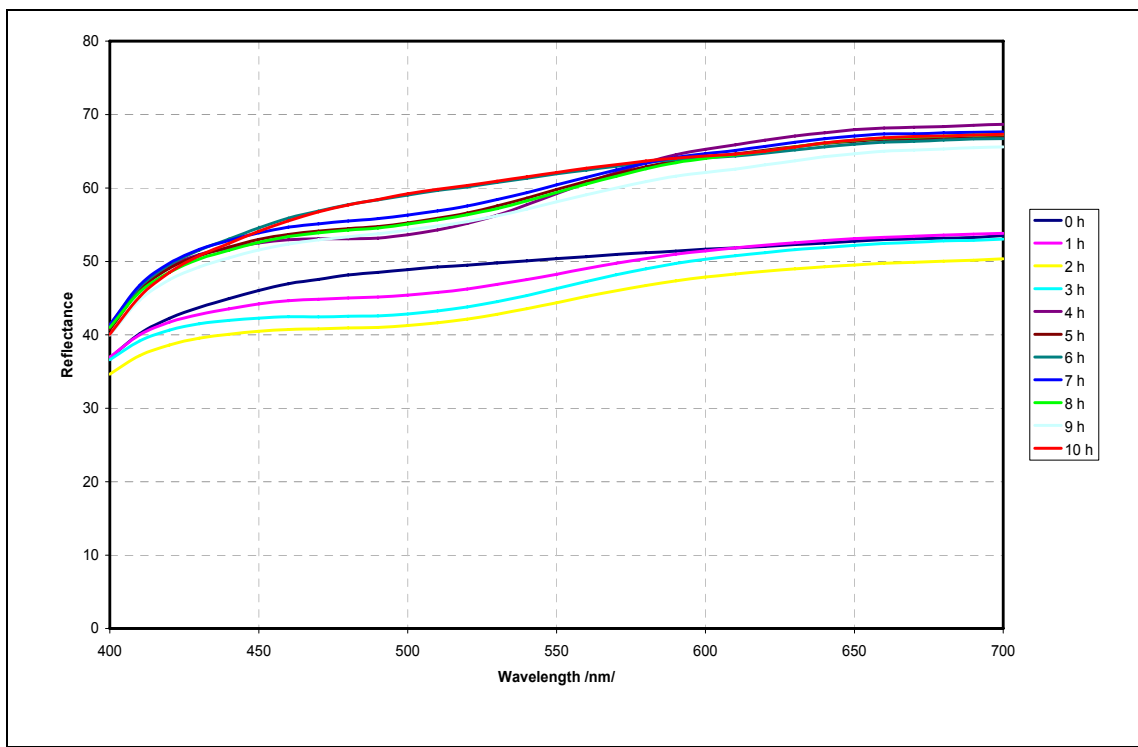Fig. 4.4.3 – Spectral data of PPT-P3 1.0g/30g – influence of number of exposure cycles in Xenotest chamber

Fig. 4.4.4 – Spectral data of NW-P2 1.0g influence of number of exposure cycles in Xenotest chamber

In Fig. 4.4.5 a decrease of shade intensity I after two or three exposure cycles (one cycle was 1 hour) is shown and following that a stable I level is achieved. This represents the significant point where the photochromic textile samples PPT lose their photochromic behaviour. This means, that the photochromic samples tested were resistant against artificial sunlight in the Xenotest chamber for only two or three hours. From Fig. 4.4.6 it is possible to observe preservation properties of the PP polymer used against artificial sunlight because NW samples have photochromic behaviour over one cycle longer than PPT samples.
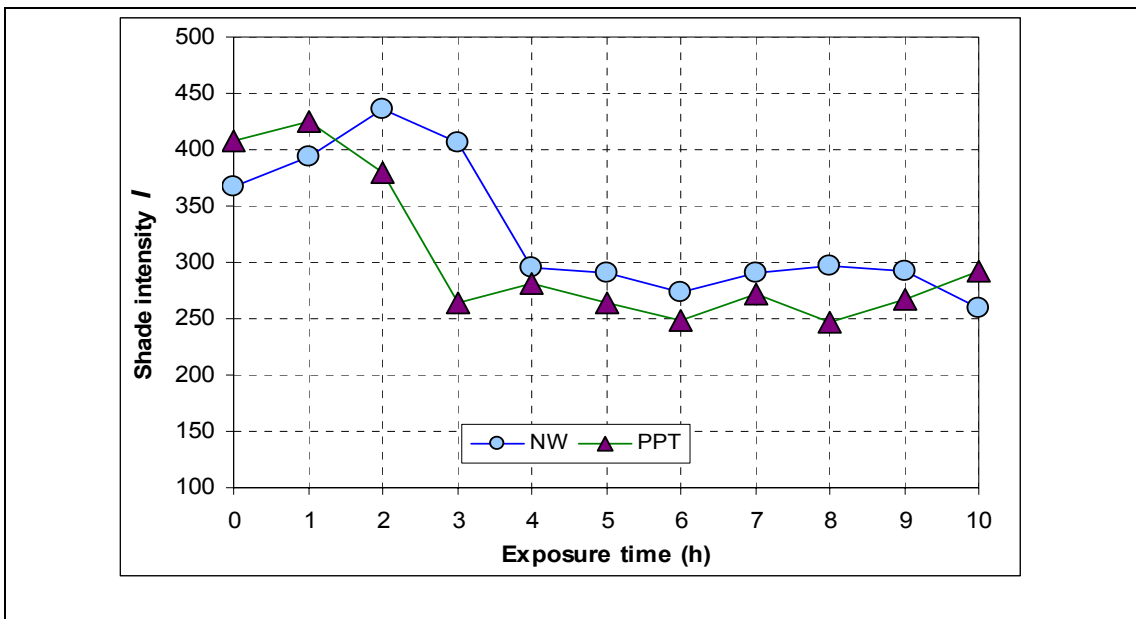
Fig. 4.4.5 – Dependence of fatigue resistance on exposure time in the XENOTEST concentration 3.0g P3   for PPT and NW samples
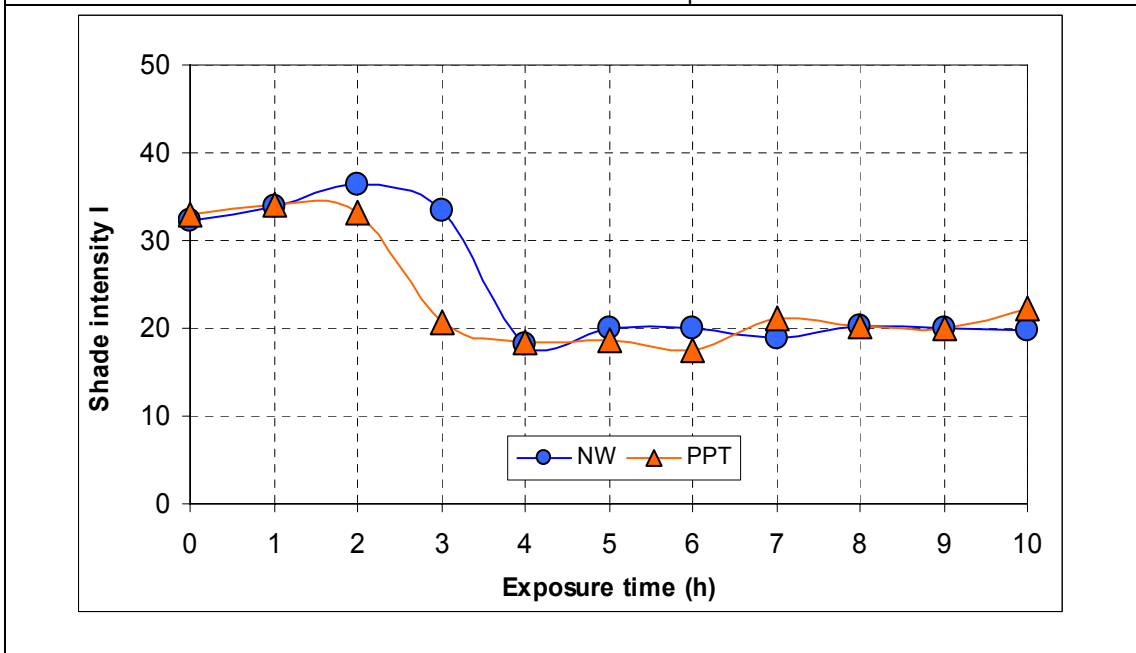
Fig. 4.4.6 – Dependence of fatigue resistance on exposure time in the XENOTEST concentration 3.0g P2   for PPT and NW samples

From Figs. 4.4.7 and 4.4.8, a colour change of the photochromic pigment is evident in CIELAB colour space as an increase in lightness of the tested samples – i.e., a decolouration or a bleaching effect. The numbering of points in the graphs given in Figs. 4.4.7 and 4.4.8 corresponds with the number of the exposure hours.
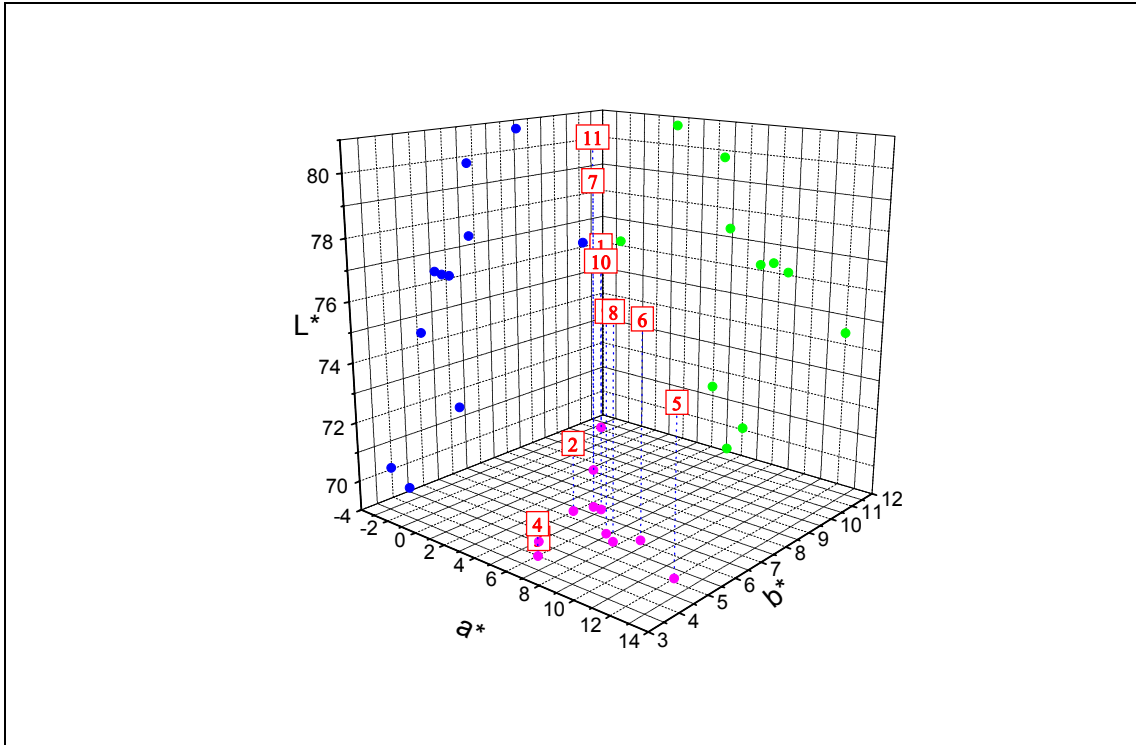

Fig. 4.4.7 – Dependence of colour change - concentration 1.0g/30g PPT-P2 on photochromic cycle number in the XENOTEST immediately after exposure
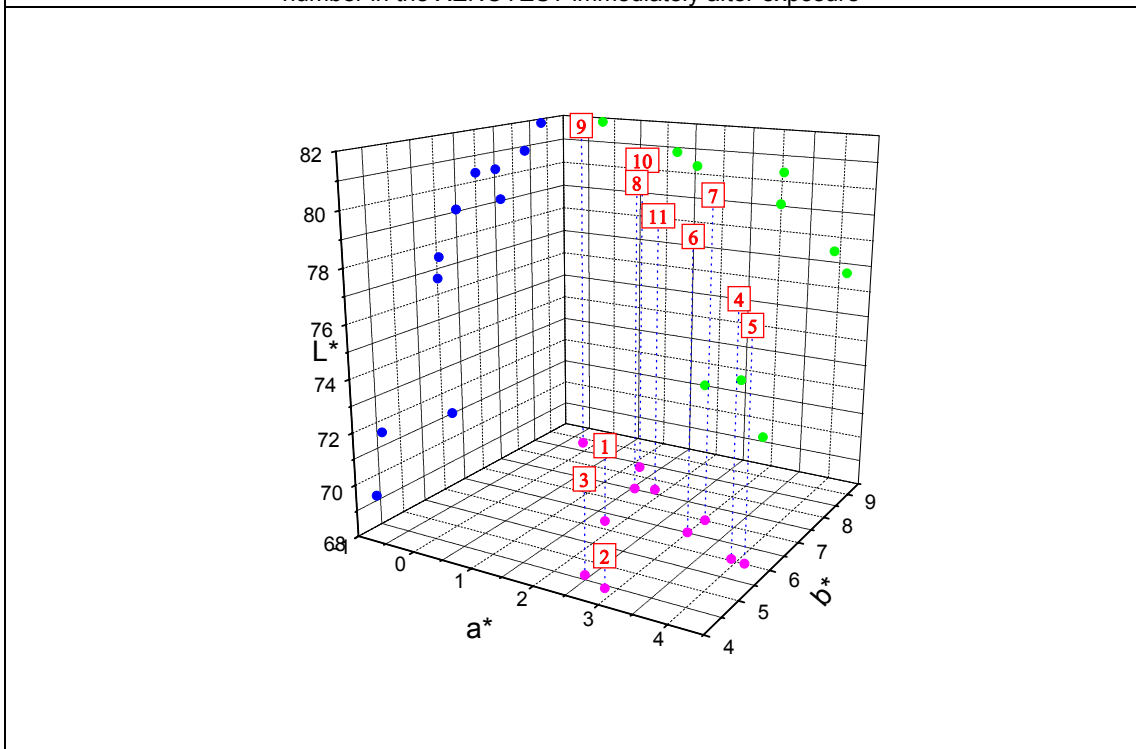

Fig. 4.4.8 – Dependence of colour change - concentration 1.0g/30g PPT-P2 on photochromic cycle number in the XENOTEST immediately after 24hours relaxation and exposure

4.5 Spectral sensitivity of the photochromic prints

UV radiation includes the wavelengths from 100-400 nm: UV-A = 315-400, UV-B = 280-315 and UV-C = 100-280 nm. It was also necessary to test for which regions of UV the new sensors are sensitive. All previous results used polychromatic illumination, i.e., for excitation illumination from 200-400 nm. For spectral sensitivity tests, a special arrangement of the measuring system developed was used, which allowed selection of variable bandwidth and dominant wavelength.

The colour response of photochromic materials depends not only on wavelength, but also on intensity of irradiance. It is possible to use different lasers or sources with a line spectrum as described in section 4.3.1. A disadvantage of this solution is a discontinuous spectrum. Furthermore, the lasers irradiate a small spot of sample, and therefore for irradiation of a large area it is necessary to use a beam expander. A side effect of this solution is a decrease in radiation intensity, and based on that, weak colour development of the photochromic pigments.

If monochromatic sources of light are used, there is a reduction in radiant flux and therefore strictly monochromatic irradiation cannot be used. In this case, band illumination may be used, where the sample is illuminated with a band of wavelengths around the dominant wavelength.

It is well known that shade depth of photochromic colour change is dependent also on irradiance. This is a major problem, because most light sources are not spectrally equi-energy. The solution to this problem is based on a diaphragm. A diaphragm is a thin opaque structure with an opening (aperture) at its centre. The role of the diaphragm is to stop the passage of light, except for the light passing through the aperture. Thus, it is also called a stop. The diaphragm is placed in the light path of an excitation beam, and the size of the aperture regulates the amount of light. The centre of the diaphragm's aperture coincides with the optical axis of the optical irradiation system of the measured sample (see Fig. 4.5.1).

By controlling the intensity of transmitted radiation, it was possible to obtain similar energy for each selected band pass of irradiation. Fig. 4.5.2 presents the spectral distribution of irradiation, which was used for the spectral sensitivity experiment. The spectral characteristic of irradiance was measured by an Avantes USB2000 spectrometer after calibration by an AvaLight-DH-CAL light source.
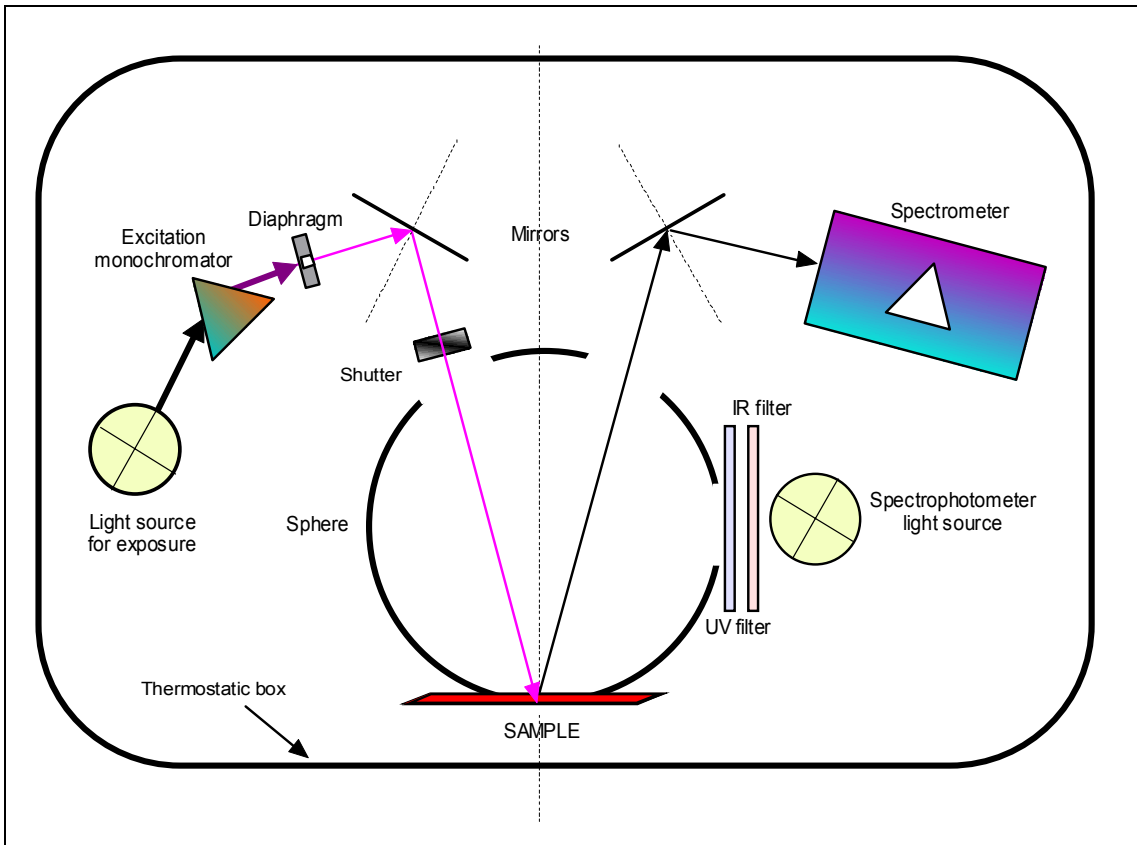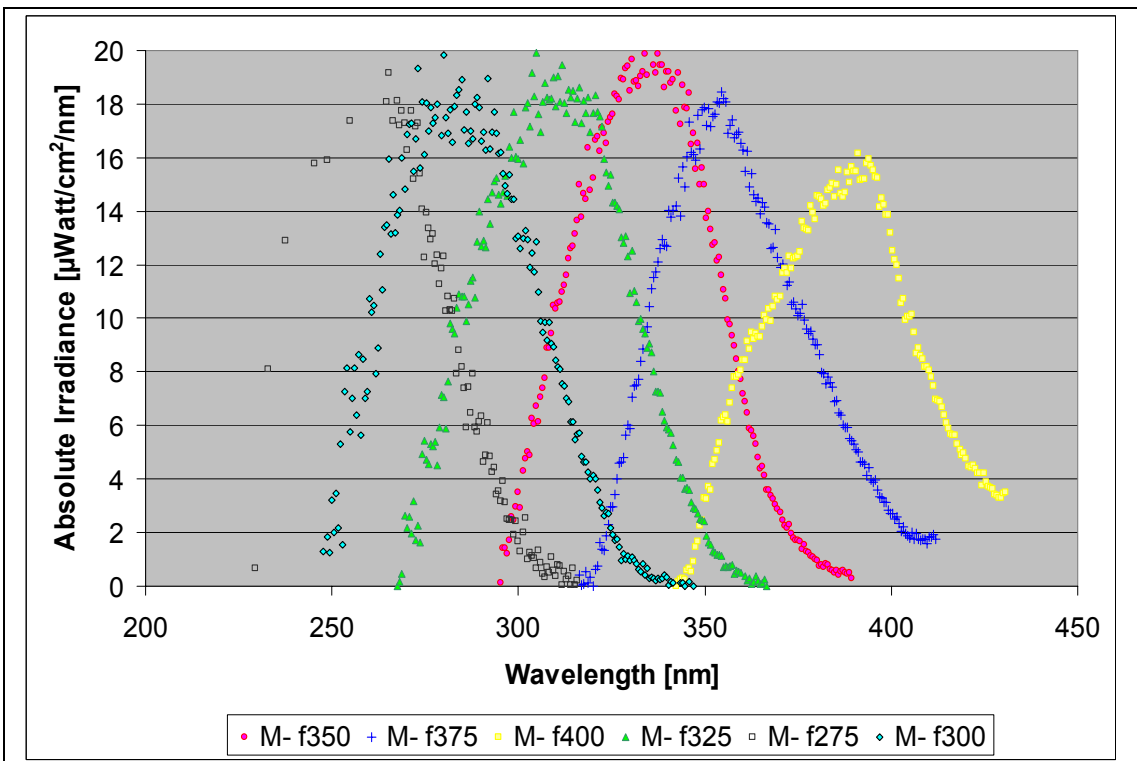
Fig. 4.5.1. Optical scheme of LCAM PHOTOCHROM3 measuring system

4.5.2. Spectral power distribution in selected band pass of irradiation

For every exciting band pass a record of on-off kinetics of the photochromic colour change was made. The following graphs in Figs. 4.5.3 – 4.5.6 present records of absolute values of the Kubelka Munk function for average energy of irradiation 800 µW.cm^{-2} for selected pigments P1-P4.

Fig. 4.5.7. documents that except for pigment P5, the pigments have their main sensitivity at 375 nm. Both spiroindolinonaphthopyran structures with the same orientation of the naphthopyran system (pigment P2: methyl2,2,6-tris(4-methoxyphenyl)-9-methoxy-2H-naphtho-[1,2-b]pyran-5-carboxylate and pigment P3: methyl 2,2-bis(4-methoxyphenyl)-6-acetoxy-2H-naphtho-[1,2-b]pyran-5-carboxylate) show the narrowest bandwidth in comparison to spironaphthooxazines (pigment P1: 3,3,5,6-tetramethyl-1-propylspiro [indoline-2,3'[3H] pyrido [3,2-f][1,4]benzoxazine] and P4:1,3,3,5,6-pentamethyl(indoline-2,3'-[3H] naphtho [2,1-b][1,4]oxazine])). Only pigment P5: 3,3-diphenyl-3H-naphtho[2,1-b]pyran, spiroindolinonaphthopyran with the opposite orientation of the naphthopyran structure, has a maximum of sensitivity shifted to lower wavelengths (to 350 nm) and a flat shape of the sensitivity curve.

Fig. 4.5.3. Spectral sensitivity during on/off kinetics of P1 pigment – concentration 1g/30g
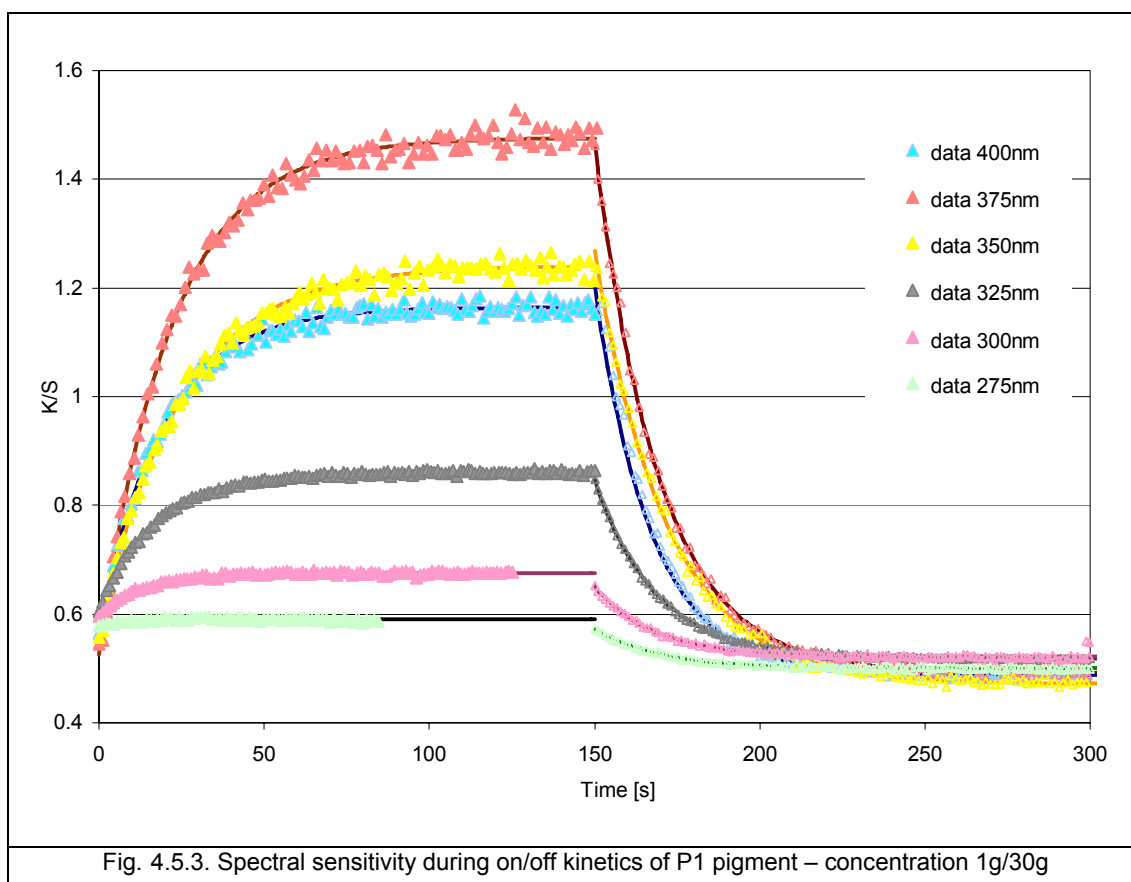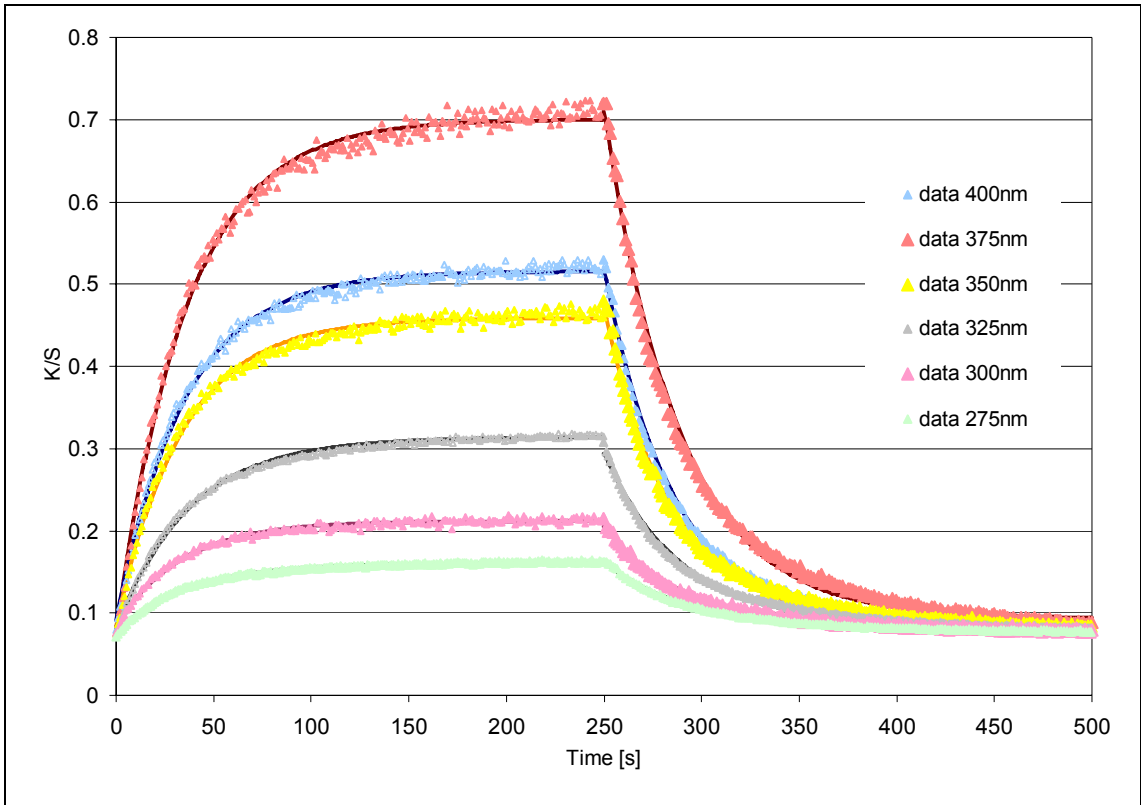
Fig. 4.5.4. Spectral sensitivity during on/off kinetics of P2 pigment – concentration 1g/30g
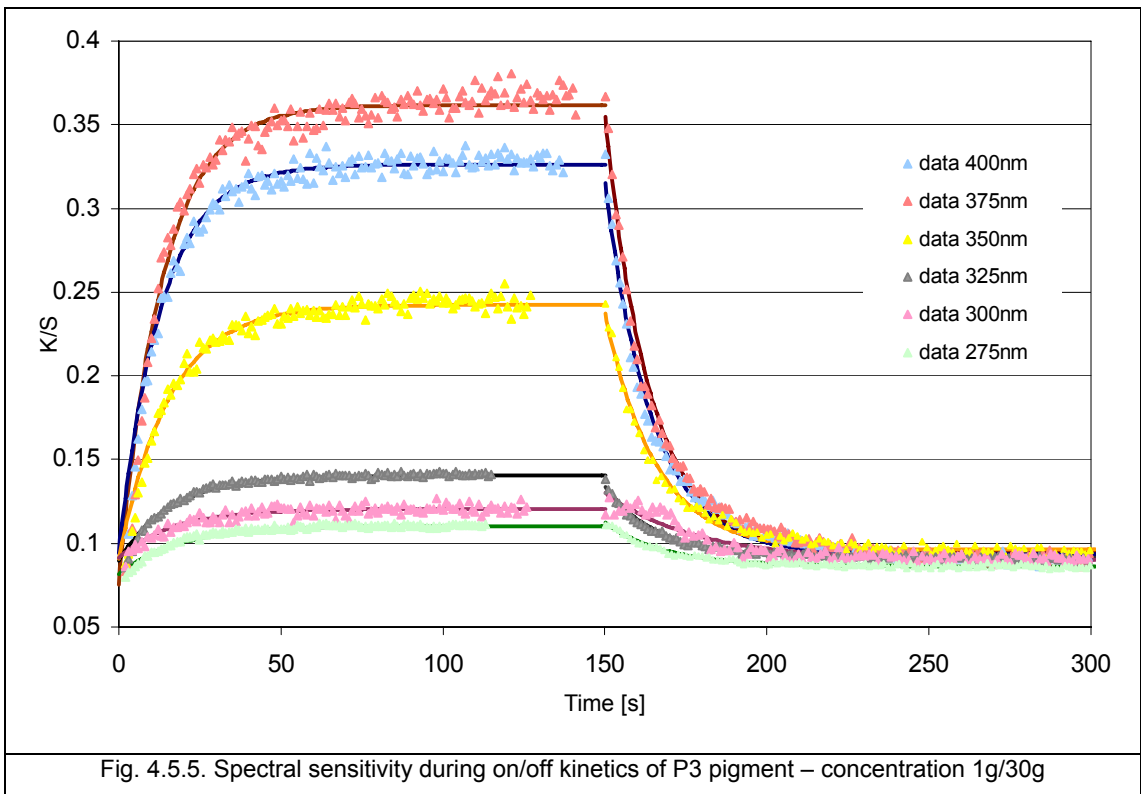

Fig. 4.5.5. Spectral sensitivity during on/off kinetics of P3 pigment – concentration 1g/30g
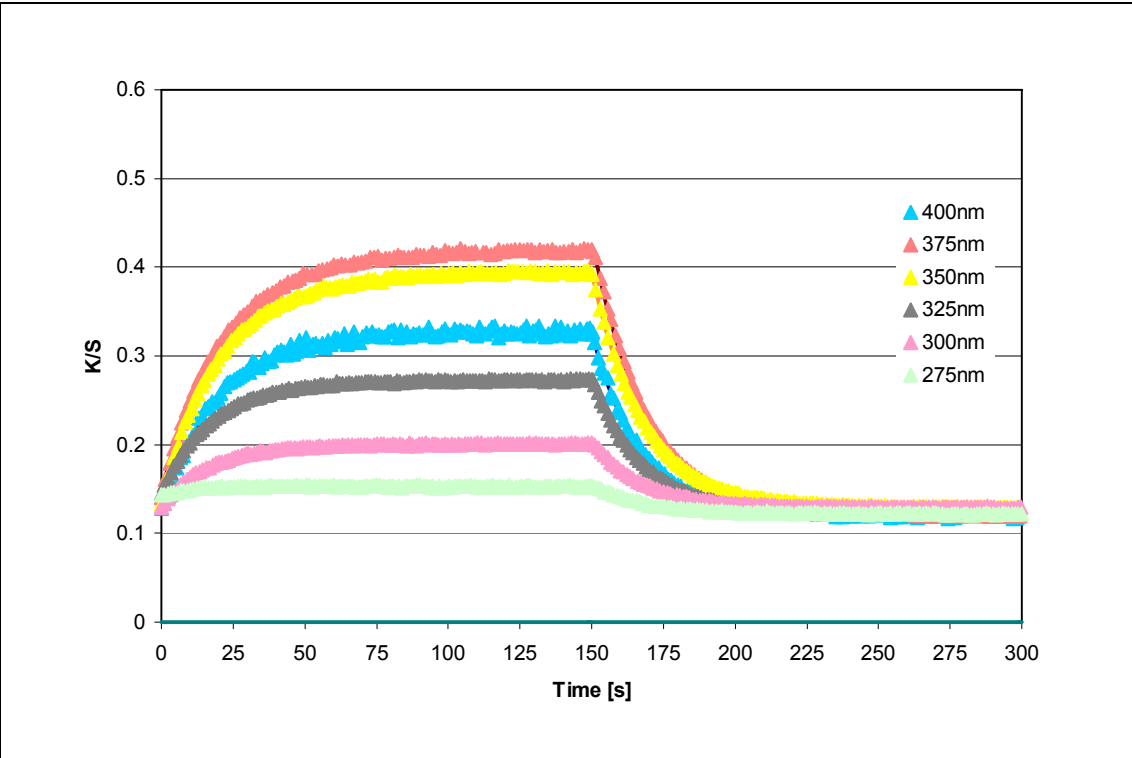
Fig. 4.5.6. Spectral sensitivity during on/off kinetics of P4 pigment – concentration 1g/30g
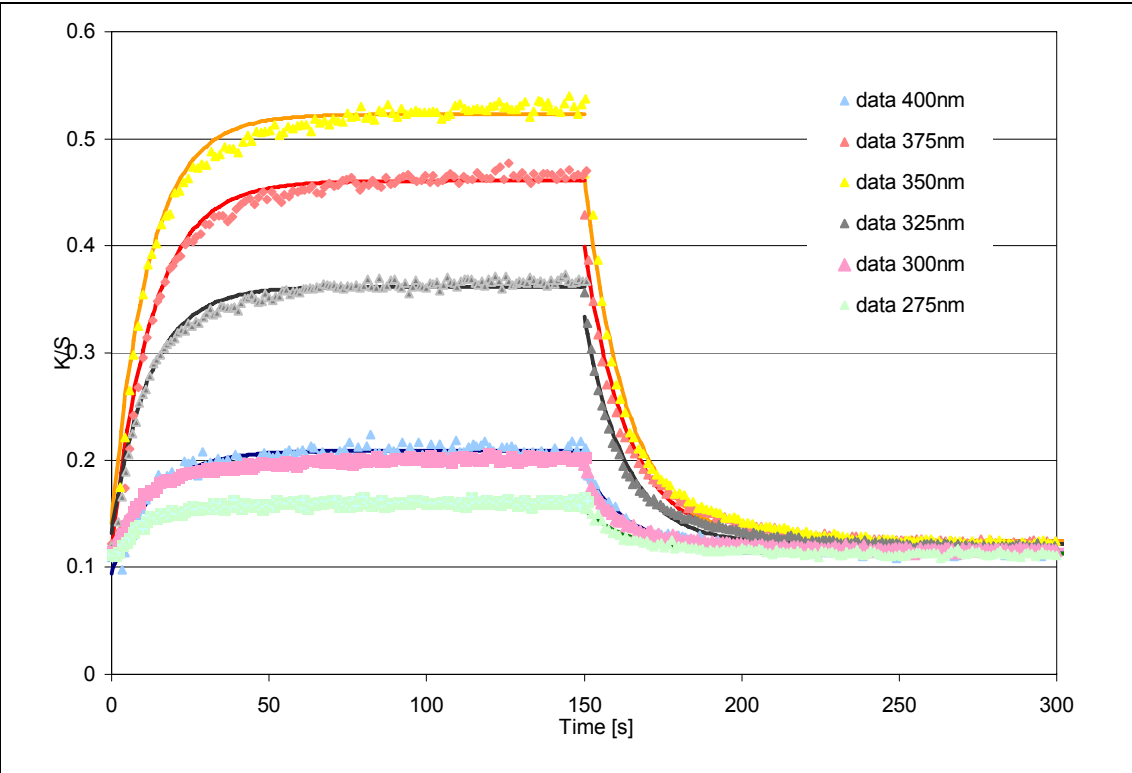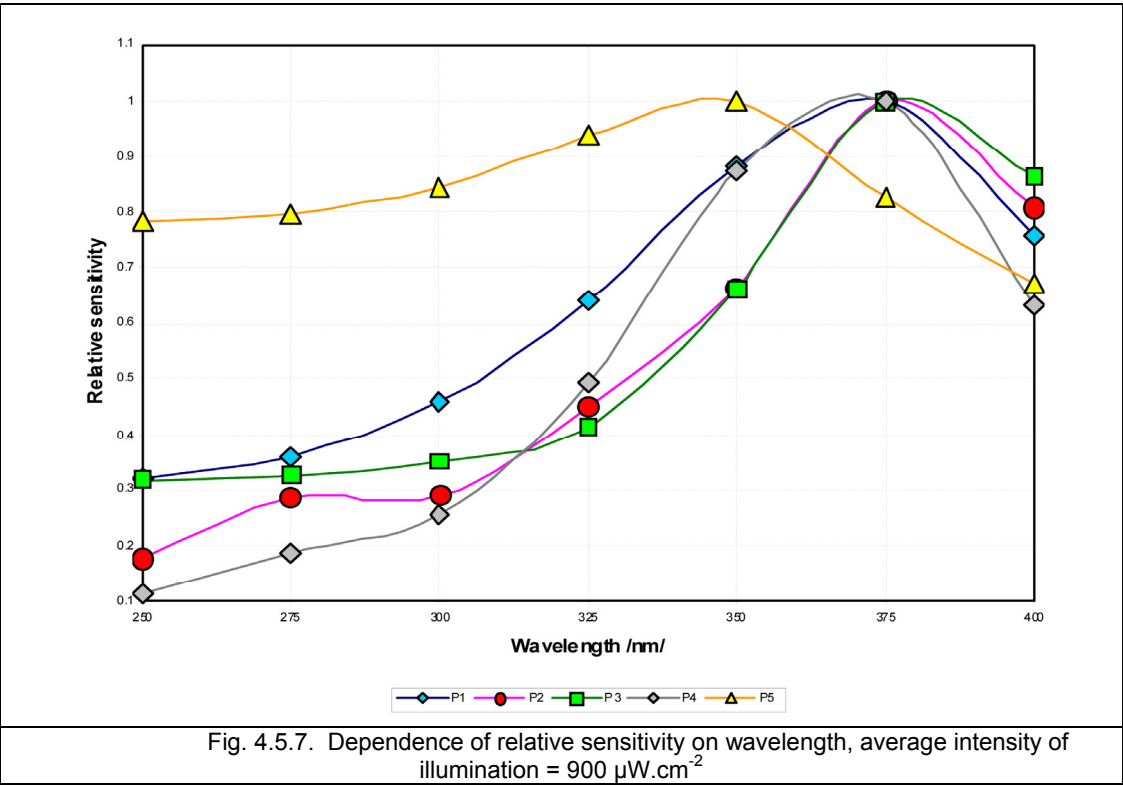

Fig. 4.5.7. Spectral sensitivity during on/off kinetics of P5 pigment – concentration 1g/30g

Fig. 4.5.7. Dependence of relative sensitivity on wavelength, average intensity of illumination = 900 $\mu W.cm^{-2}$

Chapter 5
CONCLUSION

This chapter discusses how the individual aims of the project set out in Chapter 1 have been addressed, as well as providing a summary of the main conclusions and some suggestions for how the research might be progressed into the future. The main goal of this PhD thesis was a kinetic study of the photochromic colour change and a study of the dependence of colour change on the intensity of illumination E. This study has included an evaluation of both exposure and reversion of the photochromic reaction for selected pigments in different media. For this research two spirooxazine and three naphthopyrans structures were selected. Their structures are described in section 3.2 (materials). From the results obtained from the on-line measurement method presented in section 4.1(screen –printed photochromic textiles), section 4.2 (non woven textiles containing photochromic pigments) and section 4.3 (photochromic solution), a first order kinetic model of photochromic colour change was established. The basis of the first order kinetic model is described in sections 2.5.4 and 2.5.5. The kinetic study and experimental data sets obtained clearly verify the first order kinetic model for the all applications tested using photochromic pigments (PPT, NW and PPS). Based on this kinetic model the construction of an optical yield Oy formula for the reaction of photochromic textile was proposed:

$$Oy = \int_{0}^{t_1} I_\infty + (I_0 - I_\infty) e^{-k_E t} dt - \int_{t_1}^{t_2} I_0 + (I_\infty - I_0) e^{-k_R t} dt$$
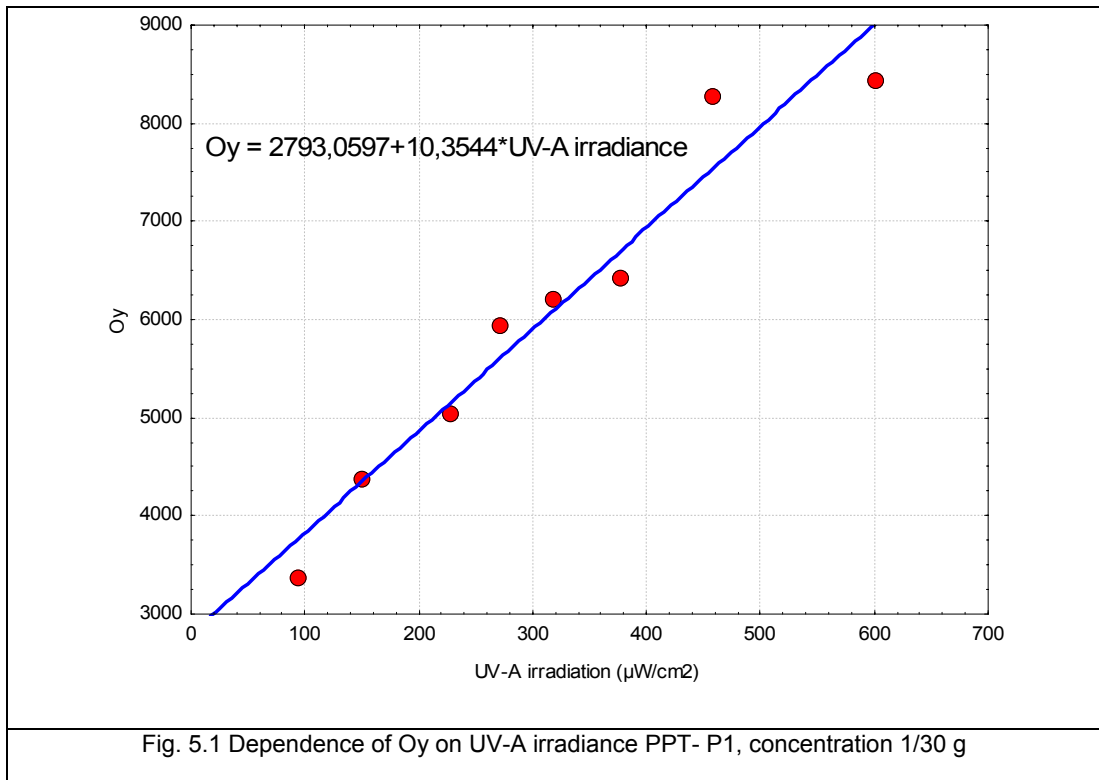
As a result of experimental observation and the calculation of the dependence of optical yield, $Oy,$ on intensity of illumination E, it was found that the optical yield of the photochromic reaction Oy depends linearly on the intensity of illumination E, as is documented in Figs. 4.1.14 a-b (for photochromic textile prints), Figs. 4.2.2a-b and 4.2.3a-b (for non wovens).

Thus a major contribution of this research to the study of photochromism is the discovery of a correlation between the optical yield of the photochromic reaction O_y and irradiance – the intensity of illumination. This correlation has the potential to be used for calibration of potential smart textile sensors with photochromic pigments

applied as indicators of UV radiation intensity. As discussed in this work, the sensorial maximum of the photochromic samples with pigments P1-P4 tested in this work is at 375 nm , which is in the UV-A radiation region. The photochromic textile with pigment P5 has a sensorial maximum at 345nm.

In Figs. 4.1.17 a-c the linear relation between optical yield, O_y, and illuminance E is shown, similar to Figs. 4.1.14 a-b where the relation to UV-A radiation is given, because in this case identical light sources are used. Illuminance E was measured by a standard luminance meter Minolta IT10, which is sensitive only in the visible part of the spectrum. The sensitivity of this luminance meter conforms to the CIE spectral luminance function V_λ.

Such a measurement method is acceptable for conditions where the ratio between the UV and visible parts of the radiation is constant. Therefore, for the newest comparisons a standard irradiance meter, which can measure radiation in UV-A, UV-B and UV-C was used. The relationship between optical yield and UV-A irradiance is shown in Fig. 5.1

Oy = 2793,0597+10,3544*UV-A irradiance

Fig. 5.1 Dependence of Oy on UV-A irradiance PPT- P1, concentration 1/30 g

The investigation of the kinetic behaviour of photochromic textiles, which is discussed in section 4.1.1, show that for the exposure period the half-life of colour change, $t_{1/2}$, is practically independent of pigment concentration. This means that the time of colour change during exposure is not influenced by increased concentration of the pigments. During reversion of photochromic colour change a slight decrease of half-life, $t_{1/2}$, with increasing photochromic pigment concentration was found. A strong negative linear relationship was found between half-life and irradiance for all photochromic pigments.

Also in this research, large differences were observed between reversion rates of the photochromic pigment applied by printing compared with solution. Differences between solution and non-woven textiles are relatively small as illustrated graphically in Fig. 4.3.13. This observation is consistent with the hypothesis that a photochromic pigment incorporated in the mass of PP fibres is in a similar state as in a saturated cyclohexane solution. The photochromic pigment is encased inside a solvent mass and values of the rate constants are therefore similar.

In this work, observation of a "transition" shade during reversion of photochromic pigments from exposed to relaxation phase in solution was discussed. For higher concentrations the time of reversion was more than 4 days (96 hours) and the time was not sufficient for the return to the original colourless form. Distribution of experimental points on the chromatic plane a*b* of CIELAB colour space represents the position of the transitional shade from the position of fully relaxed photochromic solution. From Figs. 4.3.11a-b it is evident that with an increase in concentration the extent of relaxation of the photochromic solution is reduced. A critical feature from this point of view is a concentration above 4.0 g/l, because 4 days relaxation in a dark box does not lead to full relaxation and reversion to the original colourless form. A possible explanation is that there may be a retardation influenced by agglomeration and aggregation of the photochromic pigments, which are at their limit of solubility. This phenomenon has not been reported previously, because most experiments have been realized on dilute solutions with a 1000 times smaller concentration of photochromic pigment. It was found that for formation of the transition state in saturated photochromic solutions only one exposure cycle sufficed. This phenomenon is referred to as "photochromic colour memory" - PCM. Compared to the photochromic solutions tested the effect of PCM on PPT was

minimal and the time necessary for full colour recovery was under 12 minutes. Nevertheless, during the experiments 24 hour relaxation was used.

Furthermore, it was shown that the application medium affects the colour of photochromic samples. In the applied textile media, there is a bathochromic spectral shift and the fibres or fabrics had a yellowish colour before irradiation compared with the "ideal" colourless transmittance in solvents. Simultaneously, this work demonstrates that producing photochromic textiles by melt blown technology brings no advantage in comparison to photochromic prints. On the contrary, mass dyeing technology is severely complicated and has only one benefit – marginally higher light fastness.

It is evident that the intensity of the photochromic response depends on the spectral power distribution of the exciting light source used and the absorption characteristics of the media used. The light source sensitivity study documents differences in response from the range of photochromic pigments tested. The pigments based on substituted naphthopyrans (P2 and P3) were more sensitive as illustrated in Figs. 4.3.1 and 4.3.2. These properties are believed to be due in part to the stability (lack of steric interactions) of the trans-quinoidal open form. This result is consistent with the influence of molecular orientation in the naphthopyran isomers (P5) as discussed in the literature [10, 36]. The other pigments tested were essentially insensitive to these factors.

The study of photochromic response modulation with the incorporation of UV absorbers shows that the extension of half-life of photochromic colour change caused by UV absorbers decreases with irradiance intensity. Also differences in the efficiency of the UV absorbers used were found, which is probably associated by different absorption properties.

The next main task was the study of the spectral sensitivity of photochromic textiles which showed that, except for pigment P5, the pigments tested have their main sensitivity at 375 nm as demonstrated in Fig. 4.5.8. Both [1,2-b] pyrans (pigments P2, P3) show narrower bandwidths in comparison to spirooxazines (pigments P1, P4). Pigment P5, which is a [2,1-b] pyran structure and which behaves smoothly in terms of relative spectral sensitivity shows that the orientation of the naphtho group has a strong effect. Replacement of methoxyphenyl group in pigment P2 by an acetoxy group in pigment P3 caused a difference in developed colour, but not in spectral sensitivity.

With respect to photostability, a further conclusion in this thesis is a stepwise linear trend of photochromic response decrease during fatigue resistance tests found for photochromic textile prints PPT, compared with a simple linear decrease of photochromic response for solutions, as has been previously reported in some articles [113-115]. During the first 10 cycles a large decrease in photochromic response was measured. This period is called "burning" of the photochromic system. Subsequently, the photochromic response is relatively stable (see Figs. 4.4.2 a-c.). One possible explanation for this phenomenon is the problem of low spectral sensitivity of shade intensity I compared with colour difference ΔE^*. A main reason is that the parameter of shade intensity is calculated as the integral value under the curve given by the K/S function.

In addition, an important outcome of this work is the development of a unique measuring system allowing the measurement of spectrophotometric and colorimetric values. This system is now used as prototype for measurement of photochromic and thermochromic behaviour of different materials. Due the control of excitation light source using a shutter it is possible to measure photochromic properties for one or multiple cycles. This system also allows the measurement of the thermal sensitivity of photochromic samples.

Based on this result, the possibility has been demonstrated in principle that photochromic textiles can be applied for the preparation of a sensorial system, which allows simple visual assessment of the amount of UV radiation incident on the sample. This system can be designed for example as a simple rule scale, where for comparison there is a constant coloured part made from UV stable pigments or dyestuffs. Individual parts of the constant scale can be judged as having the same colour as the photochromic part at a specific intensity of UV radiation. The observer will be able to estimate the level of UV radiation corresponding to a colour match between the photochromic colour changeable part and visual stable part of the textile UV sensor. From the point of view of future work in the photochromic textile field, optimisation of the photochromic pigment used especially in terms of fatigue resistance and spectral sensitivity criteria will be important. In this thesis, the photochromic pigments tested were sensitive in the UV - A part of the spectrum. It is well known that the UV – B part of electromagnetic spectrum is the main cause of cancerous problems. Therefore, photochromic pigments sensitive in the UV - B part will have in the near future an important role in this research field.

The development of a unique measuring system provides a starting point for the standardisation process for the measurement of colorimetric parameters of photochromic materials. Today, the situation means that the results of photochromic material properties are incomparable, when different light sources with different spectral power distribution and radiation intensity are used. Therefore, it will be necessary to discuss the question of light source specification, which should be used for excitation of photochromic materials in the future.

References

[1] Xiaoming T., Smart fibres, fabrics and clothing, The Textile Institute, Cambridge England (2001)

[2] Viková, M., Vik, M., *Some Problems in Measurement of UV Protective Textiles*, The 3rd China International Wool Textile Conference, Xi'an China 26-28 Sep. 2002, p.635-638,

[3] Vanicek, K., Frei, T., Litynska, Z., Schmalwieser, A., *UV- Index for the public*, COST-713 Action 1999

[4] Bernhard, G., Seckmeyer, G., *The uncertainty of measurements of spectral solar UV irradiance,* J. Geophys. Res. 104 14321–45, (1999)

[5] Kiedron, P. W., Michalsky, J. J., Berndt, J. L., Harrison, L. C., *Comparison of spectral irradiance standards used to calibrate shortwave radiometers and spectroradiometers*, Appl. Opt. 38 2432–9, (1999)

[6] Gardiner, B.G., P.J. Kirsch, editors, *Second European Intercomparison of Ultraviolet Spectroradiometers*, Air Pollution Research Report no. 38, Commission of European Communities, Brussels, Belgium, 1993, 38, 67

[7] Groebner, J., Blumthaler, M., Kazadzis, S., Bais, A., Webb, A., Schreder, J., Seckmayer, G., Rembges, D. , *Traveling reference spectroradiometer for routine quality assurance of spectral solar ultraviolet irradiance measurements*, Applied Optics, Vol. 44, Issue 25, pp. 5321-5331 (2005)

[8] Slaper, H., Reinen, H.A.J.M., Blumthater, M., Huber, M., Kuik, F., *Comparison ground-level spectrally resolved solar UV measurements usin various instruments: A technique resolving effects of wavelength shift and slit width,* Geophys. Res. Lett. 22 2721–4, (1995)

[9] Crano, J. C. & Guglielmetti, R. J., editors, Organic Photochromic and Thermochromic compounds, Vol 1: Main photochromic families, Plenum Press, New York (1999).

[10] Brown, G. H., editor, Techniques of Chemistry, Vol.III, Photochromism, John Wiley & Sons, New York, First edition (1971).

[11] El'tsov, A.V., editor, Organic Photochromes, Plenum Publishing Corporation, New York (1990).

[12] Stewart, J. J. P., editor, *Semiempirical molecular orbital methods.* In: Reviews in Computational Chemistry, 1, VCH New York, 45-81 (1990).

[13] Mc Ardle C. B., editor, Applied Photochromic Polymer Systems, Blackie, New York, (1992)

[14] Krongauz, V. , Weiss, V. , Berkovic, G., *Spiropyrans and Spirooxazines for Memories and Switches*, Chem. Rev., 100 1741 (2000).

[15] Hurst, J. K., Giertz, K., Khairutdinov, R. F., Voloshina, E. N., Voloshina, N. A., Minkin, V. I. , *Photochromism of Spirooxazines in Homogeneous Solution and Phospholipid Liposomes*, J. Am. Chem. Soc., 1998, 120 (49), pp 12707–12713 (1998).

[16] Bowen, C. M., Winkler, J. D., Michelet, V., *Photodynamic Fluorescent Metal Ion Sensors with Parts per Billion Sensitivity*, J. Am. Chem. Soc., 1998, 120 (13), pp 3237–3242 (1998).

[17] Pearlman, R. S., editor, 3D Molecular Structures: Generation and use in 3D searching In: 3DQSAR in Drug Design, Kubinyi, H. (Ed), Escom Science Publishers: Leiden; 41-79 (1993).

[18] Hou, L., Schmidt, H., *Effect of additives on the photostability of sol-gel-derived organic-inorganic photochromic coatings*, J. Mater. Sci. Lett, 16, 435 (1997).

[19] Kelly, J. M., Mc Ardle, C. B., Maunder, M. J., editors, Photochemistry and polymeric systems, Royal Society of Chemistry, Cambridge (1993).

[20] Viková, M., *Visual Assessment UV Radiation by Colour Changeable Textile Sensors*, AIC 2004, Color and Paints, the Interim Meeting of the International Color Association, Porto Alegre 1-5. November 2004, Brasil

[21] Galston, A.W., *Riboflavin, light, and the growth of plants*, Science 111:619-624. (1950)

[22] Bouas-Laurent, H., Dürr, H., *Organic Photochromism*, Pure Appl. Chem., Vol. 73, No. 4, pp. 639–665, (2001)

[23] Smets, G., Braeken, J., Irie, M., *Photochemical Effects in Photochromic Systems*, Pure & Appi. Chem., Vol.50, pp. 845—856, (1978)

[24] Alfimov, M.V., O.A. Fedorova, and S.P. Gromov, *Photoswitchable molecular receptors*, Journal of Photochemistry and Photobiology A: Chemistry, 158(2-3): p. 183-198, (2003)

[25] Kelly, T.R., H. De Silva, and R.A. Silva, *Unidirectional rotary motion in a molecular system*, Nature, 401(6749): p. 150-152, (1999)

[26]   Ahmed, S.A., *Photochromism of dihydroindolizines Part VI: synthesis and photochromic behavior of a novel type of IR-absorbing photochromic compounds based on highly conjugated dihydroindolizines*, J. of Phys. Org. Chem., 19: p. 402-414, (2006)

[27]   Li, J., G. Speyer, and O.F. Sankey, *Conduction Switching of Photochromic Molecules*. Physical Review Letters, 93: p. 248302, (2004)

[28]   Janus, K., Koshets, I.A., S Sworakowski, J., Nespurek, S., *An approximate non-isothermal method to study kinetic processes controlled by a distribution of rate constants: the case of a photochromic azobenzene derivative dissolved in a polymer matrix*, J. Mater. Chem., 12, 1657, (2002)

[29]   Nespurek, S., Toman, P. Sworakowski, J., *Charge carrier transport on molecular wire controlled by dipolar species: Towards light-driven molecular switch*, Thin Solid Films, 438-439: p. 268-278, (2003)

[30]   Christie, R.M., Colour Chemistry, The Royal Society of Chemistry (2001)

[31]   Nassau, K., The Physics and chemistry of color, J. Wiley and Sons, Inc., 2nd ed, New York (2001)

[32]   Bordo, V.G., Rubahn, H.G., Optics and spectroscopy at surfaces and interfaces, Wiley VCH, Weinheim, (2005)

[33]   Dürr, H., Bouas-Laurent, H., Photochromism, Molecules and systems, Elsevier, New York, (1990)

[34]   Bamfield, P., Chromic phenomena, Technological Applications of Colour Chemistry, The Royal Society of Chemistry, Cambridge, (2001)

[35]   Gerhardt, G.E.,Township, W.: *Single and Double Energy Transfer in Triplet-Triplet Photochromic Composition*, United States patent nu. 3,725, 292 (1973)

[36]   Mancheva, I., Zhivkov, I., Nešpůrek, S., *Kinetics of the Photochromic Reaction in a Polymer Containing Azobenzene Groups*, J. Opt. Adv. Materials, Vol. 7, 253-256, (2005)

[37]   Kühn, D., Balli, H., Steiner, U.E., *Kinetic study of the photodecoloration mechanism of an inversely photochromic class of compounds forming spiropyran analogues*, Journal of Photochemistry and Photobiology A: Chemistry 61, 1, 99-112, (1991)

[38]   Coelho, P.J., Salvador, M.A., Heron, B. M., Carvalho, L.M., *Spectrokinetic studies on new bi-photochromic molecules containing two naphthopyran entities*, Tetrahedron 61, 11730–11743, (2005)

[39]   Delbaere, S., Luccioni-Houze, B., Bochu, Ch., Teral, Y., Campredon, M., Vermeersch, G., *Kinetic and structural studies of the photochromic process of 3H-naphthopyrans by UV and NMR spectroscopy*, J. Chem. Soc., Perkin Trans. 2, 1153-1157, (1998)

[40]   Liu, R.S.H., Hammond, G.S., *Photochemical Reactivity of Polyenes. From Dienes to Rhodopsin; from Microseconds to Femtoseconds,* Photochem. Photobiol. Sci., 2, 835 – 844, (2003)

[41]   Ostrovskii, M. A., Fedorovich, I.B., *Photochemical transformations of the visual pigment rhodopsin,* J. Quantum Electron. 8 1274-1278, (1978)

[42]   Suzuki, T., Callender, R.H., *Primary Photochemistry and Photoisomerization of Retinal at $77^0 K$ in Cattle and Squid Rhodopsins*,   Biophys. J. 34, 5, pp. 261-270, (1981)

[43]   Nishioku, Y., Hirota, N., Nakagawa, M., Tsuda, M., Erazima, M., *The energy and dynamics of photoreaction intermediates of' Octopus rhodopsin studied by the transient grating method*, Anal.   Sci, 17, 323-325, (2001)

[44]   Kandori, H., Shichida, Y., Yoshizawa, T., *Photoisomerization in Rhodopsin*, Biochemistry, Vol. 66, 11, 1197-1209, (2001)

[45]   Yan, M., Manor, D., Weng, G., Chao, H., Rothberg, L., Jedju, T. M., Alfano, R. R., Callender, R.H., *Ultrafast spectroscopy of the visual pigment rhodopsin*, Proc. Natl. Acad. Sci. USA 88, 9809-9812, (1991)

[46]   Liu, R.S.H., Colmenares, L.U., *The molecular basis for the high photosensitivity of rhodopsin, PNAS 9*, vol. 100, 25, 14639–14644, (2003)

[47]   Han, M., Groesbeek, M., Sakmar, T.P., Smith, S.O., *The C9 methyl group of retinal interacts with glycine-121 in rhodopsin,* Proc. Natl. Acad. Sci. Vol. 94, 13442–13447, (1997)

[48]   Nakanishi, K., *Photochemical studies of visual pigments,* Pure & Appl. Chem., Vol. 49, 333-339, (1977)

[49]   Birge,R.R., Gillespie, N.B., Izaguirre, E.W., Kusnetzow, A., Lawrence, A.F., Singh, D., Song, Q.W., Schmidt, E., Stuart, J.A., Seetharaman, S., Wise, K.J., *Biomolecular Electronics: Protein-based associative processors and volumetric memories,* J. Phys. Chem. *B*, 103, pp. 10746-10766, (1999)

[50]   Lovrien, R., Waddington, J. C. B., *Photoresponsive Systems I. Photochromic Macromolecules*, J. Amer. Chem. Soc. 86, pp. 2315-2322, (1964)

[51]   Cojocariu, C., Rochon, P., *Light-induced motions in azobenzenecontaining polymers*, Pure Appl. Chem., Vol. 76, No. 7–8, pp. 1479–1497, (2004)

[52]   Maafi, M., *Useful Spectrokinetic Methods for the Investigation of Photochromic and Thermo-Photochromic Spiropyrans,* Molecules 13, pp. 2260-2302, (2008)

[53]   Tatewaki, H., Baden, N., Momotake, A., Arai, T., Erazima, M., *Dynamics of Water-Soluble Stilbene Dendrimers upon Photoisomerization*, J. Phys. Chem. B 108, 12784-12789, (2004)

[54]   Wehrle, B., Limbach H.H., *NMR study of Environment Modulated Proton Tautomerism in Crystalline and Amourphous Phatlocyanine*, Chem. Physics 136, pp.223-247 (1989)

[55]   Dürr, H., *A new photochromic system - potential limitatir and perspectives*, Pure &Appl. Chem., 62, 8, pp. 1477-1482, (1990)

[56]   Cicogna, F., Ingrosso, G., Lodato, F., Marchetti, F., Zandomeneghi, M*., 9-anthroylacetone and its photodimer,* Tetrahedron 60,   pp. 11959–11968, (2004)

[57]   Born, M. and Wolf, E., Principles of Optics: Electromagnetic Theory of Propagation, Interference and Diffraction of Light, Pergamon Press, Oxford, (1975)

[58]   Štoll, I., Tolar, J.: Teoretická fyzika (Theoretical Physics – in Czech), ČVUT Press, Prague, (1994)

[59]   Urbanova, M, Hofmann, J, Alexa, P., Fyzika II (Physics II – in Czech), VŠCHT, Prague, (2000)

[60]   Hecht, E., Optics*,* Third Edition, Addison-Wesley, Reading, Massachusetts, (1998)

[61]   Smith, W. J., "Modern Optical Engineering", Mcgraw Hill, New York, (1990)

[62]   Sillion, F. X., Peuch, C., Radiosity and Global Illumination, Morgan Kaufmann, San Francisco, CA, (1994)

[63]   Kaase, H., Fundamentals and Limitations of Optical Radiation Measurements, Berlin VDI Verlag Düsseldorf, (1999)

[64]   Bass, M, Van Stryland, E.W., Williams, D.R., Wolfe, W.L. editors, Handbook of Optics: Devices, Measurements, & Properties, Volume II, Second Edition, McGraw-Hall, New York, (1995)

[65]   Boyd, R. W., Radiometry and the Detection of Optical Radiation, John Wiley
       & Sons, New York, (1983)

[66]   Walter G. Driscoll, Vaughan, W., Handbook of Optics, McGraw-Hill,
       New York, (1978)

[67]   Grum, Becherer, R.J., Optical Radiation Measurements (Volume 1):
       Radiometry, Academic Press, New York, (1979)

[68]   Wyszecki, G., Stiles, W., Color Science: Concepts and Methods, Quantitative
       Data and Formulas, Second Edition, Wiley, New York, (1982)

[69]   Richter, M., Einführung in die Farbmetrik, Verlag de Gruyter, Berlin, New
       York, (1981)

[70]   McCluney, W.R.: Introduction to Radiometry and Photometry, Artech House
       Inc., Norwood (1994)

[71]   Giorgianni, E.J., Madden, T.E., Digital Color Management, Addison-Wesley,
       Reading, MA, (1998)

[72]   Krinov, E. L., "Spectral Reflectance Properties of Natural Formations,"
       National Research Council of Canada, Technical Translation TT-439,
       translated by G. Belkov, (1953)

[73]   MacAdam, D.L., Color Measurement Theme and Variations, Second Edition,
       Springer-Verlag, Berlin, (1985)

[74]   Shevell, S.K., Science of Color, Second Edition, Elsevier, Kidlington, Oxford,
       (2003)

[75]   Palik, E.D. ed., Handbook of Optical Constants of Solids I, Academic Press,
       Boston, (1985)

[76]   Palik, E.D. ed., Handbook of Optical Constants of Solids II, Academic Press,
       Boston, (1985)

[77]   Meyer, G.W., Wavelength Selection for Synthetic Image Generation,
       Computer Vision, Graphics, and Image Processing, 41, pp. 57-79, (1988)

[78]   Bass, M, Van Stryland, E.W., Williams, D.R., Wolfe, W.L. editors, Handbook
       of Optics: Devices, Measurements, & Properties, Volume I, Second Edition,
       McGraw-Hall, New York, (1995)

[79]   Evans, R.M., An Introduction to Color, John Wiley & Sons, New York,
       (1961)

[80]   Fairchild, M.D., Color Appearance Models, Addison-Wesley, Reading, MA,
       (1998)

[81]   Judd, D.B., Contributions to Color Science, US Department of Commerce, (1979)

[82]   Wright, W. D., The Measurement of Colours, Fourth Edition, Van Nostrand Reinhold, New York, (1969)

[83]   Hall, A., Illumination and Color in Computer Generated Imagery, Springer-Verlag, New York, (1989)

[84]   CIE: Commission Internationale de l'Eclaire, *"CIE Recomendations on Uniform Colour Space – Colour Diference Equations, Psychometric Colour Terms,"* CIE Publication. Vol. 15, (1978)

[85]   Levkowitz, H., Color Theory and Modeling for Computer Graphics, Visualization, and Multimedia Applications, Kluwer Academic, Boston, (1997)

[86]   MacDonald, L. W., Luo, M.R., Colour imaging vision and technology, Wiley and sons, Chichester, (1999)

[87]   Westland, S. , Ripamonti, C., Computational Colour Science using MATLAB, Wiley and sons, Chichester, (2004)

[88]   Ohta, N., Robertson, A.R., Colorimetry Funamental and Applications, Wiley and sons, Chichester, (2005)

[89]   Schanda, J., Colorimetry Understanding the CIE system, Wiley and sons, Hobokem, (2007)

[90]   CIE: Commission Internationale de l'Eclaire, *"Colourimetry 3-rd edition"*, CIE 15.3: (2007)

[91]   Philips-Invernizzi, B., Dupont, D., Cazé, C., *Bibliographical review for reflectance of diffusing media*, Optical Engineering, 40(6):1082–1092, (2001)

[92]   Grum, F.C., Bartleson, C. J., Optical Radiation Measurements: Color Measurement, Academic Press, (1980)

[93]   Chandrasekhar, S., Radiative Transfer, Dover, New York, (1960)

[94]   Mudgett, P.S., Richards, L.W., *Multiple Scattering Calculations for Technology*, Journal of Applied Optics, 10(7):1485-1502, (1971)

[95]   Schuster, A., *Radiation through a Foggy Atmosphere*, Astrophysics Journal, 21(1), (1905)

[96]   Kubelka, P., Munk, F., *Ein Beitrag zur Optik der Farbanstriche*, Zeits. F. techn. Physik, (12):593-601, (1931)

[97]   Judd, D.B., Wyszecki, G., Color in Bussiness, Science, and Industry, Third edition, John Wiley and Sons, New York, (1975)

[98]   Green,P., MacDonald,L., Colour Enginering, John Wiley and Sons, (2002)

[99]   Kubelka, B., *New Contributions to the Optics of Intensely Light-Scattering Materials. Part I*, J.Opt.Soc.Am. 38, 448-457, (1948)

[100]   Kubelka, B., *New Contributions to the Optics of Intensely Light-Scattering Materials. Part II*, J.Opt.Soc.Am. 44, 330-335, (1954)

[101]   McDonald, R., Colour Physics for Industry, Second edition, SDC Bradford, (1997)

[102]   Volz, H.G., Industrial Color Testing: Fundamentals and Techniques, Wiley-VCH (2002)

[103]   Randall, D. L.: COLOR TECHNOLOGY in the textile industry, Second Edition, AATCC, (1997)

[104]   Johnston, S.F., A History of Light and Colour Measurement, IOP Publishing Ltd, (2001)

[105]   Billmeyer, F.W. Jr., Hemmendinger, H., *Instrumentation for Color Measurement and its Performance*, Golden Jubilee of Colour in the CIE, Proceedings of a Symposium held by The Colour Group (Great Britain) at Imperial College, London, England on 28 and 29 September 1981

[106]   Nassau, K., Color for Science, Art and Technology, Elsevier, (1998)

[107]   Williams, T.P., *Photoreversal of Rhodopsin Bleaching,* J. Gen. Physiol. Vol. 47, 679-689, (1964)

[108]   Rullière, C., Amand, T. and Marie, X., Spectroscopic Methods for analyse of sample dynamics (Femtosecond Laser Pulses), ed. Springer-Verlag, Berlin. 203-259, (1998)

[109]   Ern, J., Petermann, M., Mrozek, T., Daub, J., Kuldov, K., Kryschi, C., *Dihydroazulene/vinylheptafulvene photochromism: dynamics of the photochemical ring-opening reaction,* Chemical Physics 259, 331-337, (2000)

[110]   Hogue, R., *'Praying Mantis' diffuse reflectance accessory for UV-Vis-NIR spectroscopy*, Fresenius J. Anal. Chem. 339, 68-69, (1991)

[111]   Boroumand, F., Moser, J.E., van den Bergh, H.: *Quantitative diffuse reflectance and transmittance infrared spectroscopy of non-diluted powders*, Appl. Spectroscopy 46, 12, 1874-1886, (1992)

[112]   Polymicro Technologies, available from: http://www.polymicro.com/products/

opticalfibers/products_opticalfibers_sr_uvmi_uvm_uvi.htm

[113] Vik, M., Viková, M., *Equipment for monitoring of dynamism of irradiation and decay phase photochromic substances* (in Czech) Czech Patent no.: PV 2007- 858 PS3546CZ

[114] Viková, M., *Selected problems of measurement of photochromic colorants*, Book of papers AIC Colour 05 - 10th Congress of the International Colour Association, Granada, p.1135-1138, 2005

[115] Viková, M., Vik, M., Accurate measurement photochromic materials, 6th International Conference - TEXSCI 2007, June 5-7, Liberec, 2007

[116] Van Gemert, B.; Kish, D.G., *The Intricacies of Color Matching Organic Photochromic Dyes*, PPG informations, Vol. 5, No. 14, 53-61, (1999)

[117] Kamata, M., Suno, H., Maeda, T., Hosikawa, R., *Reversible variable color patterning composition for synthetic resin articles*, US Patent 5431697

[118] Somani, P.R., editor, Chromic Materials, Phenomena and their Technological Applications, Applied Science Innovations, New Delhi 2010, in chapter 13. Methodology of measurement of photochromic materials - Viková, M., p.137

[119] Klukowska, A., Posset, U., Schottner, G., Jankowska-Frydel, A., Malatesta, V., *Photochromic sol-gel derived hybrid polymer coatings: the influence of matrix properties on kinetics and photodegradation*, Materilas Science-Poland, 22, 3, 187- 199, (2004)

[120] Viková, M., Vik, M., *Measurement of photochromic textiles*, ISOP07, Vancouver, Canada 7-10 Oct., 2007

[121] ISO 105-B02 Textiles - Tests for colour fastness - Part B02: Colour fastness to artificial light: Xenon arc fading lamp test

[122] Bagdon, A.M., PPG Industries Inc. – photochromic pigments - technical notes, fax 22 November 2002

[123] Czech Colourist no 43, 4, 5-37 (in Czech), (1989)

[124] Viková, M., *UV sensible sensors based on textile fibres*, International Lighting and Colour conference, Cape Town, 2-5 November 2003, book of papers 47-53, 2003

[125] Viková, M., *Intelligent textiles – UV sensors*, XXII. Course in lighting technique (in Czech), Dlouhé Stráně 23.-24. September, s.70-74, 2003

[126] Ortyl, E., Kucharski, S., *Kinetics of refractive index changes in polymeric photochromic films*, Macromol.Symp. 2004, 212, 321-326

[127] Viková,M., *Contribution to development of textile based sensors – UV sensor*, 7th Asian textile konference, New Delhi- India, Dec.1st – 3rd 2003

[128] Becker, R. S., Michl, J., *The photochromic properties of 3H-naphthopyrans (2H-benzochromenes)*, J. Am. Chem. Soc., 88, 5931–5933, (1966)

[129] Lenoble, C., Becker, R. S., *Photophysics, photochemistry and kinetics of photochromic 2H-pyrans and chromenes*, J. Photochem., 33, 187–197, (1986)

[130] Kolc, J., Becker, R. S., *The spectroscopy and photochemistry of naturally occurring and synthetic chromenes*, Photochem. Photobiol., 12, 383–393, (1970)

[131] Kolc, J., Becker, R. S., *Proofs of structure of the colored photoproducts of chromenes and spiropyrans*, J. Phys. Chem., 71, 4045–4047, (1967)

[132] Lukjanow, B. S., Knjazschanski, M. I. , Rewinski, J. W., Niworozschkin, L. E., Minkin, W. I., *Photo- und Thermochrome Spirane, III. Die Photochromie von Selenochromene*, Tetrahedron Lett., 22, 2007–2010, (1973)

[133] Becker, R. S., Dolan, E., Balke, D. E., *Vibronic effects in photochemistry. Competition between internal conversion and photochemistry*, J. Chem. Phys., 50, 239–245, (1969)

[134] Favaro, G., Romani, A., Becker, R.S., *Competition between vibrational relaxation and photochemistry: relevance of vibronic quantum effects*, Photochem. Photobiol., 74, 378–384, (2001)

[135] Becker, R. S., Pelliccioli, A. P., Romani, A., Favaro, G., *Vibronic quantum effects in fluorescence and photochemistry. Competition between vibrational relaxation and photochemistry and consequences on photochemical control*, J. Am. Chem. Soc., 121, 2104–2109, (1999)

[136] Favaro, G., Mazzucato, U., Ottavi, G., Becker, R. S., *Kinetic analysis of the photochromic behaviour of a naturally occurring chromene (lapachenole) under steady irradiation*, Mol. Cryst. Liq. Cryst., 298, 137–144, (1997)

[137] Ottavi, G., Favaro, G., Malatesta, V., *Spectrokinetic study of 2,2-diphenyl-5,6-benzo(2H)chromene: a thermoreversible and photoreversible photochromic system*, J. Photochem. Photobiol., A, 115, 123–128, (1998)

[138] Favaro, G., Romani, A., Becker, R. S., *Photochromic behavior of 2,2-spiro-adamantylidene-2H-naphtho[1,2-b]pyran: a new thermoreversible and photoreversible photochromic system*, Photochem. Photobiol., 72, 632–638, (2000)

[139] Prysztejn, H. E., Negri, R.M., *An Experiment on Photochromism and Kinetics for the Undergraduate Laboratory*, J. Chem. Ed. 78, 5, 645-648, (2001)

[140] Misra, G. P., Lavabre,D., Micheau, J.C., *Mechanistic Investigations Ans Spectrokinetic Parameter Determination During Thermoreversible Photochromism With Degradation : Example Of Application To The Triphenylimidazolyl Dimer (Tpid) System*, J. Photochem. Photobiol. A. : Chem. 80, 251-256, (1994)

[141] Crano, J.C.; Flood, T.; Knowles, D., Kumar, A.; van Gemert, B., *Photochromic compounds: Chemistry and application in ophthalmic lenses*, Pure and Appl. Chem., Vol. 68, No. 7; p. 1395-1398, (1996)

[142] Klukowska, A., Posset, U., Schottner, G., Frydel-Jankowska, A.,Malatesta,V., *Photochromic sol-gel derived hybrid polymer coatings: the influence of matrix properties on kinetics and photodegradation*, Materials Science Poland 22, p. 187-199, (2004)

[143] Zayat, M., Levy, D., *Photochromic naphthopyrans in sol–gel ormosil coatings*, J. Mater. Chem. Vol. 13, p. 727-730, (2003)

[144] Van Gemert, B., Knowles, D., *Photochromism of Diarylnaphthopyrans*, PPG informations, Vol. 1, No. 1; p. 11-17, (1995)

List of symbols

Symbol	Name	Units
ΔE^*	Color difference in CIEL*a*b* colour space	-
L^*	Lightness	-
a^*	red –green axes	-
b^*	yellow – blue axes	-
C^*	Chroma	-
H	Hue	degree
$\bar{x}$, $\bar{y}$, $\bar{z}$	CIE standard observer functions	-
K/S	Kubelka-Munk function	-
R	Reflectance	
I	Shade intensity	-
I_0	Shade intensity in time t_0	-
$I\infty$	Shade intensity in infinite time	-
λ	Wavelength	nm
λ_{max}	Dominant wavelength	nm
ε_{max}	Molar absorption coefficient in λ_{max}	$1\ mol^{-1}.cm^{-1}$
T	Time of excitation, relaxation	min
$t_{1/2(O,R)}$	Half time of excitation or relaxation of colour change	min
K	Rate constant	
Z_{20}	No. cycles after which absorption maxima	-

	is at a 20% level of the initial value	
IOD	Initial optical density v λ_{max}	-
IODF$_{10}$	Optical density 10 sec. after end of influence of UV radiation	-
Oy	Optical yield of photochromic reaction	-
F$_e$	Radiation density	$W.m^{-2}$
H$_e$	Exposure dose	$J.m^{-2}$
Φ	Luminous flux	Lm
Q$_e$	Radiant energy	J
Φ$_e$	Radiant flux	W
E	Intensity of illumination	Lx
UV	Ultraviolet radiation (100 – 380 nm)	
VIS	Visual part of electromagnetic spectrum (380 – 760 nm)	
NIR	Near infrared radiation (760 – 2500 nm)	
PPT-P1 (P2,P3,P4,P5)	Textiles with printing of pigment P1 (P2,P3,P4,P5)	
NW- P1(P2,P3,P4,P5) NW-S1	Non woven textile coloured by mass dyeing - pigment P1 (P2,P3,P4,P5,S1)	
PPS- P1(P2,P3,P4,P5)	Solution of photochromic pigment P1(P2,P3,P4,P5)	
SEM	Scanning electron microscopy	
OM	Optical microscopy	

Appendix A:

Selected measurement and their comparison with other authors

Overall Change of Absorbance after 30 sec, Change of Absorbance, half life of colour change and dominant wavelength of tested photochromic compounds

Tab. 1
Selected parameters of 3,3,5,6-tetramethyl-1-propylspiro[indoline-2,3'[3H]pyrido[3,2-f][1,4]benzoxazine]

SOURCE	SOLVENT	ΔA 30s	ΔA	$t_{1/2}$ [s]	λ_{max} [nm]
Crano &all [141]	ADC	-	0,16	8	613
Viková	Cyclohexane	0,018	0,022	6	592
Viková*	PP	-	-	-	-
Viková*	Acrylic film	0,33	0,40	13	615

* reflectance data, ADC - allyl diglycol carbonate

Tab. 2
Selected parameters of 1,3,3,5,6-pentamethyl(indoline-2,3'-[3H] naphtho [2,1-b] [1,4] oxazine])

SOURCE	SOLVENT	ΔA 30s	ΔA	$t_{1/2}$ [s]	λ_{max} [nm]
Klukowska &all [142]	Hexane	0,92	0,97	4	560
Klukowska &all	Ethanol	0,88	1,11	12	610
Viková	Cyclohexane	0,008	0,011	7	575
Viková*	PP	-	-	-	-
Viková*	Acrylic film	0,038	0,054	5	623

* reflectance data, PP – polypropylene

Tab. 3
Selected parameters of methyl 2,2,6-tris(4-methoxyphenyl)-9-methoxy-2*H*-naphtho-[1,2-*b*]pyran-5-carb-oxylate

SOURCE	SOLVENT	ΔA 30s	ΔA	$t_{1/2}$ [s]	λ_{max} [nm]
Zayat & Levy [143]	Ethanol	-	-	-	533
Zayat & Levy	Tetrahydrofuran	-	-	-	529
Zayat & Levy	Sol-Gel ormosil	0.11	0.47	27	552
Viková	Cyclohexane	0,20	0,25	19	518
Viková*	PP	0,04	0,11	42	525
Viková*	Acrylic film	0,17	0,25	33	521

* reflectance data, PP – polypropylene

Tab. 4
Selected parameters of methyl 2,2-bis(4-methoxyphenyl)-6-acetoxy-2H-naphtho-[1,2-b]pyran-5-carb-oxylate

SOURCE	SOLVENT	ΔA 30s	ΔA	$t_{1/2}$ [s]	λ_{max} [nm]
Zayat & Levy	Ethanol	-	-	-	502
Zayat & Levy	Tetrahydrofuran	-	-	-	495
Zayat & Levy	Sol-Gel ormosil	0,25	0,32	23	505
Viková	Cyclohexane	0,09	0,23	376	483
Viková*	PP	0,05	0,13	151	497

Tab. 5
Selected parameters of 3,3-diphenyl-3*H*-naphtho[2,1-*b*]pyran

SOURCE	SOLVENT	ΔA 30s	ΔA	$t_{1/2}$ [s]	λ_{max} [nm]
Coelho [39]	Toluene	-	0,27	11,5	432
Gemert , Knowles [144]	ADC	0.21	0.36	45	432
Viková	Cyclohexane	0.069	0.12	81	430
Viková*	PP	0.086	0.16	72	440
Viková*	Acrylic film	0.29	0.36	12	440

Table 6 Summary of selected properties of photochromic pigments used

	P1	P2	P3	P4	P5
Melting Pt	125-130°C	164-165°C	202-203°C	143-145°C	160-165°C
Colour	Blue	Wine purple	Red	Blue	Yellow
Assay	>95%	>98%	>98%	>98%	>97%
Appearance	Light tan powder	Off-white powder	Light tan powder	Light tan powder	White to pale yellow crystal

Appendix B:

Author`s publications relating to the thesis

/1/ Viková, M., Vik, M.: Some Problems in Measurement of UV Protective Textiles, The 3rd China International Wool Textile Conference, Xi'AN China 26-28 Sep. 2002, p.635-638, ISBN 7-5064-2373-1

/2/ Viková, M., Slabotinský, J., Musilová, M., Vik, M. Možnosti měření bariérových vlastností ochranných textilií, II. Odborný seminář „Ochranné oděvy" Prostějov, 23. 10. 2002

/3/ Viková, M., Slabotinský, J., Vik, M., Musilová, M.: Possibility of colorimetric identification of dangerous gas penetration through protective clothes, TEXSCI 03, 16.- 18. 6. 2003, Liberec, Czech Republic, ISBN 80-7083-711-X

/4/ Viková,M.: Colorimetric identification of dangerous gas penetration through protective clothes via inteligent underwear,83rd World Konference(83rd TIWC), May 23-27, 2004,Shanghai,China, p.772-774 ISBN 1870372611

/5/ Viková, M., Vik, M. : Smart textile based senzors, SUMMER SCHOOL Intelligent Textile Structures - Application, Production and Testing, Center of Excellence ITSAPT, Liberec Czech Republic, June 9 th -13 th 2003

/6/ Viková, M.: Textile photochromic sensors for protective textile, TEXSCI 03, 16.- 18. 6. 2003, Liberec, Czech Republic, 6p. on CD ROM, ISBN 80-7083-711-X

/7/ Viková, M., Vlákna a textil 10 (2), 82-85 (2003) ISSN 1335-0617

/8/ Viková, M., UV sensible sensors based on textile fibres, International Lighting and Colour conference, Cape Town 2-5 November 2003, South Africa,book of papers 47-53

/9/ Viková, M. : Inteligentní textilie - senzory UV záření, XXII. Kurs osvětlovací techniky, Dlouhé Stráně 23.-24. Září, s.70-74, ISBN 80-248 0446-8

/10/ Viková,M.: Contribution to development of textile based senzors – UV senzore, 7th Asian textile konference, New Delhi, India, Dec.1st – 3rd 2003, 6p. on CD ROM

/11/ Viková,M.: Možnosti využití pigmentů a barviv pro textilní senzory. Seminář: Textilie v novém tisíciletí I. 24. 4. 2003 Výzkumné centrum textil, Technická Universita v Liberci ISBN 55-022-03

/12/ Viková,M.: UV sensible sensors based on textile fibres. Seminář: Textilie v novém tisíciletí II. 15.4 2004 Výzkumné centrum textil, Technická Universita v Liberci ISBN 55-022-03

/13/ Viková, M., Vik,M.: Colour shift photochromic pigments in colour space CIE L*a*b*, ISOP04, Arcachon 12.-15. 9. 2004, France

/14/ Viková, M., Vik, M. : Textile sensors based on color differences, 1 st Czech-German Textile Workshop on Performance and Smart Fabrics, September 20th and 21th 2004, Dresden Germany

/15/ Viková, M. : Visual Assessment UV Radiation by Colour Changeable Textile Sensors, AIC 2004, Color and Paints, the Interim Meeting of the International Color Association, Porto Alegre 1-5. November 2004, Brasil

/16/ Viková, M.: Visual assesment UV radiation by colour changeable textile sensors, 2nd International Conference of Textile Research Division NRC, Cairo, Egypt, April 11-13, 2005

/17/ Viková, M.: SMART Textile Based Senzore - Theory and their Application, Textile Processing: State of the Art & Future Developments, 2 (7) (2005) 507 – 511,

/18/ Viková, M. : Selected problems of measurement of photochromic colorants, Book of papers AIC Colour 05 - 10th Congress of the International Colour Association, Granada, p.1135-1138, 2005

/19/ Viková, M., Vik, M.: Colour shift photochromic pigments in colour space CIE L*a*b*, Molecular Crystals and Liquid Crystals 431(2005), 103-116 [403-417]

/20/ Viková, M.: Colour change kinetic behavior of photochromic SMART textile sensors, 4th Central European Conference 2005, 7-9 September 2005, Liberec, Czech Republic

/21/ Viková, M., Vlach, P.*, Vik, M.: Textile based sensors – identification of dangerous gases penetration, 4th Central European Conference 2005, 7-9 September 2005, Liberec, Czech Republic

/22/ Viková, M.: Photochromic pigments for SMART Textiles, ITSAPT project seminar, Guimares 16. 11. 2005, Portugal

/23/ Viková, M, Vik, M.: Smart textile senzors for indication of UV radiation, AUTEX 2006 World Textile Conference, 11-14 June Raleigh, USA

/24/ Vik, M., Viková, M.: Colorimetry of Color Changeable Materials, Micro-symposium on Colour Research and Application, 8. September Kyoto, Japan

/25/ Viková, M., Vik, M.: Measurement of photochromic materials, BOLcolor 2006 - II CONGRESO BOLIVIANO DEL COLOR - 25 al 27 de septiembre de 2006 La Paz, Bolivia

/26/ Vik, M., Viková, M.: Spektrofotometrická měření v osvětlovací laboratoři, Kurz osvětlovací techniky XXV, 16. -18. 10. 2006, Hotel Dlouhé Stráně, Kouty n. Desnou

/27/ Viková, M., Vik, M.: Accurate measurement photochromic materials, 6th International Conference - TEXSCI 2007, June 5-7, Liberec

/28/ Viková, M., Vik, M.: Measurement of photochromic textiles, ISOP07, 7-10 October 2007, Vancouver, Canada

/29/ Vik, M., Viková, M.: Colorimetric Characterisation of color changeable materials, 6th BAM-DIN-Workshop on Image Technology, 3. December,Berlin 2007

/30/ Viková, M. : Colour of changeable materials, invited paper on TU Granada – Scientific Seminary, 6th February,2008

/31/ Viková, M. : Chameleonic textiles, Colour Emotion Research and Aplication, National Yunlin University of Science and Technology, Taiwan, 22-24th July 2008

/32/ Viková, M., Vik, M. : Accurate measurement of photochromic materials, Colour Emotion Research and Aplication, National Yunlin University of Science and Technology, Taiwan, 22-24th July 2008

/33/ Viková, M.: Colorimetric Measurement of Photochromic Materials, 11th Congress of the International Colour Association 2009, Sydney 27. 9-2.10. 2009, Australia

Appendix C:

Selected author's articles

COLOUR SHIFT PHOTOCHROMIC PIGMENTS IN COLOUR SPACE CIE L*a*b*

Martina Viková and Michal Vik

LCAM – Department of Textile Materials, Technical University of Liberec, Hálkova 6, CZ-461 17 Liberec, Czech Republic, martina.vikova@vslib.cz

One of possibilities for protection of human body against acute and cumulative exposure to ultraviolet is the wearing of special protective clothes. Nevertheless on the other side the protective clothes have not the same barrier features against the UV light.

The aim of present research work in LCAM on the Technical University of Liberec is research and development of original method of measurement by flexible textile based sensors reacting on the UVA part of electromagnetic radiation. In this article is publicized information about testing above mentioned sensors with weave structure and non-woven textiles. Results show that produced sensors shows sensitivity as to time of exposition so also to intensity of irradiation and their response characteristics is same as for classical luxmeters.

Key words: Sensor, photochromism, colour space, colour hysteresion area, intensity of illumination

INTRODUCTION

In present time become worse living conditions, increase harmful pollutants in environment, which can irreversible damage our health, and jeopardize full quality our life. Big attention is given in research area respectively in development and perfection of protective clothes specially their barrier features. Protective barriers we understand how the clothes or textiles protect wearer against above mentioned dangerous conditions and if the protection is only partial or the protection is time limited by ambient conditions. Most of protective clothes are not developed for long time wearing. During development of these barrier structures we have to keep in our mind full comfort of acting persons without limitation. Some of protective clothes are equipped by electronics, respectively other sensors or devices, which monitoring and quantify dangerous substances in environment. In present time is big attention given to miniaturization of electronics and also flexibility their connection with computing units [1].

Above mentioned describe concept of protective clothes we call as intelligent structure. Disadvantage of this intelligent structure is no adequate response on the external stimulus, there is only monitoring of external dangerous conditions. This structure we call as passive intelligent textile structure.

Sensors and textile structures, which react adequate response and they are able modulate protective degree in accordance on the external stimulus (change of intensity UV, temperature, press, electrical field etc.) is called as SMART textile. As example of passive intelligent textiles are optical fibres, which leading the not only signal, but they are also sensitive on the deformation, concentration of substances, press, electric power etc. As example of active intelligent textiles could be textiles which react by change own colour in dependence on external stimulus (light, temperature) and called as a chameleonic textiles or heat containing textiles, which are able to store or slack energy according external temperature. Moreover textile based sensors and active protective textiles has advantages that textile structure is easy customizable by sewing, thermal bonding or gluing. Also there are advantages of easy maintaining (washing, chemical drying) and low specific weight with good strength, tensibility and elasticity. Good features are also workability without change of technology of production and extremely large specific surface. Big advantages are possible integration these types of sensors into system of protective clothes and also their price availability. From these reason is this article directed to research of textile-based sensors with photo chromic behaviour, respectively to study of dynamic behaviour and modulation of sensitivity photo chromic sensors.

In this work is described new definition of colour reversible hysteresis, which is described by hysteresis of colour change curve. This colour hysteresis curve is described by kinetic model, which defines the speed of colour change initiated by external stimulus – UV light. Kinetic model verification is done for textile sensors with photo chromic pigment applied by textile printing, fibre mass dyeing.

MATERIALS AND USED METHODS

Our experiment was divided to 3 parts and every part is directed to special form of application of photochromic pigments and study of photochromic behaviour from point of kinetics and dynamics in different mediums:

a) Application of photochromic pigments by textile printing - **PTP**
b) Application of photochromic pigments by mass dyeing - **NWT**
c) Study of photochromic pigments behaviour in solution - **PPS**

In our research we follow the develop simple textile based sensor sensitive to UV light and kinetic study of behaviour and main attention was given to possibility use the technology of textile printing by stencil printing. This experiment was completed the study of influence of UV absorbers and ability of properties modulation of sensors. Also was studied dependence of Colour change intensity on concentration of photochromic pigment. Above mentioned studies was necessary complete by study of fatigue resistance in dependence on Intensity of source and time of exposition including also classic tests of light fastness on Xenon test and dry staining fastness, which are the same as for normal classic pigment use in textile finishing and these tests are also limitation of application offered sensors.

In second part of our experiment was studied change of photochromic behaviour tested pigments in non-woven textiles produced by technology Melt Blown (mass dyeing) and in third part was checked the photochromic behaviour used pigments in solution via measurement of transmission characteristics as completive study how is changed the photochromic response via kind application. For experiment was used commercial photochromic pigments PPG-Photosol 33672 (P1), PPG-Photosol 7106 (P2), PPG-Photosol 749 (P3), PPG-Photosol 0265 (P4) and PPG-Photosol 5-3 (P5). Chemical structure illustration is shown on FIG. 1 and FIG. 2 [2].

| **FIGURE 1** - P1 structure | **FIGURE 2** - P3 structure |
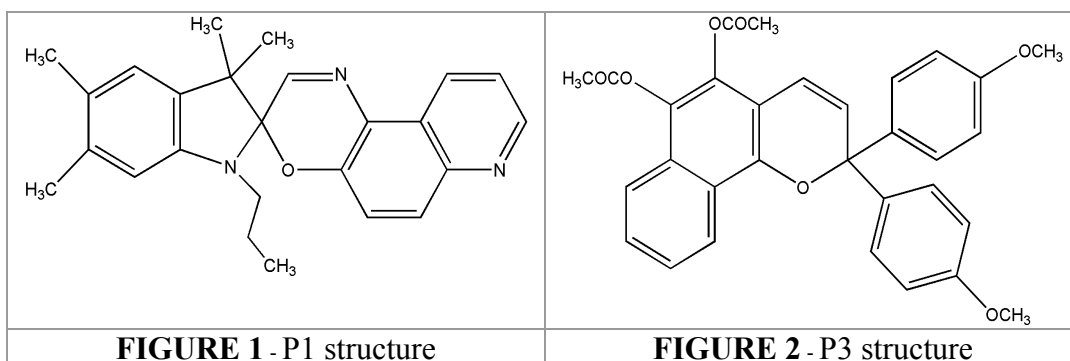
As was mentioned in our experiments were prepared two kinds of solid media – textile substrate with photochromic pigments. Illustrations of fixation of photochromic pigments on the textile substrates are shown on FIG. 3-6:
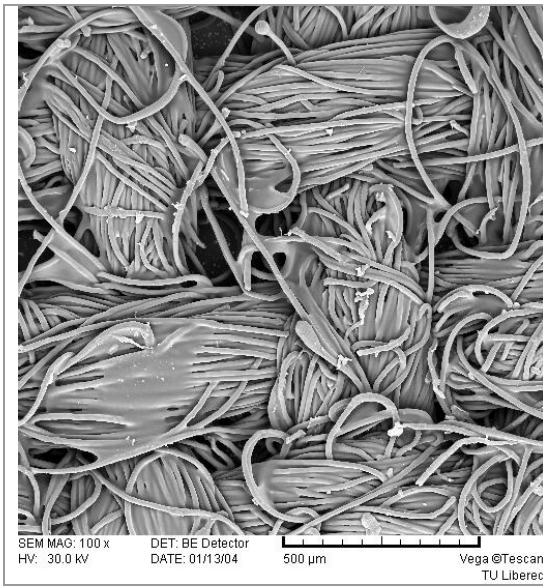
| FIGURE 3 – P1 print on PET | FIGURE 4 - P3 print on PET |

| FIGURE 5 – NWT without pigment | FIGURE 6 – NWT with P3 |
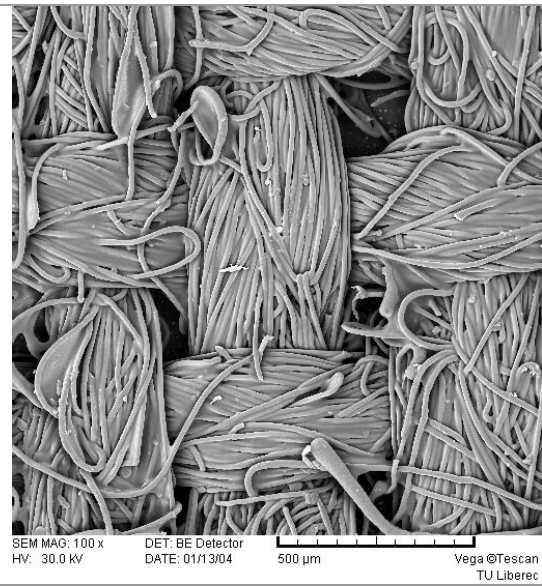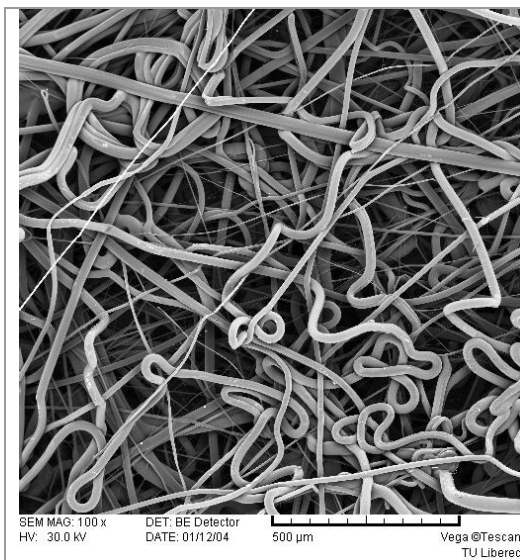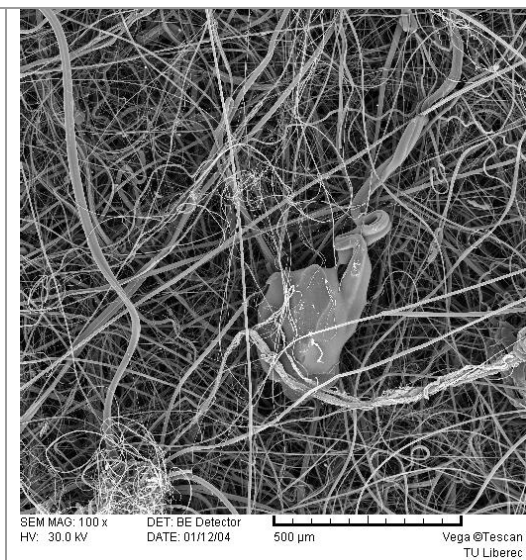
For measurement of colour response of tested photochromic media were used following spectrophotometers:

- Spectraflash SF 300 X – viewing geometry D/8, aperture 20mm, SCI

- Modified Chroma Sensor CS-5 - viewing geometry T/8, aperture 30mm in modus SCI (FIG. 7)

- AVANTES S2000 – optical fibre spectrometer arranged on 0/45 viewing geometry (FIG. 8)
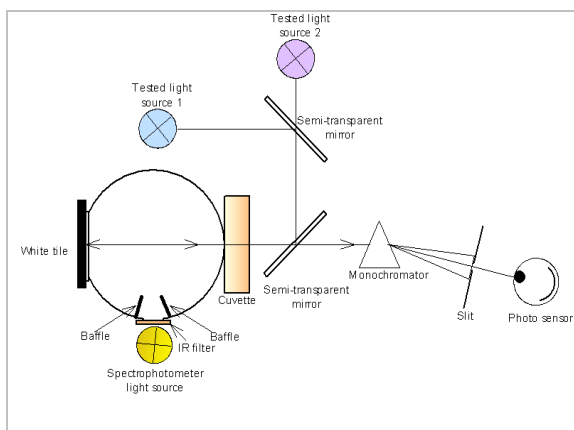
| **FIGURE 7** – CS-5 spectrophotometer modification | **FIGURE 8** – S2000 spectrometer arrangement |
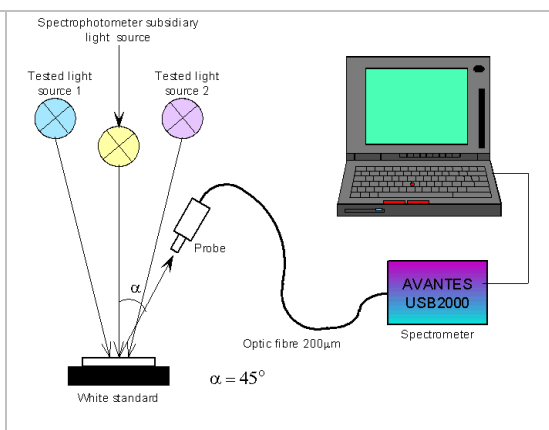
Besides measurements of prints and NWT via classical spectrophotometer Spectraflash 300UV was used arrangement of AVANTES S2000 spectrometer due to short time, continuous measurement respectively. S2000 arrangement make possible using different light sources for tested samples illumination, as is shown on the FIG. 8. Same possibility was obtained via modification of CS-5 spectrophotometer for measurement of photochromic solutions. Spectral power distribution curves of used light sources are shown on FIG. 9-10.
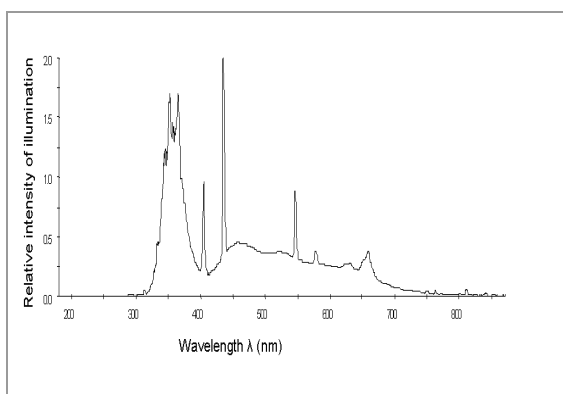
| **FIGURE 9** – Relative spectral power distribution of D65 simulator + UV tube (JUDGE II) | **FIGURE 10** – Relative spectral power distribution of tested light sources |
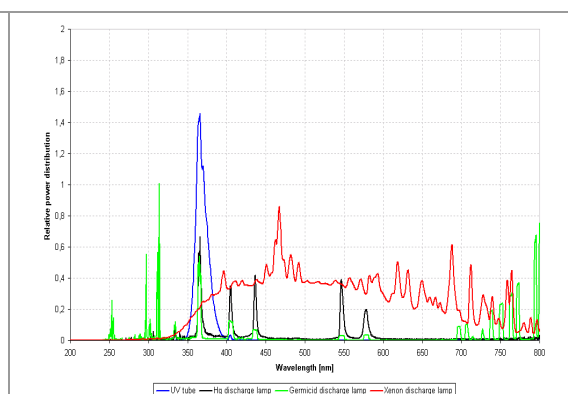
Because is relationships between remission and concentration of colorant agent non-linear, in colour measurement is obviously used relation between Kubelka-Munk function (**K/S**) and concentration, colour change intensity *I* respectively. Colour change intensity, *I* that we used, is defined as following equations:

$$\frac{K}{S} = \frac{(1 - \beta_\infty)^2}{2\beta_\infty} = f(\beta_\infty)$$

(1)

$$I = \int_{400}^{700} K/S_\lambda \, d\lambda$$

(2)

For description of kinetic behaviour of our UV sensors we used first class kinetic model as is shown in following equations [3]:

Exposition: $I = I_\infty + (I_0 - I_\infty).e^{(-kt)}$

(3)

Relaxation: $I = I_0 + (I_\infty - I_0).e^{(-kt)}$

(4)

From these equations is possible to calculate halftime of colour change $t_{1/2}$ [4] and colour hysteresis area Hp:

$$t_{1/2} = \frac{\ln 2}{k}.60 \quad,$$

(5)

$$H_P = \int I_\infty + (I_0 - I_\infty)e^{-kt} dt - \int I_0 + (I_\infty - I_0)e^{-kt} dt$$

(6)

As is from equation (6) evident that colour hysteresis area Hp arise by time reverse of reversion data as is shown on the FIG. 12.
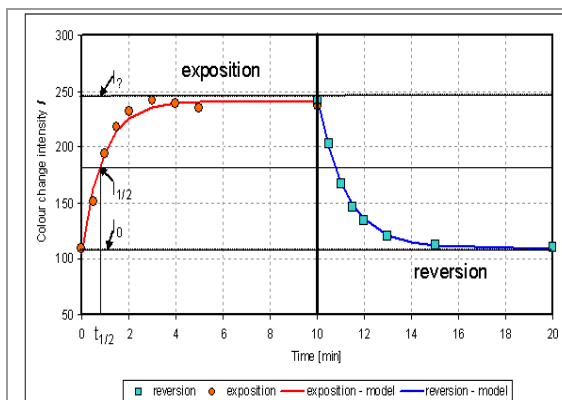
| FIGURE 11 – Typical growth and decay processes of colour change intensity for sample illumination of 714,6 µW.cm-2 power (979,3 lx) | FIGURE 12 – Colour hysteresis area Hp construction for sample at same condition as FIG. 11 |
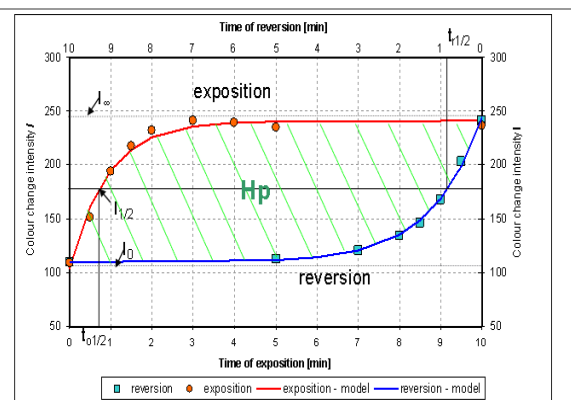
Data on both figures 11 and 12 were obtained for lowest intensity of illumination E (979,3 lx). On the FIG. 12, we can see, that already for this E in the colour change speed is higher during of exposition than reversion phase.

In our study we prepare new view on the relationship between intensity and time of exposition, time of relaxation respectively. Name of this new kind of graphs is colour hysteresis area Hp. When we will test relationship between halftime of colour change $t_{1/2}$ and intensity of illumination E, we obtain decreasing linear relation - FIG. 13. That means time of colour change is shorter during intensity of illumination increasing.
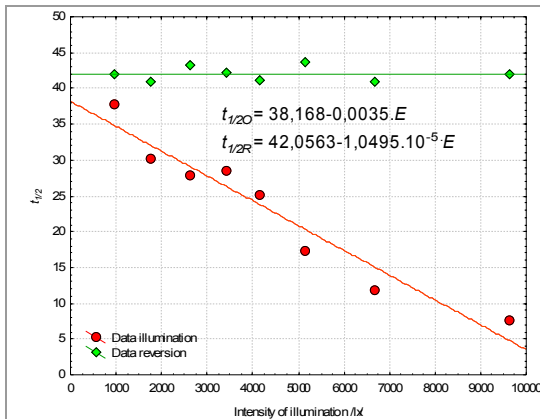
FIGURE 13 – Halftime of colour change $t_{1/2}$ relation on intensity of illumination	**FIGURE 14** – Colour hysteresis area Hp relation on intensity of illumination
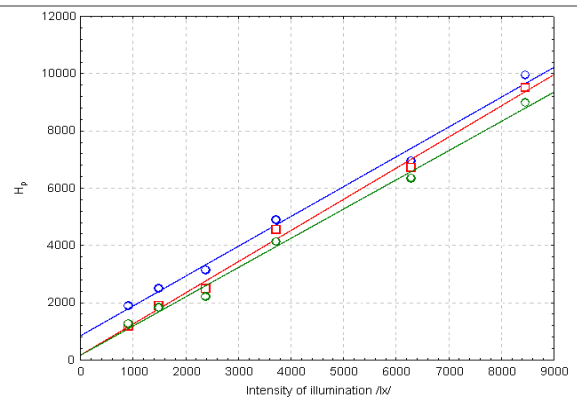
Linear relation we obtain also via dependency of hysteresis area on intensity of illumination E. On the FIG. 14, is shown dependences hysteresis area relation to UV absorber dose also. It is evident, that increasing of UV absorber dose gives decreasing of Hp.

As was mentioned before used measuring units were prepared for measuring colour change of tested samples under different light sources. On FIG. 15 and FIG. 16 are shown results for photochromic pigments solutions **PPS** and prints **PTP**.
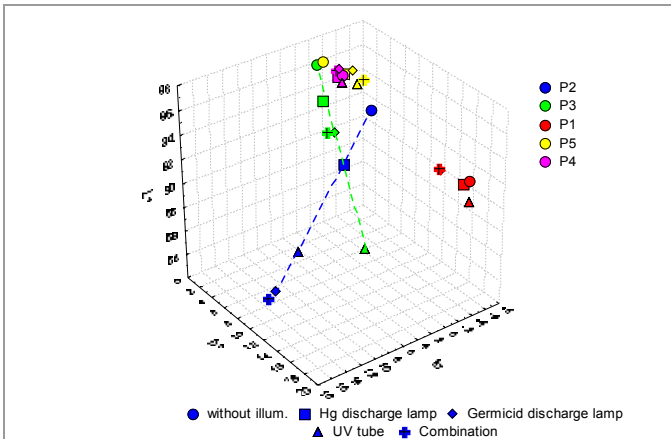
FIGURE 15 – Change of **PPS** colour position dependent on different light source
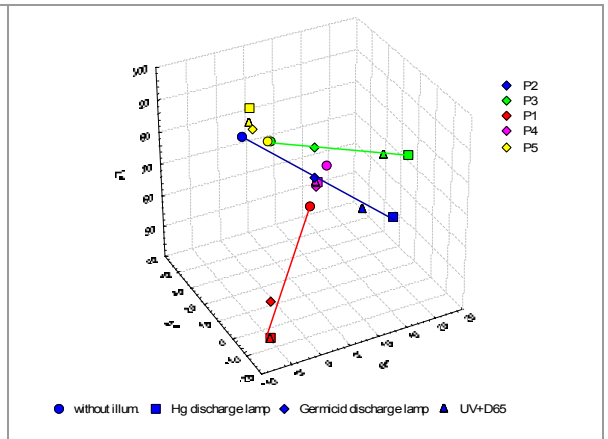
FIGURE 16 – Change of **PTP** colour position dependent on different light source

On FIG. 17 and FIG. 18 are shown results for colour shift of photochromic pigments solutions **PPS** and prints **PTP** in chromatic plane of CIELAB colour space. From these results is evident, that used media has control influence on colour shift in colour space and hysteresis trajectory is little bit complicated. At the same time we can see, that relaxation after same time and intensity illumination for samples with comparable concentration is distinctively slower for photochromic solution than for photochromic prints.
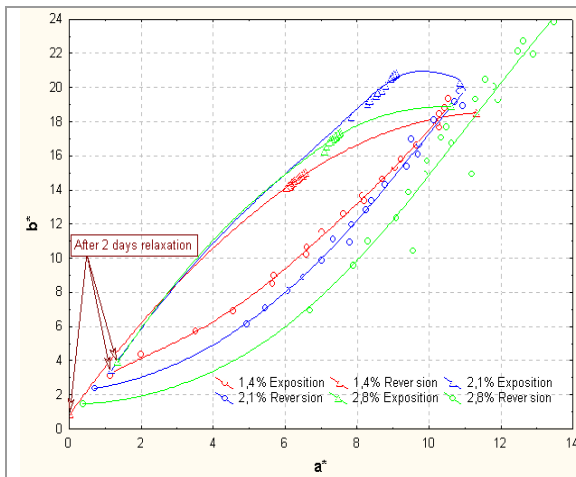
FIGURE 17 – Colour shift of **PPS** in chromatic plane of CIELAB colour space
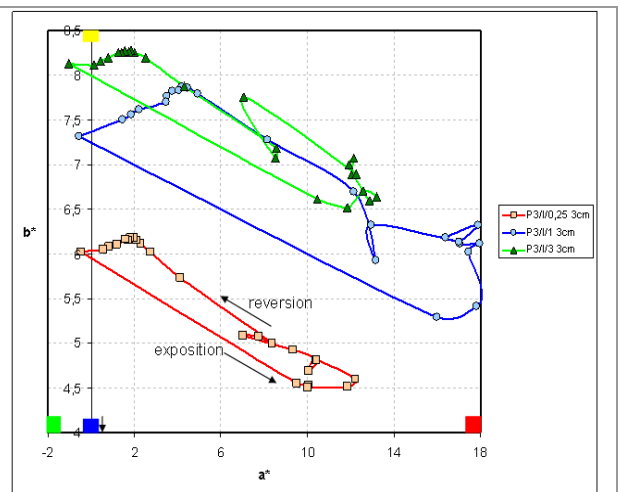
FIGURE 18 – Colour shift of **PTP** in chromatic plane of CIELAB colour space

CONCLUSION

This paper is introducing study of dynamic properties of photo chromic textile sensors. In our study we prepare new view on the relationship between intensity and time of exposition, time of relaxation respectively. That means colour hysteresis area *Hp* is linear related to the intensity of illumination *E*. Via this relation we demonstrate the possibility of flexible textile-based sensors construction in area identification of radiation intensity. Beside of this one, we demonstrate differences between photochromic pigments behaviour in solution and prints on textiles: differences in hysteresis trajectory, differences between spectral power distribution of light source sensitivity of this one's. Bi-exponential functions, which are used in *Hp* calculation, well described the kinetics of colour change intensity of photochromic pigments. They give good fits to the growth curves as well as to the relaxation one's.

REFERENCES

[1]   Tao, X.: *Smart fibres, fabric and clothing*, The Textile Institute: Cambridge England (2001)

[2]   Van Gemert, B.: *personal note*, 16. July 2004

[3]   Viková, M.:   *UV sensible sensors based on textile fibres*, International Lighting and Colour Conference, 02 to 05 November 2003, Cape Town, South Africa

[4]   Rais, J.: *Basic calculation in coloration technology* (in Czech), SNTL: Prague (1968)

SMART TEXTILE SENSORS FOR INDICATION OF UV RADIATION

M. Viková, M. Vik

ABSTRACT

Photochromism is a chemical process in which a compound undergoes a reversible change between two states having separate absorption spectra, i.e. different colours. The change of colour in one direction occurs under influence of electromagnetic radiation, usually UV light, and in the other direction by altering or removing the light source or alternatively by using thermal means. Based on photochromic pigment we developed simple textile sensor sensitive to UV light, which is usable for visual indication of intensity UV-A radiation. Main attention was given to possibility use the technology of textile printing by stencil printing. This experiment was completed the study of influence of UV absorbers and ability of properties modulation of sensors. Also was studied dependence of Colour Change Intensity (CCI) on concentration of photochromic pigment. Above mentioned studies was necessary complete by study of fatigue resistance in dependence on Intensity of source and time of exposition including also classic tests of light fastness on Xenon test and dry staining fastness, which are the same as for normal classic pigment use in textile finishing and these tests are also limitation of application offered sensors.
Also we document effectiveness of new original on-line measuring system, which was developed at Laboratory Colour and Appearance Measurement - LCAM.

1. INTRODUCTION

Sensors and textile structures, which react adequate response and they are able modulate protective degree in accordance on the external stimulus (change of intensity UV, temperature, press, electrical field etc.) is called as SMART textile. As example of passive intelligent textiles are optical fibers, which leading the not only signal, but they are also sensitive on the deformation, concentration of substances, press, electric power etc. As example of active intelligent textiles could be textiles which react by change own color in dependence on external stimulus (light, temperature) and called as a chameleonic textiles or heat containing textiles, which are able to store or slack energy according external temperature. Moreover textile based sensors and active protective textiles has advantages that textile structure is easy customizable by sewing, thermal bonding or gluing. Also there are advantages of easy maintaining (washing, chemical drying) and low specific weight with good strength, tensibility and elasticity. Good features are also workability without change of technology of production and extremely large specific surface. Big advantages are possible integration these types of sensors into system of protective clothes and also their price availability. From this reason is this article directed to research of textile-based sensors with photo chromic behaviour, respectively to study of dynamic behaviour and modulation of sensitivity photo chromic sensors. Photochromism is a chemical process in which a compound undergoes a reversible change between two states having separate absorption spectra, i.e. different colours. The change of colour

in one direction occurs under influence of electromagnetic radiation, usually UV light, and in the other direction by altering or removing the light source or alternatively by using thermal means [1].

In color science is color obviously measured by using spectrophotometers, because relationships between remission and concentration of colorant agent is non-linear, in color measurement is obviously used relation between Kubelka-Munk function (K/S) and concentration, color change intensity I respectively. Color change intensity I, that we used, is defined as following equations:

$$I = \int_{400}^{700} K/S_\lambda \, d\lambda \tag{1}$$

For description of kinetic behavior of our UV sensors we used first order kinetic model as is shown in following equations:

Exposition: $\quad CCI_{EXP} = I_0 + (I_\infty - I_0).e^{(-kt)}$ (2)

Relaxation: $\quad CCI_{REV} = I_\infty + (I_0 - I_\infty).e^{(-kt)}$ (3)

From these equations is possible to calculate halftime of color change $t_{1/2}$:

$$t_{1/2} = \frac{\ln 2}{k}.60 \tag{4}$$

2. EXPERIMENTAL PROCEDURES

2.1 Test Materials

In our research we follow the develop simple textile based sensor sensitive to UV light and kinetic study of behaviour and main attention was given to possibility use the technology of textile printing by stencil printing - **PTP**. For experiment were used five commercial photochromic pigments P1-P5. Chemical structure illustration is shown on FIG. 1 till FIG. 5 [2].
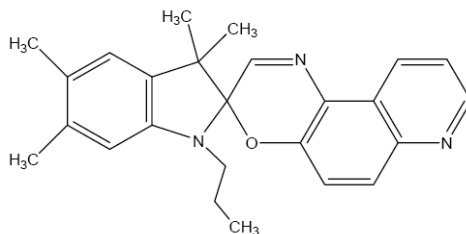
Fig.1 Structure of pigment P1
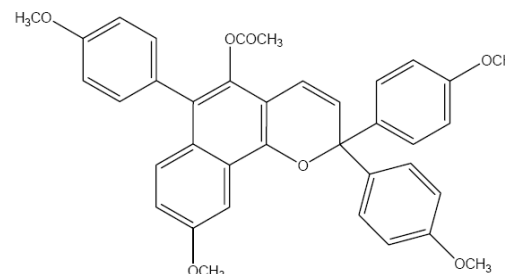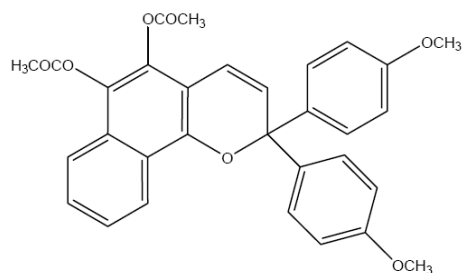

Fig.2 Structure of pigment P2
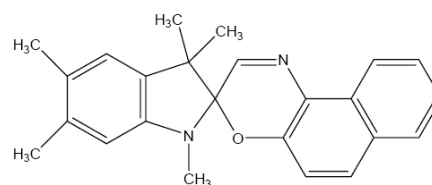
Fig.3 Structure of pigment P3
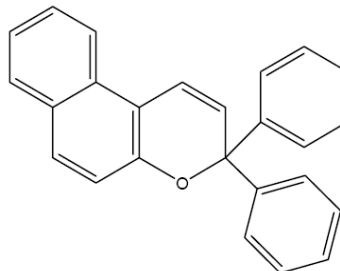

Fig.4 Structure of pigment P4

Fig.5 Structure of pigment P5

2.2 Instrumental Analysis of kinetic behaviour of photochromic materials

In our previous work, we have published some solutions of problems of photochromic textile sample measurement by classical spectrophotometer system [3]. FIG. 6 shows optical scheme of present commercial spectrophotometer and FIG. 7 shows our new experimental measuring system. Main problem with measurement of kinetic behaviour of photochromic pigments by classical spectrophotometer is relative long time period between individual measurements (cca 15s) and impossibility of measurement whole colour change during exposition without interruption of illumination of sample during measurement. That means classical commercial spectrophotometers enable off-line measurement of kinetic behaviour during exposition period and quasi on-line measurement during reversion period. Based on this problems is possible to obtain only during reversion – decay process valid data and growth process (exposition) is affected by high variation of data, as is shown on FIG. 8. Following this knowledge, we developed our original experimental system with short time scanning of colour change of photochromic samples during growth and decay period of colour change. Common period between individual measurements, which we now use is 1 s. Second difference between our experimental system and commercial system is in the usage continuous illumination by excitation and measuring light sources against discontinuous measuring light source – discharge lamp, which it is today used in commercial systems. Continuous controlled light source have smaller problems with light source drift. Third difference between classical system and our measuring system is in decomposition of time delay between excitation illumination and measurement during exposition period. Last main difference is utilization of excitation monochromator, which allow us to select variable bandwidth of wavelengths for excitation that means we use bispectral measuring configuration. In this study we have used seven excitation bands with maxima 400, 375, 350, 325, 300, 275 and 250nm (full width at half-maximum (FWHM) 50nm). Integral intensity of illumination was modified bellow average value 900 $\mu W.cm^{-2}$.
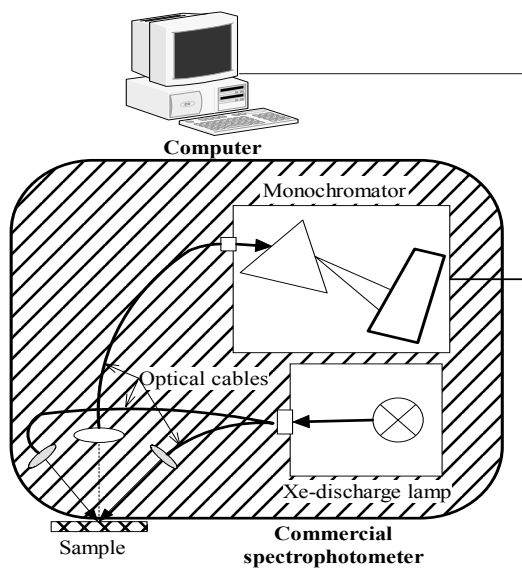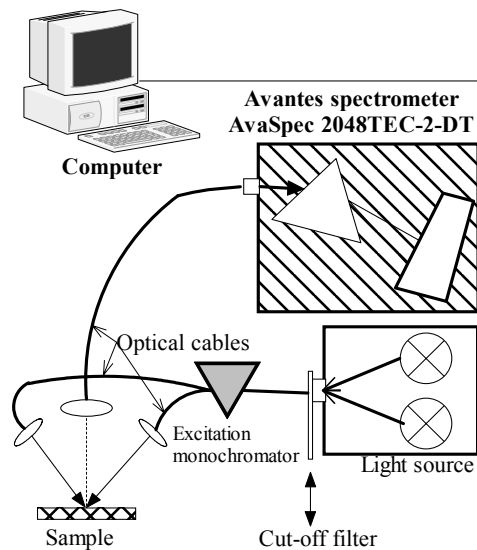
Fig.6 Off-line measurement scheme

Fig.7 On-line measurement scheme

3. RESULTS AND DISCUSSION

We describe in previous paragraph differences between commercial and our experimental measuring system. FIG. 8 shows our best results for pigment P1, which we obtain from commercial system when we used special conditions for minimizing of time delay between excitation illumination and measurement. Individual experimental points during exposition period – growth process of color change intensity we obtain via individual exposition of each point. You can see differences between experimental points and model of exposition. As we wrote, this graph document best results for adjusted commercial system, obviously was discrepancies between model and experimental points 3-5 times higher, except for time consumption of whole experiment and pure reproducibility (variation 23%-44%) - mainly in dynamic phase of kinetic curve.

On the other hand FIG. 9 show results from our experimental system for same condition of illumination intensity and pigment P1. It is evident that model fitting of experimental points is better than from commercial system, aside from shorter time consumption (20 min against 200 min). Differences between absolute levels of CCI (color change intensity) from each measuring system are occurring by differences between spectral ranges of used systems.
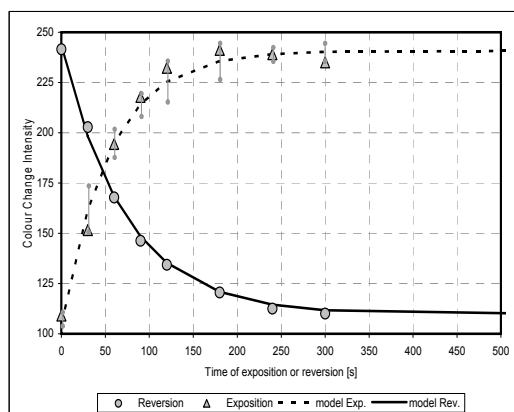

Fig.8 Off-line measurement of growth and decay processes of color change intensity for pigment P1, intensity of illumination = 714,6 µW.cm^{-2}
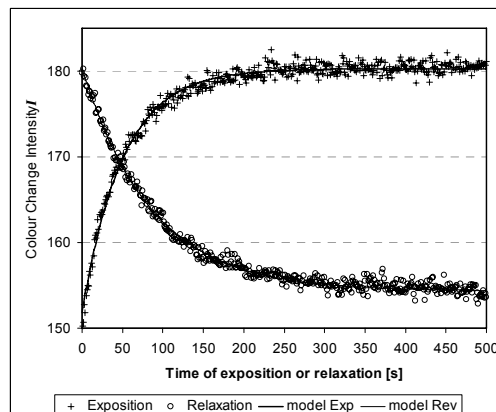

Fig.9 On-line measurement of growth and decay processes of color change intensity for pigment P1, intensity of illumination = 714,6 µW.cm^{-2}

Main reason, for which we made this experiment, is design of simple UV textile based sensor. Therefore, we need information about dependency of CCI on concentration and intensity of illumination E. Figures 10 and 11 describe us relationship between concentration and CCI over constant intensity of illumination E = 714,6 $\mu W.cm^{-2}$. When we will test relationship between halftime of color change $t_{1/2}$ and influence of pigment concentration, we obtain practically independent linear relation for exposition period of photochromic color change - FIG. 10. That means time of color change during growth process is not influenced by concentration increasing for tested pigments (constant level of $t_{1/2}$). We can see on FIG.11 that speed of color change during reversion phase is slightly dependent on pigment concentration, mainly for two pigments with slow speed of color change. It is possible to say that halftime of color change is for exposition period of CCI practically independent on concentration; on the other side for reversion period we can see decreasing of $t_{1/2}$ with increasing of concentration. We think that it is during fast recombination of chemical structure of photochromic pigment by high concentration (likewise light fastness of dyestuff).
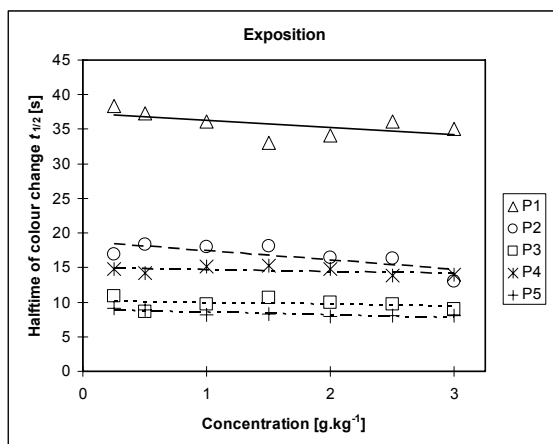

Fig.10 Dependence of Halftime of CCI on concentration of pigments, Intensity of illumination = 714,6 $\mu W.cm^{-2}$ - growth

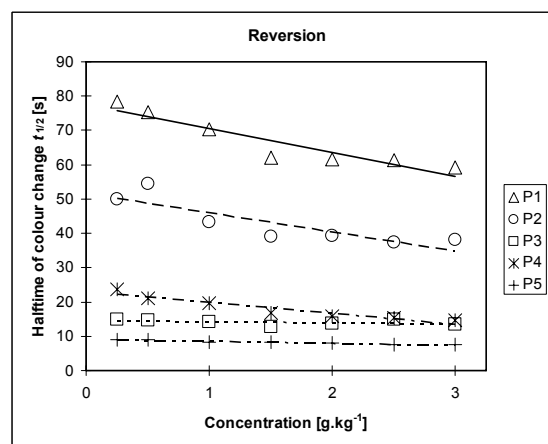Fig.11 Dependence of Halftime of CCI on concentration of pigments, Intensity of illumination = 714,6 $\mu W.cm^{-2}$ – decay

Is well known that ozone depletion in the earth's atmosphere has made the headlines on many occasions and most people would be aware of the significant problem exists. Sunburn, skin cancer, premature aging, and suppression of the immune system are some of the harmful effects of acute and cumulative exposure to ultraviolet radiation (UVR). A decrease of 1% in ozone would lead to increases in the solar UVR at the earth's surface and may eventually lead to a 2.3% increase in skin cancer. As was mentioned before, main aspect of simple textile sensor development is sensitivity of this one on amount of UV radiation, selected part of UV respectively. On the FIG. 12 is shown, that linear increasing of illumination intensity affect linear decreasing halftime of color change $t_{1/2}$, aside from that have higher illumination intensity also on CCI alone. That means higher illumination intensity is observed as deeper shade of sensor.

UV radiation includes wavelengths of 100-400 nm: UV-A = 315-400, UV-B = 280-315 and UV-C = 100-280, that means is also necessary to test for which region of UV are new sensors sensitive. All before mentioned results were made for polychromatic illumination that means for excitation illumination from 200-400 nm. For spectral sensitivity tests we have prepared special arrangement of our measuring

system, which allow to us select variable bandwidth and dominant wavelength. Because we have tested pigments with different colors is necessary to recalculate absolute sensitivity to relative sensitivity for better understanding of sensitivity spectral shape. FIG.13 documents that except pigment P5 other pigments have main sensitivity at 375 nm.
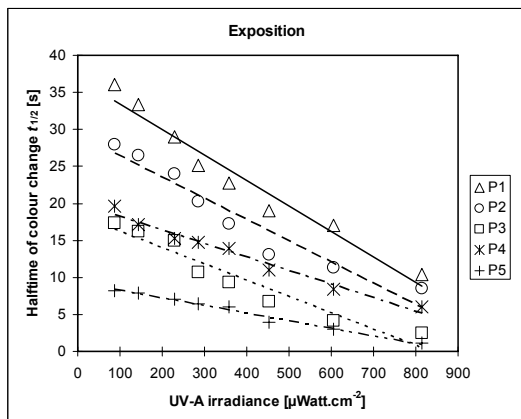

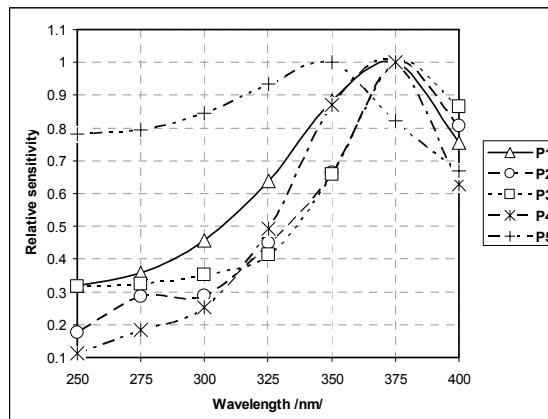Fig.12 – Halftime of color change $t_{1/2}$ relation on intensity of illumination E

Fig.13 Dependence of relative sensitivity on wavelength, average intensity of illumination = 900 µW.cm^{-2}

Both spiroindolinonaphtopyran structures with same orientation of naftopyran (P2 and P3) show narrowest bandwidth, conformable shape has also spironaphtooxazins (P1 and P4). Only pigment no P5 – spiroindolinonaphtopyran with opposite orientation of naphtopyran structure have maximum of sensitivity move to lower wavelength (350 nm) and flat shape of sensitivity curve. That means if we need sensors with low sensitivity on spectral characteristics of UV radiation we need to use pigment no. 5, if we need high sensitivity of sensors on spectral characteristics of UV radiation we need to use pigments no 2 or 3. But if we think about good selectivity of amount of UV radiation we need to use pigment no. 1 or 2.

4. CONCLUSIONS

In our study, we prepare new view on the relationship between intensity of illumination *E*, colour change halftime of exposition and halftime of relaxation respectively. Via this relation, we demonstrate the possibility of flexible textile-based sensors construction in area identification of radiation intensity. Beside of this one, we demonstrate differences between photochromic pigments behaviour concerning to spectral sensitivity. First order exponential functions, which we are used in kinetic model calculation, well described the kinetics of colour change intensity of photochromic pigments. They give good fits to the growth curves as well as to the relaxation one's. In addition, we document effectiveness of new original measuring system, which we have developed at Laboratory Colour and Appearance Measurement - LCAM.

5. REFERENCES

[1] Bamfield, P.: Chromic phenomena, technological applications of colour chemistry, RSC Cambridge 2001
[2] Van Gemert, B.: personal note, 16. July 2004
[3] Viková, M., Vik, M.: Molecular Crystals and Liquid Crystals Volume 431 (2005), p. 103-116

ACKNOWLEDGEMENTS

RESPONDENCE ADDRESS:

Laboratory Color and Appearance Measurement
Faculty of Textile Engineering,
Technical University of Liberec,
Hálkova 6, 461 17 Liberec, Czech Republic